

COMPARING RUSLE LS CALCULATION METHODS ACROSS VARYING DEM RESOLUTIONS

---

A Thesis

Presented to

The Graduate Faculty

Central Washington University

---

In Partial Fulfillment

of the Requirements for the Degree

Master of Science

Cultural and Environmental Resource Management

---

by

Amanda Moody

June 2020

CENTRAL WASHINGTON UNIVERSITY

Graduate Studies

We hereby approve the thesis of

Amanda Moody

Candidate for the degree of Master of Science

APPROVED FOR THE GRADUATE FACULTY

---

---

Dr. Robert Hickey, Committee Chair

---

---

Dr. Sterling Quinn

---

---

Dr. Michael Pease

---

---

Dean of Graduate Studies

## ABSTRACT

### COMPARING RUSLE LS CALCULATION METHODS ACROSS VARYING DEM RESOLUTIONS

by

Amanda Moody

June 2020

Soil erosion is a global problem that reduces land productivity and causes environmental degradation. Soil erosion models, such as the Revised Universal Soil Loss Equation (RUSLE), are used to estimate the severity and distribution of erosion. The topographic factor (LS), which combines slope length and angle, is an important part of RUSLE. This work compared two methods of L calculation, the grid cumulation (GC) and the contributing area (CA) methods, and two methods of S calculation, the neighborhood (NBR) and maximum downhill slope (MDS) methods. These were compared across digital elevation models (DEMs) of 1, 5, 10, and 30m resolutions. This study rectifies the lack of direct and consistent testing OF these methods across multiple sites and DEM resolutions.

The CA method produces higher mean, median, and max values of L than the GC method across all landscapes, especially along drainage channels where the greatest area accumulates to produce extremely high L values. The GC method, unlike the CA method, accounts for decreases in slope steepness that initiate deposition and reset accumulated values. Differences between these methods occur most from different

treatments of convergence. The CA method combines flow paths but the GC method only continues the one longest flow path.

The NBR and MDS method produced similar mean and median S values. However, maximum values using the NBR method are more sensitive to DEM resolution and decrease more with coarse resolutions. The NBR method produces lower S values along ridge lines and higher S values along drainage channels and concave depressions and slopes. This is due to the averaging of calculating slope angle in the NBR method. The neighborhood method smooths landscapes and reduces the ability to capture erosion variability related to S.

## TABLE OF CONTENTS (CONTINUED)

Chapter		Page
I	INTRODUCTION.....	1
	Research problem.....	1
	Purpose .....	2
II	LITERATURE REVIEW .....	5
	RUSLE History, Development, and Current Use .....	5
	L Factor Calculation Methods.....	13
	Slope Angle Calculation Methods and the S Factor .....	19
	DEM Resolution .....	21
	Research and Current Literature Gap.....	22
III	STUDY AREA.....	25
	Summary .....	38
IV	METHODS AND TECHNIQUES .....	39
	Data Gathering and Building DEMs .....	39
	Calculating L Factors .....	41
	Calculating S Factors .....	43
V	ANALYSIS AND RESULTS .....	45
	L Factor.....	46
	S Factor.....	85
VI	DISCUSSION AND FURTHER RESEARCH.....	102
	Discussion.....	102
	Further Research .....	105
	BIBLIOGRAPHY .....	107
	APPENDIXES .....	114

TABLE OF CONTENTS (CONTINUED)

Appendix A—Code.....	114
Appendix B—Raster Outputs .....	136

## LIST OF TABLES

Table		Page
1	m exponent values for USLE (Wischmeier and Smith 1978).....	10
2	Comparison of current research testing L and S factor calculation methods.....	24
3	Kolmogorov-Smirnov derived p-values for L factor outputs all sites across varying DEM resolutions.....	84
4	Kolmogorov-Smirnov derived p-values for S factor outputs all sites across varying DEM resolutions.....	88

## LIST OF FIGURES

Figure		Page
1	Site locations in Washington State .....	25
2	Climate data for Ellensburg, Washington (1893-2016) (Western Regional Climate Center n.d.) .....	26
3	Site A boundary north of Ellensburg, WA .....	28
4	Landscape view looking across the top of Site A .....	29
5	Site B boundary south of Ellensburg, WA .....	30
6	Landscape view Site B from across the Yakima River .....	31
7	Climate data for Aberdeen, Washington (1891-2016) (Western Regional Climate Center n.d.) .....	32
8	Site C boundary southwest of Olympia, WA .....	33
9	Landscape view of Site C .....	34
10	Climate data for Methow, Washington (1970-2016) (Western Regional Climate Center n.d.) .....	35
11	Site D boundary south of Twisp, WA .....	36
12	View within Site D .....	37
13	Process of calculating the RUSLE L factor using the GC method .....	41
14	Script 1 tool in ArcGIS Pro with default parameters .....	42
15	Process of calculating the RUSLE L factor using the CA method .....	43
16	L factor with the GC Method with slope cutoff at 0.5 for Site D at 1 m .....	47

LIST OF FIGURES (CONTINUED)

17	L factor with the GC Method with slope cutoff at 0.5 for Site D at 5 m.....	48
18	L factor with the GC Method with slope cutoff at 0.5 for Site D at 10 m.....	49
19	L factor with the GC Method with slope cutoff at 0.5 for Site D at 30 m.....	50
20	L factor with the GC Method without slope cutoff for Site D at 1 m.....	51
21	L factor with the GC Method without slope cutoff for Site D at 5 m.....	52
22	L factor with the GC Method without slope cutoff for Site D at 10 m.....	53
23	L factor with the GC Method without slope cutoff for Site D at 30 m.....	54
24	L factor with the CA method with a SFD algorithm for Site D at 1 m.....	55
25	L factor with the CA method with a SFD algorithm for Site D at 5 m.....	56
26	L factor with the CA method with a SFD algorithm for Site D at 10 m.....	57
27	L factor with the CA method with a SFD algorithm for Site D at 30 m.....	58
28	L factor with the CA method with a MFD algorithm for Site D at 1 m.....	59
29	L factor with the CA method with a MFD algorithm for Site D at 5 m.....	60

LIST OF FIGURES (CONTINUED)

30	L factor with the CA method with a MFD algorithm for Site D at 10 m .....	61
31	L factor with the CA method with a MFD algorithm for Site D at 30 m .....	62
32	Mean value of L factor for Site D where GC_0.5 is the GC method with slope cutoff set to 0.5, GC_1.0 is the GC method without slope cutoff, CA_SFD is the CA method using a SFD algorithm, and CA_MFD is the CA method using a MFD algorithm .....	64
33	Median value of L factor for Site D where GC_0.5 is the GC method with slope cutoff set to 0.5, GC_1.0 is the GC method without slope cutoff, CA_SFD is the CA method using a SFD algorithm, and CA_MFD is the CA method using a MFD algorithm .....	64
34	Max value of L factor for Site D where GC_0.5 is the GC method with slope cutoff set to 0.5, GC_1.0 is the GC method without slope cutoff, CA_SFD is the CA method using a SFD algorithm, and CA_MFD is the CA method using a MFD algorithm .....	65
35	Site D difference raster (1 m) for the L Factor of the GC method with slope cutoff (GC_0.5) subtracted from the GC method without slope cutoff (GC_1.0).....	67
36	Site D difference raster (5 m) for the L Factor of the GC method with slope cutoff (GC_0.5) subtracted from the GC method without slope cutoff (GC_1.0).....	68
37	Site D difference raster (10 m) for the L Factor of the GC method with slope cutoff (GC_0.5) subtracted from the GC method without slope cutoff (GC_1.0).....	69
38	Site D difference raster (30 m) for the L Factor of the GC method with slope cutoff (GC_0.5) subtracted from the GC method without slope cutoff (GC_1.0).....	70
39	Site D difference raster (1 m) for the L Factor of the CA method using a SFD algorithm (SFD) subtracted from the CA method using a MFD algorithm (MFD).....	73

LIST OF FIGURES (CONTINUED)

40	Site D difference raster (5 m) for the L Factor of the CA method using a SFD algorithm (SFD) subtracted from the CA method using a MFD algorithm (MFD).....	74
41	Site D difference raster (10 m) for the L Factor of the CA method using a SFD algorithm (SFD) subtracted from the CA method using a MFD algorithm (MFD).....	75
42	Site D difference raster (30 m) for the L Factor of the CA method using a SFD algorithm (SFD) subtracted from the CA method using a MFD algorithm (MFD).....	76
43	Site D difference raster (1 m) for the L Factor of the GC method without slope cutoff (GC_1.0) subtracted from the CA method using a SFD algorithm (CA_SFD).....	79
44	Site D difference raster (5 m) for the L Factor of the GC method without slope cutoff (GC_1.0) subtracted from the CA method using a SFD algorithm (CA_SFD).....	80
45	Site D difference raster (10 m) for the L Factor of the GC method without slope cutoff (GC_1.0) subtracted from the CA method using a SFD algorithm (CA_SFD) .....	81
46	Site D difference raster (30 m) for the L Factor of the GC method without slope cutoff (GC_1.0) subtracted from the CA method using a SFD algorithm (CA_SFD).....	82
47	Mean value of S factor for Site D .....	86
48	Median value of S factor for Site D .....	86
49	Maximum value of S factor for Site D .....	86
50	Minimum value of S factor for Site D.....	87
51	S factor with the MDS method for Site D at 1 m .....	89
52	S factor with the MDS method for Site D at 5 m .....	90

LIST OF FIGURES (CONTINUED)

53	S factor with the MDS method for Site D at 10 m .....	91
54	S factor with the MDS method for Site D at 30 m .....	92
55	S factor with the NBR method for Site D at 1 m .....	93
56	S factor with the NBR method for Site D at 5 m .....	94
57	S factor with the NBR method for Site D at 10 m .....	95
58	S factor with the NBR method for Site D at 30 m .....	96
59	Site D difference raster (1 m) for the S Factor of the MDS method subtracted from the NBR method .....	98
60	Site D difference raster (5 m) for the S Factor of the MDS method subtracted from the NBR method .....	99
61	Site D difference raster (10 m) for the S Factor of the MDS method subtracted from the NBR method .....	100
62	Site D difference raster (30 m) for the S Factor of the MDS method subtracted from the NBR method .....	101
A1	L factor with the GC Method with slope cutoff at 0.5 for Site A at 1 m .....	136
A2	L factor with the GC Method with slope cutoff at 0.5 for Site A at 5 m .....	137
A3	L factor with the GC Method with slope cutoff at 0.5 for Site A at 10 m .....	138
A4	L factor with the GC Method with slope cutoff at 0.5 for Site A at 30 m .....	139
A5	L factor with the GC Method without slope cutoff for Site A at 1 m .....	140

LIST OF FIGURES (CONTINUED)

A6	L factor with the GC Method without slope cutoff for Site A at 5 m.....	141
A7	L factor with the GC Method without slope cutoff for Site A at 10 m.....	142
A8	L factor with the GC Method without slope cutoff for Site A at 30 m.....	143
A9	Site A difference raster (1 m) for the L Factor of the GC method with slope cutoff (GC_0.5) subtracted from the GC method without slope cutoff (GC_1.0).....	144
A10	Site A difference raster (5 m) for the L Factor of the GC method with slope cutoff (GC_0.5) subtracted from the GC method without slope cutoff (GC_1.0).....	145
A11	Site A difference raster (10 m) for the L Factor of the GC method with slope cutoff (GC_0.5) subtracted from the GC method without slope cutoff (GC_1.0).....	146
A12	Site A difference raster (30 m) for the L Factor of the GC method with slope cutoff (GC_0.5) subtracted from the GC method without slope cutoff (GC_1.0).....	147
A13	L factor with the CA method with a SFD algorithm for Site A at 1 m.....	148
A14	L factor with the CA method with a SFD algorithm for Site A at 5 m.....	149
A15	L factor with the CA method with a SFD algorithm for Site A at 10 m.....	150
A16	L factor with the CA method with a SFD algorithm for Site A at 30 m.....	151
A17	L factor with the CA method with a MFD algorithm for Site A at 1 m.....	152

LIST OF FIGURES (CONTINUED)

A18	L factor with the CA method with a MFD algorithm for Site A at 5 m.....	153
A19	L factor with the CA method with a MFD algorithm for Site A at 10 m.....	154
A20	L factor with the CA method with a MFD algorithm for Site A at 30 m.....	155
A21	Site A difference raster (1 m) for the L Factor of the CA method using a SFD algorithm (SFD) subtracted from the CA method using a MFD algorithm (MFD).....	156
A22	Site A difference raster (5 m) for the L Factor of the CA method using a SFD algorithm (SFD) subtracted from the CA method using a MFD algorithm (MFD).....	157
A23	Site A difference raster (10 m) for the L Factor of the CA method using a SFD algorithm (SFD) subtracted from the CA method using a MFD algorithm (MFD).....	158
A24	Site A difference raster (30 m) for the L Factor of the CA method using a SFD algorithm (SFD) subtracted from the CA method using a MFD algorithm (MFD).....	159
A25	Site A difference raster (1 m) for the L Factor of the CA method using a SFD algorithm (CA_SFD) and the GC method without slope cutoff (GC_1.0).....	160
A26	Site A difference raster (5 m) for the L Factor of the CA method using a SFD algorithm (CA_SFD) and the GC method without slope cutoff (GC_1.0).....	161
A27	Site A difference raster (10 m) for the L Factor of the CA method using a SFD algorithm (CA_SFD) and the GC method without slope cutoff (GC_1.0).....	162
A28	Site A difference raster (30 m) for the L Factor of the CA method using a SFD algorithm (CA_SFD) and the GC method without slope cutoff (GC_1.0).....	163

LIST OF FIGURES (CONTINUED)

A29	S factor with the MDS method for Site A at 1 m .....	164
A30	S factor with the MDS method for Site A at 5 m .....	165
A31	S factor with the MDS method for Site A at 10 m .....	166
A32	S factor with the MDS method for Site A at 30 m .....	167
A33	S factor with the NBR method for Site A at 1 m .....	168
A34	S factor with the NBR method for Site A at 5 m .....	169
A35	S factor with the NBR method for Site A at 10 m .....	170
A36	S factor with the NBR method for Site A at 30 m .....	171
A37	Site A difference raster (1 m) for the S Factor of the MDS method subtracted from the NBR method.....	172
A38	Site A difference raster (5 m) for the S Factor of the MDS method subtracted from the NBR method.....	173
A39	Site A difference raster (10 m) for the S Factor of the MDS method subtracted from the NBR method.....	174
A40	Site A difference raster (30 m) for the S Factor of the MDS method subtracted from the NBR method.....	175
A41	Mean value of L factor for Site A where GC_0.5 is the GC method with slope cutoff set to 0.5, GC_1.0 is the GC method without slope cutoff, CA_SFD is the CA method using a SFD algorithm, and CA_MFD is the CA method using a MFD algorithm .....	176
A42	Median value of L factor for Site A where GC_0.5 is the GC method with slope cutoff set to 0.5, GC_1.0 is the GC method without slope cutoff, CA_SFD is the CA method using a SFD algorithm, and CA_MFD is the CA method using a MFD algorithm .....	176

LIST OF FIGURES (CONTINUED)

A43	Maximum value of L factor for Site A where GC_0.5 is the GC method with slope cutoff set to 0.5, GC_1.0 is the GC method without slope cutoff, CA_SFD is the CA method using a SFD algorithm, and CA_MFD is the CA method using a MFD algorithm .....	177
A44	Mean value of S factor for Site A .....	177
A45	Median value of S factor for Site A .....	178
A46	Maximum value of S factor for Site A .....	178
A47	Minimum value of S factor for Site A .....	179
B1	L factor with the GC Method with slope cutoff at 0.5 for Site B at 1 m.....	180
B2	L factor with the GC Method with slope cutoff at 0.5 for Site B at 5 m.....	181
B3	L factor with the GC Method with slope cutoff at 0.5 for Site B at 10 m.....	182
B4	L factor with the GC Method with slope cutoff at 0.5 for Site B at 30 m.....	183
B5	L factor with the GC Method without slope cutoff for Site B at 1 m.....	184
B6	L factor with the GC Method without slope cutoff for Site B at 5 m.....	185
B7	L factor with the GC Method without slope cutoff for Site B at 10 m.....	186
B8	L factor with the GC Method without slope cutoff for Site B at 30 m.....	187
B9	Site B difference raster (1 m) for the L Factor of the GC method with slope cutoff (GC_0.5) subtracted from the GC method without slope cutoff (GC_1.0).....	188

LIST OF FIGURES (CONTINUED)

B10	Site B difference raster (5 m) for the L Factor of the GC method with slope cutoff (GC_0.5) subtracted from the GC method without slope cutoff (GC_1.0).....	189
B11	Site B difference raster (10 m) for the L Factor of the GC method with slope cutoff (GC_0.5) subtracted from the GC method without slope cutoff (GC_1.0).....	190
B12	Site B difference raster (30 m) for the L Factor of the GC method with slope cutoff (GC_0.5) subtracted from the GC method without slope cutoff (GC_1.0).....	191
B13	L factor with the CA method with a SFD algorithm for Site B at 1 m.....	192
B14	L factor with the CA method with a SFD algorithm for Site B at 5 m.....	193
B15	L factor with the CA method with a SFD algorithm for Site B at 10 m.....	194
B16	L factor with the CA method with a SFD algorithm for Site B at 30 m.....	195
B17	L factor with the CA method with a MFD algorithm for Site B at 1 m.....	196
B18	L factor with the CA method with a MFD algorithm for Site B at 5 m.....	197
B19	L factor with the CA method with a MFD algorithm for Site B at 10 m.....	198
B20	L factor with the CA method with a MFD algorithm for Site B at 30 m.....	199
B21	Site B difference raster (1 m) for the L Factor of the CA method using a SFD algorithm (SFD) subtracted from the CA method using a MFD algorithm (MFD).....	200

LIST OF FIGURES (CONTINUED)

B22	Site B difference raster (5 m) for the L Factor of the CA method using a SFD algorithm (SFD) subtracted from the CA method using a MFD algorithm (MFD).....	201
B23	Site B difference raster (10 m) for the L Factor of the CA method using a SFD algorithm (SFD) subtracted from the CA method using a MFD algorithm (MFD).....	202
B24	Site B difference raster (30 m) for the L Factor of the CA method using a SFD algorithm (SFD) subtracted from the CA method using a MFD algorithm (MFD).....	203
B25	Site B difference raster (1 m) for the L Factor of the CA method using a SFD algorithm (CA_SFD) and the GC method without slope cutoff (GC_1.0).....	204
B26	Site B difference raster (5 m) for the L Factor of the CA method using a SFD algorithm (CA_SFD) and the GC method without slope cutoff (GC_1.0).....	205
B27	Site B difference raster (10 m) for the L Factor of the CA method using a SFD algorithm (CA_SFD) and the GC method without slope cutoff (GC_1.0).....	206
B28	Site B difference raster (30 m) for the L Factor of the CA method using a SFD algorithm (CA_SFD) and the GC method without slope cutoff (GC_1.0).....	207
B29	S factor with the MDS method for Site B at 1 m .....	208
B30	S factor with the MDS method for Site B at 5 m .....	209
B31	S factor with the MDS method for Site B at 10 m .....	210
B32	S factor with the MDS method for Site B at 30 m .....	211
B33	S factor with the NBR method for Site B at 1 m .....	212
B34	S factor with the NBR method for Site B at 5 m .....	213

LIST OF FIGURES (CONTINUED)

B35	S factor with the NBR method for Site B at 10 m .....	214
B36	S factor with the NBR method for Site B at 30 m .....	215
B37	Site B difference raster (1 m) for the S Factor of the MDS method subtracted from the NBR method.....	216
B38	Site B difference raster (5 m) for the S Factor of the MDS method subtracted from the NBR method.....	217
B39	Site B difference raster (10 m) for the S Factor of the MDS method subtracted from the NBR method.....	218
B40	Site B difference raster (30 m) for the S Factor of the MDS method subtracted from the NBR method.....	219
B41	Mean value of L factor for Site B where GC_0.5 is the GC method with slope cutoff set to 0.5, GC_1.0 is the GC method without slope cutoff, CA_SFD is the CA method using a SFD algorithm, and CA_MFD is the CA method using a MFD algorithm .....	220
B42	Median value of L factor for Site B where GC_0.5 is the GC method with slope cutoff set to 0.5, GC_1.0 is the GC method without slope cutoff, CA_SFD is the CA method using a SFD algorithm, and CA_MFD is the CA method using a MFD algorithm .....	220
B43	Maximum value of L factor for Site B where GC_0.5 is the GC method with slope cutoff set to 0.5, GC_1.0 is the GC method without slope cutoff, CA_SFD is the CA method using a SFD algorithm, and CA_MFD is the CA method using a MFD algorithm .....	221
B44	Mean value of S factor for Site B .....	221
B45	Median value of S factor for Site B .....	222
B46	Maximum value of S factor for Site B .....	222
B47	Minimum value of S factor for Site B .....	222

LIST OF FIGURES (CONTINUED)

C1	L factor with the GC Method with slope cutoff at 0.5 for Site C at 1 m.....	223
C2	L factor with the GC Method with slope cutoff at 0.5 for Site C at 5 m.....	224
C3	L factor with the GC Method with slope cutoff at 0.5 for Site C at 10 m.....	225
C4	L factor with the GC Method with slope cutoff at 0.5 for Site C at 30 m.....	226
C5	L factor with the GC Method without slope cutoff for Site C at 1 m.....	227
C6	L factor with the GC Method without slope cutoff for Site C at 5 m.....	228
C7	L factor with the GC Method without slope cutoff for Site C at 10 m.....	229
C8	L factor with the GC Method without slope cutoff for Site C at 30 m.....	230
C9	Site C difference raster (1 m) for the L Factor of the GC method with slope cutoff (GC_0.5) subtracted from the GC method without slope cutoff (GC_1.0).....	231
C10	Site C difference raster (5 m) for the L Factor of the GC method with slope cutoff (GC_0.5) subtracted from the GC method without slope cutoff (GC_1.0).....	232
C11	Site C difference raster (10 m) for the L Factor of the GC method with slope cutoff (GC_0.5) subtracted from the GC method without slope cutoff (GC_1.0).....	233
C12	Site C difference raster (30 m) for the L Factor of the GC method with slope cutoff (GC_0.5) subtracted from the GC method without slope cutoff (GC_1.0).....	234

LIST OF FIGURES (CONTINUED)

C13	L factor with the CA method with a SFD algorithm for Site C at 1 m.....	235
C14	L factor with the CA method with a SFD algorithm for Site C at 5 m.....	236
C15	L factor with the CA method with a SFD algorithm for Site C at 10 m.....	237
C16	L factor with the CA method with a SFD algorithm for Site C at 30 m.....	238
C17	L factor with the CA method with a MFD algorithm for Site C at 1 m.....	239
C18	L factor with the CA method with a MFD algorithm for Site C at 5 m.....	240
C19	L factor with the CA method with a MFD algorithm for Site C at 10 m.....	241
C20	L factor with the CA method with a MFD algorithm for Site C at 30 m.....	242
C21	Site C difference raster (1 m) for the L Factor of the CA method using a SFD algorithm (SFD) subtracted from the CA method using a MFD algorithm (MFD).....	243
C22	Site C difference raster (5 m) for the L Factor of the CA method using a SFD algorithm (SFD) subtracted from the CA method using a MFD algorithm (MFD).....	244
C23	Site C difference raster (10 m) for the L Factor of the CA method using a SFD algorithm (SFD) subtracted from the CA method using a MFD algorithm (MFD).....	245
C24	Site C difference raster (30 m) for the L Factor of the CA method using a SFD algorithm (SFD) subtracted from the CA method using a MFD algorithm (MFD).....	246

LIST OF FIGURES (CONTINUED)

C25	Site C difference raster (1 m) for the L Factor of the CA method using a SFD algorithm (CA_SFD) and the GC method without slope cutoff (GC_1.0) .....	247
C26	Site C difference raster (5 m) for the L Factor of the CA method using a SFD algorithm (CA_SFD) and the GC method without slope cutoff (GC_1.0) .....	248
C27	Site C difference raster (10 m) for the L Factor of the CA method using a SFD algorithm (CA_SFD) and the GC method without slope cutoff (GC_1.0) .....	249
C28	Site C difference raster (30 m) for the L Factor of the CA method using a SFD algorithm (CA_SFD) and the GC method without slope cutoff (GC_1.0) .....	250
C29	S factor with the MDS method for Site C at 1 m .....	251
C30	S factor with the MDS method for Site C at 5 m .....	252
C31	S factor with the MDS method for Site C at 10 m.....	253
C32	S factor with the MDS method for Site C at 30 m.....	254
C33	S factor with the NBR method for Site C at 1 m .....	255
C34	S factor with the NBR method for Site C at 5 m .....	256
C35	S factor with the NBR method for Site C at 10 m .....	257
C36	S factor with the NBR method for Site C at 30 m .....	258
C37	Site C difference raster (1 m) for the S Factor of the MDS method subtracted from the NBR method.....	259
C38	Site C difference raster (5 m) for the S Factor of the MDS method subtracted from the NBR method.....	260
C39	Site C difference raster (10 m) for the S Factor of the MDS method subtracted from the NBR method.....	261

LIST OF FIGURES (CONTINUED)

C40	Site C difference raster (30 m) for the S Factor of the MDS method subtracted from the NBR method.....	262
C41	Mean value of L factor for Site C where GC_0.5 is the GC method with slope cutoff set to 0.5, GC_1.0 is the GC method without slope cutoff, CA_SFD is the CA method using a SFD algorithm, and CA_MFD is the CA method using a MFD algorithm .....	263
C42	Median value of L factor for Site C where GC_0.5 is the GC method with slope cutoff set to 0.5, GC_1.0 is the GC method without slope cutoff, CA_SFD is the CA method using a SFD algorithm, and CA_MFD is the CA method using a MFD algorithm .....	263
C43	Maximum value of L factor for Site C where GC_0.5 is the GC method with slope cutoff set to 0.5, GC_1.0 is the GC method without slope cutoff, CA_SFD is the CA method using a SFD algorithm, and CA_MFD is the CA method using a MFD algorithm .....	264
C44	Mean value of S factor for Site C .....	264
C45	Median value of S factor for Site C .....	265
C46	Maximum value of S factor for Site C.....	265
C47	Minimum value of S factor for Site C .....	265

## CHAPTER I

### INTRODUCTION

#### Research problem

Soil erosion and related degradation continues to be a global problem (Telles, Guimarães, and Dechen 2011; Segura et al. 2014; Di Stefano and Ferro 2016). From persistent agricultural pressures to expanding infrastructures for growing populations, any activity that disturbs the Earth's surface increases soil vulnerability to detachment (Telles, Guimarães, and Dechen 2011; Laflen and Flanagan 2013; Segura et al. 2014; Di Stefano and Ferro 2016). With the geologically slow rate of soil formation, proper management of the world's current stock of fertile soil is essential to support both resilient ecosystems and human populations (Pimentel et al. 1995; Telles, Guimarães, and Dechen 2011; Segura et al. 2014; Di Stefano and Ferro 2016). Soil erosion models help land managers make informed decisions to mitigate soil erosion issues by identifying the severity and location of soil erosion (Renard et al. 1997). Conservation efforts supported by these models, include policies and programs to promote land use changes and practices that aid in reducing erosion and soil degradation (Renard et al. 1997; Di Stefano and Ferro 2016).

During the 1950s, in response to growing concerns over the loss of fertile agricultural soil in the Midwestern United States, the Universal Soil Loss Equation (USLE) was developed to estimate an average long term rate of soil erosion for a given site (Wischmeier and Smith 1978). Over time, this model evolved into the Revised Universal

Soil Loss Equation (RUSLE) with additional data, research, and computerized calculations for easier use that can better fit more landscape conditions than its predecessor (Renard et al. 1997).

The full RUSLE model is discussed in Chapter II, but two major components are the L and S factors that represent the slope length and steepness of the site. They are most commonly estimated or calculated from field measurements which can be used for local conservation planning, but this is only feasible at a small scale as using actual field measurements is labor-intensive, time consuming, and costly (Hickey, Smith, and Jankowski 1994; Van Remortel, Hamilton, and Hickey 2001; Van Remortel, Maichle, and Hickey 2004; Liu et al. 2011; Yang 2015). While there are multiple methods and algorithms for calculating the L and S factors, the comparison of these is lacking consistent testing and analysis of the differences across multiple study sites and digital elevation model (DEM) resolutions.

#### Purpose

This research tests the quantitative and spatial differences of different GIS methods and algorithms for calculating the L and S factors in the RUSLE. These differences are analyzed across varying resolutions using DEMs of 1, 5, 10, and 30 m.

Two of the most common and widely studied methods of calculating the L factor, the grid cumulation (GC) and the contributing area (CA method), are compared for this research (Winchell et al. 2008; Liu et al. 2011; Yang 2015; Zhang et al. 2017). The grid GC method calculates slope length along the flow path using a D8 flow-routing algorithm

which closely resembles the original USLE and RUSLE manual calculation methods (Hickey 2000; Van Remortel, Hamilton, and Hickey 2001; Van Remortel, Maichle, and Hickey 2004). The GC method also includes a slope cutoff factor that helps to identify breaks in slope and areas of deposition (Hickey 2000; Van Remortel, Hamilton, and Hickey 2001; Van Remortel, Maichle, and Hickey 2004). This method will be used with and without the incorporation of this slope cutoff factor to determine how much this variable influences L factor values. The CA method substitutes the linear estimate of slope length in the L factor with the upslope contributing area for a particular point (Moore and Burch 1986; Desmet and Govers 1996a, Winchell et al. 2008). For this method, two different flow-routing algorithms are used in the calculation of a cell's upslope contributing area which determine the distribution of flow from a cell to its downslope neighbors (Desmet and Govers 1996b, Wilson, Lam, and Deng 2007; Winchell et al. 2008; Liu et al. 2011).

Two different algorithms for calculating slope in the S factor will also be compared. The neighborhood (NBR) method is the standard used by the Environmental Systems Research Institute's (ESRI) ArcMap and ArcGIS Pro programs and calculates a cell's slope by averaging the elevation of that cell's eight neighbors (ESRI 2018c). The maximum downhill slope (MDS) method however, does not use an average to calculate a cell's slope; instead it considers a cell's elevation in relation to its eight neighbors to calculate the maximum value of the downhill slope for that cell (Dunn and Hickey 1998; Irfan Ashraf et al. 2012).

Given the increased pressures on soil resources from agriculture and land development and a need for improved management, this research will provide a foundation for understanding the differences between these L and S calculation methods and how they affect erosion estimates. The objectives of this thesis are to 1) compare and analyze the L and S factor outputs using the grid cumulation method and the contributing area method for L, 2) compare the neighborhood method and the maximum downhill slope method to calculate slope angle for S, and 3) quantify the effects of DEM resolution on L and S factor calculations. These objectives were accomplished by:

- Identifying four different study sites in Washington State
- Ground verifying the study site's conditions and visible evidence of erosion
- Creating a python program for ArcGIS to generate L and S output rasters
- Comparing the factor outputs mean, median, max, and standard deviations
- Comparing the spatial differences of values in the output rasters
- Identifying landscape characteristics that create these variances in the outputs
- Connecting the importance of these differences on soil erosion estimates and how that could influence policy and land management decisions

## CHAPTER II

### LITERATURE REVIEW

#### RUSLE History, Development, and Current Use

The USLE family of models estimate overland soil erosion by water from the major factors that influence this process such as climate, topography, vegetation, and land use (Wischmeier and Smith 1978; Renard et al. 1997; Gilley and Flanagan 2007; Suhua et al. 2013; Ganasri and Ramesh 2016). Of 82 different erosion from water models reviewed, Karydas, Panagos, and Gitas (2014) found that the USLE family were the most widely used empirical models. The RUSLE, especially when combined with a geographic information system (GIS), is a cost-effective management tool that can be used to determine the pattern, intensity, and cost of soil erosion on sensitive landscapes (Renard et al. 1997; Van Remortel, Maichle, and Hickey 2004; Liu et al. 2011; Telles, Guimarães, and Dechen 2011; Zhang et al. 2013, 2017; Karydas, Panagos, and Gitas 2014; Segura et al. 2014; Ganasri and Ramesh 2016; Raj et al. 2018).

In 1954 the Agricultural Research Service (an agency of the USDA) founded the National Runoff and Soil Loss Data Center at Purdue University with the goal to establish a national soil erosion equation (Wischmeier and Smith 1978; Renard et al. 1997; Gilley and Flanagan 2007). Collected and analyzed work done by researchers across the U.S. provided more than 10,000 plot-years of erosion data for the development of a overland flow soil erosion model (Wischmeier and Smith 1978; Renard et al. 1997; Gilley

and Flanagan 2007). This collaborative effort eventually led to the creation of the USLE, containing six factors to estimate the average annual soil loss for a specified area from rill and interrill erosion processes. These factors are rainfall and runoff (R), soil erodibility (K), slope length (L), slope steepness (S), cover management (C), and support practices (P). These factors are combined into the following equation (Wischmeier and Smith 1978; Renard et al. 1997):

$$A = RKLSCP$$

Where A is the long-term soil loss for the site usually presented in tons/acre/year.

In 1997 the RUSLE was published in the *Agricultural Handbook No. 703* that revised the original USLE with improvements from additional research and analysis (Renard et al. 1997). These changes updated the calculation methods for most of the factors and included updated isoerodent maps and expanded research on soil types and their erodibility.

The R factor, usually presented in hundreds of foot-ton inch per acre hour (U.S. customary units) or as  $\text{MJ mm ha}^{-1} \text{ h}^{-1}$  per year (international system of units), is the erosion that results from raindrop impact and associated storm runoff; it is proportional to the rain event parameter erosivity known as  $EI_{30}$ : total storm energy (E) times the maximum 30 minute intensity ( $I_{30}$ ) (Wischmeier and Smith 1978; Renard et al. 1997; Nearing et al. 2017). The calculation method for  $EI_{30}$  in the 1997 RUSLE Handbook was

found to significantly underestimate erosivity and was replaced in RUSLE2 as the official method of calculating the R factor for all U.S. government agencies, however the original RUSLE method is still most widely used by others (USDA-Agricultural Research Service 2013, Segura et al. 2014; Nearing et al. 2017). The R factor can be estimated directly from isoerodent maps or calculated from data from local rain gauges as the average total of the storms  $EI_{30}$  values over a number of years:

$$R = \sum_{j=1}^n EI_j$$

Where  $n$  is the number of storms and  $EI_j$  is the  $EI_{30}$  for storm  $j$  in  $n$ .

However, this requires a large amount of high frequency data for  $EI_{30}$  that may not be available (Wischmeier and Smith 1978; Renard et al. 1997; Angulo-Martínez and Beguería 2009; Beguería, Serrano-Notivoli, and Tomas-Burguera 2018). Further research has developed easier erosivity and R factor calculation from more readily available daily, monthly, or annual precipitation data online and an  $EI_{30}$  or an R factor equivalent equation can be used (Renard and Freimund 1994; Yu and Rosewell 1996; Ferro, Porto, and Yu 1999; Yu, Hashim, and Eusof 2001; Petkovšek and Mikoš 2004; Angulo-Martínez and Beguería 2009; Ganasri and Ramesh 2016; Beguería, Serrano-Notivoli, and Tomas-Burguera 2018).

Special procedures should be applied if the selected site has significant runoff from snowmelt, rain over frozen soil, or irrigation (Renard et al. 1997). This factor can

also vary dramatically from year to year with droughts or particularly wet seasons; for this reason an average over a multiple numbers of years is highly recommended (Wischmeier and Smith 1978; Renard et al. 1997; Angulo-Martínez and Beguería 2009; Beguería, Serrano-Notivolí, and Tomas-Burguera 2018).

The K factor is the susceptibility of the surface soil to detachment and the transportability of that soil material to overland flow in a storm event under reference plot conditions (Wischmeier and Smith 1978; Renard et al. 1997; Ganasri and Ramesh 2016). It is the rate of soil loss per rainfall erosion index unit and varies between zero and one where zero represents the least prone to detachment and transport (Renard et al. 1997; Ganasri and Ramesh 2016). High clay content soils produce low K values due to clays high resistance to detachment; sandy soils also produce low K values due to their high infiltration rate (Ganasri and Ramesh 2016). This factor is typically expressed as ton acre<sup>-1</sup> per erosion index unit from the R factor. Many soil types have a calculated K factor values available in the RUSLE Handbook nomograph, but if a soil is not listed a variety of K factor calculations are available dependent on the soils texture and region of the site (Renard et al. 1997; Laflen and Moldenhauer 2003).

As a part of the RUSLE update and improvement, the equations to calculate the topographic factors LS were updated and include procedures to account for convexity and concavity of a slope profile (Renard et al. 1997; Gilley and Flanagan 2007). The L factor and S factor are commonly evaluated and referred together as the topographic slope factor in most related literature (Renard et al. 1997; Winchell et al. 2008; Zhang et

al. 2013, 2017; Ganasri and Ramesh 2016). This product of LS is the ratio of soil loss from a specified slope to a reference slope that has a length of 22.13m (72.6 feet) and a steepness of 9 percent, holding all other conditions equal (Wischmeier and Smith 1978; Renard et al. 1997). The slope length is defined by Wischmeier and Smith (1978) as “the horizontal distance from the origin of overland flow to the point where either the slope gradient decreases enough that deposition begins or runoff becomes concentrated in a defined channel.” Typically, the slope length and gradient should be calculated from field measurements; however, this is labor intensive and costly, especially at large scales (Hickey, Smith, and Jankowski 1994; Van Remortel, Hamilton, and Hickey 2001; Van Remortel, Maichle, and Hickey 2004; Liu et al. 2011; Yang 2015). Deriving these from a DEM in a GIS is much more cost-effective and efficient.

The equation for the L factor in the USLE/RUSLE model is:

$$L = (\lambda/72.6)^m$$

Where  $\lambda$  is the linear measurement of slope length and the focus my research, 72.6 is the model reference plot length in feet, and m is a variable slope length exponent related to the ratio of rill to interill erosion (Foster and Wischmeier 1974; Renard et al. 1997). In the USLE, the m exponent is selected from a graduated range of slope conditions (**Table 1**).

**Table 1.** m exponent values for USLE (Wischmeier and Smith 1978).

<b>m Value</b>	<b>Slope (percent)</b>
0.5	≥ 5
0.4	3.5 - 4.5
0.3	1 - 3
0.2	< 1

For the RUSLE, m is designated by the following equation (Renard et al. 1997):

$$m = \beta / (1 + \beta)$$

$$\beta = (\sin\theta / 0.0896) / [3(\sin\theta)^{0.8} + 0.56]$$

Where  $\theta$  is the slope angle in degrees.

The USLE outlines the S factor calculation as:

$$S = 65.41 \sin^2 \theta + 4.56 \sin \theta + 0.065$$

Where  $\theta$  is the slope angle in degrees. This factor was revised for the RUSLE, involving two equations depending on the slope gradient, and is as follows:

$$S = 10.8 \sin\theta + 0.03 \text{ for slopes } < 9 \text{ percent}$$

$$S = 16.8 \sin\theta - 0.50 \text{ for slopes } \geq 9 \text{ percent}$$

Where  $\theta$  is the slope angle in degrees. Research has found that the S factor has the greater influence on RUSLE estimates, so the method of calculating the slope angle

is crucial (Wang et al. 2002; Warren et al. 2004; Irfan Ashraf et al. 2012). Slope angle calculations are a standard industry tool in GIS while slope length calculations are not.

The C factor represents the effect that cropping and management practices have on erosion rates in relation to the reference plot conditions of a continuously tilled fallow site (Wischmeier and Smith 1978; Renard et al. 1997; Laflen and Moldenhauer 2003). This means that the C factor is a ratio of soil loss at the study site to soil lost under reference plot conditions. This factor is used most commonly in conservation practices to compare different management strategies for soil conservation (Wischmeier and Smith 1978; Renard et al. 1997). This factor is calculated from the combination of soil loss ratios (SLR) calculated from the combination of sub factors over time periods where they can be assumed as remaining constant (Wischmeier and Smith 1978; Renard et al. 1997; Laflen and Moldenhauer 2003). These sub factors include the sites previous cropping and management, vegetative canopy, surface cover, surface roughness, and soil moisture (Wischmeier and Smith 1978; Renard et al. 1997; Ganasri and Ramesh 2016). These are then weighted by the fraction of  $EI_{30}$  corresponding to that SLR time period and combined into the final C factor (Wischmeier and Smith 1978; Renard et al. 1997):

$$C = (SLR_1EI_1 + SLR_2EI_2 + \dots + SLR_nEI_n) / EI_t$$

Where n is the number of time periods and  $EI_t$  is the sum of the EI percentages for the entire time period (Renard et al. 1997). This factor varies between zero and one

where values closer to zero represent sites that have high cover protection from raindrop impact and runoff (Wischmeier and Smith 1978; Renard et al. 1997; Ganasri and Ramesh 2016). If site conditions do not have large seasonal variation or are slow to change then the C factor calculation can be simplified with one annual average SLR value (Renard et al. 1997; Ganasri and Ramesh 2016).

The P factor is another ratio, between zero and one, of soil loss with the sites conservation support practices to the reference plot of straight row up and down tillage; values closer to zero represent good use of supporting practices (Wischmeier and Smith 1978; Renard et al. 1997; Laflen and Moldenhauer 2003; Ganasri and Ramesh 2016). While seemingly closely related to the C factor, the P factor does not include erosion control practices such as no-till or crop-residue management (Wischmeier and Smith 1978; Renard et al. 1997). Practices that are included for cultivated lands include contour farming, strip-cropping, terracing of various types, and contouring residue strips; while if the study area is a forest or other land use this factor can be set to one (Laflen and Moldenhauer 2003; Ganasri and Ramesh 2016). This factor represents the reduction of erosion potential by support practices influencing the drainage patterns, runoff concentration and velocity, and other forces created by runoff (Wischmeier and Smith 1978; Renard et al. 1997; Laflen and Moldenhauer 2003; Ganasri and Ramesh 2016). P factor values are available for numerous support practices in the RUSLE Handbook, these were calculated from experimental data and plot observations (Renard

et al. 1997). If multiple practices are used throughout the site, the P factor is a product of P sub factors for each subsection (Wischmeier and Smith 1978; Renard et al. 1997).

## L Factor Calculation Methods

### The Grid Cumulation Method

This method uses the length calculated along flow path as slope length ( $\lambda$ ) in the L factor calculation discussed previously. It is the summation of the non-cumulative slope length (NCSL) following flow direction, using a D8 flow routing algorithm, from high points in the landscape. This calculation conforms to USLE and RUSLE requirements where the measurements are in (x,y) space rather than (x,y,z) space.

High points are first identified as they begin all flow paths. They have an out-flow direction but no in flow, such as ridgelines and peaks, and so flow length is assumed to only occur in that half of the cell that is downhill from the center (Van Remortel, Hamilton, and Hickey 2001). These are identified by those cells that have no neighbors with corresponding flow directions, according to the D8 flow routing algorithm, pointing to that cell.

NCSL is calculated for every cell and has been updated from the previous definition of Van Remortel, Maichle, and Hickey (2004). It is calculated following the below rules:

If the cell is a high point and:

Flow direction is cardinal =  $0.5(\text{cell resolution})$

Flow direction is diagonal =  $0.5(1.4142)(\text{cell resolution})$

If the cell is not a high point and:

Flow direction is cardinal = (cell resolution)

Flow direction is diagonal =  $1.4142(\text{cell resolution})$

NCSL values are then added together for the cumulative slope length along flow direction starting at high points. The cumulative slope length is terminated either when two flow paths meet and the shorter path ends, a stream channel is reached, or the slope angle changes and decreases enough that deposition occurs (Hickey 2000; Van Remortel, Hamilton, and Hickey 2001; Van Remortel, Maichle, and Hickey 2004). The cutoff slope angle variable incorporates the occurrence of slope angles decreasing enough to initiate deposition. It assumes that at least a 50 percent slope angle decrease describes areas of deposition rather than erosion (Hickey, Smith, and Jankowski 1994; Hickey 2000). It is recommended that this value be assigned by an expert of the study area, but as this is not always feasible a default value of 0.5 can be used (Hickey 2000).

In this research, the MDS method is used to calculate slope angle for the L factor calculation (used in the rill to interrill ratio exponent). The slope raster produced is searched for flat pixels (0 degrees slope) which are re-assigned a 0.1 degree slope angle; this allows for minimal erosion within that flat area without altering flow paths (Van Remortel, Hamilton, and Hickey 2001).

Another update is the incorporation of a channel initiation threshold variable to account for areas where rill to interrill erosion is no longer the dominant erosion process, such as stream channels (Wischmeier and Smith 1978; Renard et al. 1997; Zhang et al. 2013). This is another user input value that sets the percentage of maximum cell area required to define a channel. The default value is set to 1 percent of the maximum flow accumulation value, meaning if a cell's flow accumulation is greater than 1 percent of the maximum flow accumulation value it will be considered part of a defined channel and the L factor values will be set to no data (ESRI 2018a).

After the cumulative slope length is calculated for the entire site, the L factor equation can be applied using the calculated cumulative slope length for each cell as  $\lambda$ . Van Remortel, Maichle, and Hickey (2004) worked to translate the RUSLE based AML code for the GC method to an array-based executable program using ANSI C++ software. This was also later converted to be able to run as an ArcMap extension and made available for download at <http://www.onlinegeographer.com/slope/slope.html>. Unfortunately, an error was discovered and the code was taken down with a recommendation to use the previous AML version from Van Remortel, Hamilton, and Hickey (2001). This is still available for download from the above mentioned website, while a new version will be made available to download with the above mentioned updates in 2020.

## The Contributing Area Method

The CA method substitutes slope length with upslope contributing area. This is based off the concept that overland flow and erosion does not depend on the distance of flow from a point of origin, but rather on the flow convergence and divergence over the area per unit contour length contributing flow to a specific point in the landscape (Desmet and Govers 1996a). Desmet and Govers (1996a) proposed a method of calculating the L factor in a GIS using the upslope contributing area as:

$$L_{i,j} = \frac{(A_{i,j-in} + D^2)^{m+1} - A_{i,j-in}^{m+1}}{D^{m+2} (x_{i,j}^m) 22.13^m}$$

Where  $L_{i,j}$  is the L factor for the grid cell at coordinates  $(i, j)$ ,  $A_{i,j-in}$  is the contributing area at the inlet of that grid cell,  $D$  is the grid cell size (meters), and  $x_{i,j} = \sin(a_{i,j}) + \cos(a_{i,j})$  where  $a_{i,j}$  is the aspect direction. As can be determined from the equation, the contributing area of a cell is calculated using the flow-routing algorithm, aspect direction, and grid cell size all calculated from an input DEM. The flow routing algorithm used by Desmet and Govers (1996a) is the FD8 multiple flow direction algorithm (Quinn et al. 1991) that was selected based off their previous study comparing six different flow routing algorithms (Desmet and Govers 1996b).

Another tool was published in 2003 hosted by System for Automated Geoscientific Analyses (SAGA) that has an LS Factor module available following the calculation as laid out for the USLE but only allows for the use of area to calculate the L factor and is unable to calculate slope length (SAGA 2003). This module requires the

user to input area, slope, and specify a single value for the m exponent and then outputs a single LS factor raster.

i. Flow-Routing Algorithms

Flow-routing algorithms explain how the flow from one cell is distributed to its downslope neighbors. There are two primary categories of these, single flow direction (SFD) algorithms and multiple flow direction (MFD) algorithms (Desmet and Govers 1996b; Wilson, Lam, and Deng 2007; Liu et al. 2011; Raj et al. 2018).

SFD algorithms direct all flow from one cell to only one downslope neighbor. The two most common algorithms in this category are the D8 and the Rho8 algorithms (Tarboton 1997; Wilson, Lam, and Deng 2007; Liu et al. 2011). The D8 algorithm follows flow direction and directs its flow to the steepest down slope neighbor (D. K. McCool et al. 1989; Quinn et al. 1991; Wilson, Lam, and Deng 2007; Liu et al. 2011; Raj et al. 2018). The Rho8 algorithm attempts to generate random variability to the D8 algorithm by weighting the chance of a downslope neighbor receiving all flow in portion to its downslope gradient from the center cell (Fairfield and Leymarie 1991; Wilson, Lam, and Deng 2007; Liu et al. 2011). While this can help to reduce the banding and parallel effects of the D8 algorithm, it also makes calculating that should be deterministic quantities in these models non-repeatable, as every run of this produces a slightly different output (Tarboton 1997; Wilson, Lam, and Deng 2007).

There are many various MFD algorithms that all differ in the way they distribute flow to two or more downslope neighbors. Common algorithms include the FD8,  $D_{\infty}$ , FRho8, DEMON, and ANSWERS (Quinn et al. 1991; Desmet and Govers 1996b; Tarboton 1997; Wilson, Lam, and Deng 2007; Liu et al. 2011). ANSWERS only considers the cardinal downslope neighbors while the others consider all downslope neighbors (Quinn et al. 1991; Desmet and Govers 1996b; Tarboton 1997; Wilson, Lam, and Deng 2007; Liu et al. 2011). SFD algorithms typically produce the lowest contributing area values, and therefore L factor values, while the MFD algorithms that consider fewer neighbors produce lower values than those that consider all downslope neighbors (Desmet and Govers 1996b; Wilson, Lam, and Deng 2007). Considering more neighbors distributes flow to more areas which results in the higher contributing area values.

Differences between the single and multiple flow routing algorithms have also been found to increase for the steeper upslope areas than the lower valley or flat areas, indicating that the choice of the flow-routing algorithm could be more influential in steep or complex terrain (Quinn et al. 1991; Wilson, Lam, and Deng 2007; Liu et al. 2011). SFD algorithms produce sharper features and can have a banding or parallel effect: where once an area becomes a part of a flow path it cannot be later distributed (Quinn et al. 1991; Desmet and Govers 1996b; Tarboton 1997; Wilson, Lam, and Deng 2007; Raj et al. 2018). This can be a more realistic representation of pathways in valley floors where permanent drainage systems become more easily established (Quinn et al. 1991). MFD algorithms typically do not have any banding effects and can produce more

realistic patterns on hillslopes with greater dispersion of area instead of staying in a concentrated path, but have a tendency to ‘braid’ cumulative area across valley floors (Quinn et al. 1991; Desmet and Govers 1996b; Tarboton 1997; Wilson, Lam, and Deng 2007).

## Slope Angle Calculation Methods and the S Factor

### Neighborhood Method

The NBR method of slope angle calculation, which is used by the Environmental Systems Research Institute (ESRI) in their ArcGIS programs, is an averaging method where a 3x3 window moves over the DEM and calculates the center cell’s slope by averaging the rate of change in elevation of the surrounding eight neighbors.

Geographic Resources Analysis Support System (GRASS) and Quantum GIS (QGIS) also uses a similar averaging method for its slope calculation tool (GDAL 2020; GRASS 2020).

The equation used for the NBR method (in degrees) is (Dunn and Hickey 1998; ESRI 2018b):

$$\theta = \tan^{-1} \left( \sqrt{\left(\frac{dz}{dx}\right)^2 + \left(\frac{dz}{dy}\right)^2} \right)$$

Where  $\frac{dz}{dx}$  is the east to west slope and  $\frac{dz}{dy}$  is the north to south slope. This leads to inaccuracies where lower slope estimates are calculated in steep terrain and higher estimates are calculated in flat terrain (Dunn and Hickey 1998; Hickey 2000; Irfan Ashraf et al. 2012, ESRI 2018c). This calculation is also inconsistent with flow direction, which

follows the steepest downslope direction, making its use inconsistent and problematic for models that rely on flow direction (Dunn and Hickey 1998).

#### Maximum Downhill Slope Method

The maximum downhill slope method is able to retain local variability and small scale features as it does not use an average for calculating slope (Dunn and Hickey 1998; Hickey 2000). This method also uses a 3x3 window, but considers the center cell's elevation and its difference between one of the eight neighbors that gives the maximum downhill slope (Dunn and Hickey 1998; Hickey 2000). The consideration of only downhill neighbors for maximum value ensures that slope calculations are not overestimated (Dunn and Hickey 1998; Hickey 2000). The equation is as follows:

$$\theta = \tan^{-1}\left(\max \frac{(z_9 - z_i)}{L_e}\right)$$

Where  $L_e$  is the distance between the midpoints of the center and neighboring cell (if neighboring cell diagonally adjacent then multiply by  $\sqrt{2}$ ),  $z_9$  is the center cell, and  $z_i$  is neighboring cell 1-8. Unfortunately, the advantage of this method being able to retain small scale features can also result in a disadvantage to being sensitive to local errors in DEMs (Hickey 2000; Irfan Ashraf et al. 2012). However, this method more accurately represents true landscape variability, especially in combination with high quality fine resolution DEMs, producing greater variance in values of slope steepness and the S factor (Dunn and Hickey 1998; Hickey 2000). This method is consistent with

flow direction, making it the better method to use for models that require flow direction.

#### DEM Resolution

For L factor estimates, coarse DEM resolutions have been shown to result in larger mean slope lengths, contributing area, and L values (Quinn et al. 1991; Zhang et al. 1999; Liu et al. 2011; Fu et al. 2015). Coarse resolutions (typically greater than 10 m) smooth over and lose landscape features important to hydrological processes which are apparent in finer resolutions (Quinn et al. 1991; Fu et al. 2015). For the GC method, increased cell size creates longer slope lengths for each cell and small-scale features that would otherwise break slope length are lost (Fu et al. 2015). One exception that has been found has been in gently rolling landscapes where the opposite occurs (Liu et al. 2011). The wave like features of the landscape are lost at coarse resolutions and turned into dramatically changing slopes that trigger the slope cutoff angle variable into smaller slope lengths (Liu et al. 2011). Similarly, increased cell size increases the minimum area used in the CA method (Quinn et al. 1991; Liu et al. 2011). Overall, coarse DEM resolutions increase the mean values and standard deviations of L Factor outputs regardless of calculation method (Liu et al. 2011; Fu et al. 2015).

Higher resolutions DEMs produce estimates of slope angle that are more representative of the landscape's true slope, while coarse DEM resolutions reduce the mean and standard deviation of S values (Zhang et al. 1999; Warren et al. 2004; Irfan Ashraf et al. 2012; Fu et al. 2015). The S factor calculation only requires one input, the

slope angle, and underestimating this directly influences the S Factor and produces correspondingly lower values.

#### Research and Current Literature Gap

Various research (Wischmeier and Smith 1978; Pimentel et al. 1995; Renard et al. 1997; Nearing 2001; Telles, Guimarães, and Dechen 2011; Telles et al. 2013; Segura et al. 2014) using the USLE family of models has been done assessing the environmental and economic impacts of soil erosion to society. Other studies (Jabbar 2003; Yang 2015; Ganasri and Ramesh 2016; Di Stefano, Ferro, and Pampalone 2017) use the USLE and RUSLE models to assess a specific sites erosion when there is strong concern over the soil loss, future productivity, or water quality of the area. This information can be used to mitigate areas of high erosion and conserve valuable topsoil.

In the agricultural industry, a loss of valuable topsoil results in decreased yield from lost nutrients, stability, and water holding capacity which forces the farmer to use more fertilizers and pesticides to continue producing greater harvests (Pimentel et al. 1995; Renard et al. 1997; Telles et al. 2013; Di Stefano and Ferro 2016). This increased input by the farmer results in environmental degradation with fertilizer, pesticide, and soil runoff. This also results in a raised cost to the consumer paying for the farmers increased effort. The combination of these costs cumulates into approximately 44 billion dollars a year for the U.S. (Telles, Guimarães, and Dechen 2011; Telles et al. 2013).

As water is one of the primary driving forces in erosion, the effects and costs of soil erosion can be expected to rise with the effects of climate-related hydrologic variability. Segura et al. (2014) used RUSLE and several projected climate change scenarios to assess those impacts on soil erosion. Her results agreed with similar past research (Nearing 2001) that the climatic changes in rainfall erosivity (R factor) and temperature will increase projected soil erosion and runoff. However, this is not spatially uniform across the U.S. (Segura et al. 2014). Sound management decisions concerning soil erosion are critical with the increasing effects of climatic change and stress of expanding populations on land use.

At present, the existing studies on L and S factor calculation methods and algorithms lack a cohesive and easy to interpret comparison of the differences they produce, especially across multiple study sites and regulations (**Table 2**). This makes it difficult to know if the differences presented in one study about one particular site can be related to other research. Determining if these differences are consistent and predictable across similar landscapes and DEM resolutions will aid in understanding RUSLE erosion estimates. This knowledge can be used to influence policy and land management decisions concerned with soil conservation.

**Table 2.** Comparison of current research testing L and S factor calculation methods

Study	Model			L Factor			Slope Angle for S Factor			DEM Scale (m)	# of Study Areas
	USLE	RUSLE	Other USLE Related Model	GC Method	CA Method	Other	Neighborhood Method	Maximum Downhill Slope	Other		
Liu et al. 2011	X			X	X		Not Applicable			5, 10, 25, 50, 100	1
Zhang et al. 2013		X		X	X	X		X		5	1
Zhang et al. 2017		X			X	X			X	5	1
Suhua et al. 2013		X		X				X		5	2
Lee and Choi 2010	X					X	Undefined			10-200 at 10m intervals	1
Ganasri and Ramesh 2016		X			X		X**			30	1
Raj et al. 2018		X				X	X**			18cm, 10, 30	1
Yang 2015		X		X				X		30	1***
Rodríguez and Suárez 2010		X		X		X	Not Applicable			10	1
Schmidt, Tresch, and Meusburger 2019		X				X			X	2	1
Winchell et al. 2008		X			X		X	X		30	40
Fu et al. 2015			X*	X			X**			3-30 at 1m intervals	1
Nakil and Khire 2016		X				X			X	20	1
Warren et al. 2004	X			Not Applicable					X	1-12.5	1
Irfan Ashraf et al. 2012	Not Applicable			Not Applicable			X	X		1, 5, 10	1

*\*Chinese Soil Loss Equation (derived from USLE)*

*\*\*When not explicitly stated, and the study used ESRI programs, it was assumed the researchers used the standard ESRI slope command*

*\*\*\*Merged hydrologically corrected DEMs together for New South Wales, Australia*

This research provides a cohesive comparison of these methods and algorithms across multiple study sites and DEM resolutions. This aids in determining the differences these methods have on the L and S factors and if they are consistent and predictable across varying conditions. Recommendations of which methods to use for certain landscape conditions and DEM availability can then be derived from these observations.

## CHAPTER III

### STUDY AREA

There are four different sites used in this study (**Figure 1**), each located in Washington State in the northwestern United States, that encapsulate varying terrain conditions. The sites were selected based on the availability of high point density LiDAR (Light Detection And Ranging) data, catchment areas of at least 1 km<sup>2</sup>, no paved roads dividing the hillslopes, and avoiding sites that have water manually controlled to best conform to conditions under which the RUSLE model is most applicable.



**Figure 1.** Site locations in Washington State.

Site visits were done to verify that the landscape condition was appropriately represented by the downloaded LiDAR data and to identify areas that may alter flow that were not captured in the DEMs. The intensity and distribution of erosion was visually gauged, allowing for improved evaluations of GIS results.

The first two selected study sites, Sites A and B, are located near Ellensburg in Kittitas County, Washington. Ellensburg is located east of the Cascade Range within the Kittitas Valley. Known for growing timothy hay, much of this region is dedicated to irrigated agriculture (Bowen and Hultquist 2013). As a cool semi-arid climate, this area is characterized by warm dry summers and cold winters as depicted in **Figure 2** (Kottek et al. 2006, Western Regional Climate Center n.d). The majority of the precipitation occurs between October and March and is a mix of rain and snow (Western Regional Climate Center n.d.).

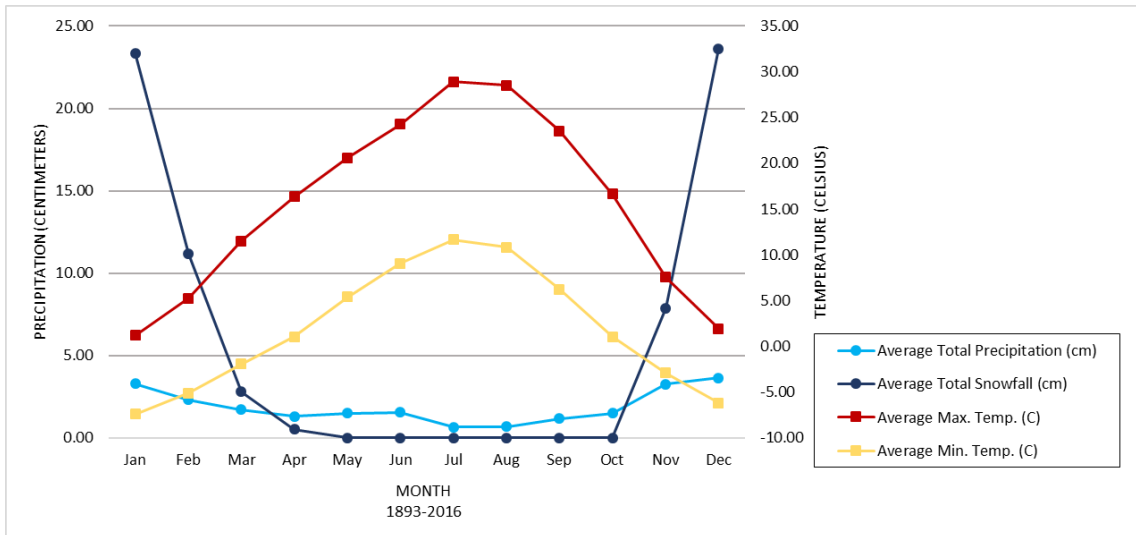


**Figure 2.** Climate data for Ellensburg, Washington (1893-2016) (Western Regional Climate Center n.d.).

Site A is ~ 7 km north of Ellensburg, east of Reecer Creek Road and north of Hungry Junction Road. It is 2.7 km<sup>2</sup> with elevations ranging from 509 m to 662 m and slope steepness from 0 degrees up to 71 degrees with a mean of 3 degrees (**Figure 3**). This site is characterized by only a few narrow drainage channels that capture flow and concentrate it, with most of the area gently sloping down to the southern border. The southern end of this catchment is terminated by a large irrigation channel that captures overland flow and directs it elsewhere for mainly agricultural purposes.

The landscape is gently sloping, arid, and predominately used for cattle grazing. Vegetation is predominately bunchgrasses, fescues, sagebrush, and bitterbrush (**Figure 4**). There are a few dirt roads that crisscross the site as well as power lines and cattle fencing. Visually, erosion appears as interrilling that follows along roads and in some highly exposed areas where no soil cover, such as shrubs and grasses, exist. Areas that are unable to grow protective cover are areas of high traffic use for cattle feeding. No identifiable larger rills were found for the site, and even the steepest slopes appeared to be relatively short in length and had established vegetative cover.

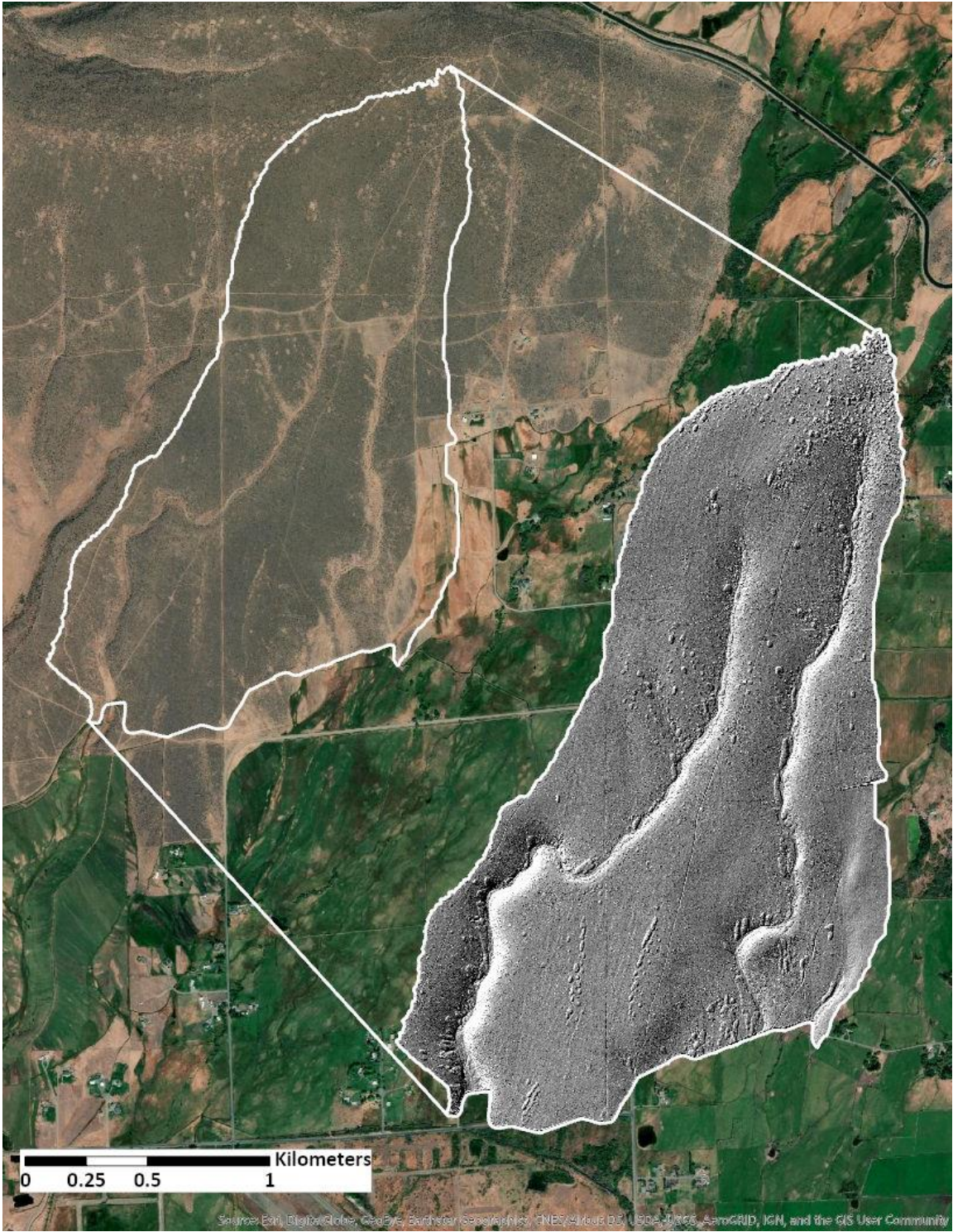


**Figure 3.** Site A boundary north of Ellensburg, WA.



**Figure 4.** Landscape view looking across the top of Site A.

Site B is 2.5 km<sup>2</sup> and located ~ 11 kilometers south of Ellensburg along the eastern side of Canyon Road that follows the Yakima River (**Figure 5**). It is a typical arid rangeland with complex topography of slope steepness from 0 degrees up to 78 degrees, with a mean of 23 degrees, and elevation from about 395 m to 930 m. The elevation increases in a SW to NE direction along three prominent drainage channels.

Vegetation is similar to site A with the inclusion of a few willows in the main drainage channels and areas of exposed basalt (**Figure 6**). The lower half along Canyon Road is managed by the Bureau of Land Management; the upper portion is privately owned and appears to be used for cattle grazing. Vegetation and climatic conditions are similar to Site A; the most significant difference is the terrain. While Site A is a large open gentle terrain, this site is more complex and steeper which is valuable in comparing output erosion differences due to terrain.



**Figure 5.** Site B boundary south of Ellensburg, WA.



**Figure 6.** Landscape view Site B from across the Yakima River.

Many of the slopes are covered in large basalt rocks and boulders which makes visually identifying soil erosion difficult. These features appear to make establishment of vegetation difficult but prevent water forming channels on these slopes. Rills, drainage channel outlets, and a water burst area are evidence of erosion at the bottom of this catchment along Canyon Road. The larger drainage channel walls are lacking surface vegetation and appear most vulnerable with loose material easily dislodging and rolling to the bottom of the channel.

Site C is located in Grays Harbor County, on the west side of Washington, ~ 37 km southwest of Olympia and ~ 34 km east of Aberdeen. Aberdeen is located on Washington's coast just south of the Olympic Peninsula and is dominated by a wet coastal climate. Most precipitation falls as rain from fall through spring since temperatures remain fairly constant throughout the year (**Figure 7**). Excess water that cannot infiltrate the soil contributes to overland flow, however the large amounts of

vegetation act as a barrier of protection to soil erosion that is not present in arid climates. Finding visual evidence of erosion is difficult as the soil surface is entirely covered by thick vegetation.

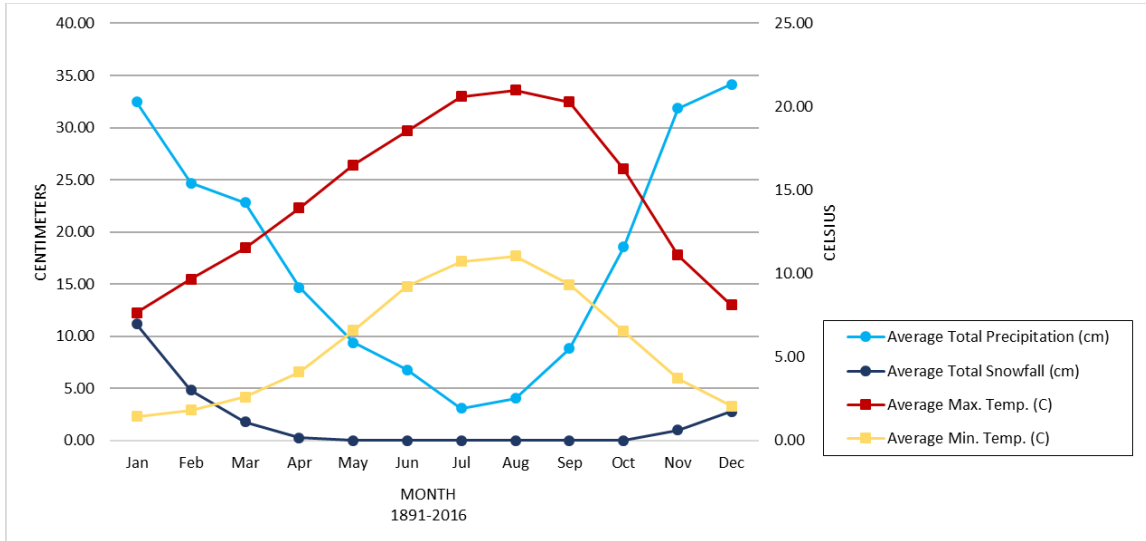


**Figure 7.** Climate data for Aberdeen, Washington (1891-2016) (Western Regional Climate Center n.d.).

Site C is 5.8 km<sup>2</sup> with elevations ranging from 41 m to 1191 m, and slopes vary from 0 degrees up to 89 degrees with a mean of 50 degrees (**Figure 8**). This site is the largest and most topographically complex site in this study. It is heavily forested with predominately Douglas-fir; about half the area appears to have been harvested within the last 10-15 years (**Figure 9**). The high level of precipitation promotes rapid regrowth of vegetation. Gaddis Creek runs east to west through the site alongside a dirt road. Various patches of big leaf maple follow the roads and creeks that run through the site. Most of this site is owned by the Washington State Department of Natural Resources, and the outlet opens up to privately owned pastures.

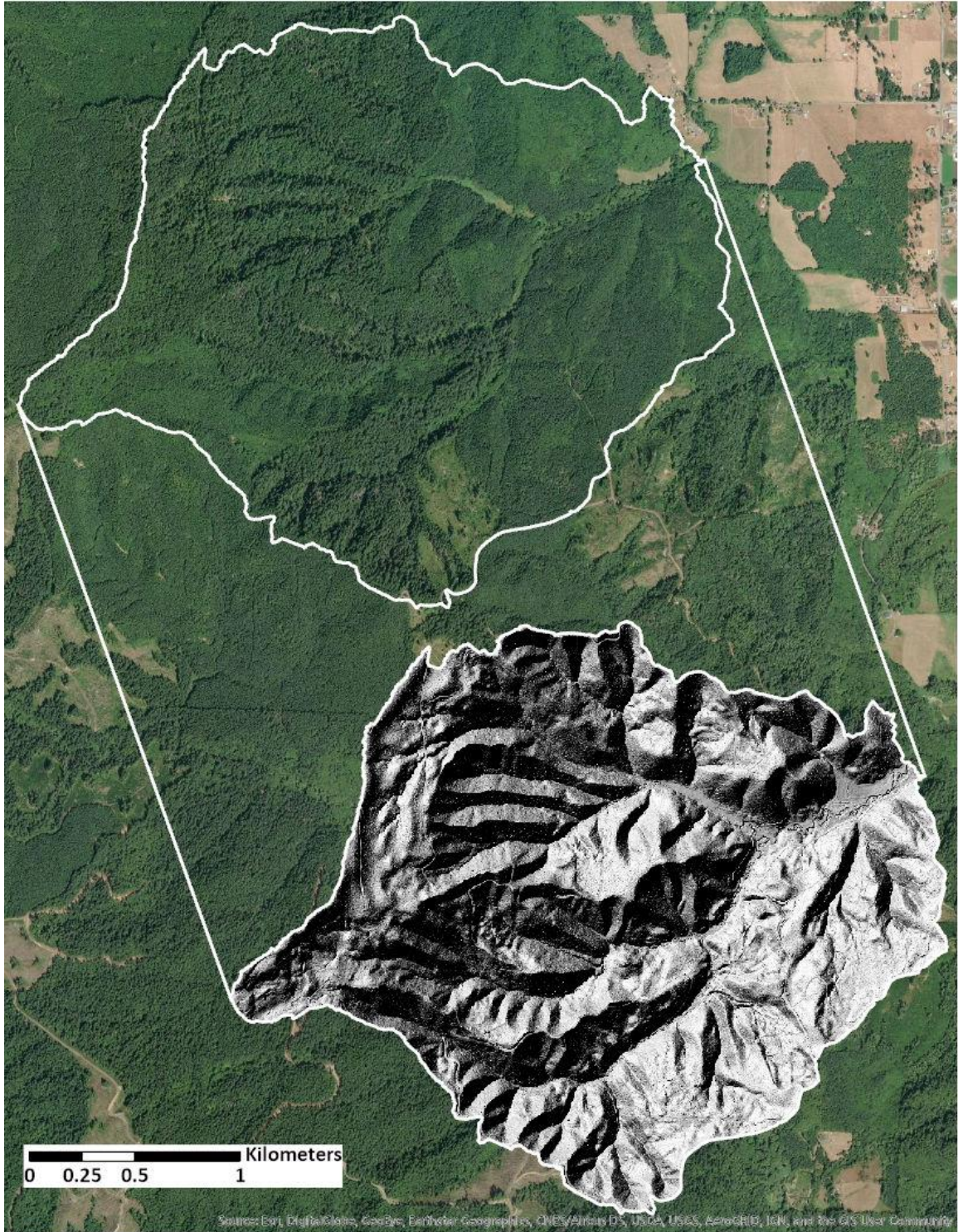


**Figure 8.** Site C boundary southwest of Olympia, WA.



**Figure 9.** Landscape view of Site C.

The final site is located in the southern portion of Okanogan County in central Washington near Methow. This area is largely open arid rangeland, similar to Ellensburg, with ponderosa pine dominated forests and woodlands. Precipitation occurs predominantly in winter and spring as rain and snowmelt (**Figure 10**). Large erosion events can occur with a fast snow melt and heavy spring rains, especially in recently burned areas without vegetation to slow water flow and protect bare ground.

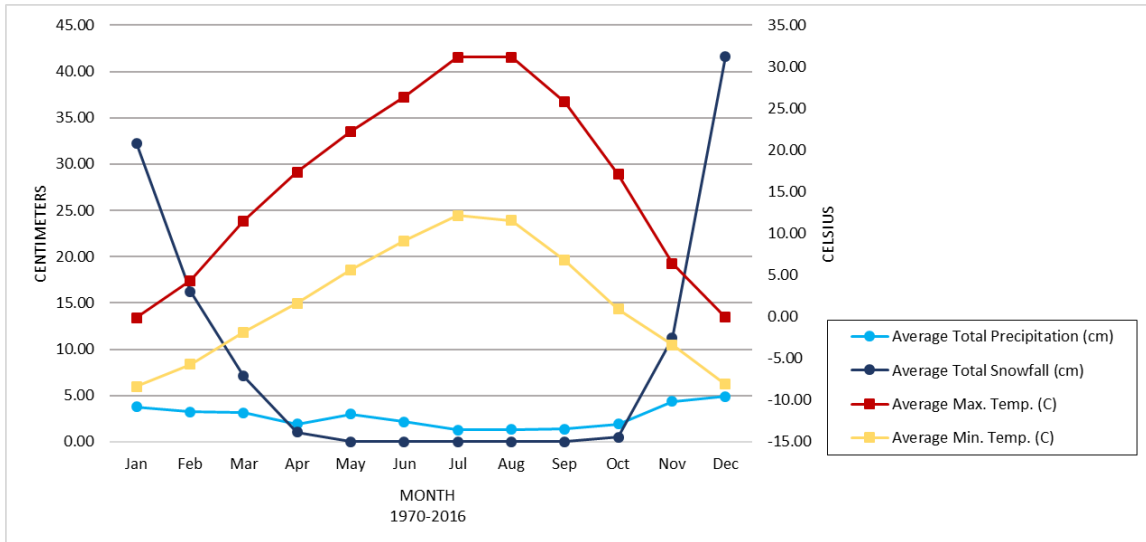


**Figure 10.** Climate data for Methow, Washington (1970-2016) (Western Regional Climate Center n.d.).

Site D is in the McCall Basin of Okanogan County, Washington ~ 8 km north west of Methow along the south side of State Route 153 and ~ 21 km south of Twisp. It is 2.6 km<sup>2</sup> with elevation ranging from 385 m to 920 m and slopes varying from 0 degrees to 84 degrees with a mean of 19 degrees. There are mostly east and west facing slopes with the main drainage channel moving south to north in the center of the catchment (**Figure 11**).

This area of the Methow, along State Route 153, burned in the summer of 2015. The severity of the burn was patchy, with the dense areas of Douglas-fir and ponderosa pine completely burned and areas of open ponderosa pine woodland recovering quickly (**Figure 12**). The DNR reseeded burned areas the following fall with native herbs and grasses which appear to have successfully established.

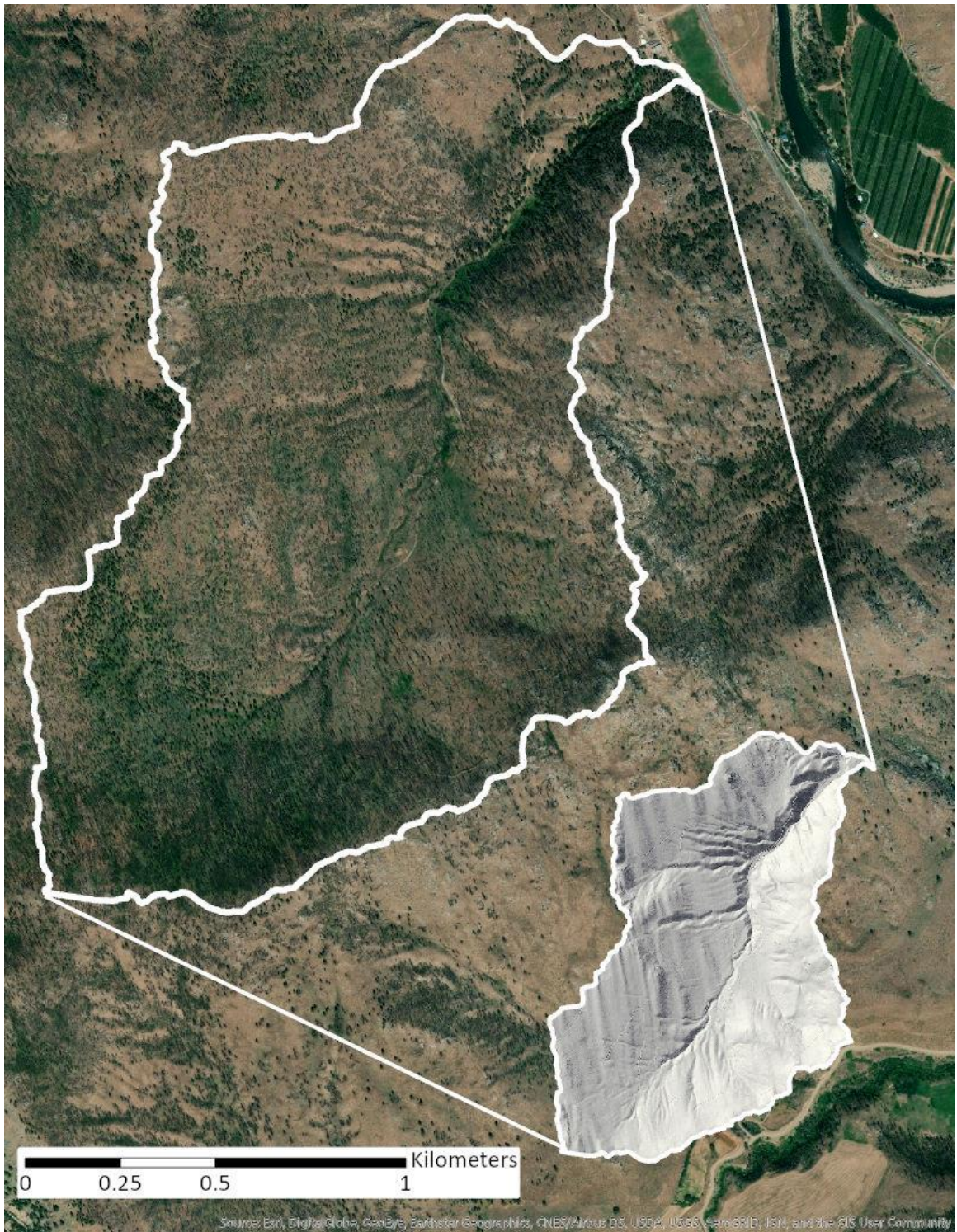


**Figure 11.** Site D boundary south of Twisp, WA.



**Figure 12.** View within Site D.

The DNR access road at the outlet of this catchment had been washed out in the immediate area surrounding the drainage channel, but this is an extreme event and not indicative to average annual erosion. As of spring 2020, this road still had not been repaired and vehicle use of the roads has been limited to one or two private landowners with smaller all-terrain vehicles. Otherwise, visual evidence of other erosion includes interrilling around rock outcroppings and the occasional small deposition site on old access roads that intercept the hill slopes and break slope length. These roads break the slope and have allowed for greater establishment of grasses and herbs around that area to protect the soil from erosion. No major rills or gullies were found stemming from road edges. This is different from Site A and Site B that, due to regular disturbances of

vehicle and cattle traffic, do not have this healthy establishment of surface vegetation as protection on these sorts of areas.

### Summary

In total, there are four sites of various landscape type, complexity, and catchment size. Landscape types consist of two arid rangelands, one ponderosa pine woodland, and one dense Douglas-fir forest. Site A is the simplest landscape with little slope variability and Site C is the most complex. Site C is also the largest catchment, being over twice as large as Site A which is the second largest site.

## CHAPTER IV

### METHODS AND TECHNIQUES

This chapter discusses the procedures used in this research to obtain the L and S factor outputs used in the research analysis. A program was written using Python to automate the following processes and produce rasters for the L and S factors, as well as a raster for slope angle using the maximum downhill slope method. The code calculates the L and S factors according to the methods discussed in Chapter II. A copy of the script can be found in Appendix A.

#### Data Gathering and Building DEMs

The four study sites selected had their corresponding LiDAR data downloaded from either The National Map hosted by the United States Geological Survey (n.d.), The Department of Natural Resources Washington LiDAR Portal (n.d.), or OpenTopography (2020). The downloaded LiDAR data was used to create 1, 5, 10, and 30 m DEMs using the ArcGIS Pro 2.4 LAS Dataset to Raster tool. The interpolation type was set to binning interpolation (output cell uses those points that fall within its extent) with the cell assignment method set to average and the void fill method set to linear (ESRI 2018d). These are the default settings for this tool. The default settings are used to reduce complexity of the method and replicate realistic use by land managers and others. The binning approach is also supported by the idea that DEM cells can be interpreted as an average elevation over the area that that cell represents, and so the average of that cell can be the average of LiDAR points that fall within the cell (Zhang et al. 1999). This is

why high density ground points from the downloaded LiDAR are required, so more points are available to represent the creation of a DEM cell over that area.

While LiDAR is becoming more readily available, the number of areas with LiDAR ground point spacing less than 1-2 per m<sup>2</sup> is difficult to find (LiDAR is available with overall point spacing < 1 per m<sup>2</sup> but filtering for ground points only means spacing is > 1 per m<sup>2</sup> for that classification). This problem is especially true when searching for study sites on the more heavily populated west side of the Cascades. While considerable data exists in this area, a high ground point density is difficult to find. This problem occurred for Site C with dense tree cover, where there are a few patchy parts in the LiDAR data with ground point density < 1 per m<sup>2</sup>.

If an irrigation channel or major road was found to intersect the catchment, I adjusted the site boundary so these features act as a border or termination of the catchment. An irrigation ditch ran through Site A, so the catchment boundary was reduced on the southern end to account for this feature artificially channeling flow. Site B's boundary was adjusted so that Canyon Road and the Yakima River terminated the catchment. Catchments were defined using the 1 m DEMs with the basin tool. A catchment was selected if it was entirely within the DEM (no border of the catchment being a border of the DEM edge) and the area met the above stated requirements.

## Calculating L Factors

The procedure for calculating the L factor using the GC method is displayed in **Figure 13**. The inputs to the tool include a DEM larger than site boundary, a cutoff slope angle, and an optional channel initiation threshold value. The tool was run twice for each DEM with slope cutoff values at 0.5 and then at 1.0; the channel initiation threshold value was always set to 1.0 (**Figure 14**).

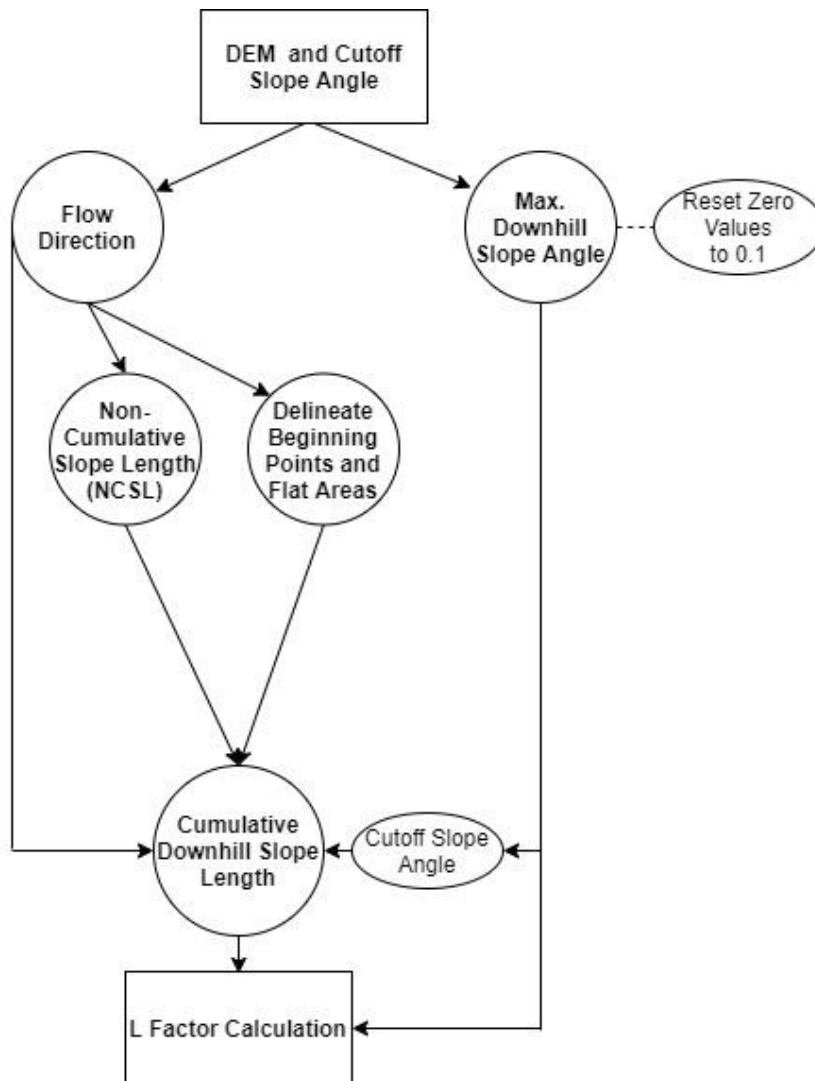


**Figure 13.** Process of calculating the RUSLE L factor using the GC method.

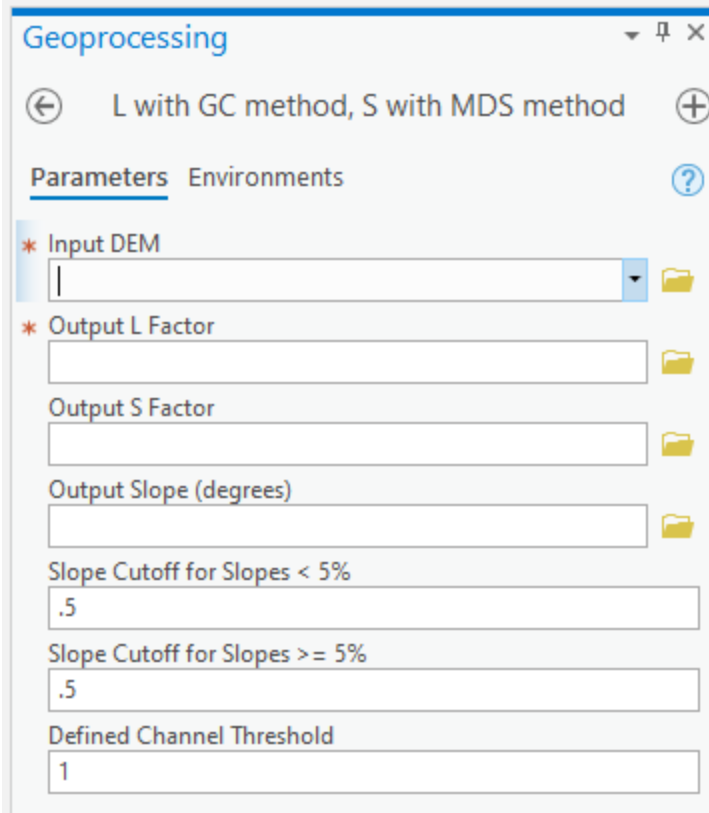


**Figure 14.** Script 1 tool in ArcGIS Pro with default parameters.

In order to maintain the single L algorithm as previously discussed for this study, it is assumed that slope lengths are longer than 15 ft, since the RUSLE includes alternate L algorithms for slopes less than 15 ft (Renard et al. 1997; Van Remortel, Hamilton, and Hickey 2001). It is possible to include these alternate algorithms for slopes less than 15 feet for the 1 m DEMs but not for the 5, 10, or 30 m DEM. To allow for proper comparison of L factor calculation methods across all DEM scales, these alternate algorithms have not been incorporated.

A separate script was created to simplify and automate the creation of the L Factor with the CA method (**Figure 15**).

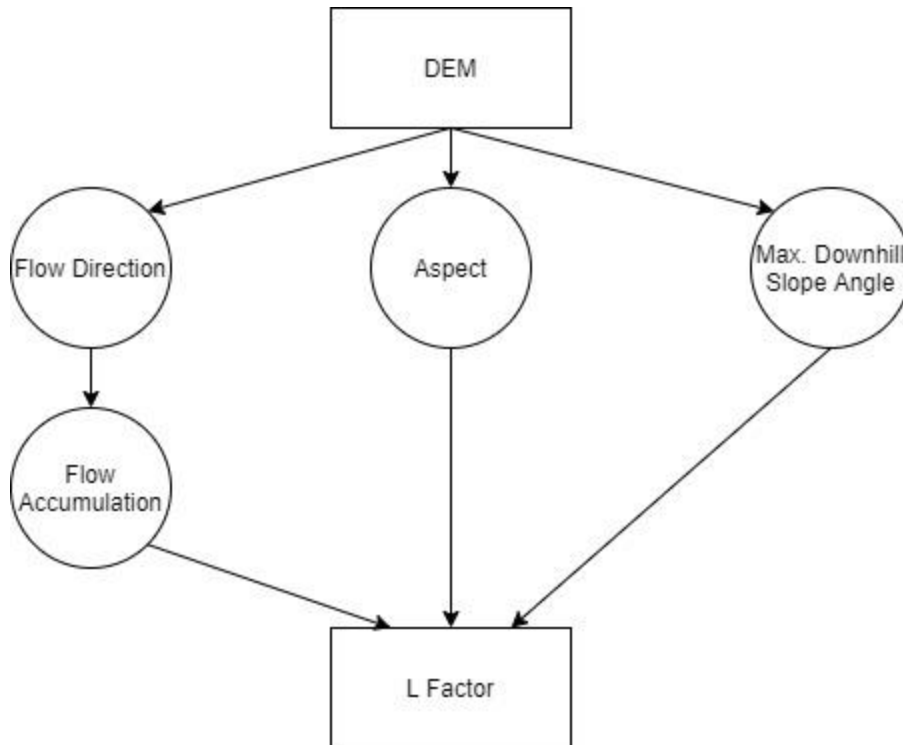


**Figure 15.** Process of calculating the RUSLE L factor using the CA method.

This script was run with two different flow-routing algorithms, D8 and D $\infty$ , to calculate the unit contributing area. The channel initiation threshold stayed at 1.0, just as it was with the GC method. This method also requires the incorporation of an aspect raster that is used to calculate  $x_{i,j}$  as discussed in Chapter II.

#### Calculating S Factors

S factor outputs are produced through the same code as the L factor outputs. The S factors using the MDS and NBR method are produced at the same time as the L factor outputs and follows all the same input variables. Slope calculated using the MDS and then the NBR method are input into the S factor equations discussed in Chapter II.

## Summary

Following the steps just described for L and S factor calculations, the following raster outputs were produced:

1. L Factor: 4 outputs per site per DEM resolution
  - a. GC method: 2 outputs per site per DEM resolution
    - i. Slope cutoff set to 0.5
    - ii. Slope cutoff set to one
  - b. CA method: 2 outputs per site per DEM resolution
    - i. SFD algorithm
    - ii. MFD algorithm
2. S Factor: 2 outputs per site per DEM
  - a. MDS method: 1 output per site per DEM
  - b. NBR method: 1 output per site per DEM

## CHAPTER V

### ANALYSIS AND RESULTS

The below additional outputs were generated to spatially compare differences between the various L and S factor calculation methods. The difference rasters mentioned below take one output and subtract it from another to show where values differ in the site.

#### 1. L Factor

- a. Difference rasters: 3 outputs per site per DEM resolution
  - i. GC method with slope cutoff vs. without slope cutoff
  - ii. CA with a SFD algorithm vs a MFD algorithm
  - iii. GC method without slope cutoff vs CA method with a SFD algorithm

#### 2. S Factor

- a. Difference rasters: 1 output per site per DEM
  - i. MDS method vs the NBR method

These difference rasters highlight areas within each site where the two methods being compared are similar and dissimilar and what method produces higher or lower values where. From this, landscape changes or features can be identified that regularly produce higher/lower values in comparison to another method.

In addition, the L and S factor outputs mean, median, and maximum values were compared for each individual site across DEM resolutions and between each site. The S factor also includes minimum values for each site at each DEM resolution.

Maps of the L and S factor outputs for all sites, except for Site D, at each DEM resolution can be found in Appendix B. Otherwise, Site D's outputs and difference rasters are shown throughout Chapter V. This site was selected as the most representative site of the four. Site D's landscape type and complexity is a medium between the simple and open landscape of Site A and the steep complex and dense forest of Site C.

#### L Factor

The L factor is reviewed across DEM resolutions for each site and each method as well as comparing two methods at a time for each site at each DEM resolution using difference rasters.

This allows for understanding where change occurs within each individual method across DEM scales as well as change between methods for each DEM at each site. The difference rasters are made from subtracting one L factor method output from another. Shown below are the L factor outputs for each method for Site D. L factor outputs using the GC method with a slope cutoff of 0.5 (**Figures 16 - 19**), GC method with a slope cutoff of one (**Figures 20 - 23**), CA method with a SFD algorithm (**Figures 24 - 27**), and the CA method with a MFD algorithm (**Figures 28 - 31**).

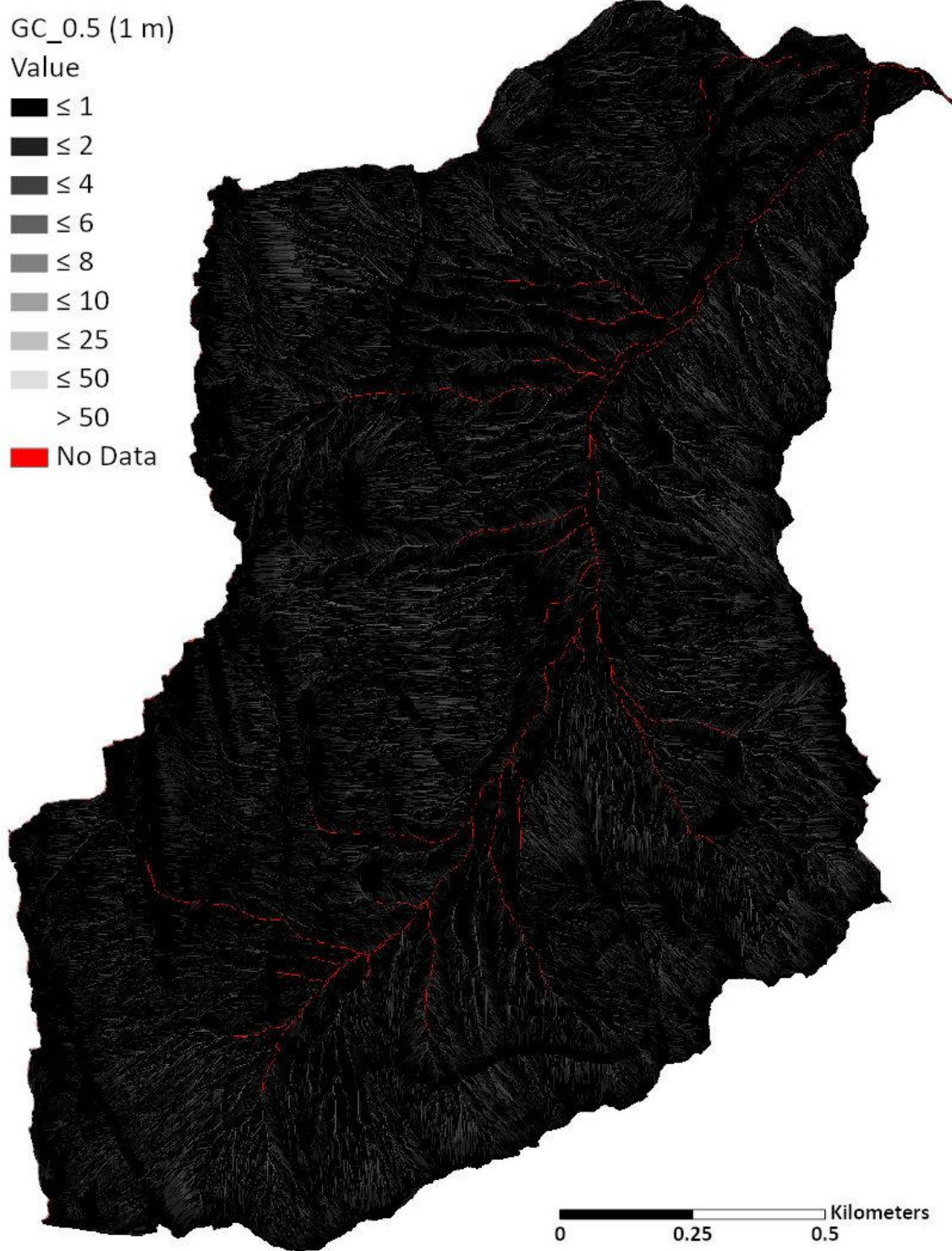


**Figure 16.** L factor with the GC Method with slope cutoff at 0.5 for Site D at 1 m.

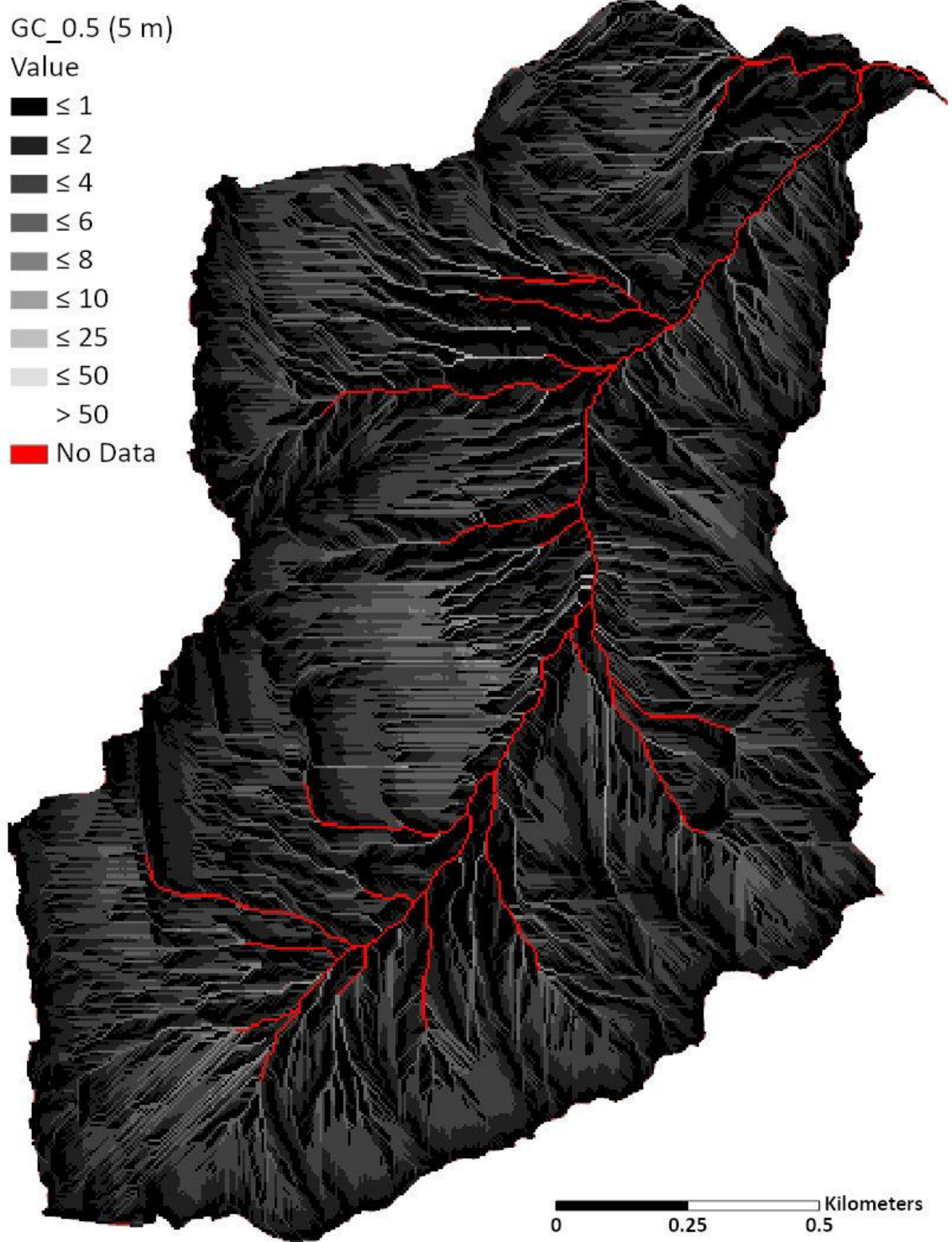


**Figure 17.** L factor with the GC Method with slope cutoff at 0.5 for Site D at 5 m.

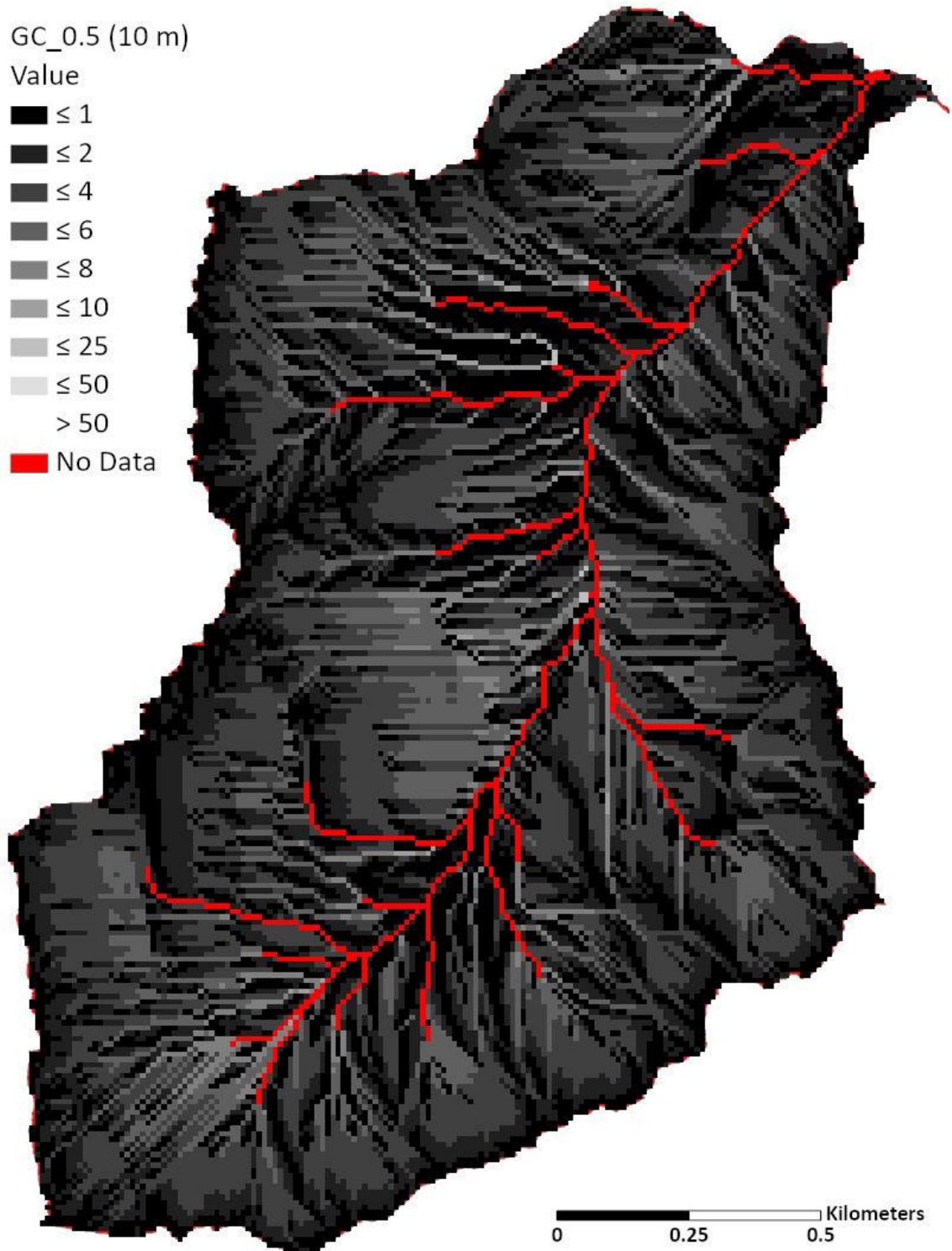


**Figure 18.** L factor with the GC Method with slope cutoff at 0.5 for Site D at 10 m.

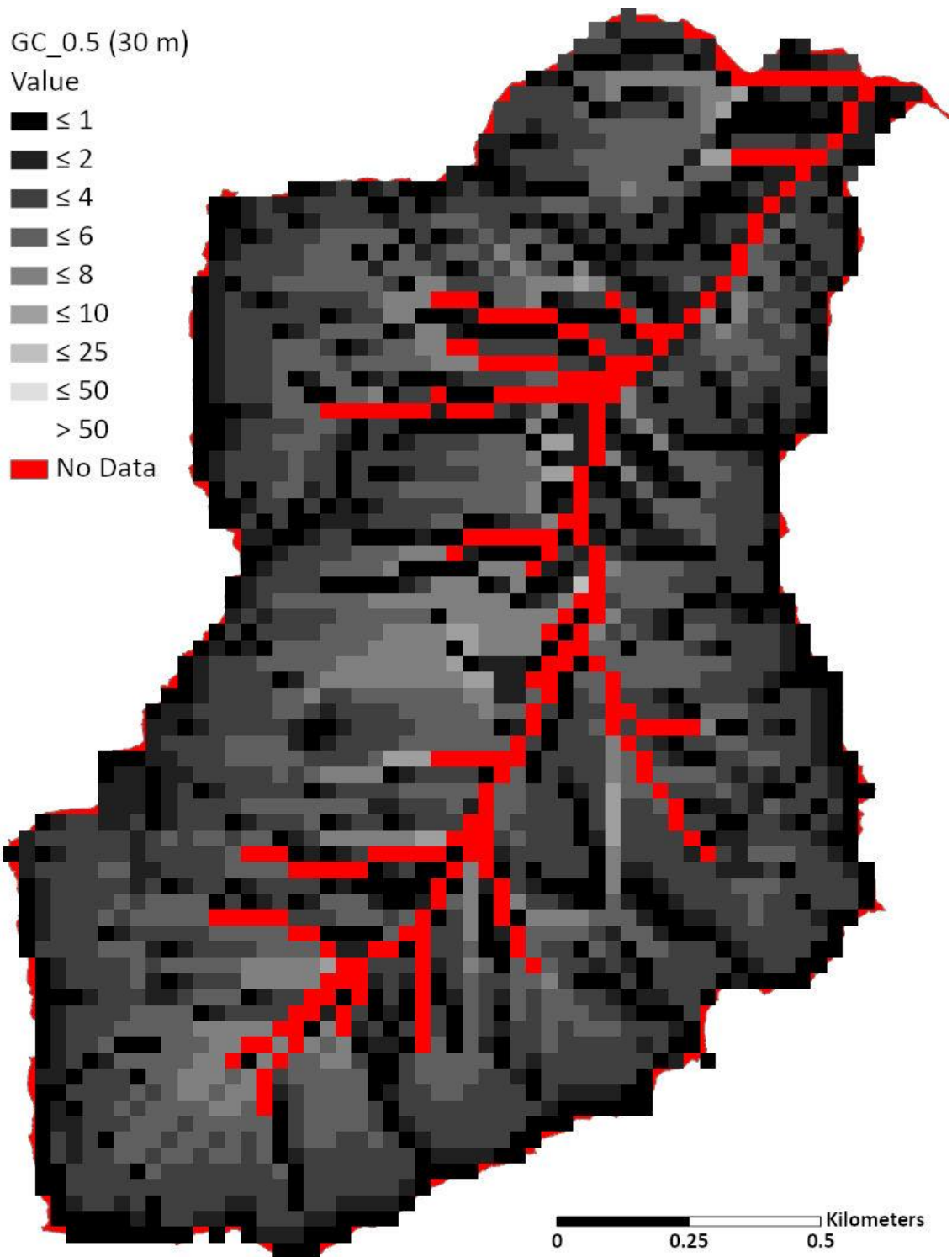


**Figure 19.** L factor with the GC Method with slope cutoff at 0.5 for Site D at 30 m.

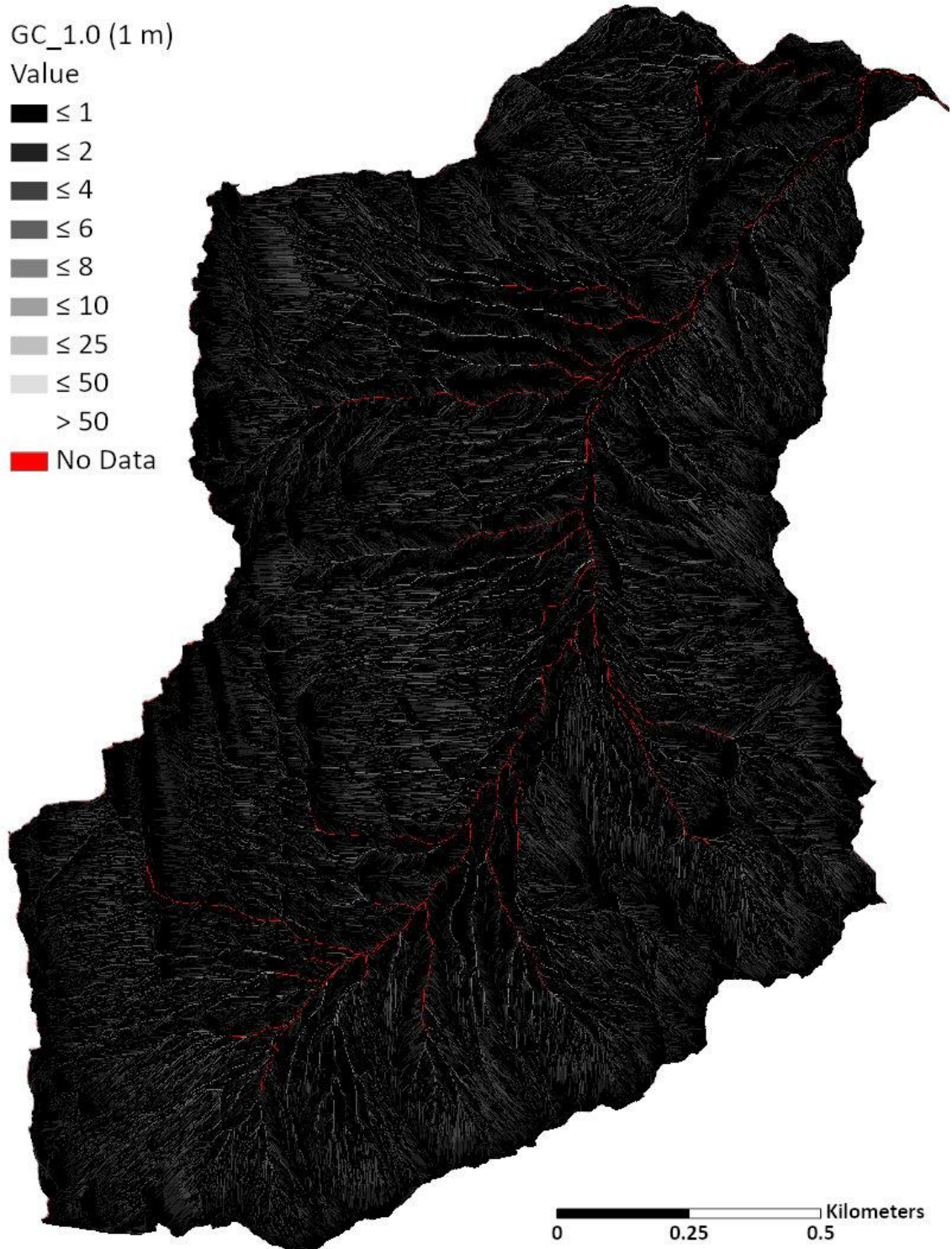


**Figure 20.** L factor with the GC Method without slope cutoff for Site D at 1 m.

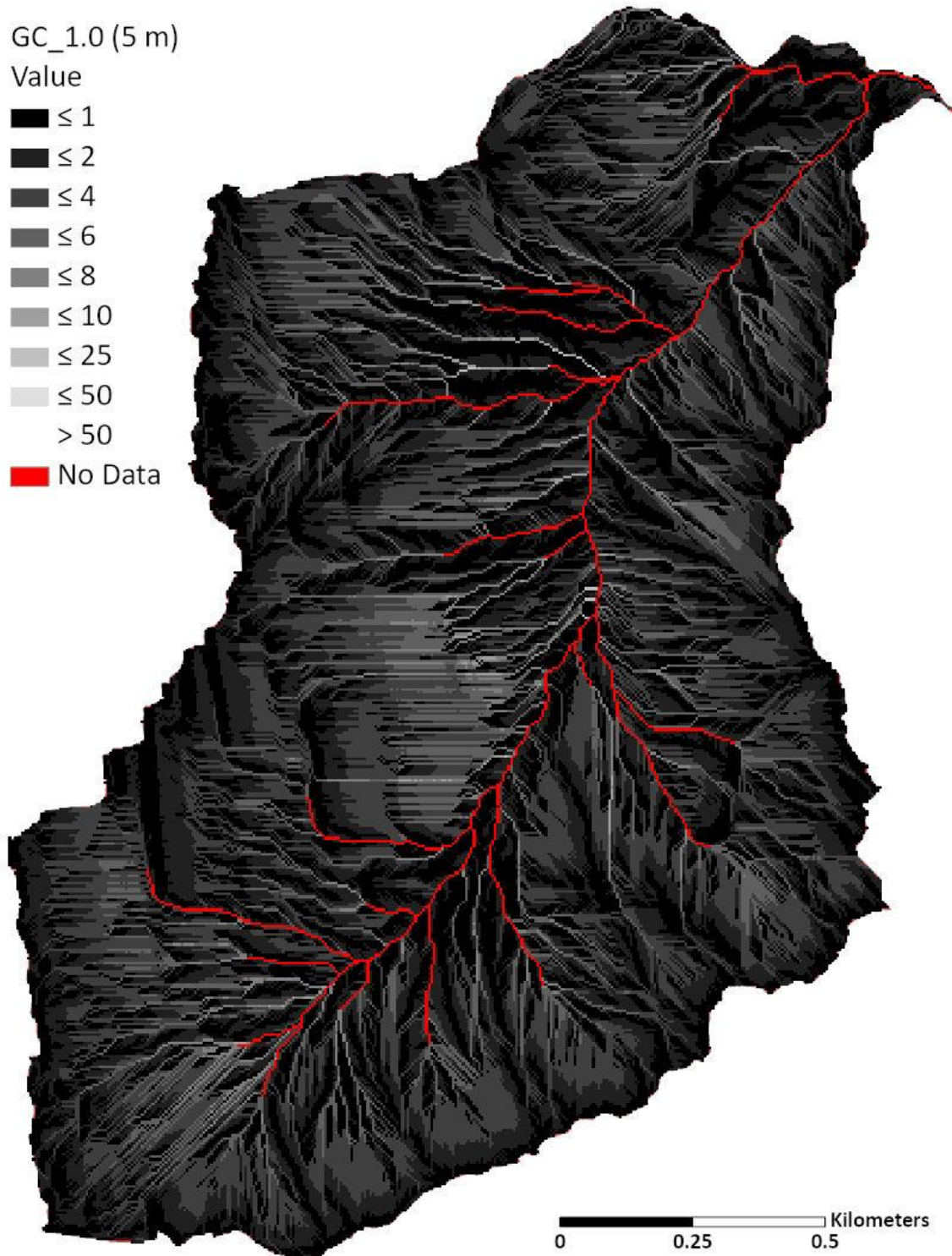


**Figure 21.** L factor with the GC Method without slope cutoff for Site D at 5 m.

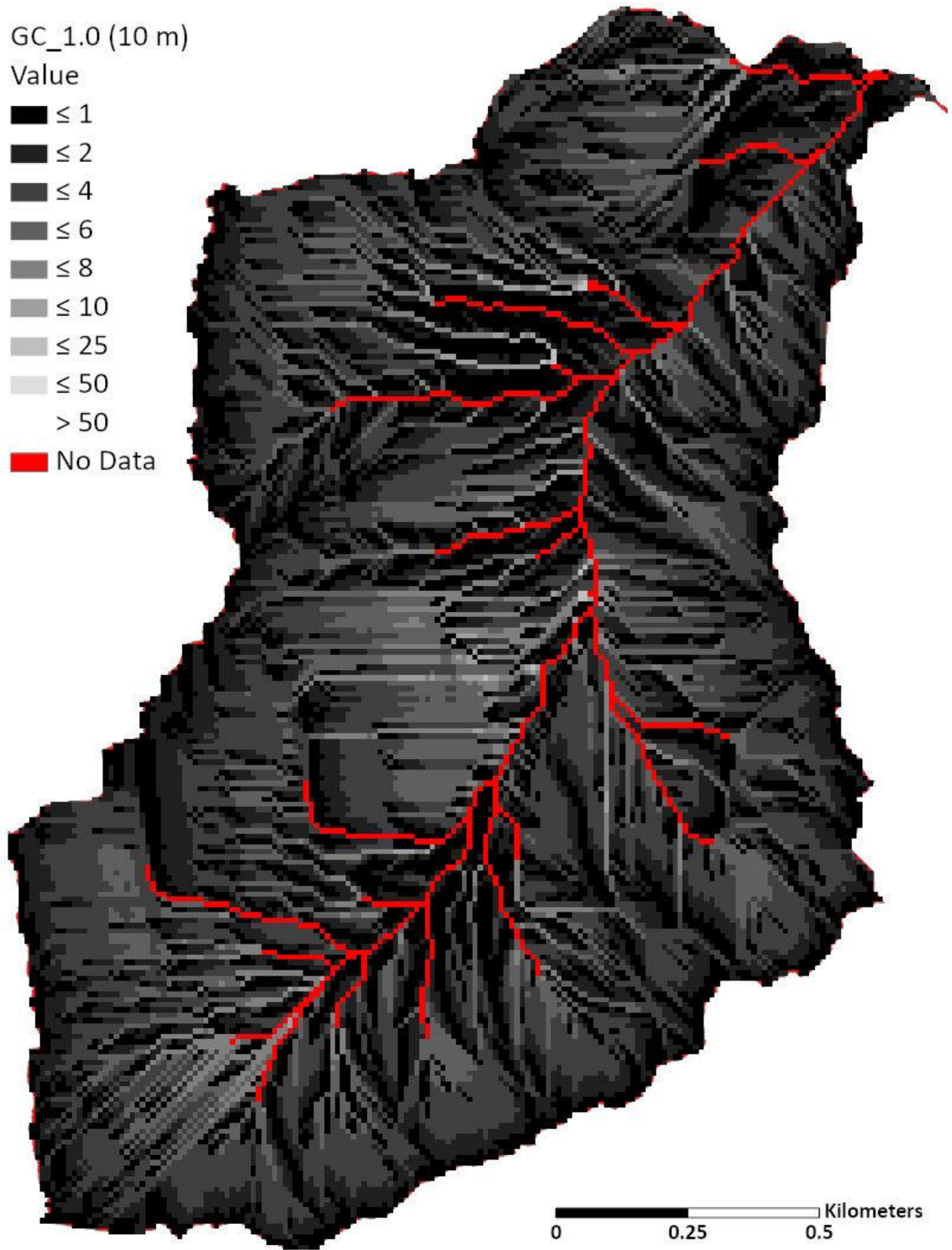


**Figure 22.** L factor with the GC Method without slope cutoff for Site D at 10 m.

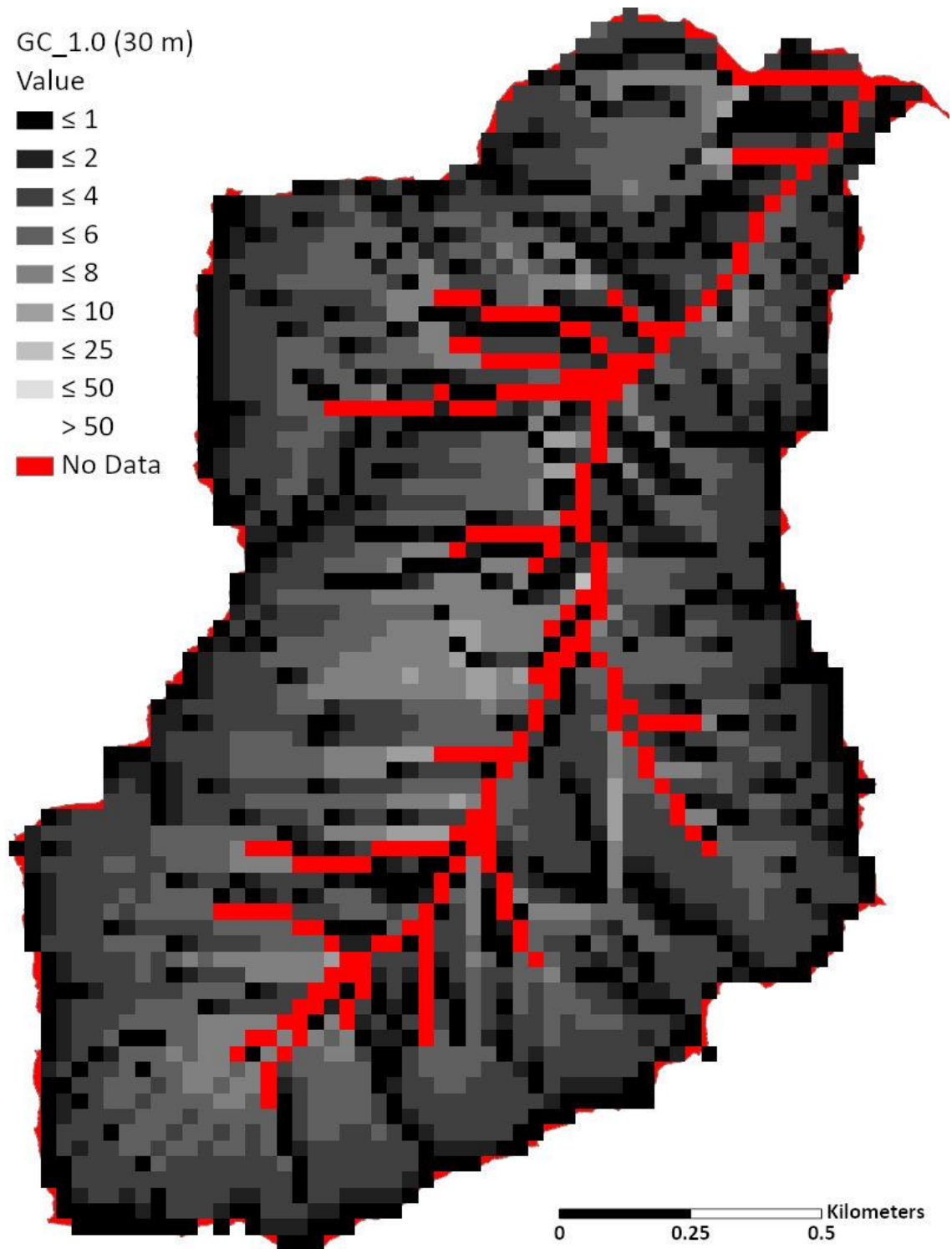


**Figure 23.** L factor with the GC Method without slope cutoff for Site D at 30 m.

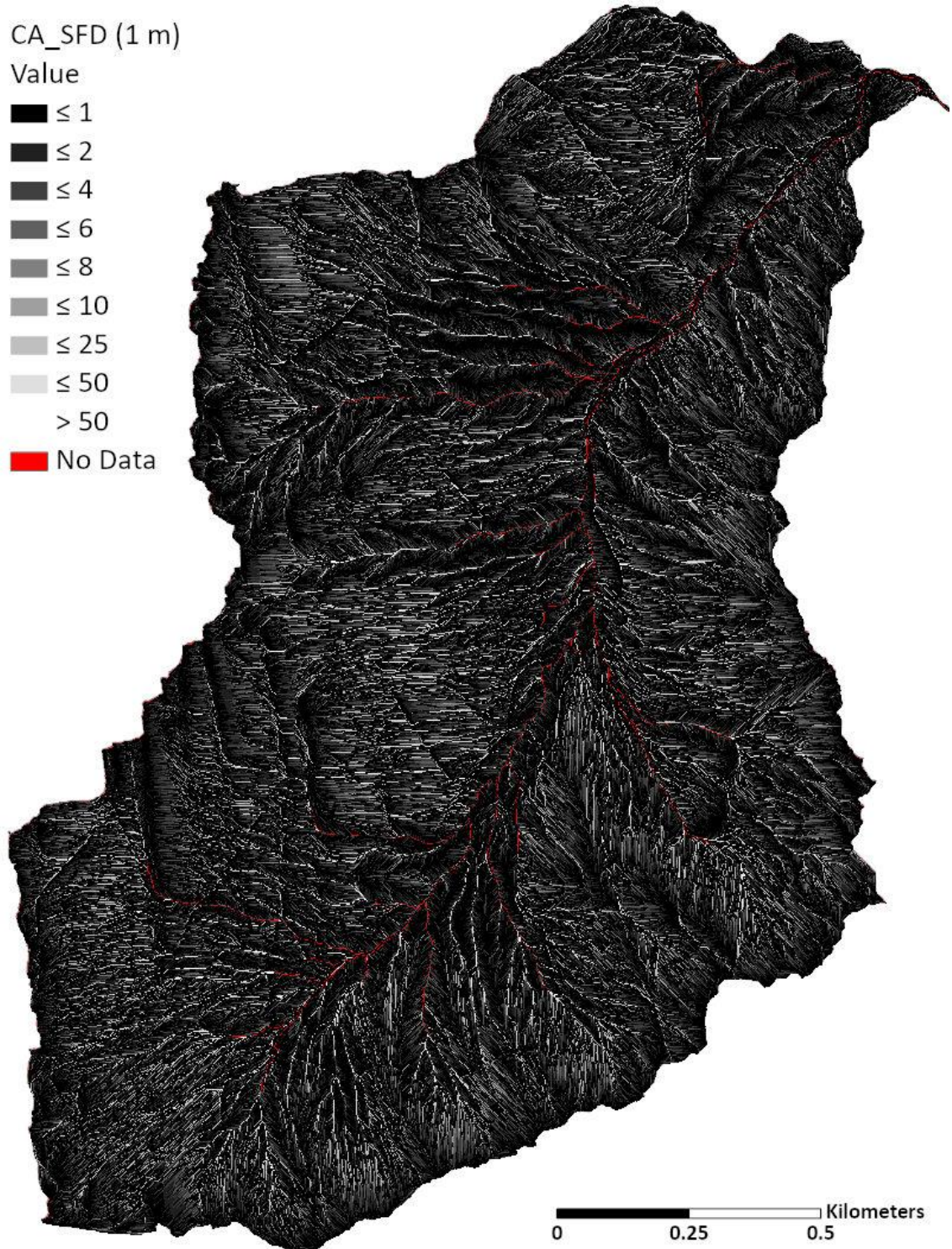


**Figure 24.** L factor with the CA method with a SFD algorithm for Site D at 1 m.

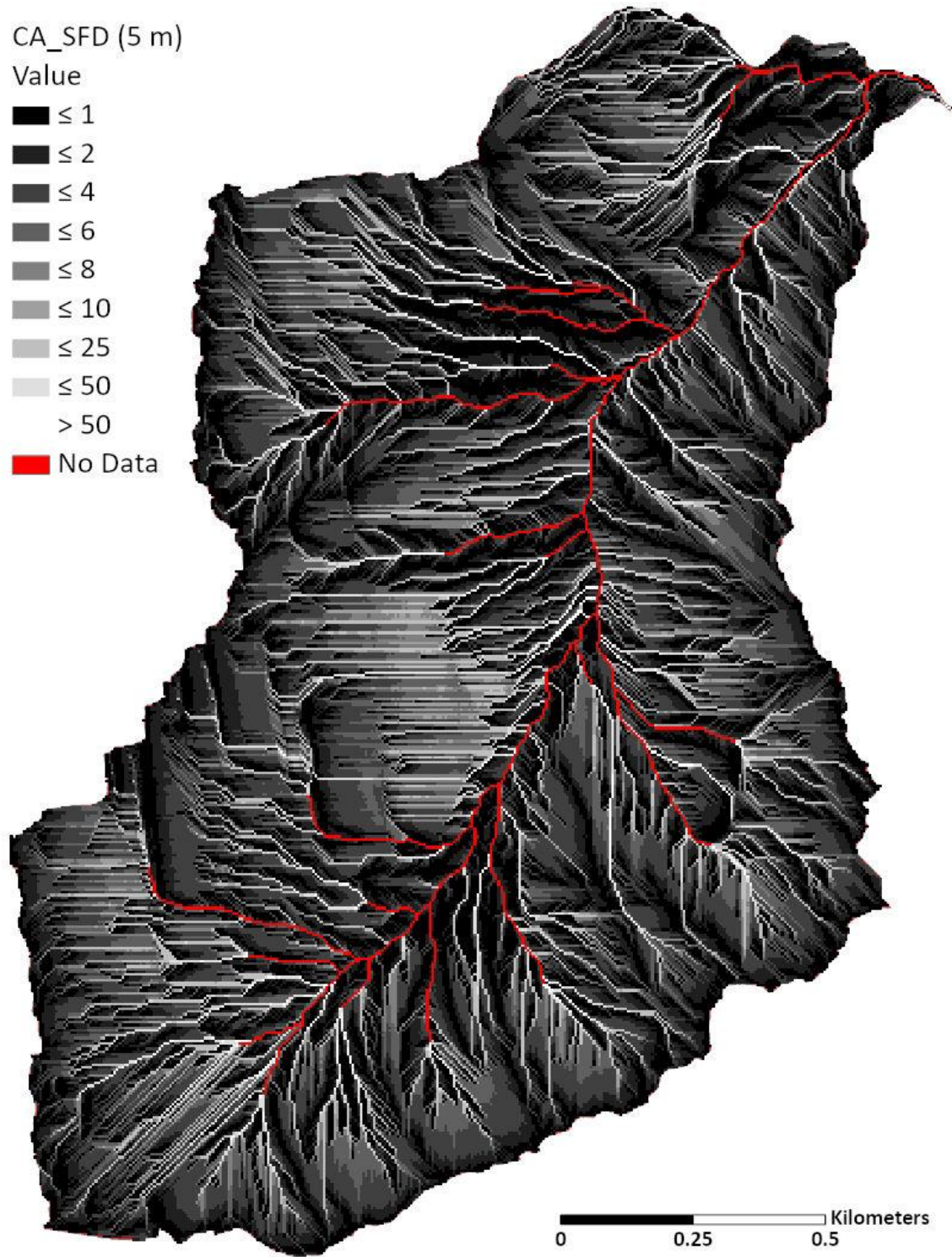


**Figure 25.** L factor with the CA method with a SFD algorithm for Site D at 5 m.

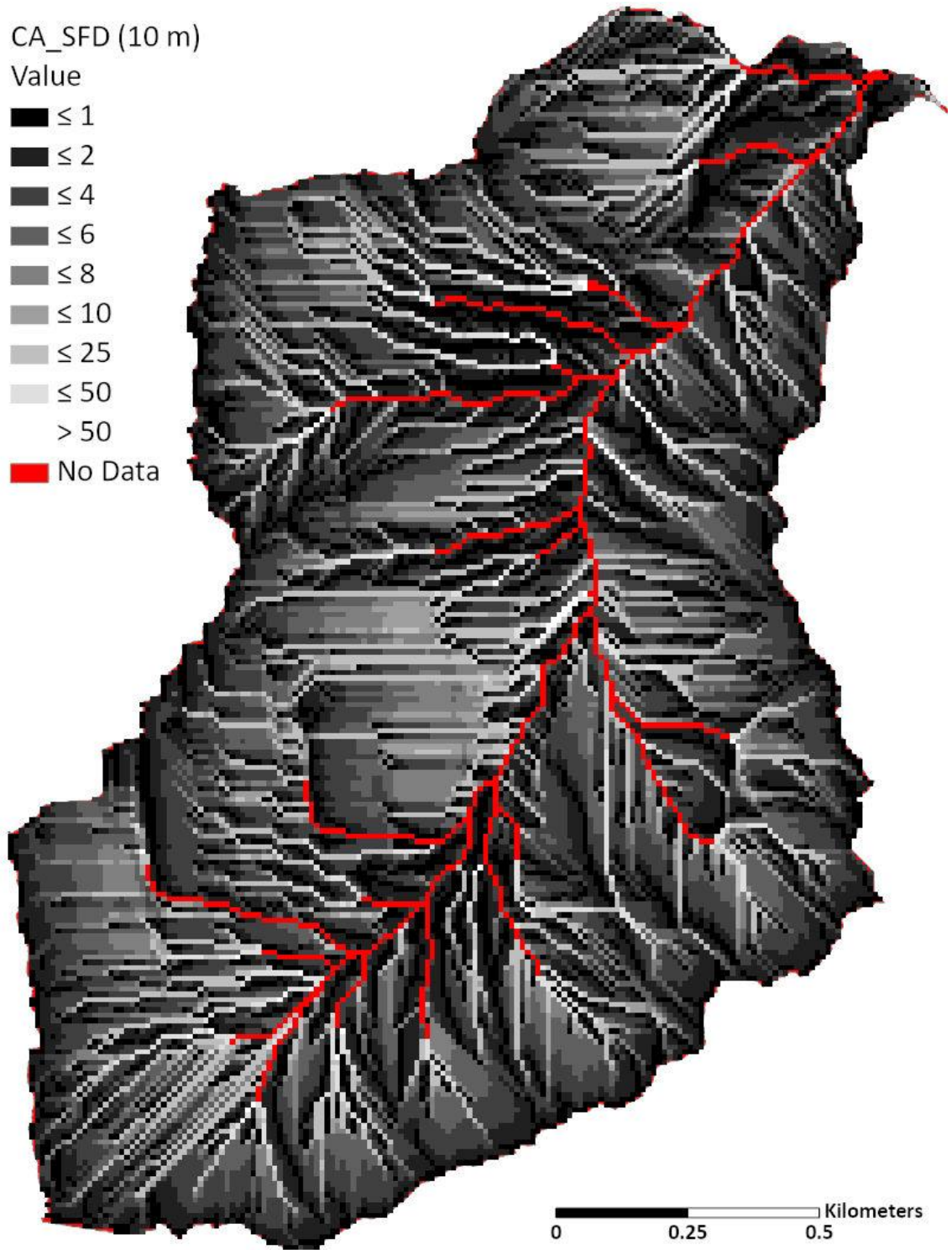


**Figure 26.** L factor with the CA method with a SFD algorithm for Site D at 10 m.

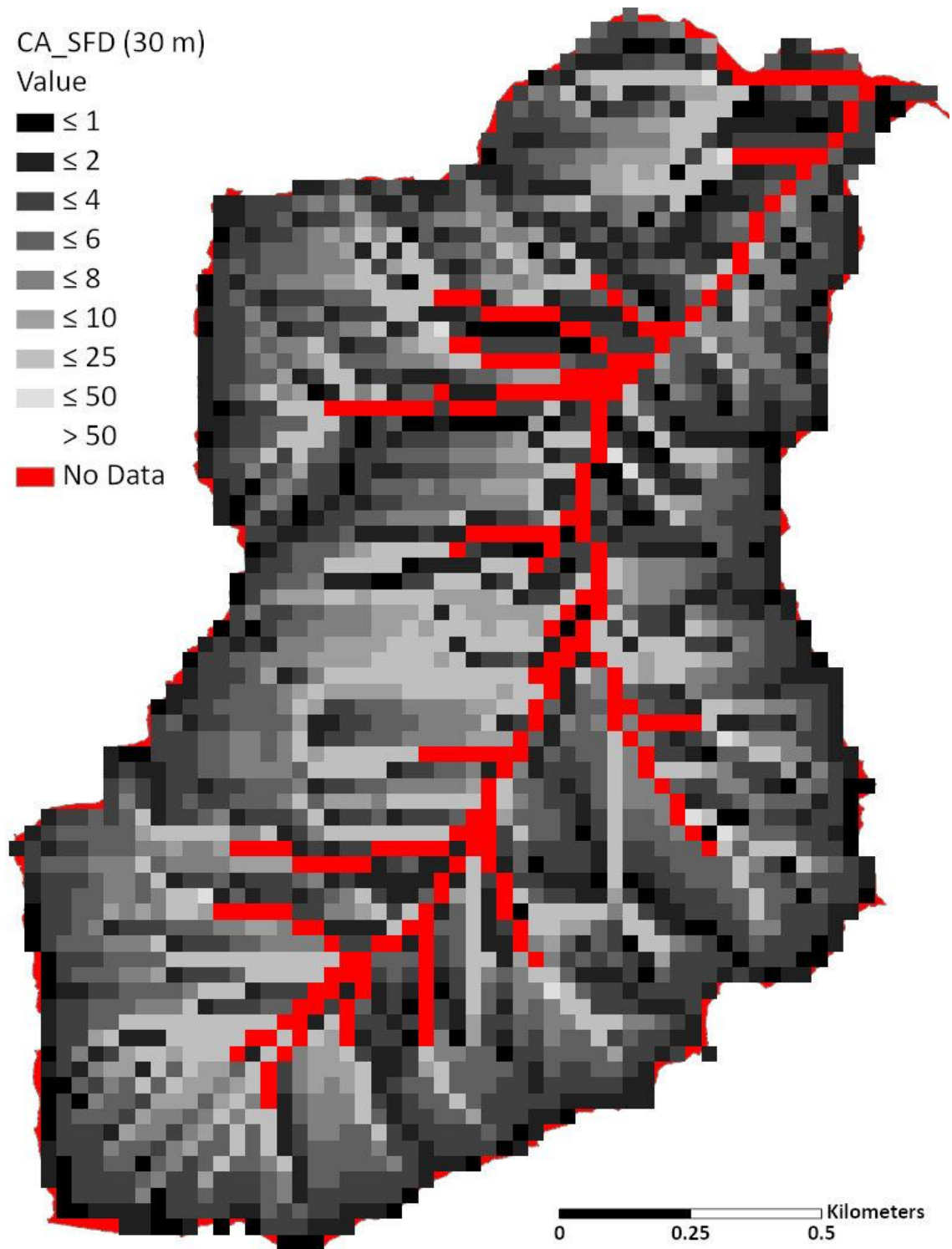


**Figure 27.** L factor with the CA method with a SFD algorithm for Site D at 30 m.

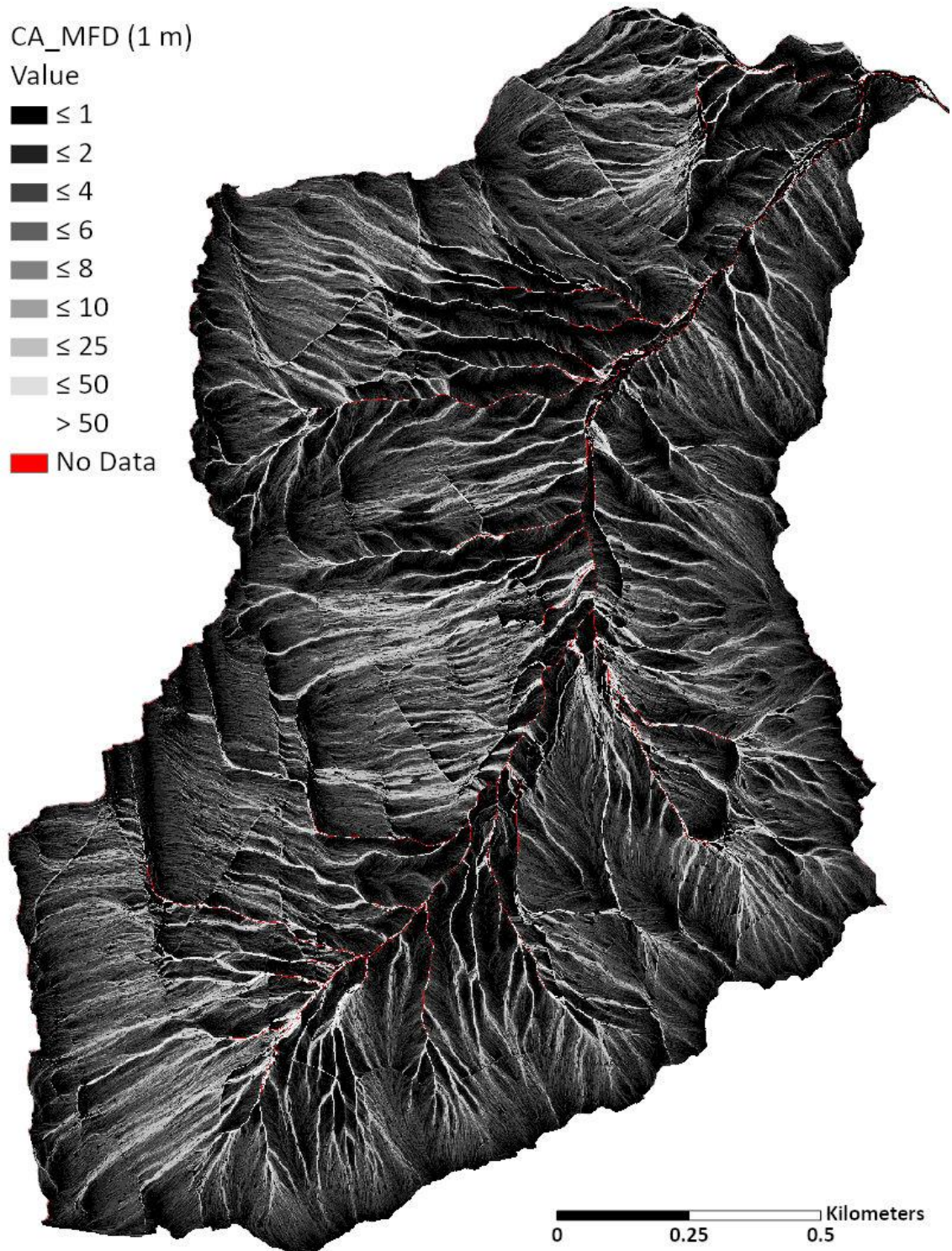


**Figure 28.** L factor with the CA method with a MFD algorithm for Site D at 1 m.

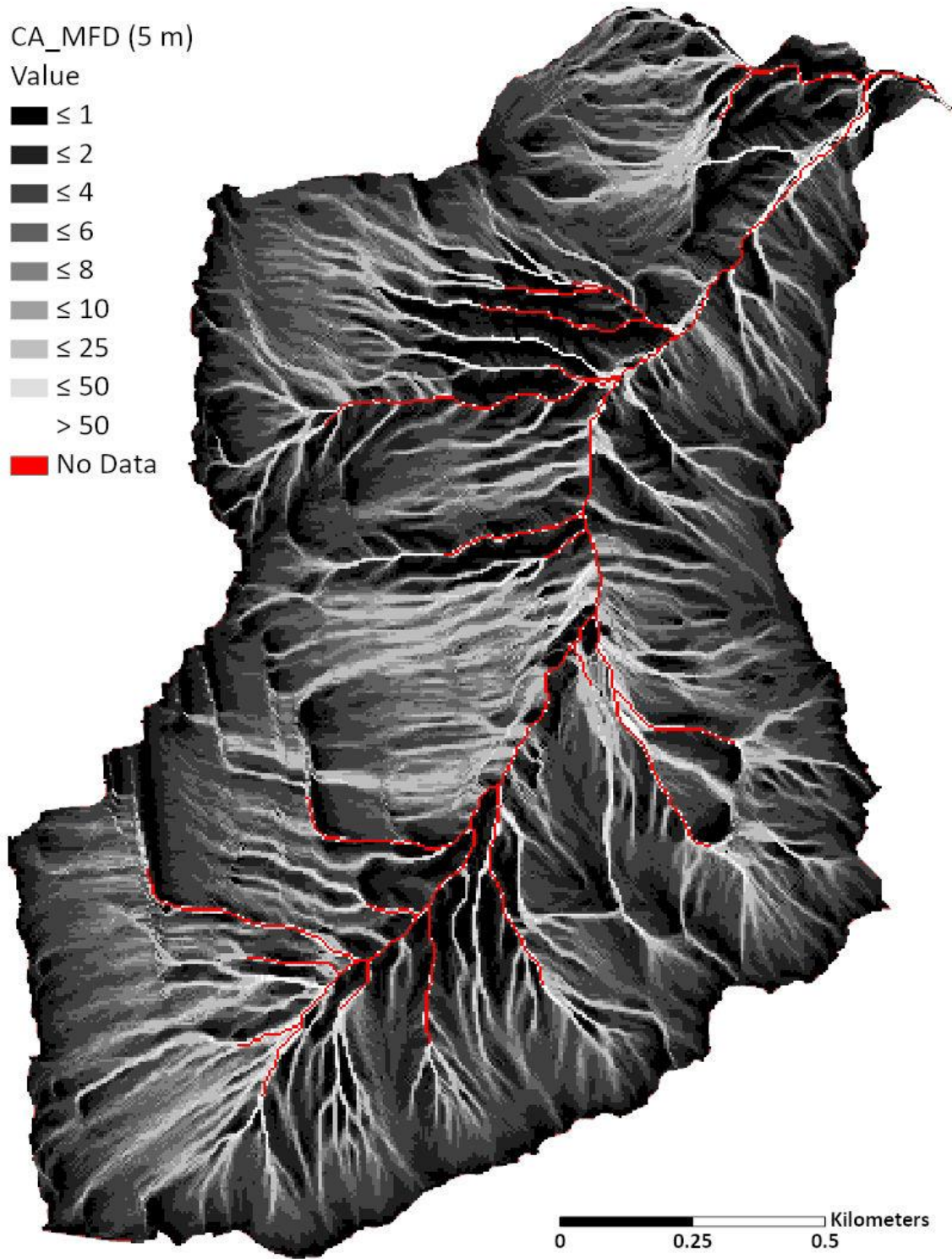


**Figure 29.** L factor with the CA method with a MFD algorithm for Site D at 5 m.

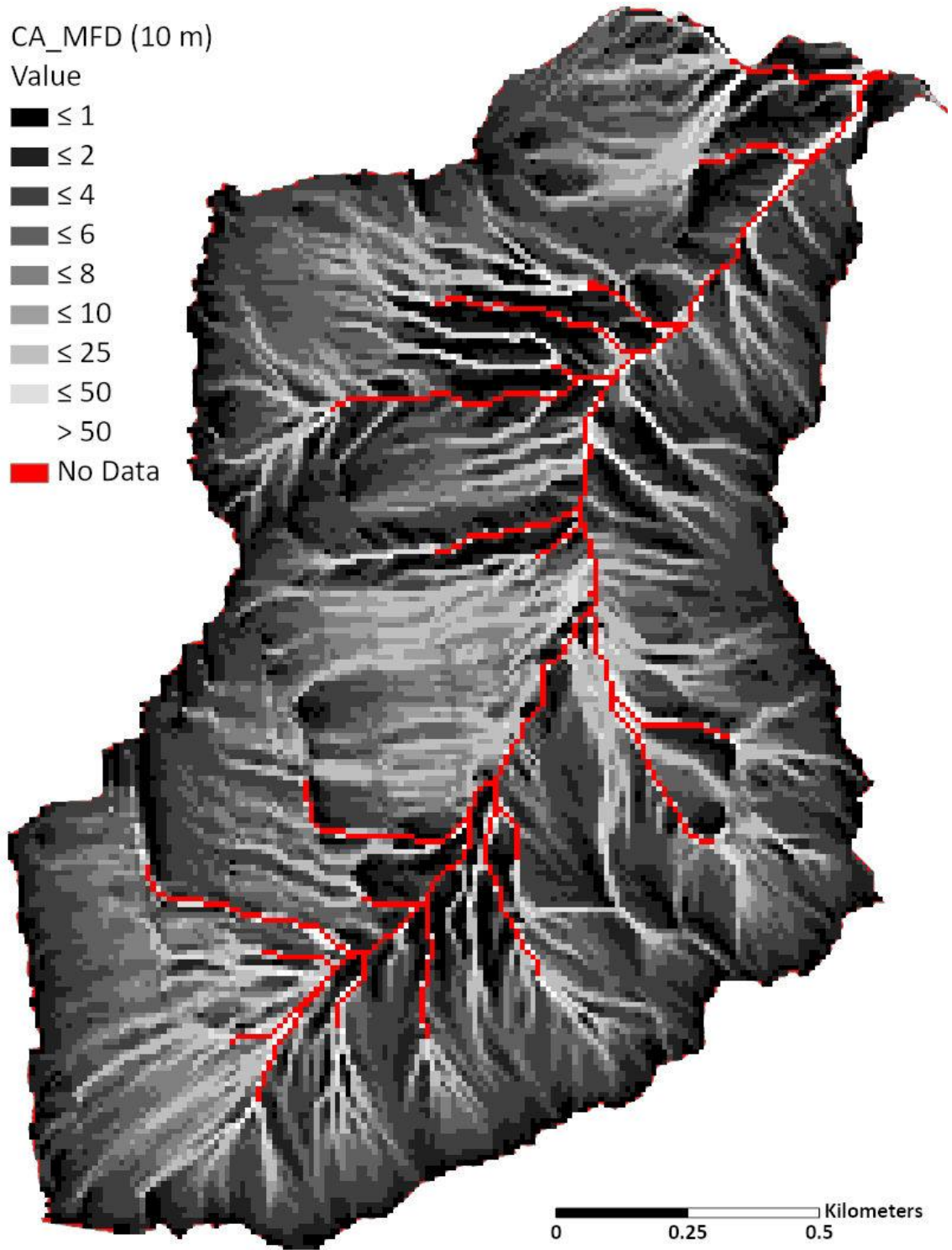


**Figure 30.** L factor with the CA method with a MFD algorithm for Site D at 10 m.

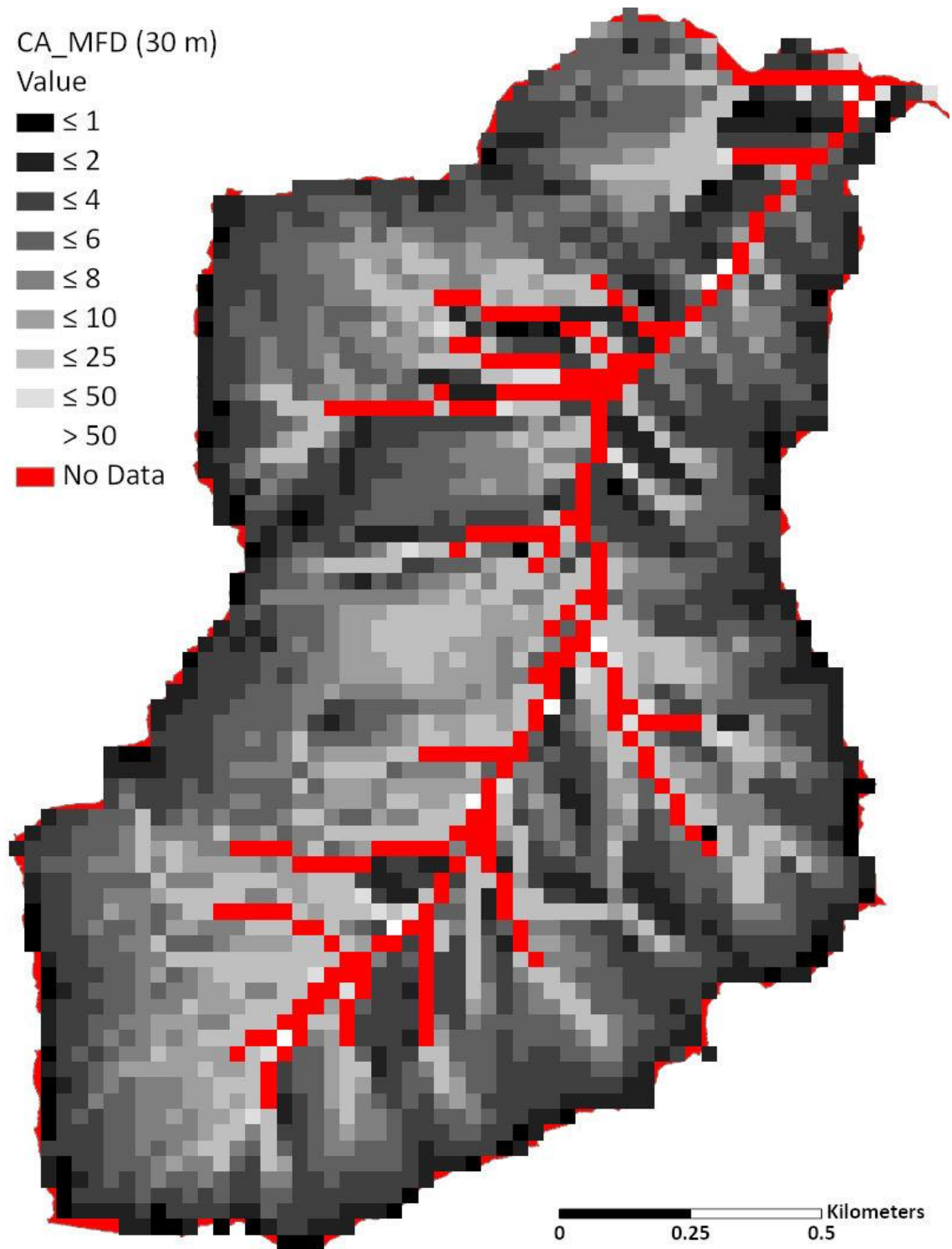


**Figure 31.** L factor with the CA method with a MFD algorithm for Site D at 30 m.

The biggest differences in all outputs occur between the choice of SFD and MFD algorithms for the CA method as well as between the GC and the CA methods. Differences between the outputs of these methods decrease as resolution of the DEM becomes coarser. For the CA method, the choice of flow routing algorithm has the least impact on L values in comparison to the effects of degrading DEM resolution and in comparison to the GC method, which was also found in Liu et al. (2011). However, within the choice of flow-routing algorithms for only the CA method, SFD algorithms produce lower mean contributing area and L factor values than MFD algorithms which has also been shown in Desmet and Govers (1996b), Wilson, Lam, and Deng (2007), and Liu et al. (2011).

The CA method produces higher mean, median, and maximum values of L than the GC method, in all landscapes, since accumulating cell area yields higher values than accumulating cell length and values are combined when flow paths converge (**Figures 32 - 34**). It is also sensitive to areas along prominent drainage channels where the greatest area accumulates and produces extremely high L values.

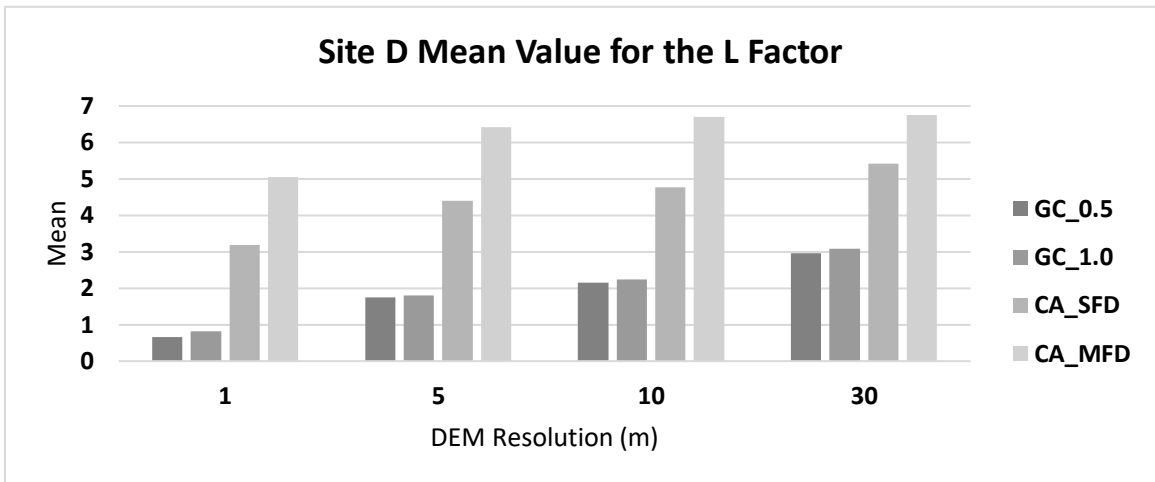


**Figure 32.** Mean value of L factor for Site D where GC\_0.5 is the GC method with slope cutoff set to 0.5, GC\_1.0 is the GC method without slope cutoff, CA\_SFD is the CA method using a SFD algorithm, and CA\_MFD is the CA method using a MFD algorithm.

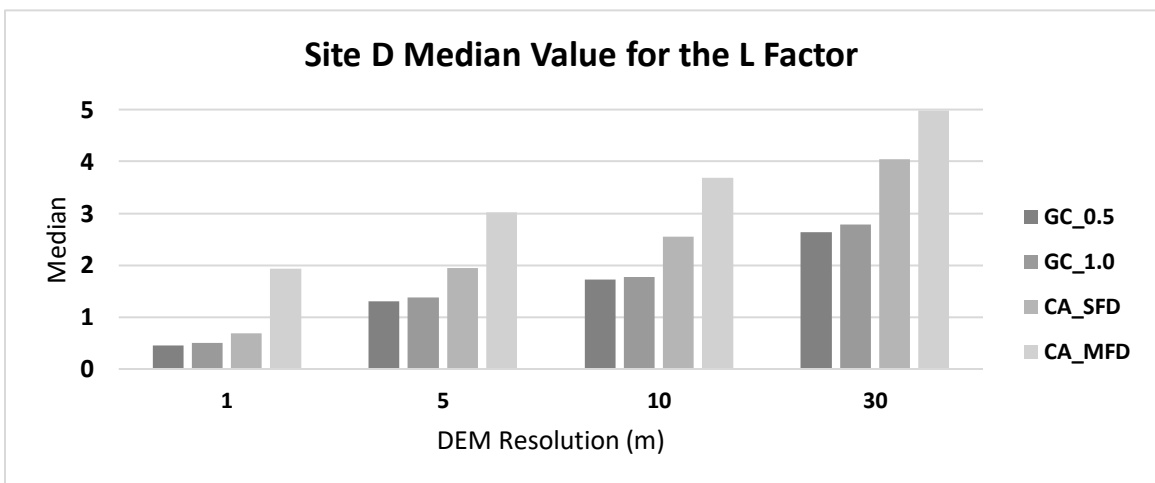


**Figure 33.** Median value of L factor for Site D where GC\_0.5 is the GC method with slope cutoff set to 0.5, GC\_1.0 is the GC method without slope cutoff, CA\_SFD is the CA method using a SFD algorithm, and CA\_MFD is the CA method using a MFD algorithm.

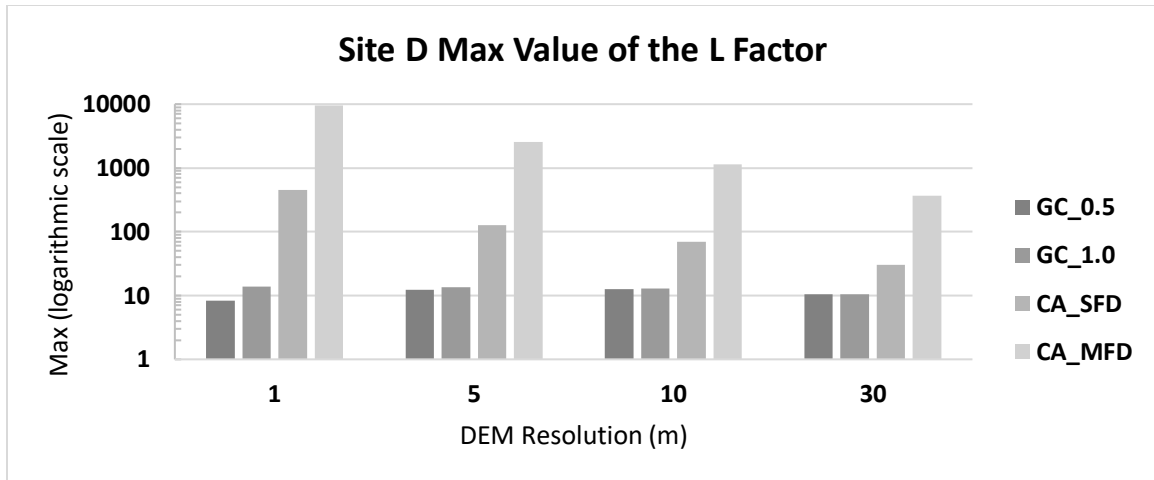


**Figure 34.** Max value of L factor for Site D where GC\_0.5 is the GC method with slope cutoff set to 0.5, GC\_1.0 is the GC method without slope cutoff, CA\_SFD is the CA method using a SFD algorithm, and CA\_MFD is the CA method using a MFD algorithm.

The recommended resolution for capturing L factor estimates derived from this study is 5 m. This resolution easily depicts identifiable drainage patterns and overall landscape flow for useful qualitative visual analyses. A 1 m resolution is of such high detail that it appears “noisy” and being able to visually identify sensitive areas typically becomes impossible as the previously identifiable networks at 5 m are lost. At such a fine resolution, ephemeral details are displayed over the more sustained drainage patterns of the site.

#### GC Method

L factor mean and median values produced by the GC method with slope reset varied little from those produced without slope reset. However, a difference raster of the GC without slope reset minus the GC with slope reset shows significant spatial variability (**Figures 35 - 38**). Maximum values varied the most at 1 m, where the

resolution can capture landscape features that reset slope length. In the figures below, as DEM resolution becomes coarser spatial differences decrease to being less than 2.

The GC method without slope cutoff is able to produce maximum values, and also longer slope lengths, of more than double those when using slope cutoff for Sites A and B. These differences between using and not using the slope cutoff are linked with the catchment size and landscape complexity. Site A is the simplest while site C is the most complex with sites B and D in-between in terms of size and complexity.

In simple terrains and/or small catchments, the areas that change the most with the slope cutoff variable appear to be long smooth hill sides without any defined channels, where flow continues predominately in one direction. For this landscape type flow paths continue to accumulate with the only condition of breaking slope length to be a change in slope steepness. Sites A and a bit of site B depict this landscape type the most and have the greatest differences in maximum values and flow paths at 1 m. At coarse resolutions of 10 m or more, this landscape loses the micro features that alter flow and becomes smoothed, so differences from using the slope cutoff are lost. More complex landscapes and/or larger catchments, such as Sites C and D, have proportionally smaller differences in maximum values between using or not using the slope cutoff variable, but the longest flow paths are still greater than those in the simpler or smaller landscapes and differences remain detectable even at coarser resolutions of 10 m or greater.

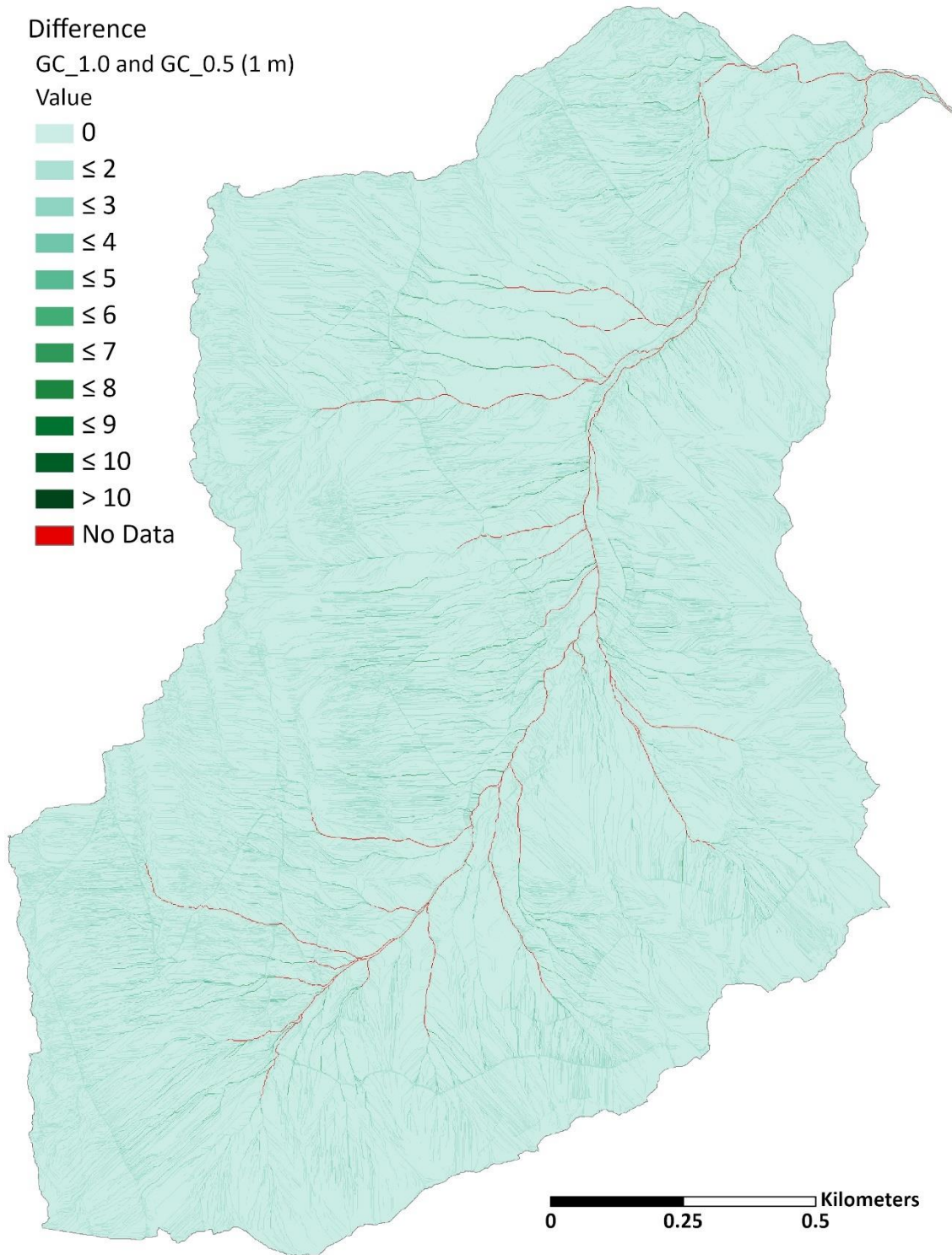


**Figure 35.** Site D difference raster (1 m) for the L Factor of the GC method with slope cutoff (GC\_0.5) subtracted from the GC method without slope cutoff (GC\_1.0).

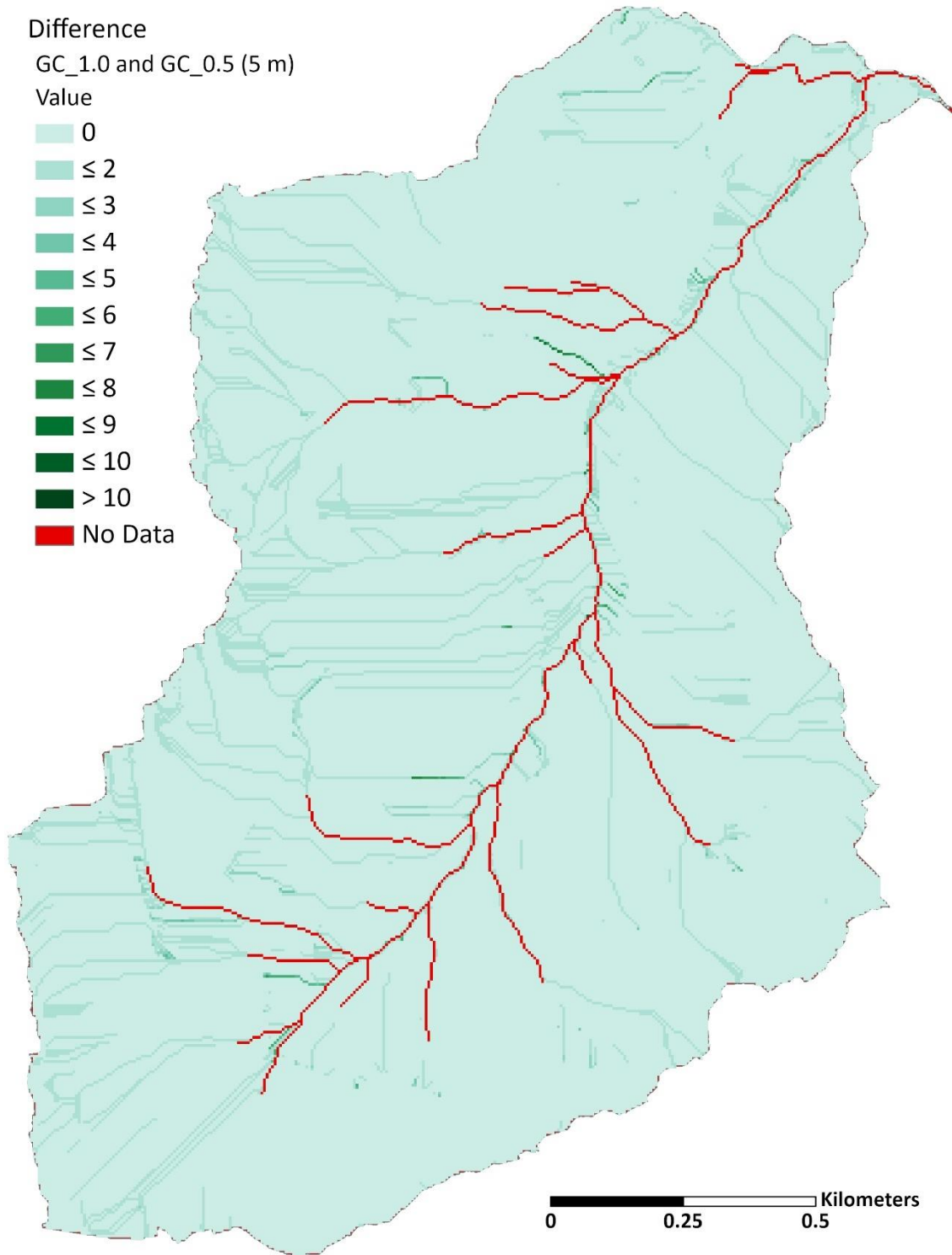


**Figure 36.** Site D difference raster (5 m) for the L Factor of the GC method with slope cutoff (GC\_0.5) subtracted from the GC method without slope cutoff (GC\_1.0).

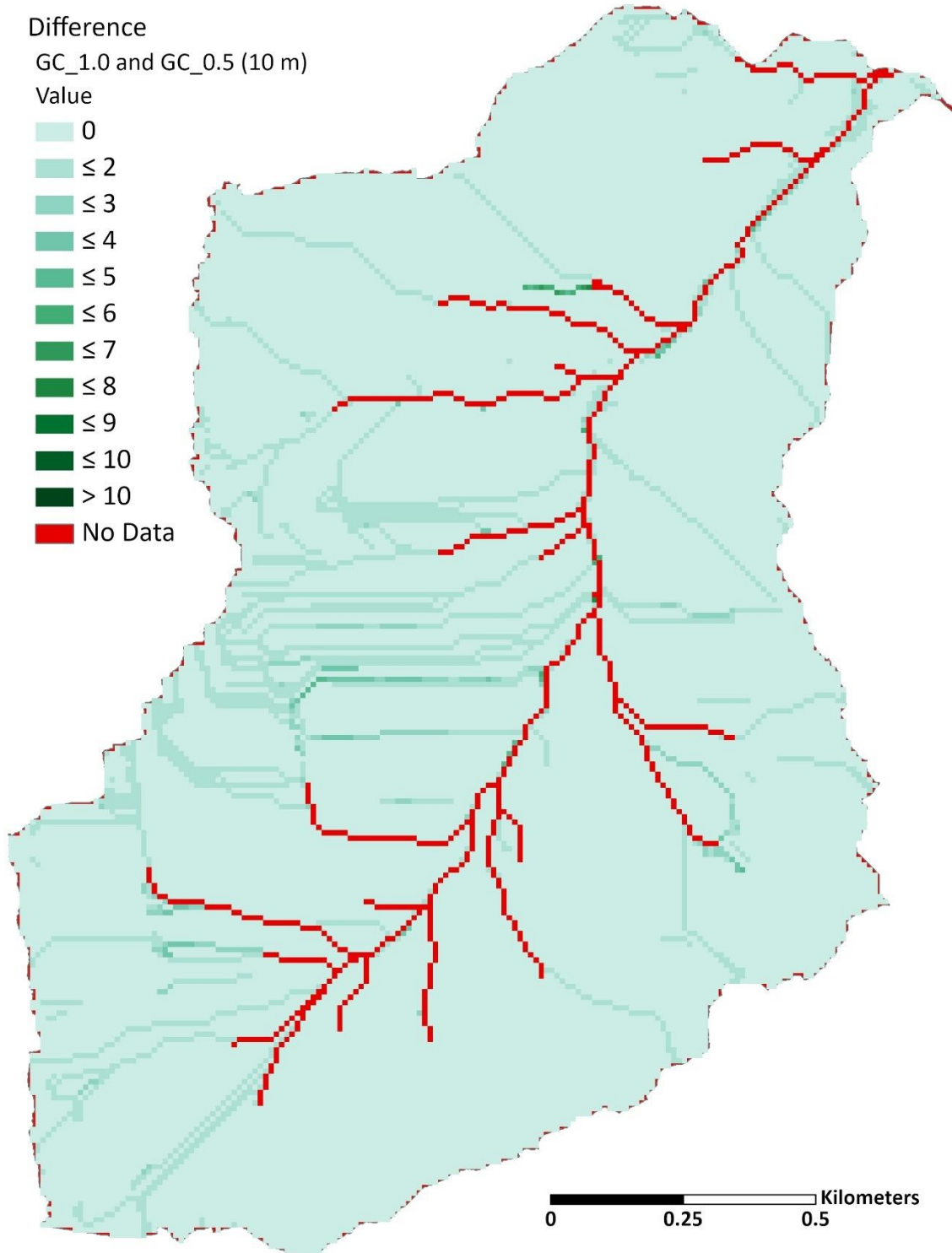


**Figure 37.** Site D difference raster (10 m) for the L Factor of the GC method with slope cutoff (GC\_0.5) subtracted from the GC method without slope cutoff (GC\_1.0).

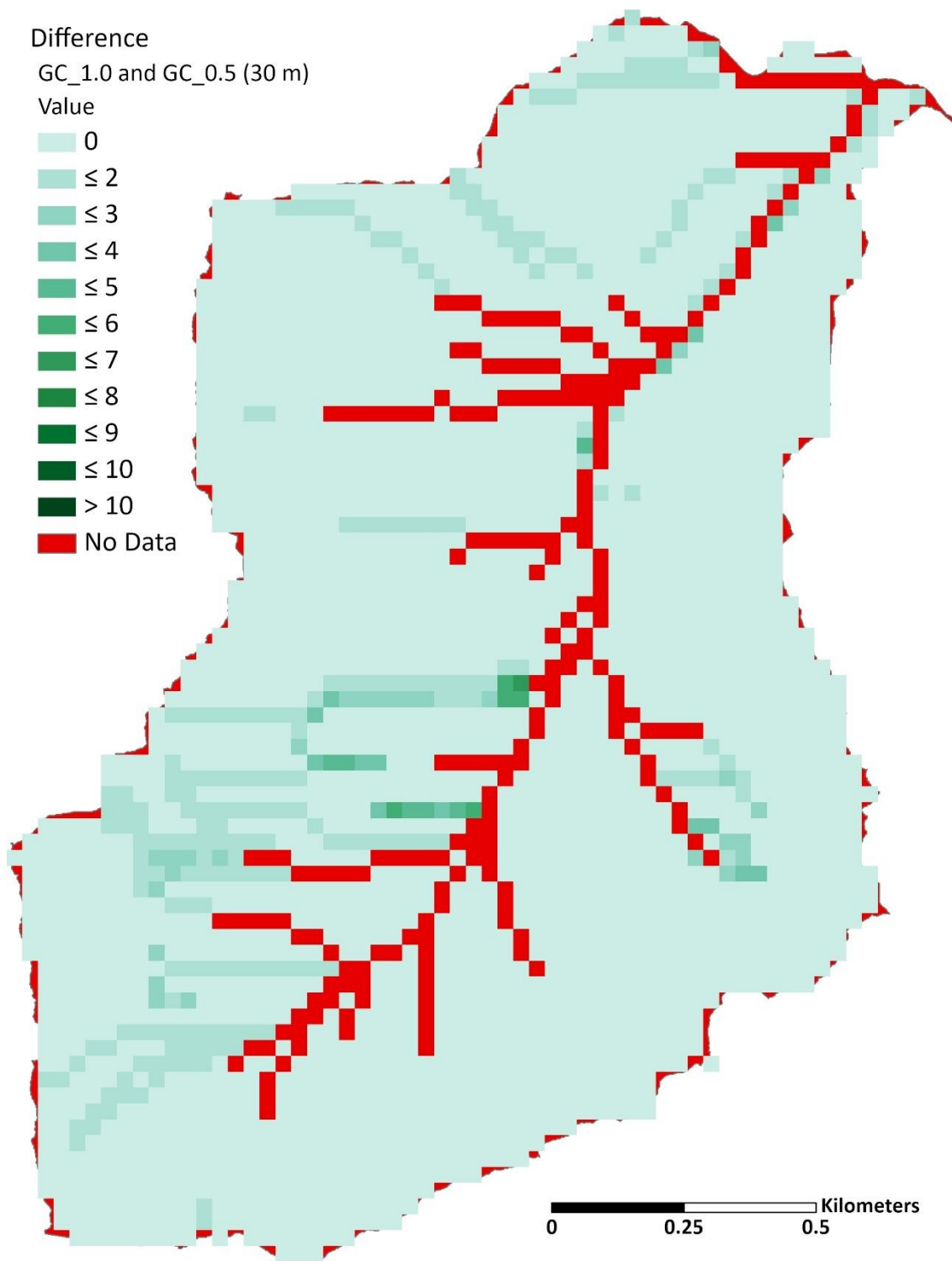


**Figure 38.** Site D difference raster (30 m) for the L Factor of the GC method with slope cutoff (GC\_0.5) subtracted from the GC method without slope cutoff (GC\_1.0).

For most landscapes, the incorporation of the slope cutoff variable at high resolution 1 m DEMs accounts for fine scale variability. Sudden changes in steepness that occur from barriers or micro features that interrupt flow and break slope length are detected. However, the problem still remains that visually interpreting erosion estimates for these areas at 1 m is noisy, and it is difficult to identify patterns or locate problem areas. For example, using satellite imagery in combination with visual on-site verification, the micro features that are captured at 1 m and not 5 m for Site B are cattle paths that create small bench features and the exposed rocky basalt slides where the surface roughness of the rip-rap like material increases the chance of meeting the slope cutoff variable to break slope length (**Appendix B**). However, 5 m resolutions are still able to capture the influence of other small scale features such as dirt roads.

The 1 m resolution can be difficult to visually interpret, especially for more complex landscapes, but may produce more meaningful estimates of total erosion occurring in the site if looking at a sum total of RUSLE estimates. The 5 m resolution visually highlights patterns and specific areas within the study site that have the highest erosion related to slope length. This provides a valuable resource for useful qualitative visual analyses. Resolutions coarser than 5 m smooth landscapes and lose small scale features, producing less meaningful outputs.

Lower resolutions mean that the minimum slope lengths for every pixel are increased with the greater pixel size and increase L mean and median values. The mean

and median increase also due to the decrease in the number of starting point pixels of flow paths (low L values) that occur at the top of slopes.

The GC method without slope cutoff continues to cumulate longer slopes and produce higher L factor values in the above-mentioned areas. Using the slope cutoff variable better refines the spatial distribution of erosion estimates across slopes and identifies areas in a slope where slope change can be initiating deposition instead of continuing to accumulate slope length for greater erosion.

#### CA Method

The CA method produces extremely high L factor values that skew the distribution and create higher mean values. The median value is more representative of the central values for the greatly skewed distributions. This method will produce increasingly higher L values with increasing catchment area, greater elevation change, and decreased number of main drainage channels. These factors control available area to distribute flow down the slopes and the amount of area draining down around any one defined channel.

Difference rasters of the CA method with the MFD and then the SFD algorithm are shown below (**Figures 39 - 42**). The MFD diffuses the contributing area, while the SFD concentrates that area into a single flow to produce easily identifiable drainage patterns. The MFD algorithm splits and distributes area to more downslope neighbors so there are more cells with overall higher L values; leading to a higher mean, median,

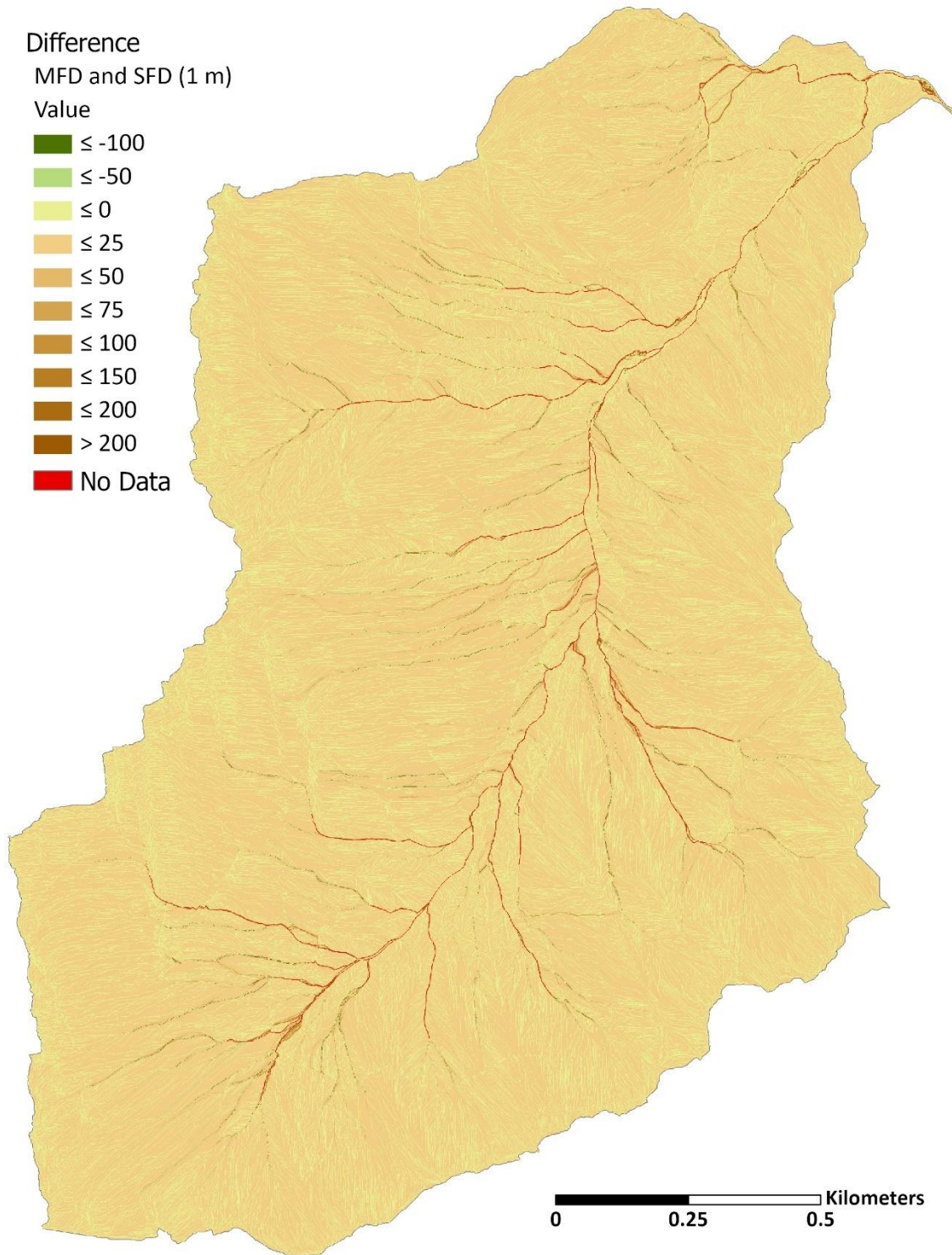


**Figure 39.** Site D difference raster (1 m) for the L Factor of the CA method using a SFD algorithm (SFD) subtracted from the CA method using a MFD algorithm (MFD).

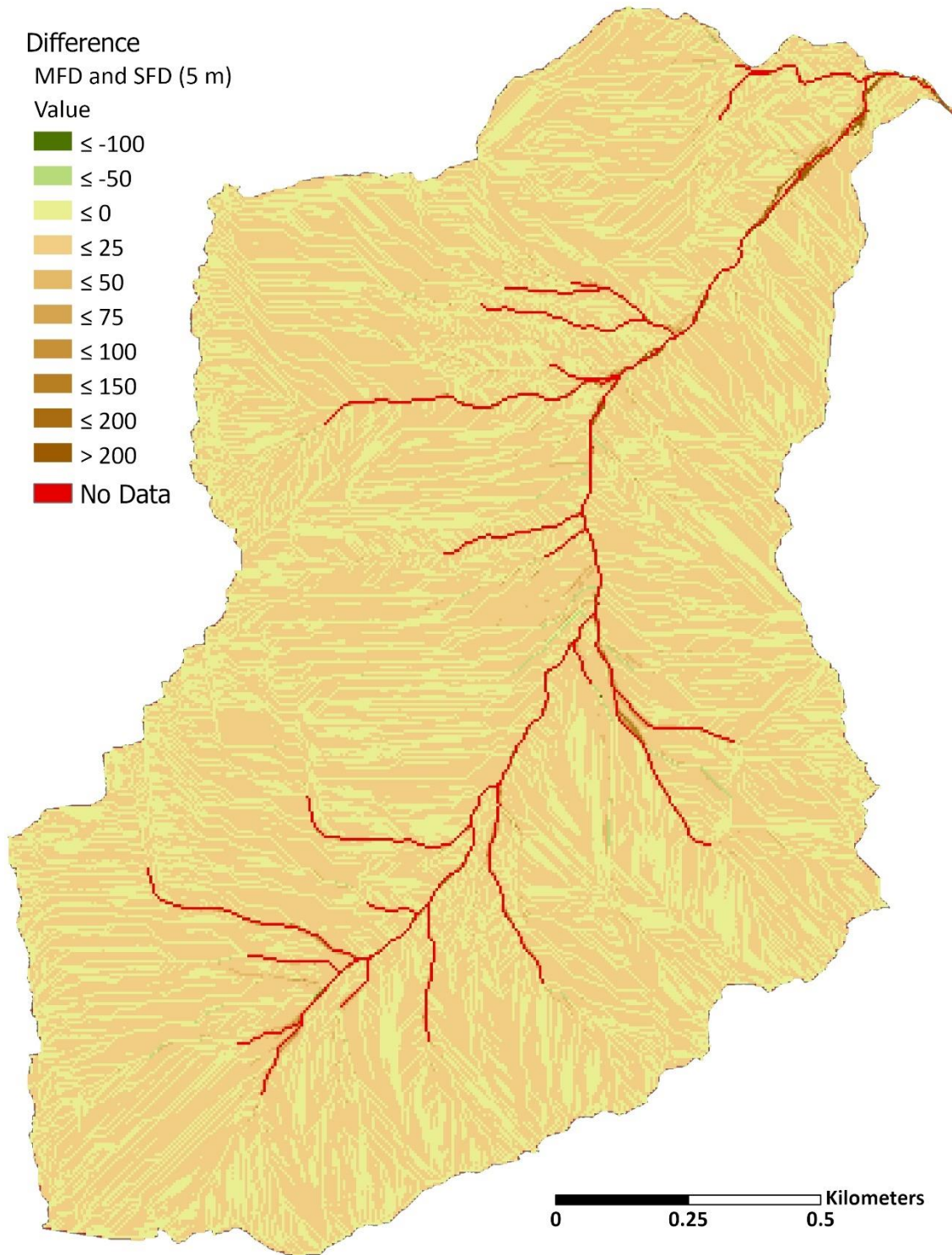


**Figure 40.** Site D difference raster (5 m) for the L Factor of the CA method using a SFD algorithm (SFD) subtracted from the CA method using a MFD algorithm (MFD).

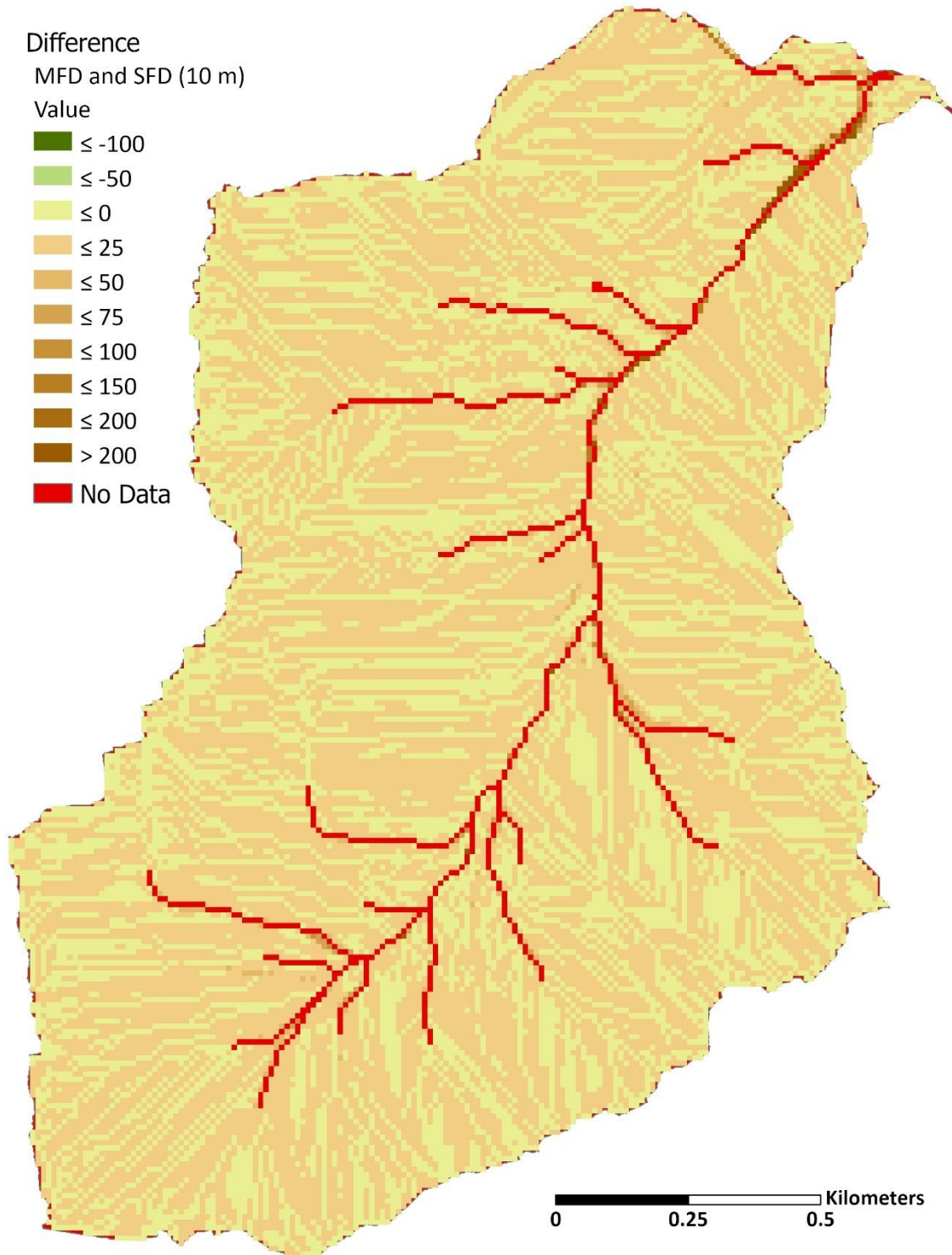


**Figure 41.** Site D difference raster (10 m) for the L Factor of the CA method using a SFD algorithm (SFD) subtracted from the CA method using a MFD algorithm (MFD).

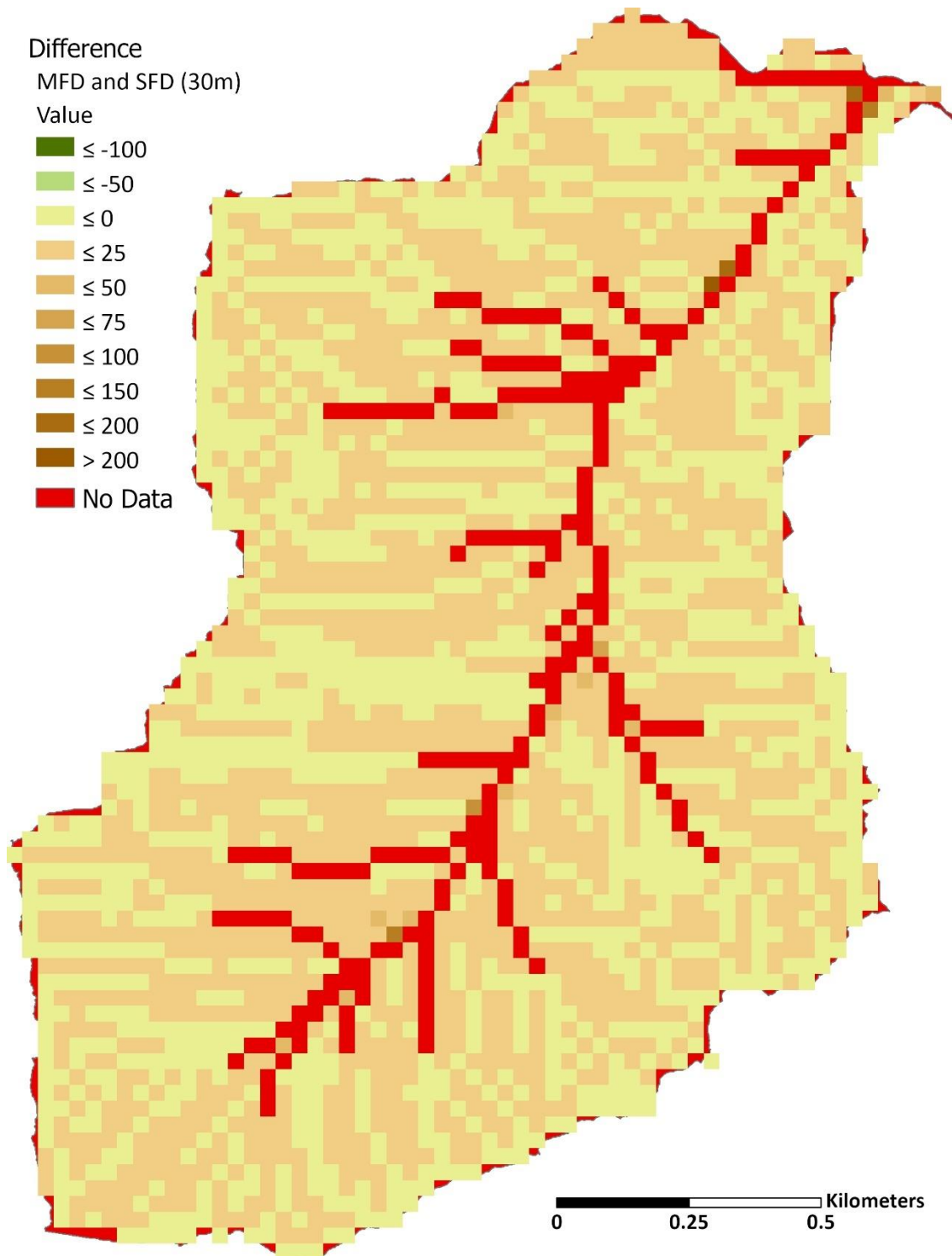


**Figure 42.** Site D difference raster (30 m) for the L Factor of the CA method using a SFD algorithm (SFD) subtracted from the CA method using a MFD algorithm (MFD).

and maximum values when using the MFD algorithm. Most of the smaller differences between the SFD and MFD algorithms appear to occur in open gentle slopes where topography does not naturally aggregate flow into drainage channels so the MFD has more neighbors to split flow to while the larger differences occur closer to the defined channels as more area is braided and then concentrated by the MFD.

The CA method overall is sensitive where flow begins to concentrate near a defined channel, producing exceptionally high values as almost all upslope area is combined. For the SFD algorithm these high values are concentrated in easily identifiable drainage patterns while the MFD algorithm disperses area in a fan like pattern before converging and reaching the defined channels. These areas are in a zone that is no longer applicable to the RUSLE model, where flow concentrates enough that the dominant erosional process is greater than rill and interill erosion becoming either gullies or stream channels (Wischmeier and Smith 1978; Renard et al. 1997; Zhang et al. 2013). The defined channel threshold is meant to minimize the effect of this occurrence and is best set by an expert of the study site and drainage network. A detailed stream network file, built from topographical data of at least the same resolution and timeframe of the site's DEM, could also be used if available.

Coarse resolutions increase the pixel size and minimum area to disperse downslope which increases L mean and median values from 1 to 30 m resolutions. However, maximum value decreases as the landscape is smoothed and simplified and

there are fewer cells to disperse downslope area to before reaching defined drainage channels or catchment boundaries.

#### GC and CA Method

To compare the two methods, the CA method using the SFD algorithm and the GC method without slope cutoff are used for difference rasters. This is done since these are most similar, the CA with the MFD algorithm producing higher mean, median, and max will have even greater differences to the GC method with a slope cutoff of 0.5. The differences identified with CA using the SFD and GC without slope cutoff, will be increased with other combinations such as CA using a MFD and GC with slope cutoff.

Differences between the methods grow larger as flow becomes concentrated moving downslope, especially along drainage channels (**Figures 43 - 46**). This corresponds to how each method treats convergence in the landscape. The CA method combines accumulated area where two or more paths converge, allowing for all area in the site to influence values downslope. The GC method only continues the longest flow path; the flow paths that are ended no longer influence values downslope.

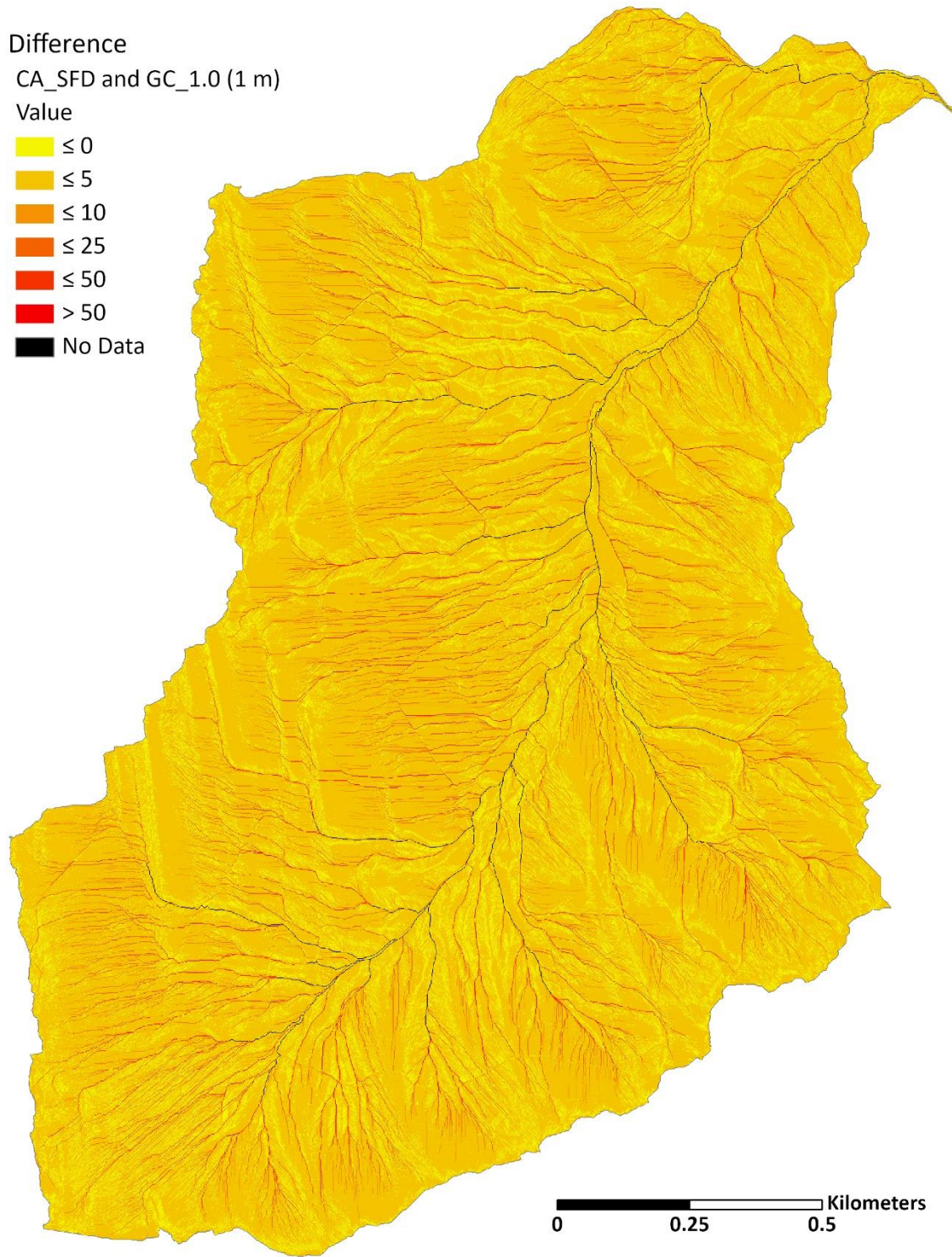


**Figure 43.** Site D difference raster (1 m) for the L Factor of the GC method without slope cutoff (GC\_1.0) subtracted from the CA method using a SFD algorithm (CA\_SFD).

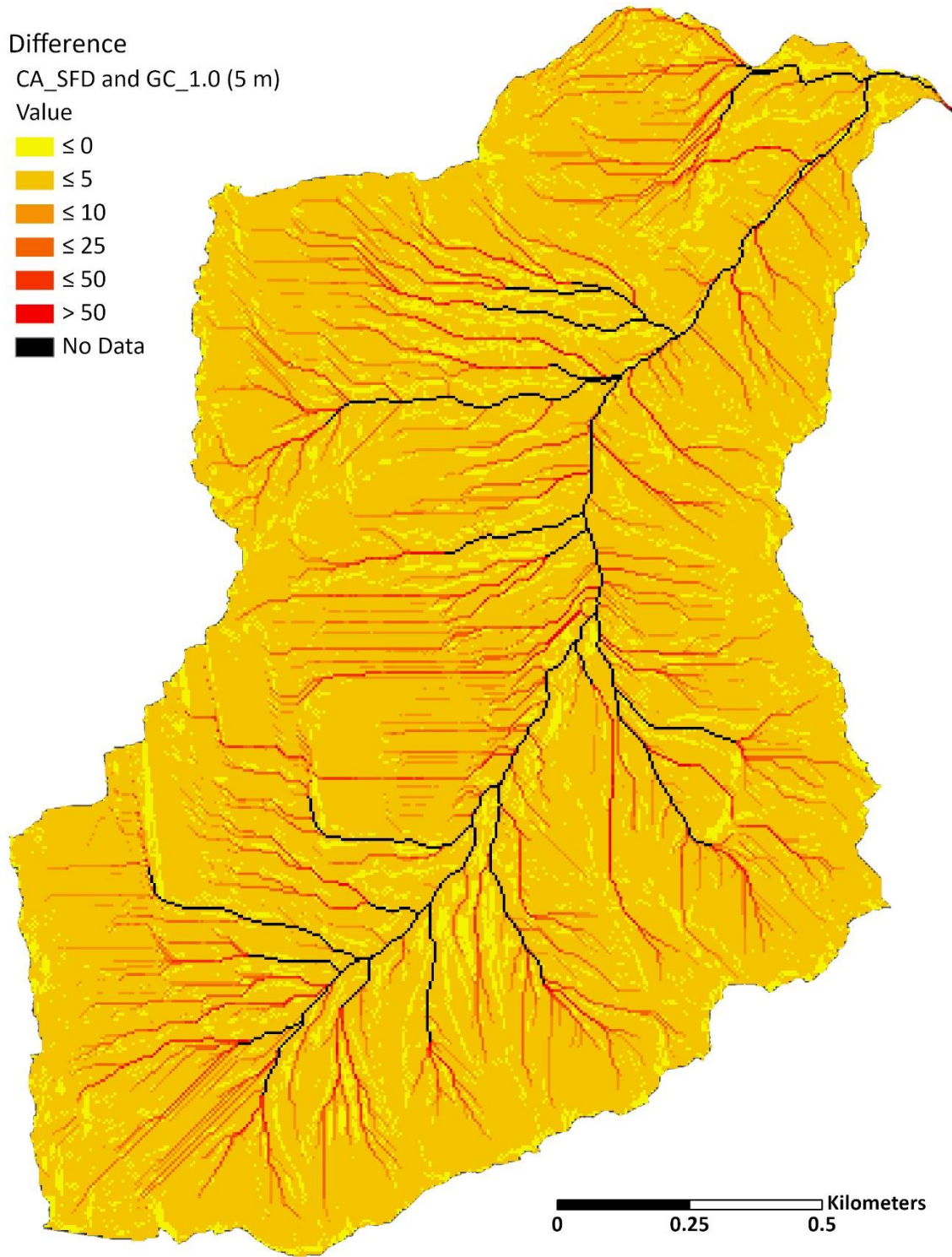


**Figure 44.** Site D difference raster (5 m) for the L Factor of the GC method without slope cutoff (GC\_1.0) subtracted from the CA method using a SFD algorithm (CA\_SFD).

Difference

CA\_SFD and GC\_1.0 (10 m)

Value

≤ 0

≤ 5

≤ 10

≤ 25

≤ 50

> 50

No Data

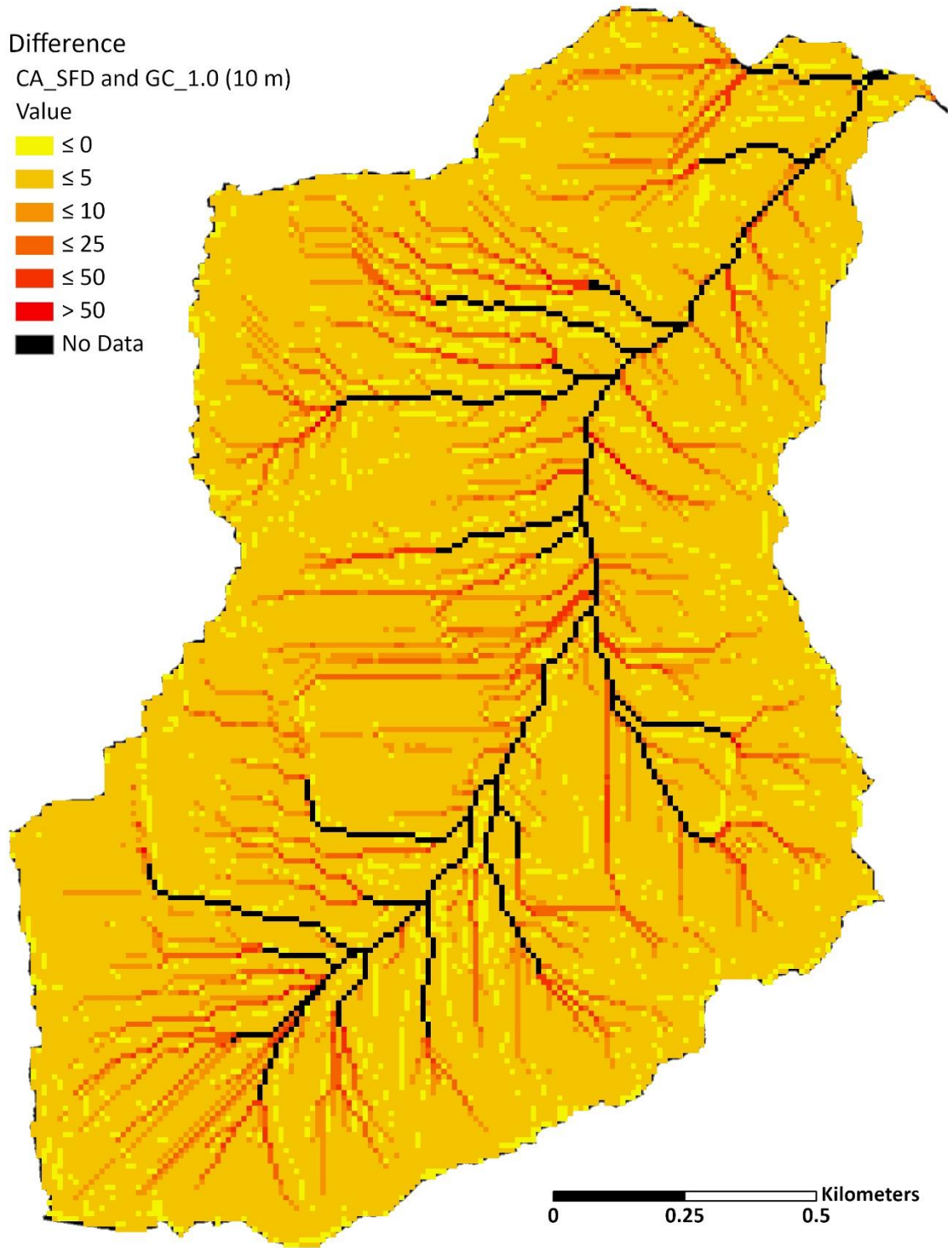


**Figure 45.** Site D difference raster (10 m) for the L Factor of the GC method without slope cutoff (GC\_1.0) subtracted from the CA method using a SFD algorithm (CA\_SFD).

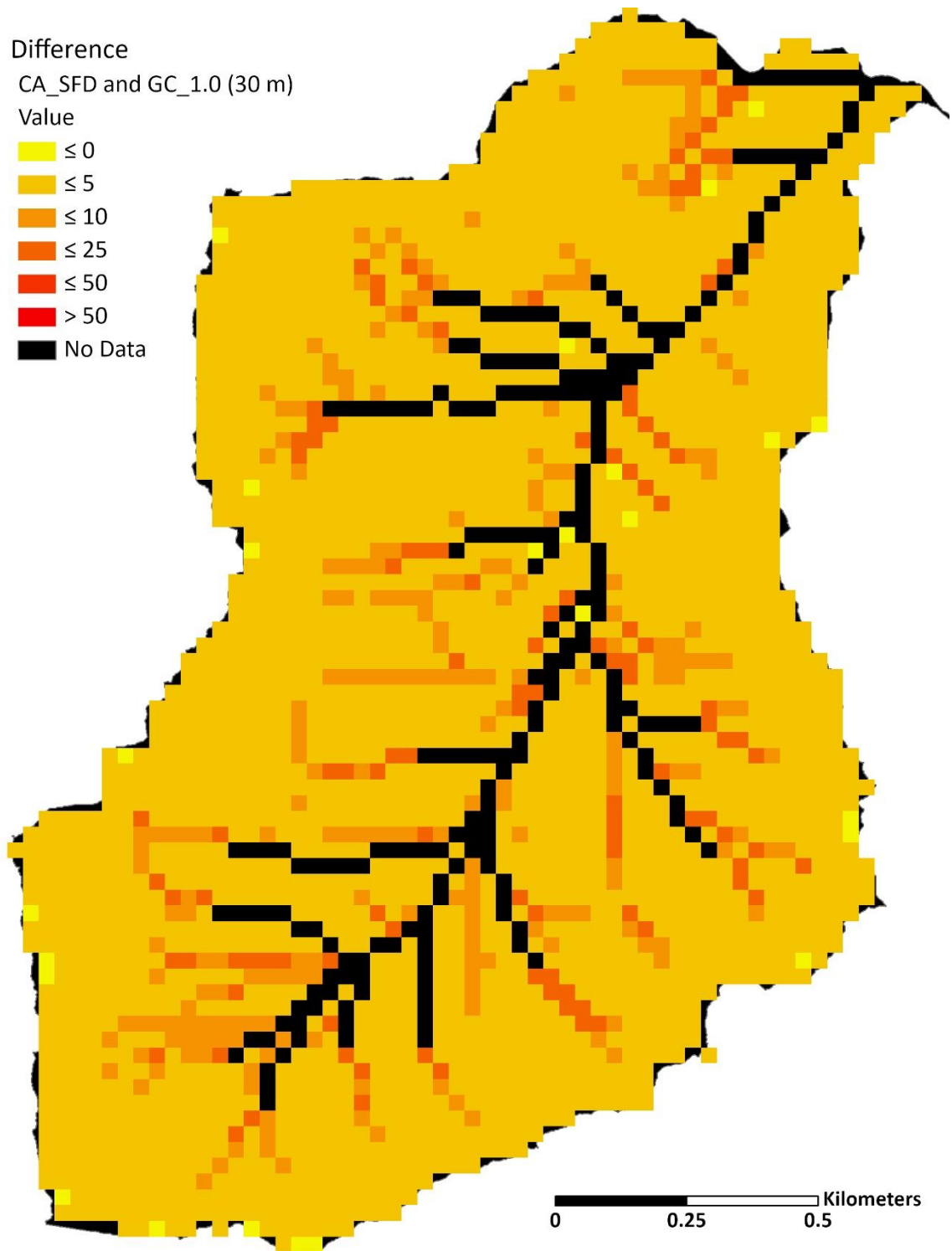


**Figure 46.** Site D difference raster (30 m) for the L Factor of the GC method without slope cutoff (GC\_1.0) subtracted from the CA method using a SFD algorithm (CA\_SFD).

The CA method has no equivalent for the slope cutoff that is incorporated in the GC method. This means the greater values of area accumulating in the CA method will continue to accumulate while the GC method has the opportunity to reset slope length values. The CA method creates overall higher L values than using slope length which alters the weight of the L factor in the RUSLE model, potentially overestimating erosion.

This treatment of convergence and no equivalent of a slope cutoff variable becomes increasingly important in large catchments and/or catchments with large elevation change. The CA method will increasingly produce higher values in these conditions, with greater available area to distribute, that could lead to an overprediction of erosion in a larger area of the landscape. The L calculation equation differs for the CA method, and at the high spots in the landscape, the input length and area can be similar which produces instances where the GC method produces minimally higher L values (GC method greater by less than one), but this effect does not last as area accumulates into larger values and the two methods have different treatments of convergence.

To determine the statistical significance of the differences between these methods, a two-sided hypothesis test with a null hypothesis that two independent methods at the same resolution were drawn from the same distribution was conducted. **Table 3** shows the corresponding p-values using the Kolmogorov-Smirnov test. For each method pairing, at each resolution, the null hypothesis is that the distribution values for both methods are the same. It was found that the GC methods were statistically different from the CA methods at the 1% significance level for all resolutions. The CA

method using the SFD algorithm (CA\_SFD) is also statistically different to the CA method using the MFD algorithm (CA\_MFD) at the 1% significance level for all resolutions.

**Table 3.** Kolmogorov-Smirnov derived p-values for L factor outputs all sites across varying DEM resolutions.

Site A - Resolution (m)												
	1			5			10			30		
	GC_1.0	CA_SFD	CA_MFD									
GC_0.5	0.0	0.0	0.0	0.0	0.0	0.0	0.2424	0.0	0.0	1.0	0.0	0.0
GC_1.0		0.0	0.0		0.0	0.0		0.0	0.0		0.0	0.0
CA_SFD			0.0			0.0			0.0			0.0

Site B - Resolution (m)												
	1			5			10			30		
	GC_1.0	CA_SFD	CA_MFD									
GC_0.5	0.0	0.0	0.0	0.1084	0.0	0.0	0.9204	0.0	0.0	0.9826	0.0	0.0
GC_1.0		0.0	0.0		0.0	0.0		0.0	0.0		0.0	0.0
CA_SFD			0.0			0.0			0.0			0.0

Site C - Resolution (m)												
	1			5			10			30		
	GC_1.0	CA_SFD	CA_MFD									
GC_0.5	0.0	0.0	0.0	0.0	0.0	0.0	0.0	0.0	0.0	0.0	0.0	0.0
GC_1.0		0.0	0.0		0.0	0.0		0.0	0.0		0.0	0.0
CA_SFD			0.0			0.0			0.0			0.0

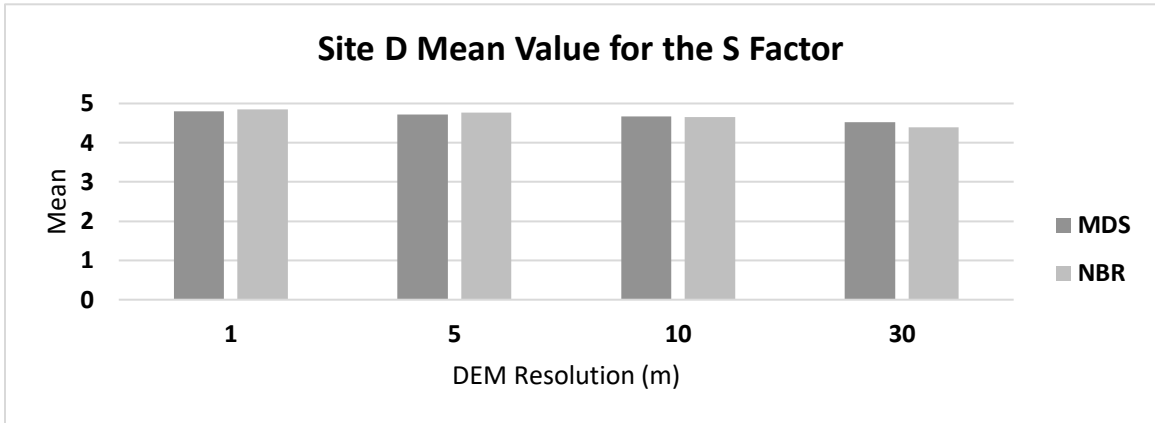
  

Site D - Resolution (m)												
	1			5			10			30		
	GC_1.0	CA_SFD	CA_MFD									
GC_0.5	0.0	0.0	0.0	0.0	0.0	0.0	0.0046	0.0	0.0	0.3061	0.0	0.0
GC_1.0		0.0	0.0		0.0	0.0		0.0	0.0		0.0	0.0
CA_SFD			0.0			0.0			0.0			0.0

The GC method using slope cutoff (GC\_0.5) remained statistically significant at the 1% level compared to the GC method without slope cutoff (GC\_1.0) for all sites at a 1 m resolution. However, Site B loses statistical significance at 5 m, Site A loses it at 10 m, and Site D loses it at 30 m. Site C, which is by far the largest and most complex site, remains statistically significant at all resolutions for all method pairings. This provides support to the assertion that as resolution degrades, differences between using these methods are lost to landscape smoothing.

## S Factor

Overall, the MDS method appears to be less sensitive to changing DEM resolutions than the NBR method (**Figures 47 - 50**). As resolution becomes coarser the mean, median, and maximum values for both methods decrease. The mean and median values for the MDS method are more resilient to coarser DEM resolutions and typically exhibit a smaller degree of change in comparison to the changes the NBR method mean and median values experience. The most significant change that occurs is the increase in minimum values for both methods using a resolution of 30 m. Minimum values can increase by more than ten times the value at 1 m with the MDS having the largest increase for Sites B and D. The only site to not follow this trend is Site A. This Site has the gentlest terrain and while minimum values do increase, it is not as dramatic as with the other sites. Instead, the maximum values for Site A, for both methods, exhibit a similarly dramatic decrease from maximum values ~15 down to 1 – 2 at the 30 m resolution. This suggests that the smoothing effect of decreasing resolution is most noticeable on those slope categories that are most scarce in the landscape. Site A has limited area of steep short slopes that occur only along the main drainage channel. When the cell resolution changed from 1 m to 5 m this area was lost and the slope calculations that use the surrounding cell's elevation could only represent the dominant terrain type of gentle long slopes.



**Figure 47.** Mean value of S factor for Site D.

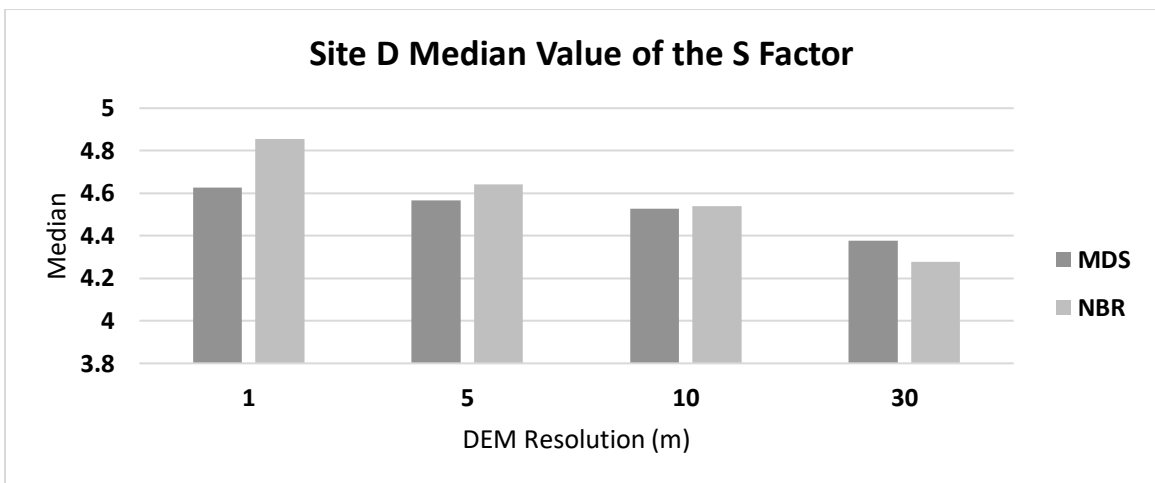


**Figure 48.** Median value of S factor for Site D.

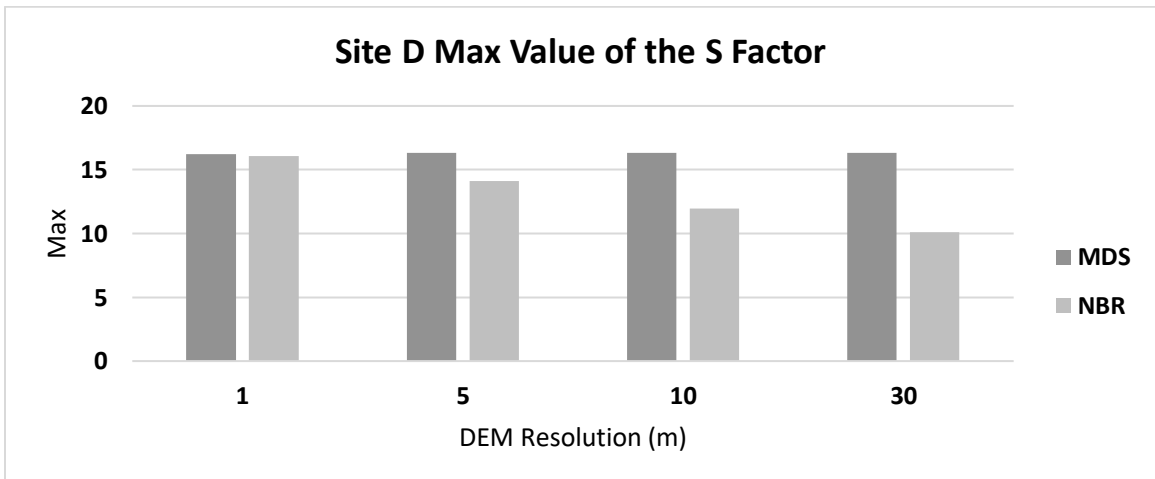


**Figure 49.** Maximum value of S factor for Site D.

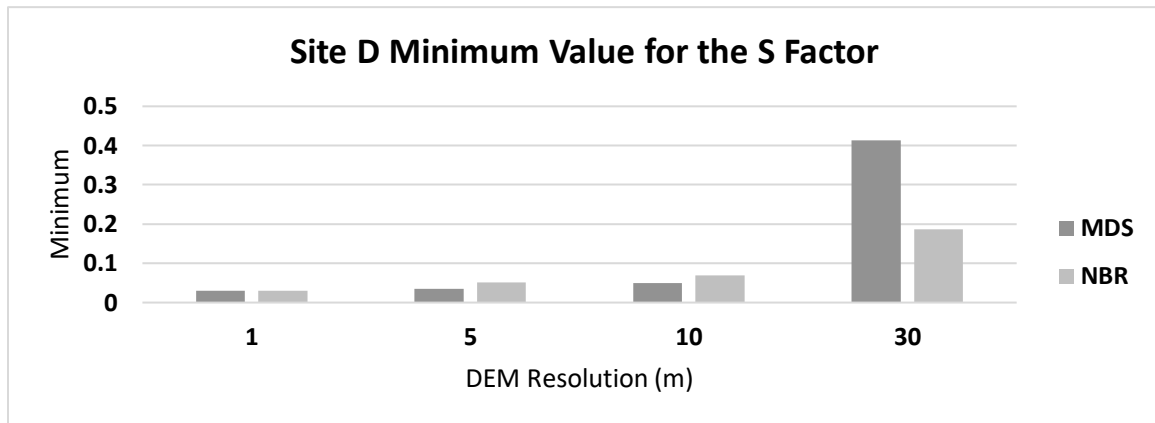


**Figure 50.** Minimum value of S factor for Site D.

Overall mean and median values from each method produce similar results in all sites, especially at finer resolutions, but are strongly influenced by changing DEM resolutions. As resolution decreases across all sites, the methods begin to produce outputs that are no longer statistically different at the 1% significance level using the same Kolmogorov-Smirnov test as was done with the L factor outputs (**Table 14**). The null hypothesis is that the NBR and MDS method produce results that come from the same data distribution. This was rejected for all sites at the 1 and 5 m resolution. At the 10 m resolution Sites A, C, and D still rejected the null hypothesis and at 30 m Sites B and C produced statistically different outputs. As with the L factor outputs, the S factor is vulnerable to losing small scale features to landscape smoothing with 10 and 30 m resolutions. At these coarse resolutions, differences between the MDS and NBR methods decrease since the larger cell sizes homogenize the landscape.

S outputs using the MDS method reflect the landscape more accurately and are more detailed for resolutions coarser than 1 m. Features such as roads and trails are still

identifiable at the 5 m resolution using the MDS method, while they are lost in the NBR method at 5 m. Small scale features are able to be represented by the MDS method and are persistent to 5 m resolutions.

**Table 4.** Kolmogorov-Smirnov derived p-values for S factor outputs all sites across varying DEM resolutions.

	<b>Resolution (m)</b>			
	<b>1</b>	<b>5</b>	<b>10</b>	<b>30</b>
Site A	0.0	0.0	0.0061	0.2380
Site B	0.0	0.0	0.0727	0.0011
Site C	0.0	0.0	0.0	0.0
Site D	0.0	0.0	0.0057	0.0242

The smoothing effect of decreasing resolution is most noticeable on those slope categories that are most scarce in the landscape. If the landscape is predominately a gentle flat terrain, than the minority of area that exhibits steep slopes is going to be minimized further or even lost. The MDS method is the best method to retain variability of slope steepness in the landscape, picking up small scale features at fine resolutions (**Figures 51 - 54**). Coarse resolution DEMs smooth the landscape and using the NBR method on those DEMs further smooths landscapes and dramatically reduces variability (**Figures 55 - 58**). This can be seen from the loss of detecting roads in the 1 m resolution to the 5 m resolution using the NBR method. As was seen with the L factor, features such as roads are important influences on water flow and erosion. Being able to detect these features and their influences is important in obtaining representative outputs of the landscape. The NBR method is not as effective at detecting these features as the MDS method is.

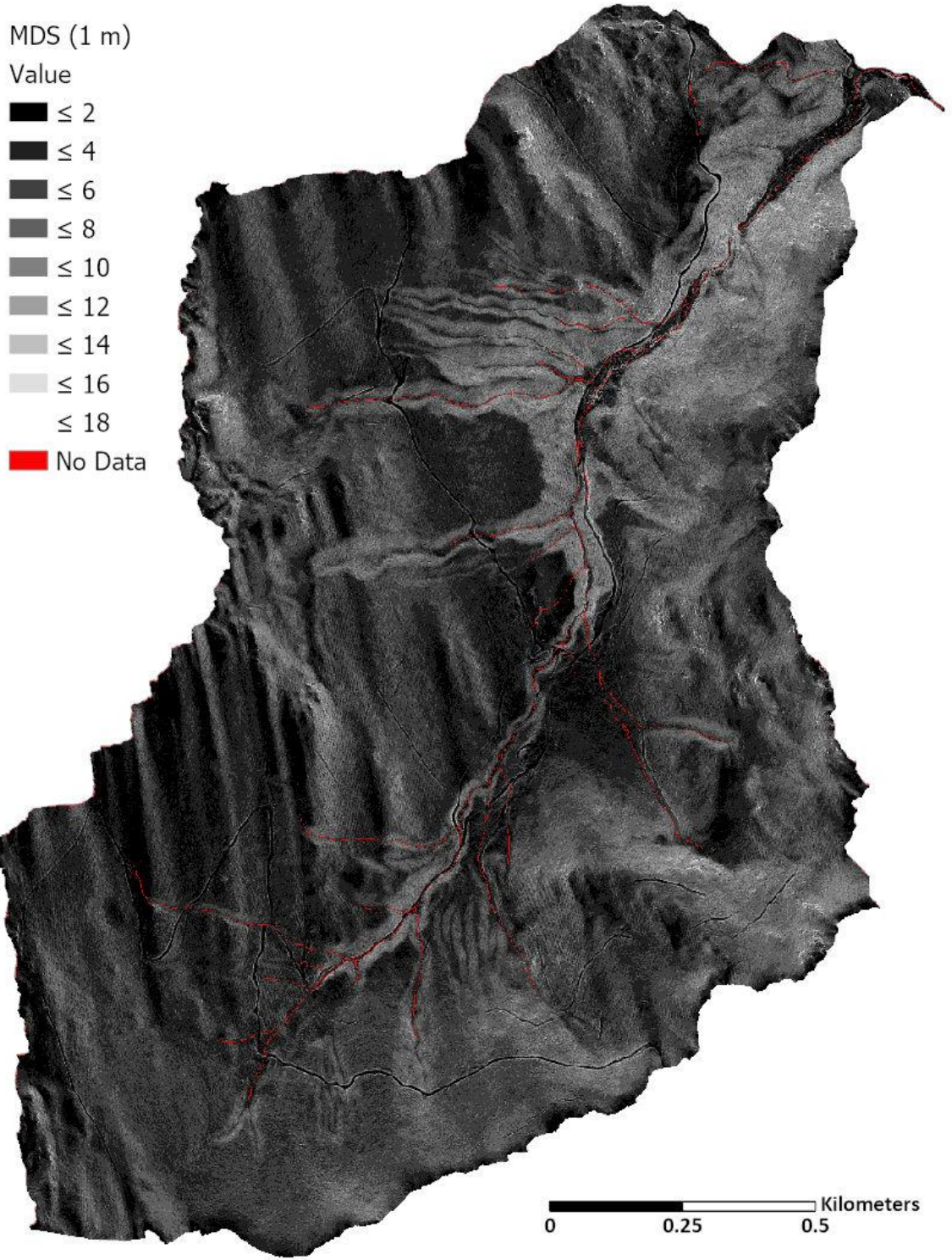


**Figure 51.** S factor with the MDS method for Site D at 1 m.

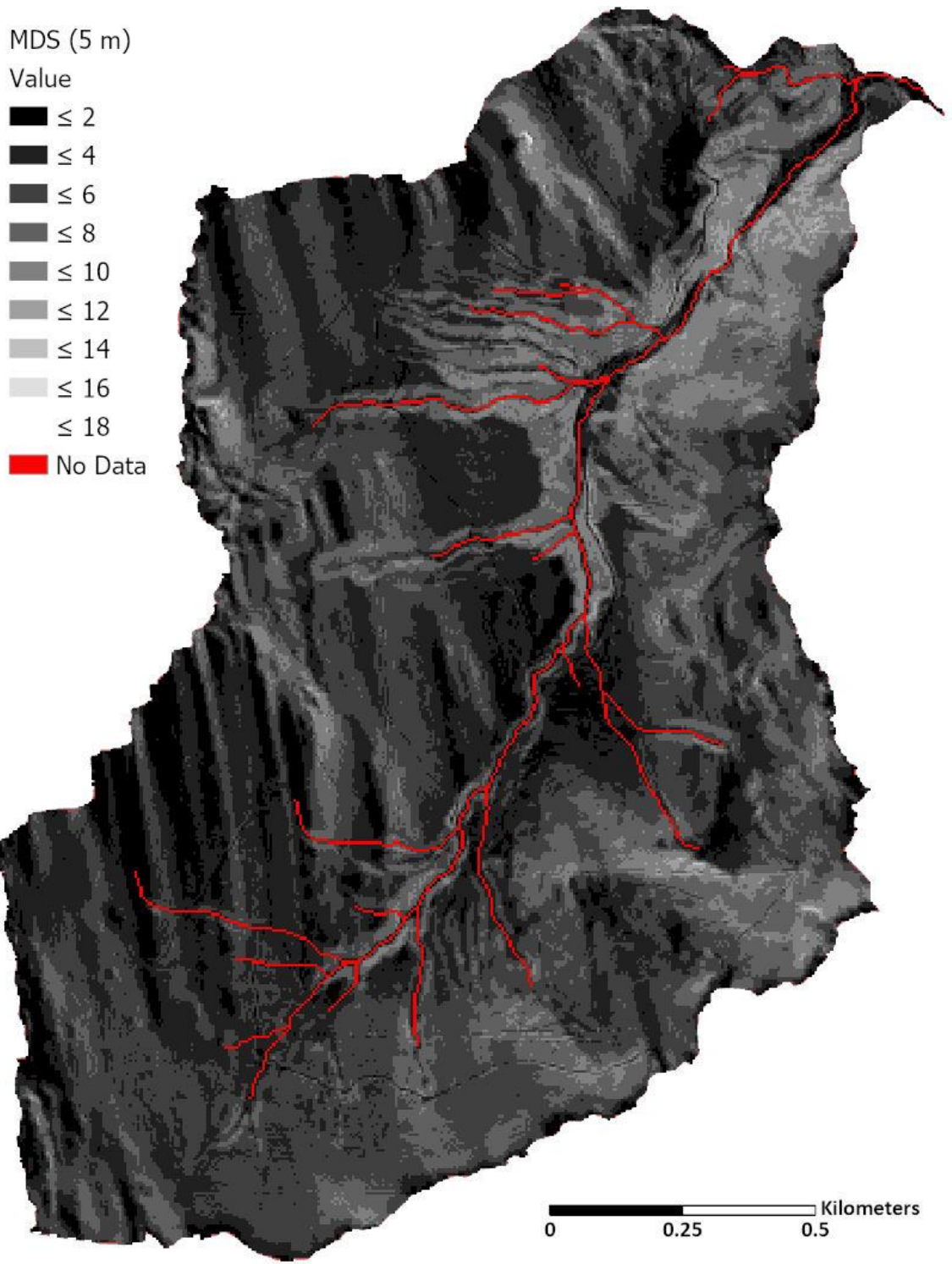


**Figure 52.** S factor with the MDS method for Site D at 5 m.

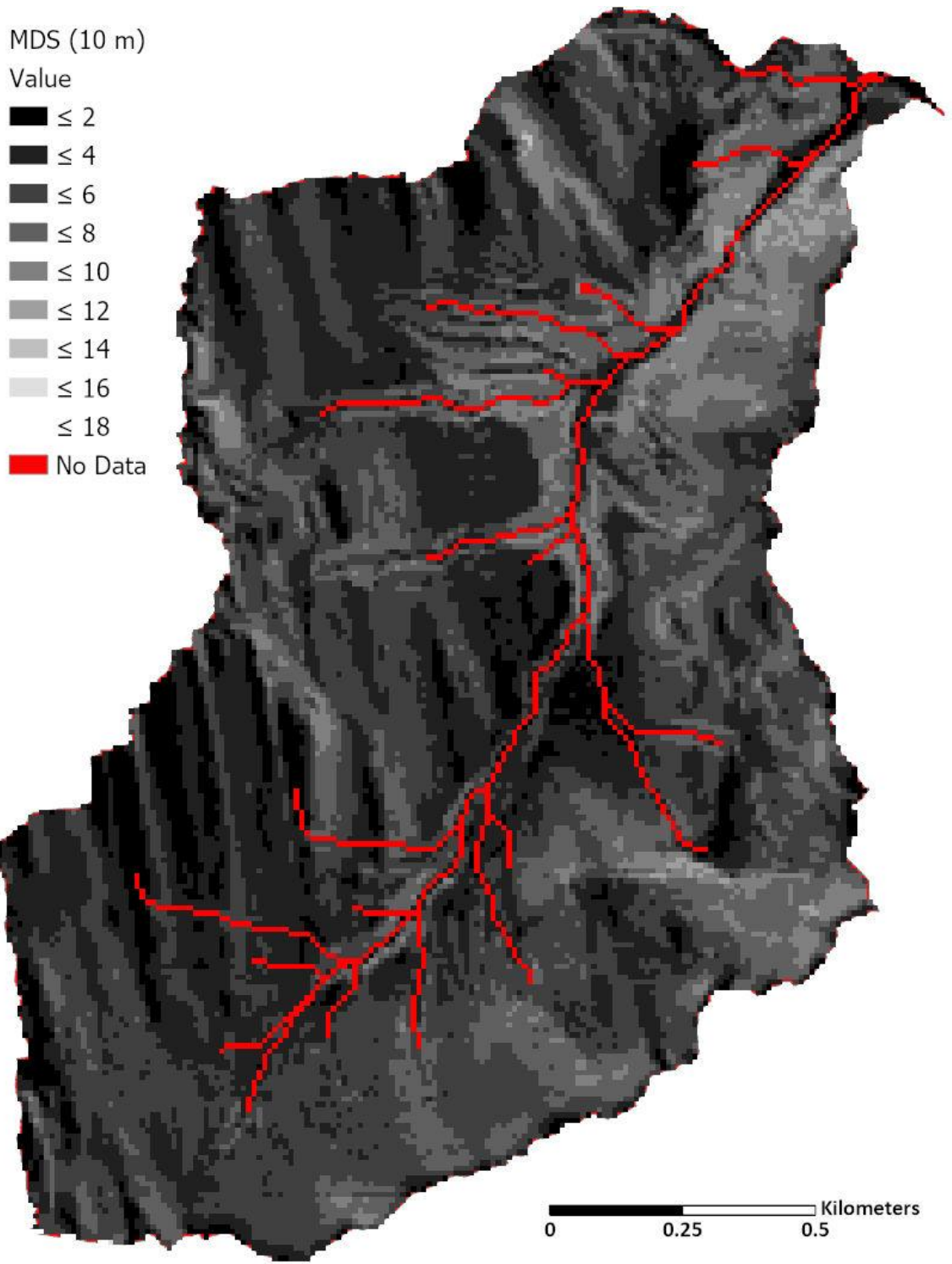


**Figure 53.** S factor with the MDS method for Site D at 10 m.

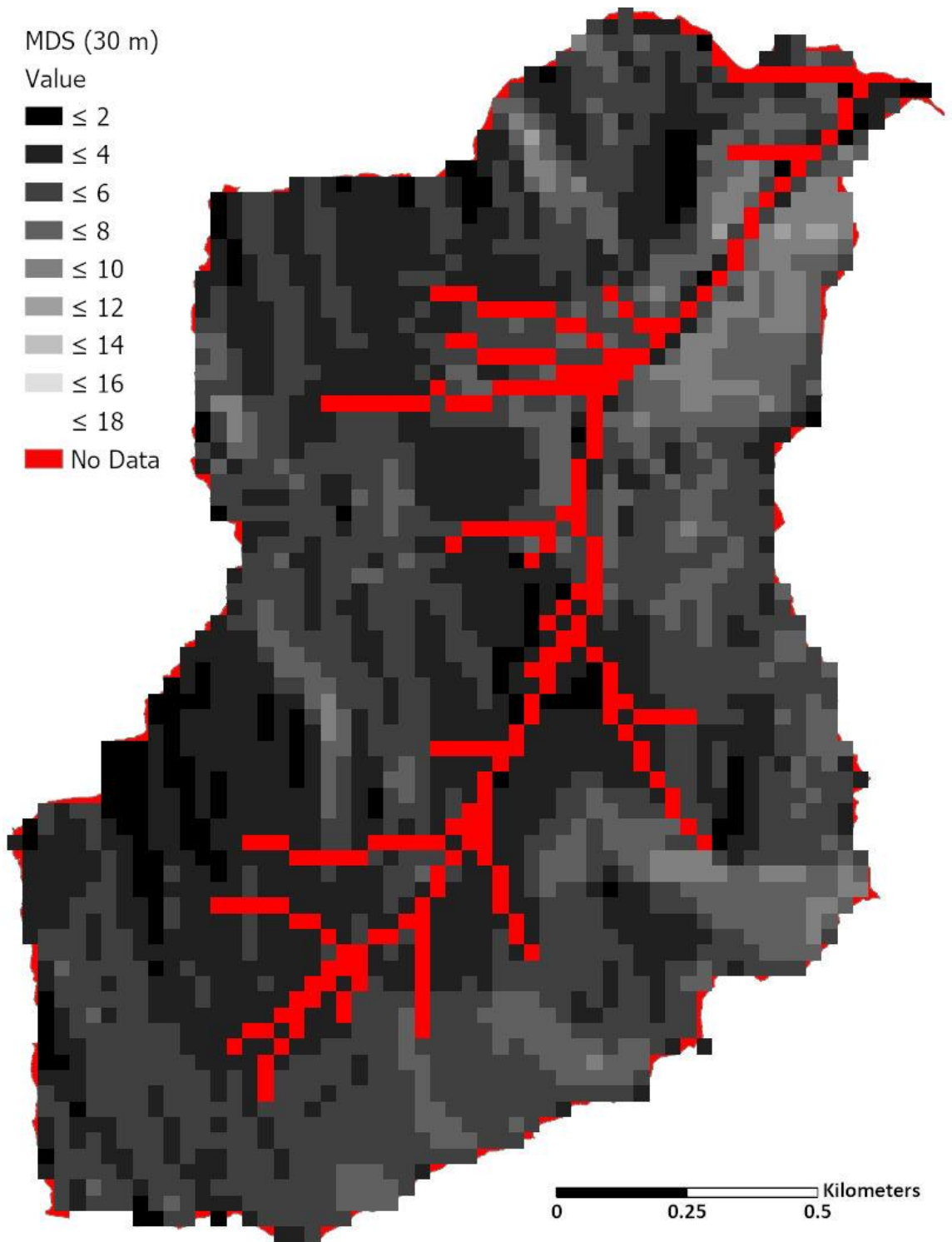


**Figure 54.** S factor with the MDS method for Site D at 30 m.

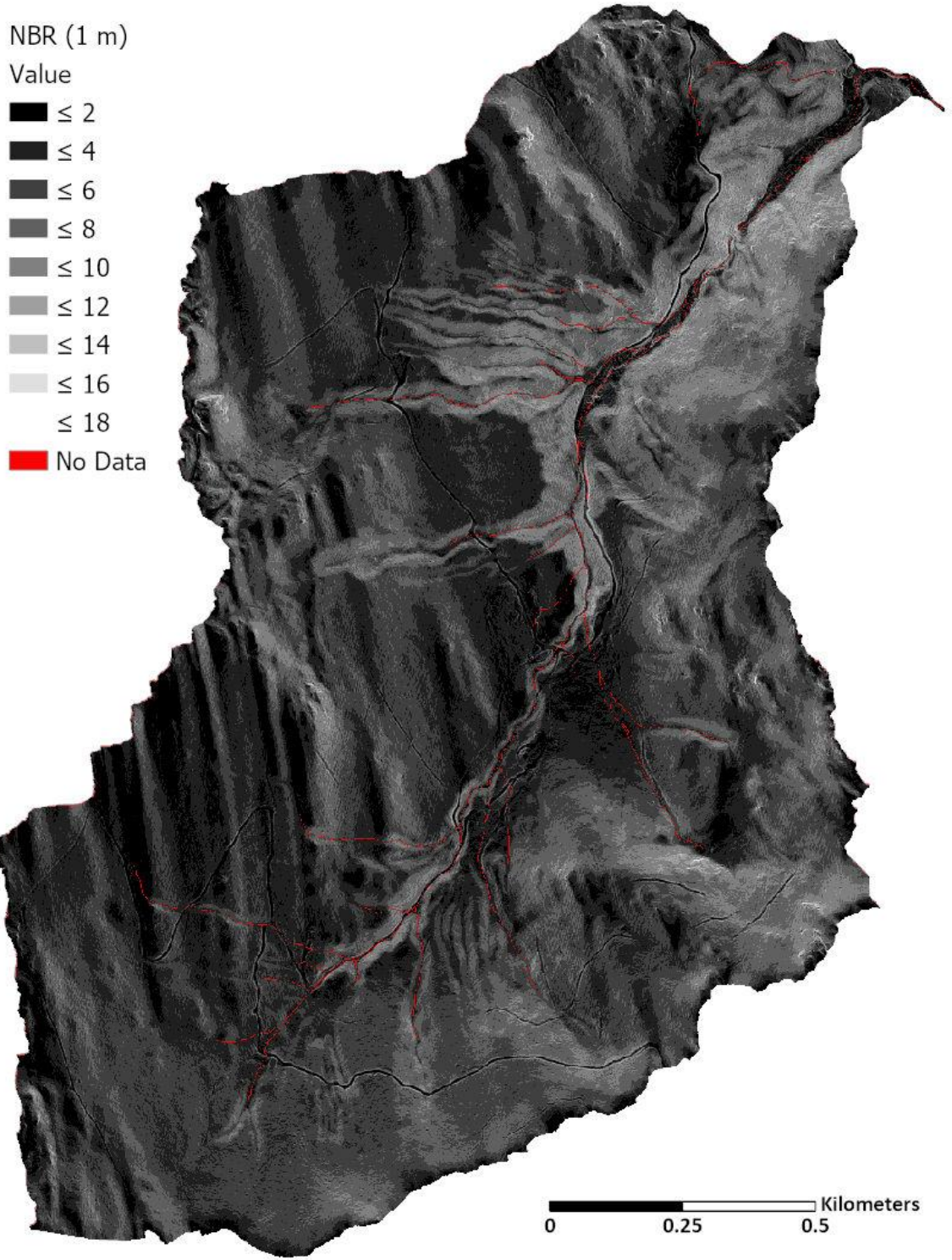
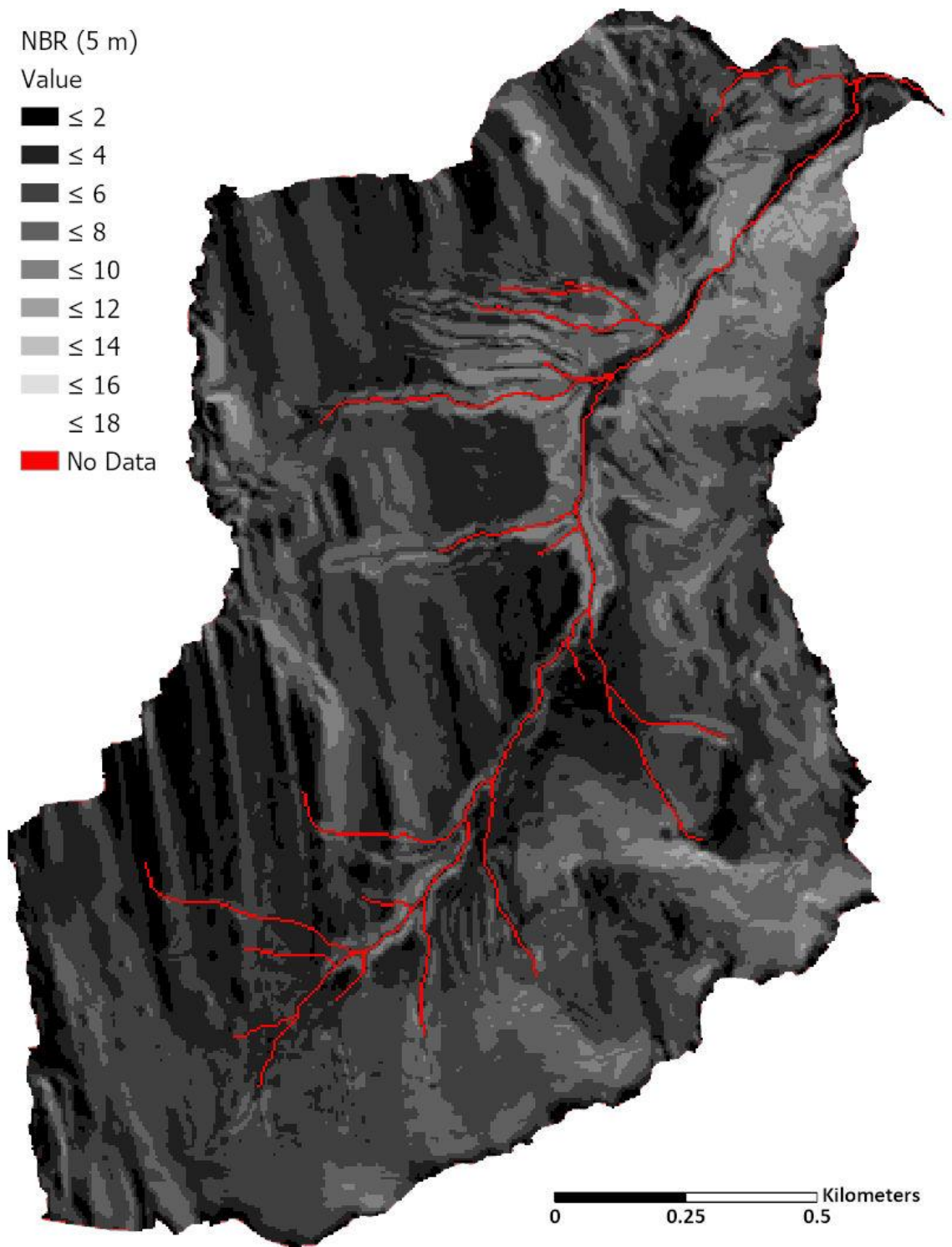
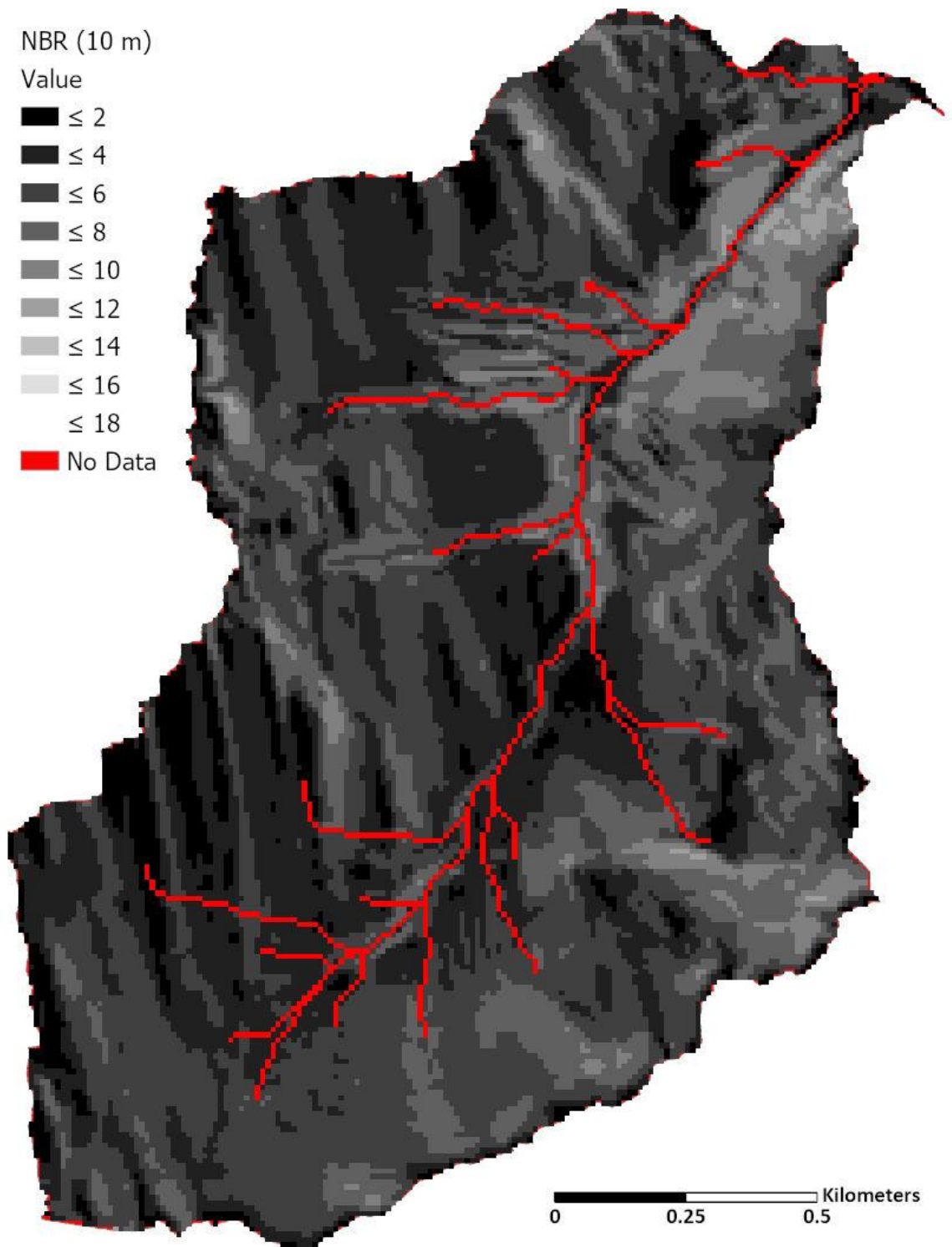


Figure 55. S factor with the NBR method for Site D at 1 m.



**Figure 56.** S factor with the NBR method for Site D at 5 m.



**Figure 57.** S factor with the NBR method for Site D at 10 m.

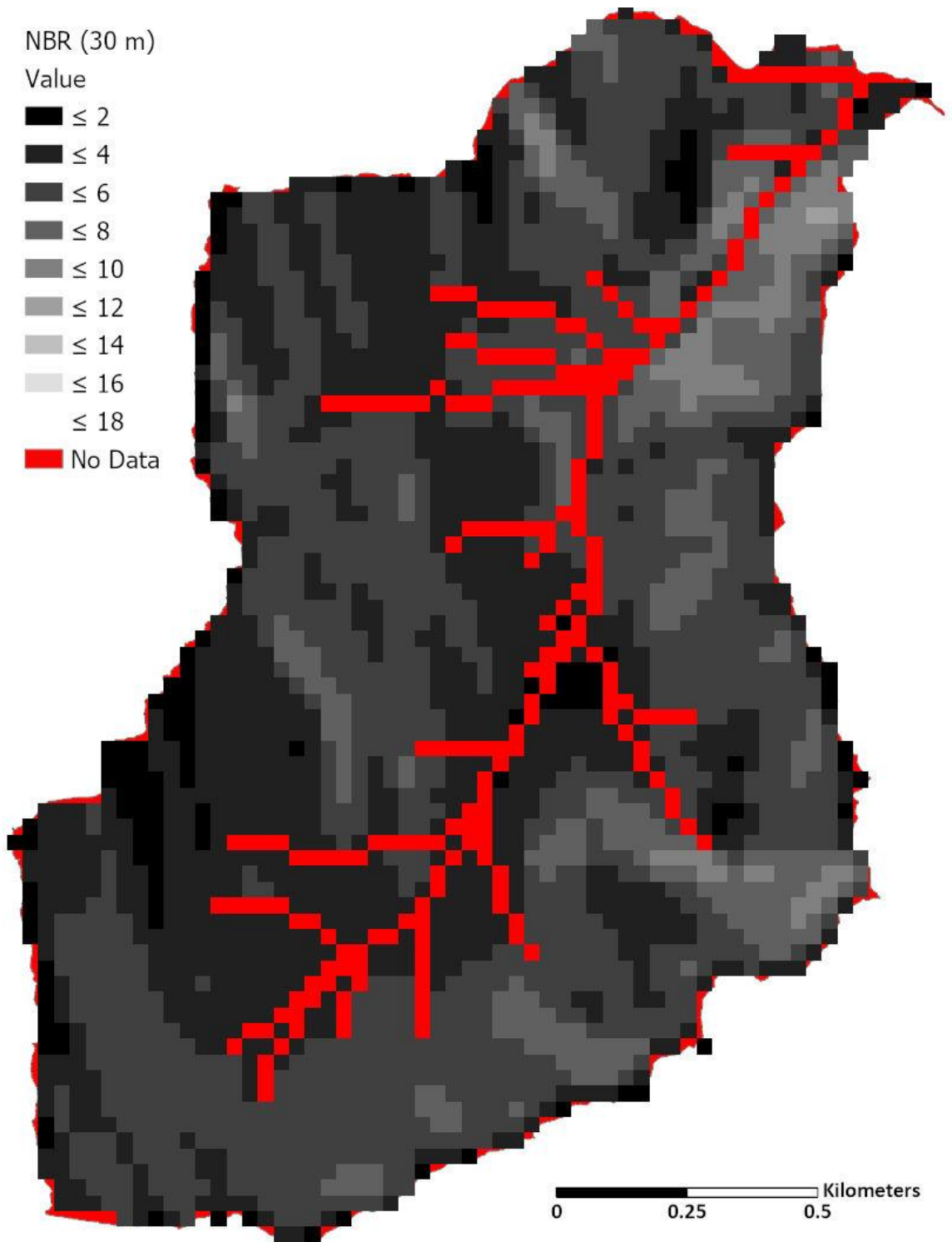


**Figure 58.** S factor with the NBR method for Site D at 30 m.

The MDS method produces higher maximum values which confirms existing understanding that the NBR method underestimates steep slopes. At coarse resolutions, the MDS method is more likely to produce higher maximum values than the NBR method. However, the MDS does not always produce lower minimum values. Minimum values stay relatively similar until 30 m resolutions where the MDS method produces significantly larger minimum values than the NBR method for Sites A, B, and C. At coarse resolutions the landscape is smoothed over which means that local depressions that could have been picked up with the MDS method at fine resolutions, but averaged by the NBR method, are lost. This significantly raises the minimum values calculated by the MDS method.

Difference rasters across the DEM resolutions highlights where the MDS method typically produces higher S values along ridges and the start of the slopes where the NBR method most strongly underestimates slope steepness and produces lower S values (**Figures 59 - 62**). The NBR method appears to produce higher S values around drainage channels and concave depressions or slopes where this method overestimates slope angle. This is due to the NBR method's choice of calculating slope by averaging using all the surrounding cell's neighbors.

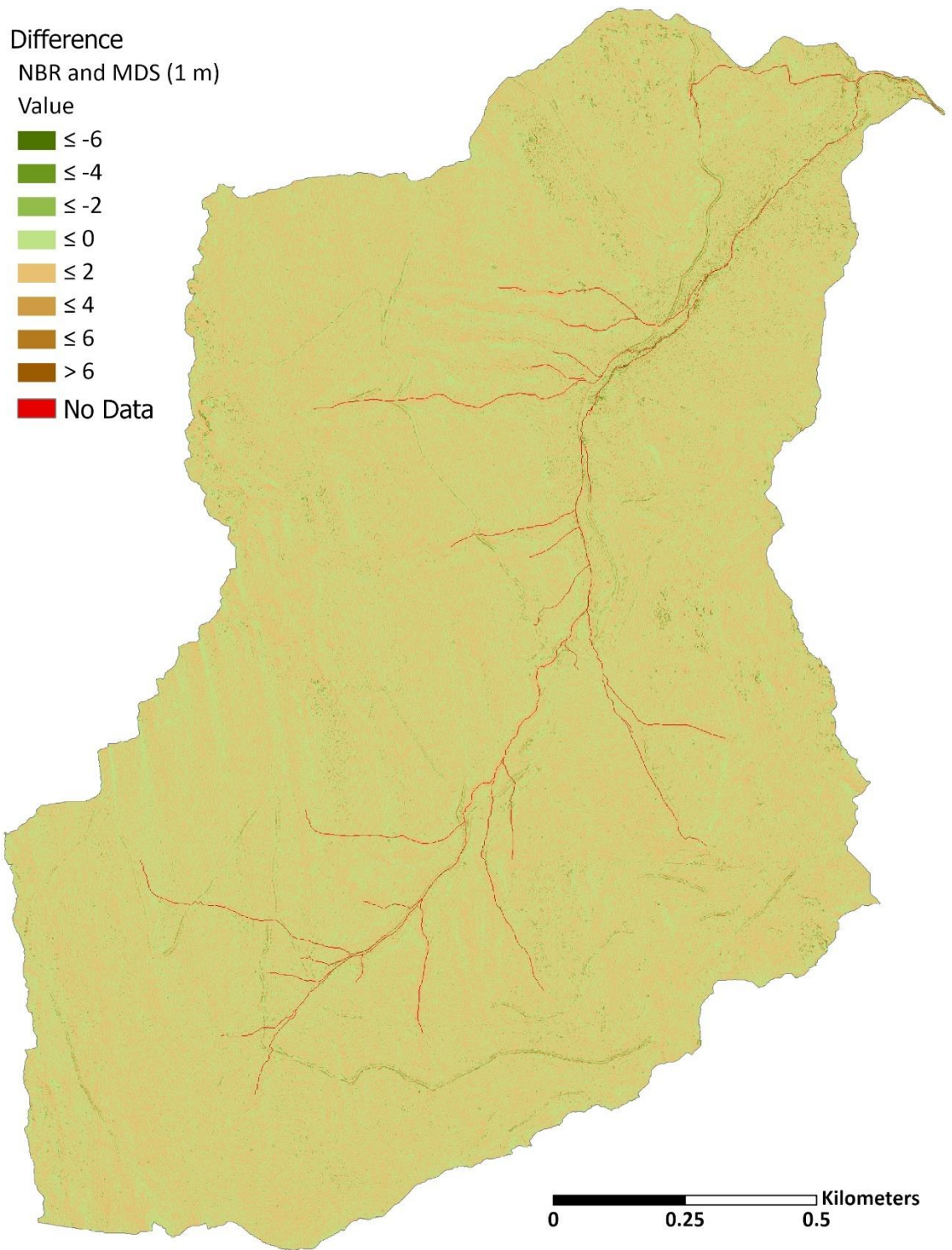


**Figure 59.** Site D difference raster (1 m) for the S Factor of the MDS method subtracted from the NBR method.

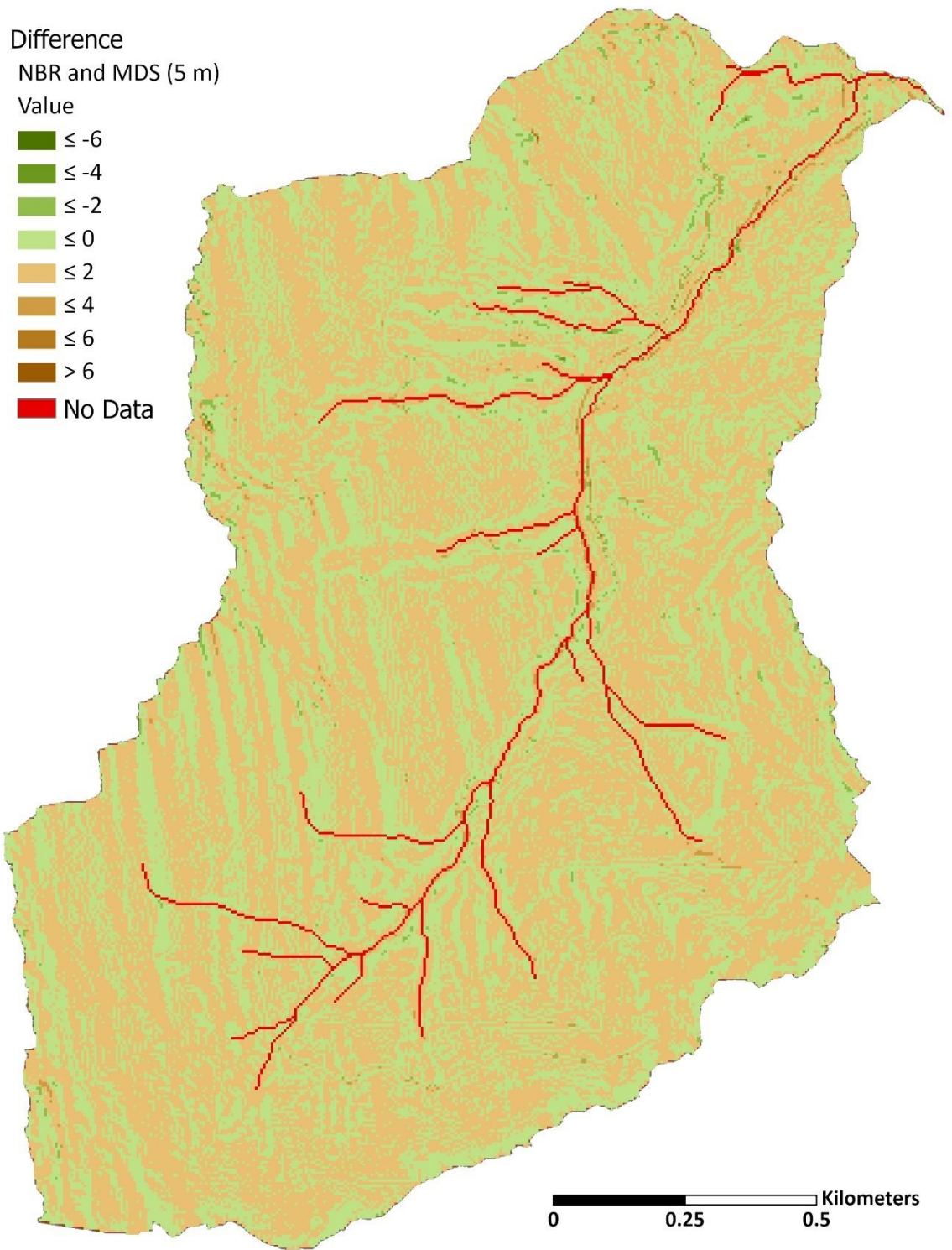


**Figure 60.** Site D difference raster (5 m) for the S Factor of the MDS method subtracted from the NBR method.

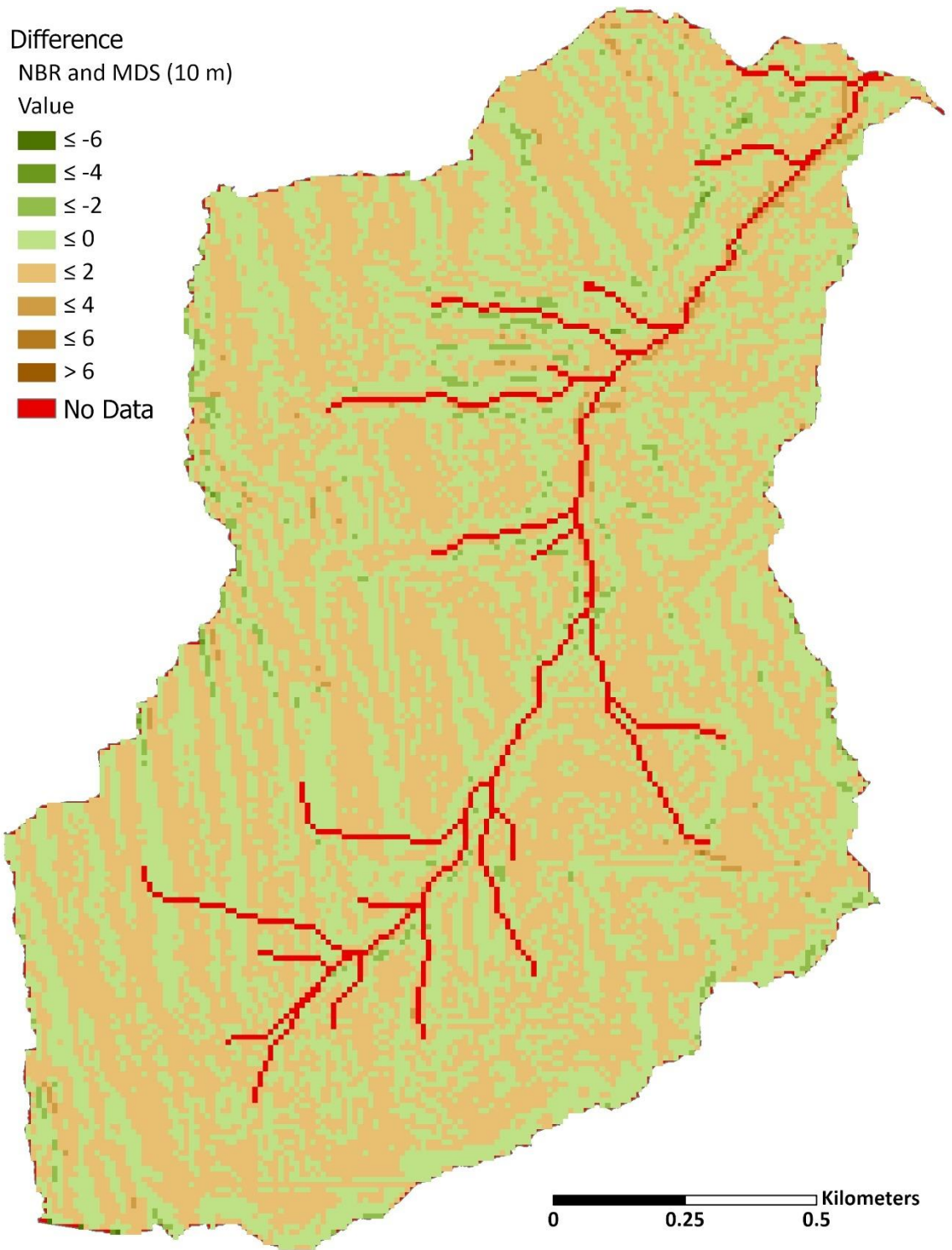


**Figure 61.** Site D difference raster (10 m) for the S Factor of the MDS method subtracted from the NBR method.

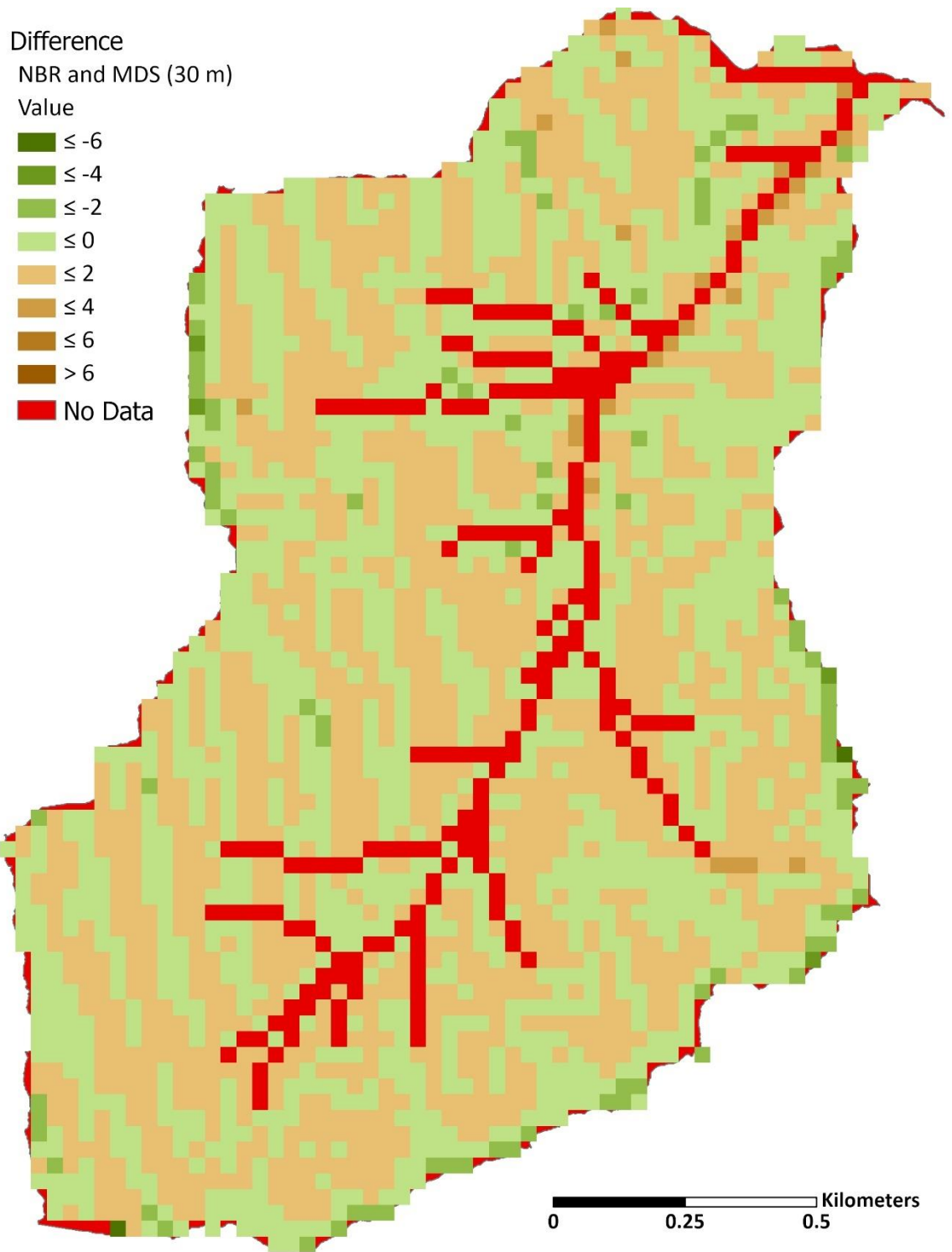


**Figure 62.** Site D difference raster (30 m) for the S Factor of the MDS method subtracted from the NBR method.

## CHAPTER VI

### DISCUSSION AND FURTHER RESEARCH

#### Discussion

Soil erosion models aid land managers and policy makers in the use, management, and conservation of soil resources. Understanding the differences in method choices when producing RUSLE estimates helps to discern the validity and confidence in the estimates provided. RUSLE estimates that incorporate the CA method could improperly influence policy and land management decisions, especially when used in economic models that estimate the cost of soil erosion. For example, Telles et al. (2013) estimates that soil erosion costs the US 44 billion dollars a year.

Using the CA method for the L factor cannot be recommended without extensive research comparing L values to real world erosion rates, as its calculation fundamentals are outside the construction of the RUSLE model. Using this on large sites and sites with great elevation change increases the magnitude of area available and produces much higher L values than what is seen in small sites with little elevation change. The weight of the L factor is changed by using area that was not accounted for in the original construction of this model. Since RUSLE is concerned with the erosion of soil across the land surface and is not applicable to other erosional processes, the CA method could be overestimating the L factor's influence on erosion estimates by using area and allowing convergence to dominate the output rather than slope length. If analysts do not clearly

define drainage channels, outlets, and other areas where this model is not applicable, then the CA method will greatly exaggerate soil erosion estimates and improperly represent RUSLE erosional process. Differences between using the GC and the CA method grow as the size of the study area enlarges, landscape complexity increases, and the number of drainage channels increase. For large and complex sites especially, the GC method is strongly advised since the CA method will produce very high L factor values.

The slope cutoff variable should be used with the GC method, especially at resolutions less than or equal to 5 m. While the range in values are similar, the spatial distribution and occurrence of lower values around slope steepness changes is statistically different at these fine resolutions. Once the landscape loses its microfeatures at resolutions of 10 m or greater, there is a low chance that outputs incorporating slope cutoff will be statistically different at the 1% significance level. This helps to refine where in the landscape the greatest risk of erosion is occurring by reducing the occurrence of high L estimates on long slopes that would accumulate length and therefore produce high L values. Using the slope cutoff variable identifies where in these long slopes that a change in slope steepness occurs and initiates deposition, otherwise these areas would result with higher L values and overestimate erosion. If a local expert of the site is available, then the use of a slope cutoff value can be assessed.

The MDS method is recommended for slope calculations, particularly at fine resolutions. This method retains landscape variability and creates more realistic estimates related to slope steepness. Small scale features such as roads and cattle trails were still detectable at a 5 m resolution, while many were lost using the NBR method. The NBR method underestimates slope at ridges and produces lower S factor values while overestimating in flatter regions. The MDS is superior at fine resolutions to capture micro features while also being more resilient to the smoothing effects of decreased resolutions at 5 or 10 m. If possible, its recommended to use resolutions finer than 30 m due to the dramatic effect that this coarse resolution has on slope values. At this coarse of a resolution, there may also not be statistical significance between using the MDS and NBR method, as using coarse resolutions reduces the differences between the two methods.

Overall, very fine resolution does not necessarily produce the best outputs. A resolution of 5 m is recommended for most uses since it is still able to detect fine scale features that alter flow in the landscape while using the MDS method for the S factor and the GC method with slope cutoff for the L factor. This resolution allows for meaningful interpretation of the spatial distribution of erosion without showing an overwhelming amount of variation in the values across the site that can make visual interpretation difficult. A 1 m resolution can be too fine, producing a very busy L factor output. This makes it difficult to interpret the spatial distribution of where high vs low erosion estimates are occurring most prominently in the landscape. It is also possible

that a 1 m resolution is so fine that it is picking up small-scale ephemeral erosion patterns rather than established and consistent landscape pattern of erosion. Coarse resolutions lose fine scale variability and smooth the landscape too much to produce meaningful outputs.

The research done in this project is a valuable resource that provides a cohesive comparison of these methods across multiple sites and DEM resolutions. Researchers can use this to guide efforts in undertaking these other future research paths.

#### Further Research

Further research looking at terrain differences in L and S estimates from these varying methods between gentle slopes and complex steep slopes would aid in further verifying terrain influence on outputs. The differences between 1 and 5 m resolutions should also be further investigated on smaller, easy to study plots, observed over a longer time period, to determine if the spatial patterns of erosion being depicted at the 1 m resolution is more or less representative of long-term and established erosion patterns for the plot than the 5 m resolution.

The code to calculate the L factor using the GC method will be made publicly available. Future researchers will be able to use this to continue developing this method. Recommendations for development are improving run time for calculating cumulative slope length and further research on the slope steepness trigger for the slope cutoff variable. Specifically, the slope cutoff variable can be set differently for

slopes less than 5 percent and slopes greater than or equal to 5 percent. It would be beneficial research to observe the differences changing this 5 percent trigger to 9 percent trigger to mirror the slope steepness calculation differences used by the S factor.

Availability of these methods as built-in GIS tools would greatly aid in the availability, understanding, and use of these methods for soil erosion estimates and other terrain modelling needs. Alternate methods of calculating slope angle would be the easiest to implement, as the structure already exists for slope angle calculation as built-in tools. The most helpful advantage by implementing all of these methods as built-in GIS tools is the reliable source of proper documentation detailing how and why to use each method.

Perhaps the most influential research that can be done for this model now would require real world soil erosion measures. Real soil erosion data measuring the movement of soil over the landscape of multiple sites is needed to compare against L and S estimates using each method. No existing data could be found, and even the data used to create the original USLE model has been lost. Further, the size of the plots originally used are not representative to the sizes of areas that this model is now regularly being applied to. Collecting these data would require huge resource and time dedication that was far outside the scope of this project.

## BIBLIOGRAPHY

- Angulo-Martínez, M., and S. Beguería. 2009. Estimating rainfall erosivity from daily precipitation records: A comparison among methods using data from the Ebro Basin (NE Spain). *Journal of Hydrology* 379 (1–2):111–121.  
<http://dx.doi.org/10.1016/j.jhydrol.2009.09.051>.
- Beguería, S., R. Serrano-Notivoli, and M. Tomas-Burguera. 2018. Computation of rainfall erosivity from daily precipitation amounts. *Science of the Total Environment* 637–638:359–373. <https://doi.org/10.1016/j.scitotenv.2018.04.400>.
- Bob's Slope Page. 2009. RUSLE Calculations.  
<http://www.onlinegeographer.com/slope/slope.html> (last accessed 6 March 2019).
- Bowen, J. T., and N. B. Hultquist. 2013. Compressing Nature: The Development of the Export Hay Industry in the Western United States. *Yearbook of the Association of Pacific Coast Geographers* 75 (1):83–103.
- D. K. McCool, L. C. Brown, G. R. Foster, C. K. Mutchler, and L. D. Meyer. 1989. Revised Slope Length Factor for the Universal Soil Loss Equation. *Transactions of the ASAE* 32 (5): 1571–1576.
- Desmet, P. J. J., and G. Govers. 1996a. A GIS procedure for automatically calculating the USLE LS factor on topographically complex landscape units. *Journal of Soil and Water Conservation* 51:427–433. <http://www.jswnonline.org/content/51/5/427.full.pdf+html>.
- . 1996b. Comparison of routing algorithms for digital elevation models and their implications for predicting ephemeral gullies. *International Journal of GIS* 10 (3):311–331.
- Di Stefano, C., and V. Ferro. 2016. Establishing soil loss tolerance: An overview. *Journal of Agricultural Engineering* 47 (3):127–133.
- Di Stefano, C., V. Ferro, and V. Pampalone. 2017. Applying the USLE Family of Models at the Sparacia (South Italy) Experimental Site. *Land Degradation and Development* 28 (3):994–1004.
- Dunn, M., and R. Hickey. 1998. The effect of slope algorithms on slope estimates within a GIS. *Cartography* 27 (1):9–15.  
<http://www.tandfonline.com/doi/abs/10.1080/00690805.1998.9714086>.

- ESRI. 2018a. Flow Accumulation. <https://pro.arcgis.com/en/pro-app/tool-reference/spatial-analyst/flow-accumulation.htm> (last accessed 30 April 2020).
- . 2018b. Flow Direction. <http://desktop.arcgis.com/en/arcmap/latest/tools/spatial-analyst-toolbox/flow-direction.htm> (last accessed 21 February 2019).
- . 2018c. How Slope Works. <http://desktop.arcgis.com/en/arcmap/10.3/tools/spatial-analyst-toolbox/how-slope-works.htm> (last accessed 6 March 2019).
- . 2018d. LAS Dataset To Raster (Conversion). <https://pro.arcgis.com/en/pro-app/tool-reference/conversion/las-dataset-to-raster.htm> (last accessed 20 May 2020).
- Fairfield, J., and P. Leymarie. 1991. Drainage networks from grid digital elevation models. *Water Resources Research* 27 (5):709–17.
- Ferro, V., P. Porto, and B. Yu. 1999. A comparative study of rainfall erosivity estimation for southern Italy and southeastern Australia. *Hydrological Sciences Journal* 44 (1):3–24.
- Foster, G. R., and W. H. Wischmeier. 1974. Evaluating Irregular Slopes for Soil Loss Prediction. *Transactions of the ASAE* 17 (2):305–309. <http://www.scopus.com/inward/record.url?eid=2-s2.0-0016035813&partnerID=40&md5=f9e25c6a6c0aa3250bff5639d327fcce>.
- Freeman, T. G. 1991. Calculating catchment area with divergent flow based on a regular grid. *Computers and Geosciences* 17 (3):413–22.
- Fu, S., L. Cao, B. Liu, Z. Wu, and M. R. Savabi. 2015. Effects of DEM grid size on predicting soil loss from small watersheds in China. *Environmental Earth Sciences* 73 (5):2141–2151. <http://link.springer.com/10.1007/s12665-014-3564-3>.
- Ganasri, B. P., and H. Ramesh. 2016. Assessment of soil erosion by RUSLE model using remote sensing and GIS - A case study of Nethravathi Basin. *Geoscience Frontiers* 7 (6):953–961. <http://dx.doi.org/10.1016/j.gsf.2015.10.007>.
- GDAL. 2020. gdaldem. <https://gdal.org/programs/gdaldem.html> (last accessed 26 May 2020)

- Gilley, J. E., and D. C. Flanagan. 2007. Early investment in soil conservation research continues to provide dividends. *Transactions of the ASABE* 50 (5):1595–1601. [http://www.ars.usda.gov/SP2UserFiles/ad\\_hoc/36021500WEPP/Gilley\\_Flanagan\\_2007a.pdf](http://www.ars.usda.gov/SP2UserFiles/ad_hoc/36021500WEPP/Gilley_Flanagan_2007a.pdf).
- GRASS. 2020. r.slope.aspect. <https://grass.osgeo.org/grass78/manuals/r.slope.aspect.html> (last accessed 26 May 2020).
- Hickey, R. 2000. Slope angle and slope length solutions for GIS. *Cartography* 29 (1):1–8.
- Hickey, R., A. Smith, and P. Jankowski. 1994. Slope length calculations from a DEM within ARC/INFO grid. *Computers, Environment and Urban Systems* 18 (5):365–380.
- Horn, B. K. P. 1981. Hill Shading and the Reflectance Map. *Proceedings of the IEEE* 69 (1):14–47.
- Irfan Ashraf, M., Z. Zhao, C. P. A. Bourque, and F. R. Meng. 2012. GIS-evaluation of two slope-calculation methods regarding their suitability in slope analysis using high-precision LiDAR digital elevation models. *Hydrological Processes* 26 (8):1119–1133.
- Jabbar, M. 2003. Application of gis to estimate soil erosion using rusle. *Geo-Spatial Information Science* 6 (1):34–37.
- Karydas, C. G., P. Panagos, and I. Z. Gitas. 2014. A classification of water erosion models according to their geospatial characteristics. *International Journal of Digital Earth* 7 (3):229–250. <http://www.tandfonline.com/doi/abs/10.1080/17538947.2012.671380>.
- Kottek, M., J. Grieser, C. Beck, B. Rudolf, and F. Rubel. 2006. World Map of the Köppen-Geiger climate classification updated. *Meteorologische Zeitschrift* 15 (3):259–263. [http://www.schweizerbart.de/papers/metz/detail/15/55034/World\\_Map\\_of\\_the\\_Kopp en\\_Geiger\\_climate\\_classificat?af=crossref](http://www.schweizerbart.de/papers/metz/detail/15/55034/World_Map_of_the_Kopp en_Geiger_climate_classificat?af=crossref).
- Lafren, J. M., and D. C. Flanagan. 2013. The development of U. S. soil erosion prediction and modeling. *International Soil and Water Conservation Research* 1 (2):1–11. [http://dx.doi.org/10.1016/S2095-6339\(15\)30034-4](http://dx.doi.org/10.1016/S2095-6339(15)30034-4).
- Lafren, J. M., and W. C. Moldenhauer. 2003. *Pioneering Soil Erosion Prediction: The USLE Story*.
- Lea, N. 1992. An aspect driven kinematic routing algorithm. In *Overland Flow: Hydraulics and Erosion Mechanics*, ed. By A. Parsons and A. Abrahams, 374–388. Taylor & Francis.

Liu, H., J. Kiesel, G. Hörmann, and N. Fohrer. 2011. Effects of DEM horizontal resolution and methods on calculating the slope length factor in gently rolling landscapes. *Catena* 87 (3):368–375. <http://dx.doi.org/10.1016/j.catena.2011.07.003>.

Moore, I. D., and G. J. Burch. 1986. Modelling erosion and deposition: topographic effects. *Transactions of the ASAE* 29 (6):1624–30.

Nearing, M. A. 2001. Potential changes in rainfall erosivity in the US with climate change during the 21st century. *Journal of Soil and Water Conservation* 56 (3):229–32.

Nearing, M. A., S. qing Yin, P. Borrelli, and V. O. Polyakov. 2017. Rainfall erosivity: An historical review. *Catena* 157 (June):357–362.

OpenTopography. 2020. Find Topography Data. <https://portal.opentopography.org/datasets> (last accessed 9 2020).

Petkovšek, G., and M. Mikoš. 2004. Estimating the R factor from daily rainfall data in the sub-Mediterranean climate of southwest Slovenia. *Hydrological Sciences Journal* 49 (5).

Pimentel, D., C. A. Harvey, P. Resosudarmo, K. Sinclair, D. Kurz, M. Mcnair, S. Crist, L. Shpritz, L. Fitton, R. Saffouri, and others. 1995. Environmental and Economic Costs of Soil Erosion and Conservation Benefits. *Science* 267 (5201):1117–1123.

Quinn, P., K. Beven, P. Chevallier, and O. Planchon. 1991. The Prediction of Hillslope Flow Paths for Distributed Hydrological Modelling using Digital Terrain Models. *Hydrological Processes* 5 (i):59–79.

Raj, A. R., J. George, S. Raghavendra, S. Kumar, and S. Agrawal. 2018. Effect of Dem Resolution on Ls Factor Computation. *International Archives of the Photogrammetry, Remote Sensing & Spatial Information Sciences* (January).

Renard, K., G. Foster, G. Weesies, D. McCool, and D. Yoder. 1997. Predicting soil erosion by water: a guide to conservation planning with the Revised Universal Soil Loss Equation (RUSLE). *Agricultural Handbook No. 703* :404. [http://www.ars.usda.gov/SP2UserFiles/Place/64080530/RUSLE/AH\\_703.pdf](http://www.ars.usda.gov/SP2UserFiles/Place/64080530/RUSLE/AH_703.pdf).

Renard, K. G., and J. R. Freimund. 1994. Using monthly precipitation data to estimate the R-factor in the revised USLE. *Journal of Hydrology*.

SAGA. 2003. Module LS Factor. [http://www.saga-gis.org/saga\\_tool\\_doc/2.1.4/ta\\_hydrology\\_22.html](http://www.saga-gis.org/saga_tool_doc/2.1.4/ta_hydrology_22.html) (last accessed 25 May 2020).

- Segura, C., G. Sun, S. McNulty, and Y. Zhang. 2014. Potential impacts of climate change on soil erosion vulnerability across the conterminous United States. *Journal of Soil and Water Conservation* 69 (2):171–81.
- Suhua, F., W. Zhiping, L. Baoyuan, and C. Longxi. 2013. Comparison of the Effects of the Different Methods for Computing the Slope Length Factor at a Watershed Scale. *International Soil and Water Conservation Research* 1 (2):64–71.
- Tarboton, D. G. 1997. A new method for the determination of flow directions and upslope areas in grid digital elevation models. *Water Resources Research* 33 (2):309–19.
- Telles, T. S., S. C. F. Dechen, L. G. Antonio de Souza, and M. de F. Guimarães. 2013. Valuation and assessment of soil erosion costs. *Scientia Agricola* 70 (3):209–216. [http://www.scielo.br/scielo.php?script=sci\\_arttext&pid=S0103-90162013000300010&lng=en&tlng=en](http://www.scielo.br/scielo.php?script=sci_arttext&pid=S0103-90162013000300010&lng=en&tlng=en).
- Telles, T. S., M. D. F. Guimarães, and S. C. F. Dechen. 2011. The Cost of Soil Erosion - Literature Review. *SciELO Analytics* 35 (2):287–298. [http://www.scielo.br/scielo.php?script=sci\\_arttext&pid=S0100-06832011000200001&lng=en&tlng=en](http://www.scielo.br/scielo.php?script=sci_arttext&pid=S0100-06832011000200001&lng=en&tlng=en).
- United States Department of Agriculture. 2013. Science Documentation Revised Universal Soil Loss Equation Version 2. [https://www.ars.usda.gov/ARSUserFiles/60600505/RUSLE/RUSLE2\\_Science\\_Doc.pdf](https://www.ars.usda.gov/ARSUserFiles/60600505/RUSLE/RUSLE2_Science_Doc.pdf) (last accessed 12 December 2019).
- — —. 2016. USLE History. <https://www.ars.usda.gov/midwest-area/west-lafayette-in/national-soil-erosion-research/docs/usle-database/usle-history/> (last accessed 7 February 2019).
- United States Geological Survey. n.d. TNM Download (v1.0). <https://viewer.nationalmap.gov/basic/> (last accessed 9 June 2020).
- Van Remortel, R. D., M. E. Hamilton, and R. J. Hickey. 2001. Estimating the LS factor for RUSLE through iterative slope length processing of DEM elevation data. *Cartography* 30 (1):27–35. <http://www.mappingsciences.org.au/journal.htm>.
- Van Remortel, R. D., R. W. Maichle, and R. J. Hickey. 2004. Computing the LS Factor for the RUSLE through array based slope processing of digital elevation data using a C++ executable. *Computers & geosciences* (April):1043–1053.

- Wang, G., Fang, S., Shinkareva, S., Gertner, G., Anderson, A. 2002. Spatial uncertainty in prediction of the topographical factor for the revised universal soil loss equation (RUSLE). *Transactions of the American Society of Agricultural Engineers* 45 (1):109–118. [https://www.researchgate.net/publication/275515101\\_Spatial\\_prediction\\_and\\_uncertainty\\_analysis\\_of\\_topographic\\_factors\\_for\\_the\\_Revised\\_Universal\\_Soil\\_Loss\\_Equation\\_RUSLE](https://www.researchgate.net/publication/275515101_Spatial_prediction_and_uncertainty_analysis_of_topographic_factors_for_the_Revised_Universal_Soil_Loss_Equation_RUSLE).
- Warren, S. D., H. Mitasova, K. Auerswald, and M. G. Hohmann. 2004. An evaluation of methods to determine slope using digital elevation data. *Catena* 58 (3):215–233.
- Washington State Department of Natural Resources. n. d. Washington LiDAR Portal. <https://lidarportal.dnr.wa.gov/> (last accessed 9 June 2020).
- Western Regional Climate Center. n.d. Climate Summaries. <https://wrcc.dri.edu/summary/Climismwa.html> (last accessed 9 June 2020).
- Wilson, J. P., C. S. Lam, and Y. Deng. 2007. Comparison of the performance of flow-routing algorithms used in GIS-based hydrologic analysis. *Hydrological Processes* 21 (8):1026–1044. <http://jamsb.austms.org.au/courses/CSC2408/semester3/resources/ldp/abs-guide.pdf>.
- Winchell, M. F., S. H. Jackson, A. M. Wadley, and R. Srinivasan. 2008. Extension and validation of a geographic information system-based method for calculating the Revised Universal Soil Loss Equation length-slope factor for erosion risk assessments in large watersheds. *Journal of Soil and Water Conservation* 63 (3):105–111.
- Wischmeier, W., and D. Smith. 1978. *Predicting Rainfall Erosion Losses: A Guide to Conservation Planning*. (Agriculture Handbook No. 537). <https://naldc.nal.usda.gov/download/CAT79706928/PDF>.
- Yang, X. 2015. Digital mapping of RUSLE slope length and steepness factor across New South Wales, Australia. *Soil Research* 53 (2):216.
- Yu, B., G. M. Hashim, and Z. Eusof. 2001. Estimating the R-factor with limited rainfall data: A case study from peninsular Malaysia. *Journal of Soil and Water Conservation* 56 (2):101–5.
- Yu, B., and C. J. Rosewell. 1996. A Robust estimator of the R-factor for the universal soil loss equation. *Transactions of the ASAE* 39 (2):559–61.
- Zevenbergen, L. W., and C. R. Thorne. 1987. Quantitative analysis of land surface topography. *Earth Surface Processes and Landforms* 12 (1):47–56.

Zhang, H., J. Wei, Q. Yang, J. E. M. Baartman, L. Gai, X. Yang, S. Q. Li, J. Yu, C. J. Ritsema, and V. Geissen. 2017. An improved method for calculating slope length ( $\lambda$ ) and the LS parameters of the Revised Universal Soil Loss Equation for large watersheds. *Geoderma* 308 (December 2016):36–45. <http://dx.doi.org/10.1016/j.geoderma.2017.08.006>.

Zhang, H., Q. Yang, R. Li, Q. Liu, D. Moore, P. He, C. J. Ritsema, and V. Geissen. 2013. Extension of a GIS procedure for calculating the RUSLE equation LS factor. *Computers and Geosciences* 52:177–188. <http://dx.doi.org/10.1016/j.cageo.2012.09.027>.

Zhang, X., N. A. Drake, J. Wainwright, and M. Mulligan. 1999. Comparison of slope estimates from low resolution dems: Scaling issues and a fractal method for their solution. *Earth Surface Processes and Landforms* 24 (9):763–779.

## APPENDIXES

### Appendix A - Code

Script 1: L with GC method, S with MDS method

*# Written by Amanda Moody, Central Washington University, Ellensburg, WA. 2019.*

*Provided freely "as is."*

*# RUSLE L Factor calculation according to the RUSLE Handbook (Renard et al. 1997) and following the Grid Cumulation (GC)*

*# method for calculating slope length originally proposed by Hickey et al. (1994) for USLE.*

*# Original RUSLE based AML code published by Van Remortel et al. (2001). Major revisions include no longer using*

*# ESRI focal flow tool to define high points and updating the non-cumulative slope length (NCSL) calculations for*

*# high points. S Factor calculation uses the Max. Downhill Slope method (Hickey 2000).*

*# It is highly recommended to run code with a 64-bit download of python and a solid state hard drive.*

*# If unsure open python command line and read the top line of code to determine if you are using 32 or 64-bit python.*

*### Navigation ### approx. lines*

*# Maximum Downhill Slope calculation (MDS) - LINE 114*

*# S Factor calculation - LINE 191*

*# L Factor components - line 222*

*# NCSL - LINE 223*

*# CDHSL - LINE 333*

*# L Factor Calculation - LINE 539*

**import** arcpy, numpy, math, time, sys

arcpy.AddMessage("Beginning process at " + time.ctime())

myRaster = arcpy.GetParameterAsText(0) *# input DEM*

outputL = arcpy.GetParameterAsText(1) *# output location for L factor raster*

outputS = arcpy.GetParameterAsText(2) *# output location for S factor raster*

outputSlope = arcpy.GetParameterAsText(3) *# output location for slope raster (no slope will equal 0 degrees)*

*# slope cutoff angles for slopes less than 5% and those greater or equal to 5%*

less5 = float(arcpy.GetParameterAsText(4)) *# if unsure, recommended value .5*

great5 = float(arcpy.GetParameterAsText(5)) *# if unsure, recommended value .5*

*# this is the percent of max flow accumulation value to designate defined channels (where RUSLE is not applicable)*

*# rule of thumb for stream threshold is 1% while 100% would nullify this variable*

```

threshold = float(arcpy.GetParameterAsText(6)) # if unsure, .5 for more aggressive
channel definition,
# 1 for general stream channels, or 100 if you don't want this to influence results

# custom raise statement for inappropriate inputs by the user
class InputError(Exception):
    pass

if less5 < 0 or less5 > 1:
    raise InputError("Invalid slope cutoff value. Please input a value between 0 and 1.")

if great5 < 0 or great5 > 1:
    raise InputError("Invalid slope cutoff value. Please input a value between 0 and 1.")

if threshold < 0 or threshold > 100:
    raise InputError("Invalid defined channel threshold value. Please input a value
between 0 and 100.")

# get working raster's info. to use when turning l factor array into a raster
desc = arcpy.Describe(myRaster)
sr = desc.spatialReference
lLeft = desc.extent.lowerLeft
cSize = arcpy.Raster(myRaster).meanCellHeight
units = sr.linearUnitName

# units must be either feet or meters, output l factor will be in the same units as DEM.
while RUSLE guidelines use
# feet, users continue l factor calculation with meters as that is the international system
of measurement for length.
if "Feet" in units or "Foot" in units or "Meter" in units:
    pass
else:
    raise InputError("Invalid linear unit. Please input a DEM using feet or meters.")

### Step: Define Functions ###
# buffer edge cells to nodata (can't know true value at edge cells, missing surrounding
spatial info.) for any function
# that uses surrounding cells to calculate center cell value
def noDataBuff(noArray, topLeft, bottomRight):
    noArray[:, topLeft] = -9999 # first column starts at 0
    noArray[topLeft, :] = -9999 # first row starts 0
    noArray[:, (nCols - bottomRight)] = -9999 # last column in array is the # of columns - 1

```

*(0 indexed)*

```
noArray[(nRows - bottomRight), :] = -9999 # last row in array is the # of row - 1 (0 indexed)
```

*# locate and define new row and col for a specific neighboring cell. example, neighbor cell above origin cell has*

*# coordinates originRow-1, originCol. if no change for row/col use 0. used in "Step: Calc NCSL" and "Step: Calc CDHSL"*

```
def nbrCell(originRow, originCol, nbrRow, nbrCol):
```

```
  varR = originRow + nbrRow
```

```
  varC = originCol + nbrCol
```

```
  if varR < 0 or varR == nRows:
```

```
    return "Invalid"
```

```
  elif varC < 0 or varC == nCols:
```

```
    return "Invalid"
```

```
  else:
```

```
    return varR, varC
```

*# calc. a cell's S Factor value, input cell slope in degrees and percent*

```
def sCalc(slope, percent):
```

```
  if percent < 9:
```

```
    sValue = 10.8 * (math.sin(math.radians(slope))) + 0.03
```

```
  elif percent >= 9:
```

```
    sValue = 16.8 * (math.sin(math.radians(slope))) - 0.50
```

```
  return sValue
```

*# calc. a cell's L Factor value, input the slope angle, length, and if unit plot is 22.13 (m) or 72.6 (ft)*

```
def Lcalc(slopeVar, lengthVar, unit):
```

```
  beta =
```

```
(math.sin(math.radians(slopeVar))/0.0896)/(3*((math.sin(math.radians(slopeVar)))**0.8)+0.56)
```

```
  m = (beta/(1+beta))
```

```
  if "Foot" in units or "Feet" in units:
```

```
    lValue = (lengthVar/72.6)**m
```

```
  elif "Meter" in units:
```

```
    lValue = (lengthVar/22.13)**m
```

```
  return lValue
```

*# calculate slope percent used in "Step: Calc S Factor" and "Step: Calc CDHSL"*

```
def slopePerc(value):
```

```
  return (math.tan(math.radians(value))*100)
```

```

arcpy.CheckOutExtension("Spatial")
### Step: fill DEM ###
fillRaster = arcpy.sa.Fill(myRaster)

### Step: Calc flow direction using D8 algorithm (ESRI 2019 Flow Direction) ###
arcpy.AddMessage("Getting flow direction.")
flowDir = arcpy.sa.FlowDirection(fillRaster, "FORCE")
# force edge cells to flow outwards to keep edge effect errors consistent across site
arcpy.CheckInExtension("Spatial")

### Step: Calc max. downhill slope angle (Dunn and Hickey 1998) ###
# Original code written by Dr. Sterling Quinn with some logic adapted from code posted
# by user FelixIP on StackExchange
# https://gis.stackexchange.com/questions/136715/getting-cell-value-along-flow-
# direction-using-arcpy
arcpy.AddMessage("Calculating maximum downhill slope angle.")

fDir = (1, 2, 4, 8, 16, 32, 64, 128)
rookDir = (1, 4, 16, 64)
diagDir = (2, 8, 32, 128)
# fdCol and fdRow are used from indexed fDir value to correctly reference cell in the
# flow direction
fdCol = (1, 1, 0, -1, -1, -1, 0, 1)
fdRow = (0, 1, 1, 1, 0, -1, -1, -1)

fDirArray = arcpy.RasterToNumPyArray(flowDir, "", "", "", -9999)

fAccD8 = arcpy.sa.FlowAccumulation(flowDir) # for defined channel threshold
del flowDir, myRaster

# this is the array shape of original DEM, used for any new array being built
nRows, nCols = fDirArray.shape
cTotal = nRows * nCols

elevArray = arcpy.RasterToNumPyArray(fillRaster, "", "", "", -9999)
del fillRaster

maxDHSArray = numpy.empty((nRows, nCols))

for nRow in range(nRows):
    for nCol in range(nCols):

```

```

# find elevation and flow direction of current cell at location nRow, nCol
elevPixel = elevArray[nRow, nCol]
if elevPixel == -9999: # nodata value
    maxDHSArray[nRow, nCol] = -9999
    continue

fDircPixel = fDircArray[nRow, nCol]
if fDircPixel == -9999:
    maxDHSArray[nRow, nCol] = -9999
    continue

# this indicates the pixel in the direction of fDircPixel's flow
i = fDirc.index(fDircPixel)
# get location of the comparing cell (the cell in the flow direction)
newRow = nRow + fdRow[i]
# this accounts for those instances where
# the flow direction points to a non-existent row outside raster coverage
if newRow < 0 or newRow == nRows:
    maxDHSArray[nRow, nCol] = -9999
    continue
newCol = nCol + fdCol[i]
if newCol < 0 or newCol == nCols:
    maxDHSArray[nRow, nCol] = -9999
    continue

# now the elevation of that comparing cell can be referenced
newElevPixel = elevArray[newRow, newCol]
# calculate the difference
elevDiff = elevPixel - newElevPixel

# calculate max downhill slope for current cell
# if comparing cell in diagonal direction then divide by orthogonal size
if fDircPixel in diagDirc:
    maxDHSArray[nRow, nCol] =
math.degrees(math.atan(float(elevDiff)/(1.4142*cSize)))
# if comparing cell in cardinal direction then divide by cell size
elif fDircPixel in rookDirc:
    maxDHSArray[nRow, nCol] = math.degrees(math.atan(float(elevDiff)/cSize))
else:
    maxDHSArray[nRow, nCol] = -9999

if outputSlope and outputSlope != "#":
    maxDHSraster = arcpy.NumPyArrayToRaster(maxDHSArray, lLeft, cSize, cSize, -9999)

```

```

arcpy.DefineProjection_management(maxDHSraster, sr)
maxDHSraster.save(outputSlope)
del maxDHSraster

# value = 0 change to 0.1. this allows for erosion in every cell without altering flow paths
(following the GC method)
maxDHSArray[maxDHSArray == 0] = 0.1
noDataBuff(maxDHSArray, 0, 1)

### Step: Calc S Factor ### following RUSLE guidelines (Agricultural Handbook No. 703)
# use the maximum downhill slope angle calculated previously because the
neighborhood method (ESRI 2019) averages
# slope from all neighbors and smooths the landscape and local variability
faccD8Array = arcpy.RasterToNumPyArray(fAccD8, "", "", "", -9999)
del fAccD8
flowAccD8Max = numpy.nanmax(faccD8Array)
streamsD8 = float(threshold / 100) * flowAccD8Max

if outputS and outputS != "#":
    arcpy.AddMessage("Calculating S Factor.")

    sFactorArray = numpy.empty((nRows, nCols))

    for nRow in range(nRows):
        for nCol in range(nCols):
            slope = maxDHSArray[nRow, nCol]
            slopeP = slopePerc((maxDHSArray[nRow, nCol]))
            faccPixel = faccD8Array[nRow, nCol]

            if slope == -9999:
                sFactorArray[nRow, nCol] = -9999
            elif faccPixel > streamsD8: # if location is designated as a "defined" channel,
RUSLE does not apply
                sFactorArray[nRow, nCol] = -9999
            else:
                sFactorArray[nRow, nCol] = sCalc(slope, slopeP)

    SFactor = arcpy.NumPyArrayToRaster(sFactorArray, lLeft, cSize, cSize, -9999)
    arcpy.DefineProjection_management(SFactor, sr)
    SFactor.save(outputS)
del sFactorArray, SFactor

```

```

### Step: L Factor Calc Components (GC Method)###
## Step: Calc NCSL ##
# NCSL for each cell calculated by flow direction and designation as a high point or flat
area
arcpy.AddMessage("Calculating non-cumulative slope length.")
NCSLArray = numpy.empty((nRows, nCols))

# loop through rasters high points and flow direction
for nRow in range(nRows):
    for nCol in range(nCols):

        fDircPixel = fDircArray[nRow, nCol]

        # set row and column locations for all cell neighbors around current cell, this helps
        # determines those cells
        # that have no inflow from their surrounding neighbors, according to the D8
        algorithm
        tCell = nbrCell(nRow, nCol, -1, 0)
        if tCell == "Invalid":
            tFD = -9999
        else:
            tFD = fDircArray[tCell]

        rCell = nbrCell(nRow, nCol, 0, 1)
        if rCell == "Invalid":
            rFD = -9999
        else:
            rFD = fDircArray[rCell]

        bCell = nbrCell(nRow, nCol, 1, 0)
        if bCell == "Invalid":
            bFD = -9999
        else:
            bFD = fDircArray[bCell]

        lCell = nbrCell(nRow, nCol, 0, -1)
        if lCell == "Invalid":
            lFD = -9999
        else:
            lFD = fDircArray[lCell]

        trCell = nbrCell(nRow, nCol, -1, 1)

```

```

if trCell == "Invalid":
    trFD = -9999
else:
    trFD = fDircArray[trCell]

tlCell = nbrCell(nRow, nCol, -1, -1)
if tlCell == "Invalid":
    tIFD = -9999
else:
    tIFD = fDircArray[tlCell]

brCell = nbrCell(nRow, nCol, 1, 1)
if brCell == "Invalid":
    brFD = -9999
else:
    brFD = fDircArray[brCell]

blCell = nbrCell(nRow, nCol, 1, -1)
if blCell == "Invalid":
    bIFD = -9999
else:
    bIFD = fDircArray[blCell]

# apply NCSL rules to write NSCLArray values
# if cell high point (no flow into it) then multiply by .5 to account for only length
downhill from center
if fDircPixel == -9999:
    NCSLArray[nRow, nCol] = -9999
elif tFD != 4 and trFD != 8 and rFD != 16 and brFD != 32 and bFD != 64 and bIFD !=
128 and lFD != 1 and tIFD != 2:
    if fDircPixel in rookDirc:
        NCSLArray[nRow, nCol] = .5 * cSize
    elif fDircPixel in diagDirc:
        NCSLArray[nRow, nCol] = .5 * 1.4142 * cSize
# if receiving cell in cardinal direction then set equal to cell size
elif fDircPixel in rookDirc:
    NCSLArray[nRow, nCol] = cSize
# if receiving cell in diagonal direction than multiply cell size by orthogonal distance
elif fDircPixel in diagDirc:
    NCSLArray[nRow, nCol] = 1.4142 * cSize
else:
    NCSLArray[nRow, nCol] = -9999

```

```

# loop through again to check for flat areas that should be changed to .5 that value
for nRow in range(nRows):
    for nCol in range(nCols):

        elevPixel = elevArray[nRow, nCol]
        fDircPixel = fDircArray[nRow, nCol]
        if fDircPixel == -9999:
            continue
        i = fDirc.index(fDircPixel)

        newRow = nRow + fdRow[i]
        if newRow < 0 or newRow == nRows:
            continue
        newCol = nCol + fdCol[i]
        if newCol < 0 or newCol == nCols:
            continue

        newElevPixel = elevArray[newRow, newCol]

        # if cell's elevation is equal to receiving cell's elevation, then receiving cell is a flat
        area
        if elevPixel == newElevPixel:
            if fDircArray[newRow, newCol] in rookDirc:
                NCSLArray[newRow, newCol] = .5 * cSize
            elif fDircArray[newRow, newCol] in diagDirc:
                NCSLArray[newRow, newCol] = .5 * 1.4142 * cSize
            else:
                continue

noDataBuff(NCSLArray, 0, 1)
del elevArray

## Step: Calc cumulative downhill slope length (CDHSL) ##
try:
    CDHSLArray = numpy.zeros((nRows, nCols))

    # identify high points and no data values in CHDSL, these are the points that will start
    the cumulation process
    for nRow in range(nRows):
        for nCol in range(nCols):

```

```

NCSLPixel = NCSLArray[nRow, nCol]

if NCSLPixel == (.5 * cSize) or NCSLPixel == (.5 * 1.4142 * cSize):
    CDHSLArray[nRow, nCol] = NCSLArray[nRow, nCol]
elif NCSLPixel == -9999:
    CDHSLArray[nRow, nCol] = -9999
else:
    continue

# iterate through array adding NCSL from the high points/flat areas down along flow
direction. since any cell that
# does not have flow into it is defined as a high/flat area and given a value above, all
remaining cells should
# receive some length value (no cell has 0 degree slope so always some slope length).
this can take up to 12 hours.
arcpy.AddMessage("Beginning cumulative downhill slope calculations at " +
time.ctime() + ". This may take a while.")
computron = 0
while 0 in CDHSLArray:
    computron += 1
    if (computron/50.0).is_integer():
        arcpy.AddMessage("Calculating...")
    for nRow in range(nRows):
        for nCol in range(nCols):

            CDHSLPixel = CDHSLArray[nRow, nCol]
            # must start where a CDHSL value exists, this means first iteration at high points
            if CDHSLPixel == -9999 or CDHSLPixel == 0:
                continue

            fDircPixel = fDircArray[nRow, nCol]
            i = fDirc.index(fDircPixel)
            newRow = nRow + fdRow[i]
            if newRow < 0 or newRow == nRows:
                continue
            newCol = nCol + fdCol[i]
            if newCol < 0 or newCol == nCols:
                continue

            NCSLPixel = NCSLArray[nRow, nCol]
            newNCSL = NCSLArray[newRow, newCol]
            newCDHSL = CDHSLArray[newRow, newCol]

```

```

    if newCDHSL != 0: # if receiving cell has CDHSL then all in flows already
considered and calculated
        # for that cell. No need to repeat lengthy calculation process over again.
        continue

    if maxDHSArray[newRow, newCol] == -9999: # slope value must exist for L
factor and slope cutoff consideration
        CDHSLArray[newRow, newCol] = -9999
        continue
    else:
        newSlope = math.tan(math.radians(maxDHSArray[newRow, newCol]))*100
        # set rows & columns locations for all neighbors around the receiving cell (cell in
the flow direction)
        tCell = nbrCell(newRow, newCol, -1, 0)
        if tCell == "Invalid":
            tFD = -9999
            tCDHSL = -9999
            tSlope = -9999
        else:
            tFD = fDirArray[tCell]
            tCDHSL = CDHSLArray[tCell]
            tSlope = slopePerc((maxDHSArray[tCell]))

        rCell = nbrCell(newRow, newCol, 0, 1)
        if rCell == "Invalid":
            rFD = -9999
            rCDHSL = -9999
            rSlope = -9999
        else:
            rFD = fDirArray[rCell]
            rCDHSL = CDHSLArray[rCell]
            rSlope = slopePerc((maxDHSArray[rCell]))

        bCell = nbrCell(newRow, newCol, 1, 0)
        if bCell == "Invalid":
            bFD = -9999
            bCDHSL = -9999
            bSlope = -9999
        else:
            bFD = fDirArray[bCell]
            bCDHSL = CDHSLArray[bCell]
            bSlope = slopePerc((maxDHSArray[bCell]))

```

```

lCell = nbrCell(newRow, newCol, 0, -1)
if lCell == "Invalid":
    lFD = -9999
    lCDHSL = -9999
    lSlope = -9999
else:
    lFD = fDircArray[lCell]
    lCDHSL = CDHSLArray[lCell]
    lSlope = slopePerc((maxDHSArray[lCell]))

trCell = nbrCell(newRow, newCol, -1, 1)
if trCell == "Invalid":
    trFD = -9999
    trCDHSL = -9999
    trSlope = -9999
else:
    trFD = fDircArray[trCell]
    trCDHSL = CDHSLArray[trCell]
    trSlope = slopePerc((maxDHSArray[trCell]))

tlCell = nbrCell(newRow, newCol, -1, -1)
if tlCell == "Invalid":
    tlFD = -9999
    tlCDHSL = -9999
    tlSlope = -9999
else:
    tlFD = fDircArray[tlCell]
    tlCDHSL = CDHSLArray[tlCell]
    tlSlope = slopePerc((maxDHSArray[tlCell]))

brCell = nbrCell(newRow, newCol, 1, 1)
if brCell == "Invalid":
    brFD = -9999
    brCDHSL = -9999
    brSlope = -9999
else:
    brFD = fDircArray[brCell]
    brCDHSL = CDHSLArray[brCell]
    brSlope = slopePerc((maxDHSArray[brCell]))

blCell = nbrCell(newRow, newCol, 1, -1)

```

```

if blCell == "Invalid":
    bIFD = -9999
    bICDHSL = -9999
    bISlope = -9999
else:
    bIFD = fDircArray[blCell]
    bICDHSL = CDHSLArray[blCell]
    bISlope = slopePerc((maxDHSArray[blCell]))

    # if empty receiving cell then cont. check other neighbors if they also flow to the
same receiving cell
    pNeighbors = []
    slopes = []
    if tFD == 4 and tCDHSL != -9999 and tSlope != -9999:
        pNeighbors.append(tCDHSL)
        slopes.append(tSlope)
    if trFD == 8 and trCDHSL != -9999 and trSlope != -9999:
        pNeighbors.append(trCDHSL)
        slopes.append(trSlope)
    if rFD == 16 and rCDHSL != -9999 and rSlope != -9999:
        pNeighbors.append(rCDHSL)
        slopes.append(rSlope)
    if brFD == 32 and brCDHSL != -9999 and brSlope != -9999:
        pNeighbors.append(brCDHSL)
        slopes.append(brSlope)
    if bFD == 64 and bCDHSL != -9999 and bSlope != -9999:
        pNeighbors.append(bCDHSL)
        slopes.append(bSlope)
    if blFD == 128 and blCDHSL != -9999 and blSlope != -9999:
        pNeighbors.append(blCDHSL)
        slopes.append(blSlope)
    if lFD == 1 and lCDHSL != -9999 and lSlope != -9999:
        pNeighbors.append(lCDHSL)
        slopes.append(lSlope)
    if tlFD == 2 and tlCDHSL != -9999 and tlSlope != -9999:
        pNeighbors.append(tlCDHSL)
        slopes.append(tlSlope)

    if 0 in pNeighbors: # don't need to calculate slope changes if one of the
neighbors CDHSL is still a zero
        continue
    else:

```

```

        # neighbors who are eligible to pass length. slope change doesn't trigger their
slope to reset
        finalNeighbors = []
        # check if slope cutoff is triggered for any neighbors, they will not be eligible
to pass length
        if newSlope >= 5:
            slopeIndex = 0
            for neighbor in pNeighbors: # starts at neighbor index 0 which corresponds
to start slopeIndex 0
                if ((slopes[slopeIndex] - newSlope) / (slopes[slopeIndex]) * 100) >=
(great5*100):
                    slopeIndex += 1
                    # if slope cutoff not triggered, CDHSL neighbor able to pass on length
                    else:
                        finalNeighbors.append(neighbor)
                        slopeIndex += 1
                del slopeIndex
            elif newSlope < 5:
                slopeIndex = 0
                for neighbor in pNeighbors:
                    if ((slopes[slopeIndex] - newSlope) / (slopes[slopeIndex]) * 100) >=
(less5*100):
                        slopeIndex += 1
                    else:
                        finalNeighbors.append(neighbor)
                        slopeIndex += 1
                del slopeIndex
            del slopes, pNeighbors

        # determine cell's CDHSL value
        if len(finalNeighbors) == 0: # slope cutoff met for all neighbors and cell resets
slope length
            CDHSLArray[newRow, newCol] = newNCSL
        else: # from neighbors list, use max value (greatest slope length) to add for
new CDHSL
            CDHSLArray[newRow, newCol] = max(finalNeighbors) + newNCSL
        del finalNeighbors
    except:
        message = sys.exc_info()[1]
        arcpy.AddError(message.args[0])

del fDirArray, NCSLArray

```

```

arcpy.AddMessage("Completed cumulative downhill slope calculations at " +
time.ctime() + ".")

noDataBuff(CDHSLArray, 1, 2)

## Step: L factor calculation ## following RUSLE guidelines (Agricultural Handbook No.
703)
arcpy.AddMessage("Calculating L Factor.")

try:
    IFactorArray = numpy.empty((nRows, nCols))

    for nRow in range(nRows):
        for nCol in range(nCols):
            slope = maxDHSArray[nRow, nCol]
            length = CDHSLArray[nRow, nCol]
            faccPixel = faccD8Array[nRow, nCol]

            if slope == -9999 or length == -9999:
                IFactorArray[nRow, nCol] = -9999
            elif faccPixel > streamsD8: # if location is designated as a "defined" channel,
RUSLE does not apply
                IFactorArray[nRow, nCol] = -9999
            else:
                IFactorArray[nRow, nCol] = Lcalc(slope, length, units)

    del CDHSLArray, faccD8Array
    LFactor = arcpy.NumPyArrayToRaster(IFactorArray, lLeft, cSize, cSize, -9999)
    arcpy.DefineProjection_management(LFactor, sr)
    LFactor.save(outputL)
    del IFactorArray, LFactor
except:
    message = sys.exc_info()[1]
    arcpy.AddError(message.args[0])

```

```

Script 2: L with CA method, S with NBR method
# Written by Amanda Moody, Central Washington University, Ellensburg, WA. 2019.
# Provided freely "as is."
# RUSLE L-Factor calculation according to Desmet and Govers (1996) Contributing Area
# (CA) method. This uses the max.
# downhill slope method (Dunn and Hickey 1998) to calculate slope used in the m
# exponent of the L calculation.
# Optional S Factor is calculated using normal ESRI slope tool which uses the
# neighborhood method.
# Other tool available online at WEBSITE
# provides an L Factor output using the Grid Cumulation method (Hickey et al. 1994) and
# an S Factor and a slope raster
# output using the max. downhill slope method.

import arcpy, numpy, math, time
arcpy.AddMessage("Beginning process at " + time.ctime())

inputDEM = arcpy.GetParameterAsText(0)
outputS = arcpy.GetParameterAsText(1)
outputLD8 = arcpy.GetParameterAsText(2)
outputLDi = arcpy.GetParameterAsText(3)
# this is the percent of max flow accumulation (D8 algorithm) value to designate defined
# channels
# (where RUSLE is not applicable) rule of thumb for stream threshold is 1% while 100%
# would nullify this variable
threshold = float(arcpy.GetParameterAsText(4)) # if unsure, .5 for more defined
# channels, 1 for general stream channels, or
# 100 if you don't want this to influence results

desc = arcpy.Describe(inputDEM)
sr = desc.spatialReference
lLeft = desc.extent.lowerLeft
cSize = arcpy.Raster(inputDEM).meanCellHeight
units = sr.linearUnitName

# units must be either feet or meters, output L factor will be in the same units as DEM.
# while RUSLE guidelines use
# feet, users continue L factor calculation with meters as that is the international system
# of measurement for length.
class InputError(Exception):
    pass

```

```

if "Feet" in units or "Foot" in units or "Meter" in units:
    pass
else:
    raise InputError("Invalid linear unit. Please input a DEM using feet or meters.")

if threshold < 0 or threshold > 100:
    raise InputError("Invalid defined channel threshold value. Please input a value
between 0 and 100.")

# buffer edge cells to nodata (can't know true value at edge cells, missing surrounding
spatial info.) for any function
# that uses surrounding cells to calculate center cell value
def noDataBuff(noArray, topLeft, bottomRight):
    noArray[:, topLeft] = -9999 # first column starts at 0
    noArray[topLeft, :] = -9999 # first row starts 0
    noArray[:, (nCols - bottomRight)] = -9999 # last column in array is the # of columns - 1
(0 indexed)
    noArray[(nRows - bottomRight), :] = -9999 # last row in array is the # of row - 1 (0
indexed)

def lcalc(facc, aspect, maxDHS, cell, unit):
    area = facc*((cell)**2)
    aX = abs(math.sin(math.radians(aspect))) + abs(math.cos(math.radians(aspect)))
    beta = (math.sin(math.radians(maxDHS))/0.0896) /
(3*((math.sin(math.radians(maxDHS)))**0.8)+0.56)
    m = beta/(1 + beta)
    if "Foot" in unit or "Feet" in unit:
        lValue = (((area+(cell**2))*(m+1))-
area**(m+1))/((cell**(m+2))*(aX**m)*(72.6**m))
    elif "Meter" in unit:
        lValue = (((area+(cell**2))*(m+1))-
(area**(m+1)))/((cell**(m+2))*(aX**m)*(22.13**m))
    return lValue

def sCalc(slope, percent):
    if percent < 9:
        sValue = 10.8 * (math.sin(math.radians(slope))) + 0.03
    elif percent >= 9:
        sValue = 16.8 * (math.sin(math.radians(slope))) - 0.50
    return sValue

```

```

arcpy.CheckOutExtension("Spatial")

### Step: fill DEM ###
fillRaster = arcpy.sa.Fill(inputDEM)

### Step: Calc flow direction using D8 algorithm (ESRI 2019 Flow Direction) ###
flowDirD8 = arcpy.sa.FlowDirection(fillRaster, "FORCE")
flowDirDi = arcpy.sa.FlowDirection(fillRaster, "FORCE", "", "DINF")

### Step: Aspect ###
aspect = arcpy.sa.Aspect(fillRaster)

### Step: MDS for m exponent ###
# this uses the flow direction with the D8 algorithm as that follows the direction of max.
# downhill slope change
fDir = (1, 2, 4, 8, 16, 32, 64, 128)
rookDir = (1, 4, 16, 64)
diagDir = (2, 8, 32, 128)
# fdCol and fdRow are used from indexed fDir value to correctly reference cell in the
# flow direction
fdCol = (1, 1, 0, -1, -1, -1, 0, 1)
fdRow = (0, 1, 1, 1, 0, -1, -1, -1)

fDirArray = arcpy.RasterToNumPyArray(flowDirD8, "", "", "", -9999)
del inputDEM

# this is the array shape of original DEM, used for any new array being built
nRows, nCols = fDirArray.shape
cTotal = nRows * nCols

elevArray = arcpy.RasterToNumPyArray(fillRaster, "", "", "", -9999)
maxDHSArray = numpy.empty((nRows, nCols))

for nRow in range(nRows):
    for nCol in range(nCols):

        # find elevation and flow direction of current cell at location nRow, nCol
        elevPixel = elevArray[nRow, nCol]
        if elevPixel == -9999:
            maxDHSArray[nRow, nCol] = -9999
            continue

```

```

fDircPixel = fDircArray[nRow, nCol]
if fDircPixel == -9999:
    maxDHSArray[nRow, nCol] = -9999
    continue
# this indicates the pixel in the direction of fDircPixel's flow
i = fDirc.index(fDircPixel)
# get location of the comparing cell (the cell in the flow direction)
newRow = nRow + fdRow[i]
# this accounts for those instances where flow direction points to a non-existent row
outside raster coverage
if newRow < 0 or newRow == nRows:
    maxDHSArray[nRow, nCol] = -9999
    continue
newCol = nCol + fdCol[i]
if newCol < 0 or newCol == nCols:
    maxDHSArray[nRow, nCol] = -9999
    continue

# now the elevation of that comparing cell can be referenced
newElevPixel = elevArray[newRow, newCol]
# calculate the difference to get max change
elevDiff = float(elevPixel - newElevPixel)

# calculate max downhill slope for current cell
# if comparing cell in diagonal direction then divide by orthogonal size
if fDircPixel in diagDirc:
    maxDHSArray[nRow, nCol] = math.degrees(math.atan(elevDiff/1.4142*cSize))
# if comparing cell in cardinal direction then divide by cell size
elif fDircPixel in rookDirc:
    maxDHSArray[nRow, nCol] = math.degrees(math.atan(elevDiff/cSize))
else:
    maxDHSArray[nRow, nCol] = -9999

# buffer outer cells to nodata value (cannot know true value at edge cells, missing
surrounding spatial info.)
noDataBuff(maxDHSArray, 0, 1)
# if any value = 0 change to 0.1. this allows for erosion in every cell without altering flow
paths
maxDHSArray[maxDHSArray == 0] = 0.1

#### S Factor ####
fAccD8 = arcpy.sa.FlowAccumulation(flowDircD8)

```

```

faccD8Array = arcpy.RasterToNumPyArray(fAccD8, "", "", "", -9999)
noDataBuff(faccD8Array, 0, 1) # outer edge is force flow out, these cells don't qualify to
be included for L Fctor
del fAccD8, flowDirD8

flowAccD8Max = numpy.nanmax(faccD8Array)
streamsD8 = float(threshold / 100) * flowAccD8Max

if outputS and outputS != "": # optional
    nbrSlope = arcpy.sa.Slope(fillRaster)
    nbrSlopeArray = arcpy.RasterToNumPyArray(nbrSlope, "", "", "", -9999)
    del nbrSlope
    sFactorArray = numpy.empty((nRows, nCols))

    for nRow in range(nRows):
        for nCol in range(nCols):
            slope = nbrSlopeArray[nRow, nCol]
            slopeP = math.tan(math.radians(nbrSlopeArray[nRow, nCol]))*100
            faccPixel = faccD8Array[nRow, nCol]

            # S Factor is different for slopes < 9 % or >= 9%
            if slope == -9999:
                sFactorArray[nRow, nCol] = -9999
            elif faccPixel > streamsD8:
                sFactorArray[nRow, nCol] = -9999
            else:
                sFactorArray[nRow, nCol] = sCalc(slope, slopeP)

    del nbrSlopeArray
    SFactor = arcpy.NumPyArrayToRaster(sFactorArray, lLeft, cSize, cSize, -9999)
    arcpy.DefineProjection_management(SFactor, sr)
    SFactor.save(outputS)
    del sFactorArray, SFactor
arcpy.AddMessage("Completed S Factor Calculations at " + time.ctime() + ".")

### Step: L Calc. ###
aspectArray = arcpy.RasterToNumPyArray(aspect, "", "", "", -9999)

## D8 (optional)##
if outputLD8 and outputLD8 != "": # optional
    lFactD8 = numpy.empty((nRows, nCols))

```

```

for nRow in range(nRows):
    for nCol in range(nCols):
        maxDHSpixel = maxDHSArray[nRow, nCol]
        aspectPixel = aspectArray[nRow, nCol]
        faccPixel = faccD8Array[nRow, nCol]

        if maxDHSpixel == -9999:
            lFactD8[nRow, nCol] = -9999
        elif aspectPixel == -9999:
            lFactD8[nRow, nCol] = -9999
        elif faccPixel == -9999:
            lFactD8[nRow, nCol] = -9999
        elif faccPixel > streamsD8:
            lFactD8[nRow, nCol] = -9999
        else:
            lFactD8[nRow, nCol] = lcalc(faccPixel, aspectPixel, maxDHSpixel, cSize, units)

lFactorD8 = arcpy.NumPyArrayToRaster(lFactD8, lLeft, cSize, cSize, -9999)
arcpy.DefineProjection_management(lFactorD8, sr)
lFactorD8.save(outputLD8)
del lFactD8, lFactorD8

## D-Infinity ##
fAccDi = arcpy.sa.FlowAccumulation(flowDircDi, "", "", "DINF")
faccDiArray = arcpy.RasterToNumPyArray(fAccDi, "", "", "", -9999)
noDataBuff(faccDiArray, 0, 1)
del fAccDi, flowDircDi

lFactDi = numpy.empty((nRows, nCols))

for nRow in range(nRows):
    for nCol in range(nCols):
        maxDHSpixel = maxDHSArray[nRow, nCol]
        aspectPixel = aspectArray[nRow, nCol]
        faccPixel = faccDiArray[nRow, nCol]
        faccD8Pixel = faccD8Array[nRow, nCol]

        if maxDHSpixel == -9999 or aspectPixel == -9999 or faccPixel == -9999:
            lFactDi[nRow, nCol] = -9999
        elif faccD8Pixel > streamsD8:
            lFactDi[nRow, nCol] = -9999
        else:

```

```
IFactDi[nRow, nCol] = lcalc(faccPixel, aspectPixel, maxDHSpixel, cSize, units)
```

```
del faccDiArray
```

```
LFactorDi = arcpy.NumPyArrayToRaster(IFactDi, lLeft, cSize, cSize, -9999)
```

```
arcpy.DefineProjection_management(LFactorDi, sr)
```

```
LFactorDi.save(outputLDi)
```

```
del IFactDi, LFactorDi, aspect, aspectArray, maxDHSArray
```

```
arcpy.AddMessage("Completed L Factor Calculations at " + time.ctime() + ".")
```

```
arcpy.CheckInExtension("Spatial")
```

Appendix B – Raster Outputs

Site A outputs:

GC\_0.5 (1 m)

Value

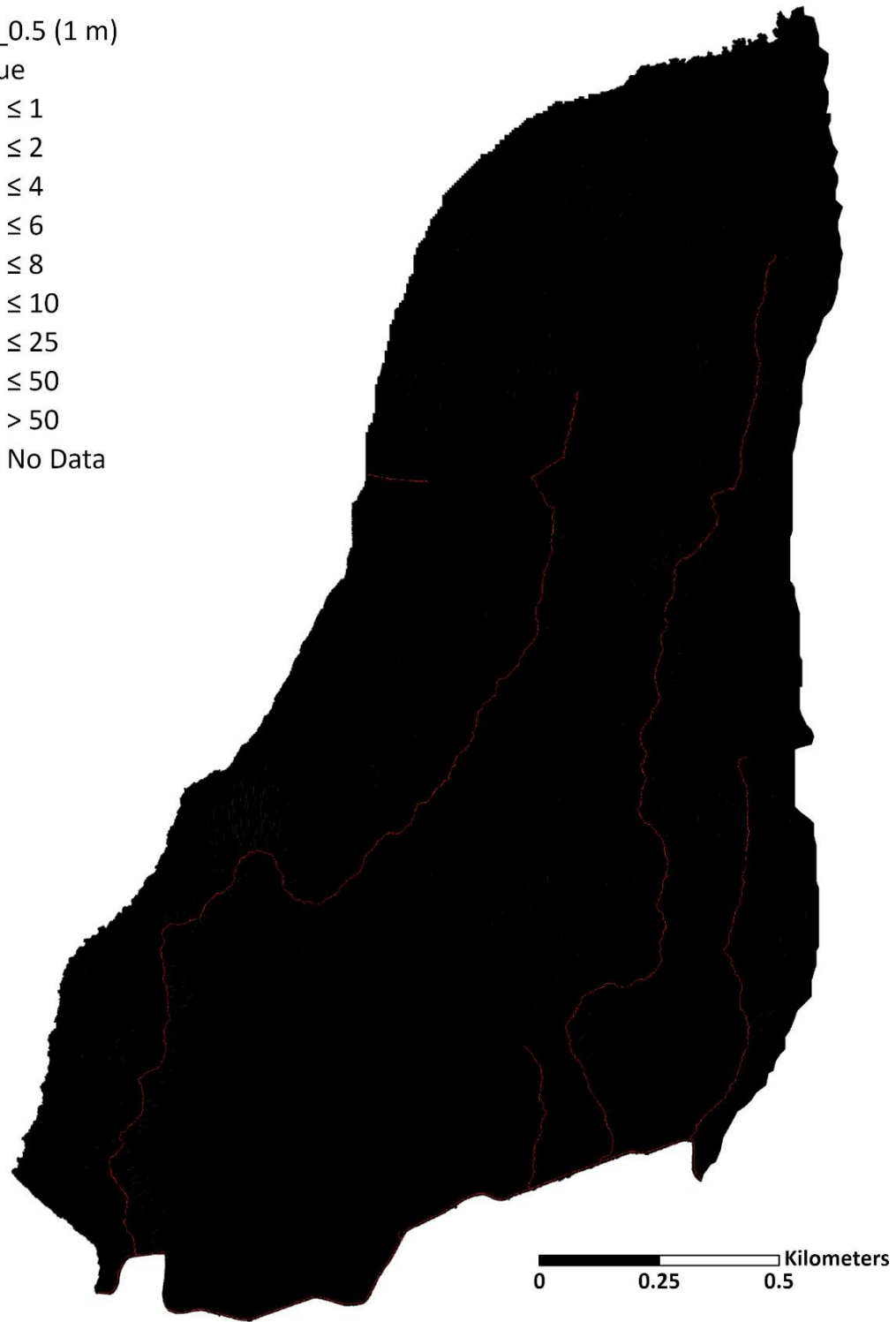
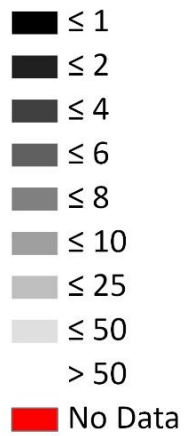
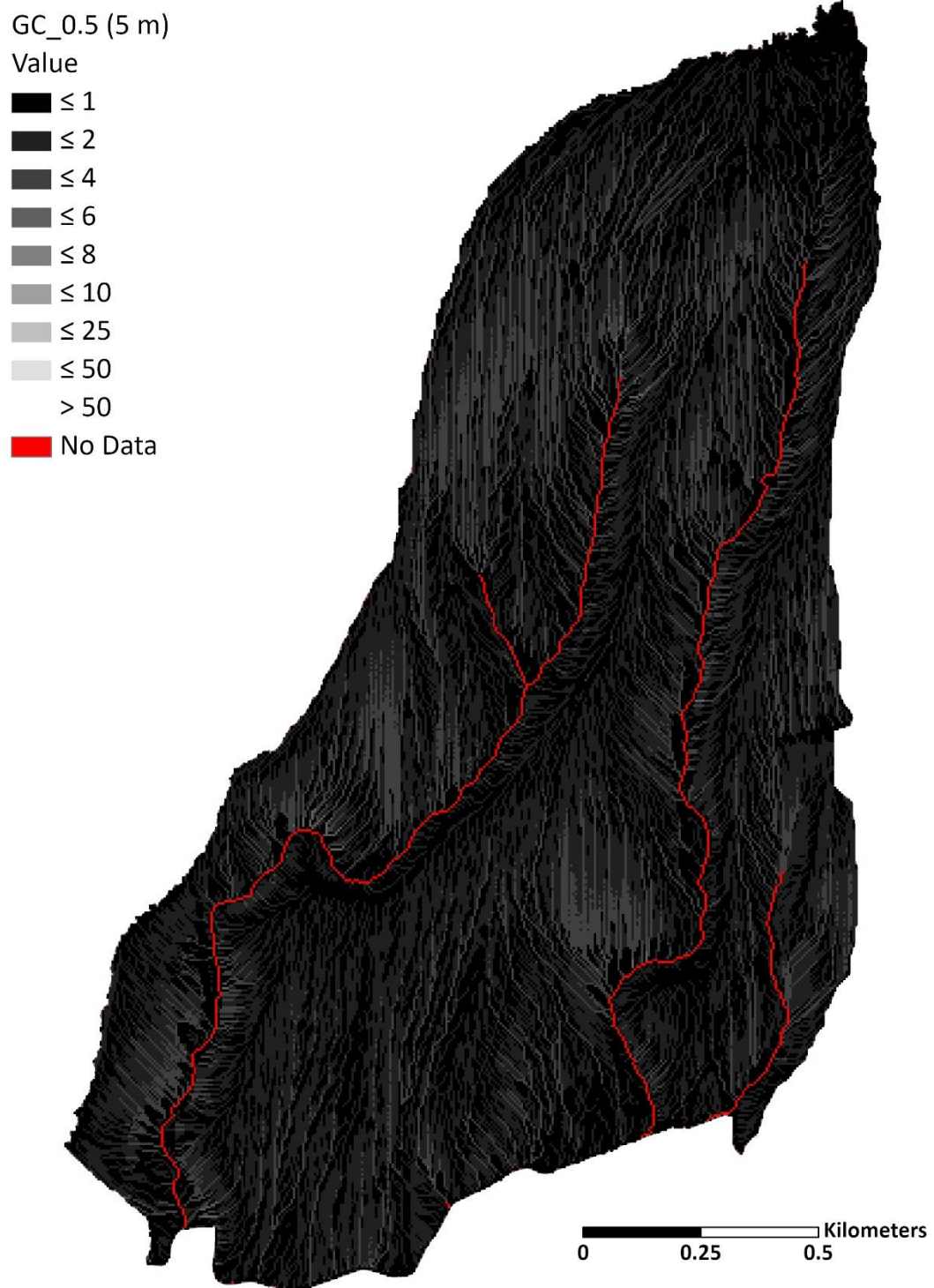
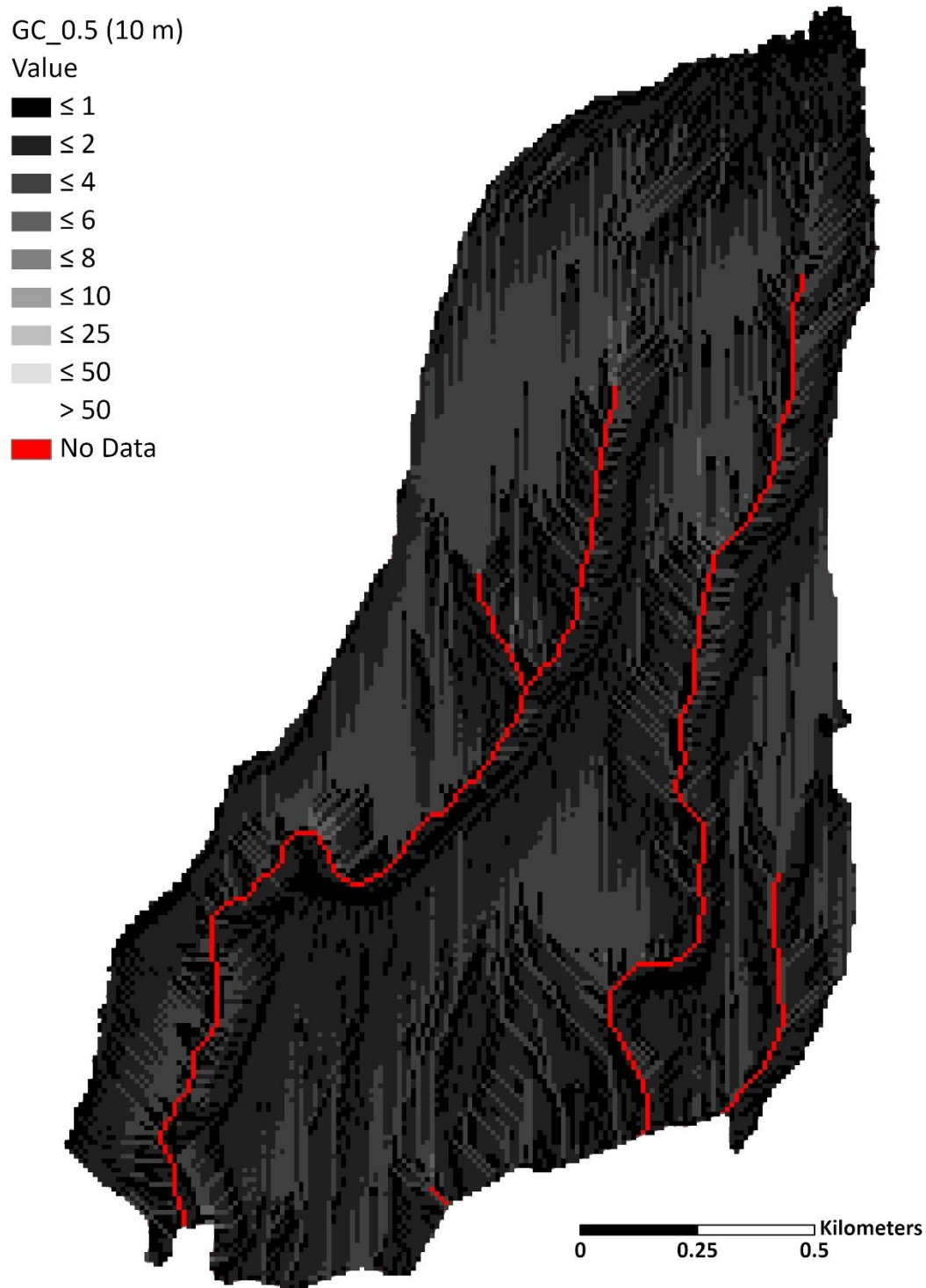


Figure A1. L factor with the GC Method with slope cutoff at 0.5 for Site A at 1 m.



**Figure A2.** L factor with the GC Method with slope cutoff at 0.5 for Site A at 5 m.



**Figure A3.** L factor with the GC Method with slope cutoff at 0.5 for Site A at 10 m.

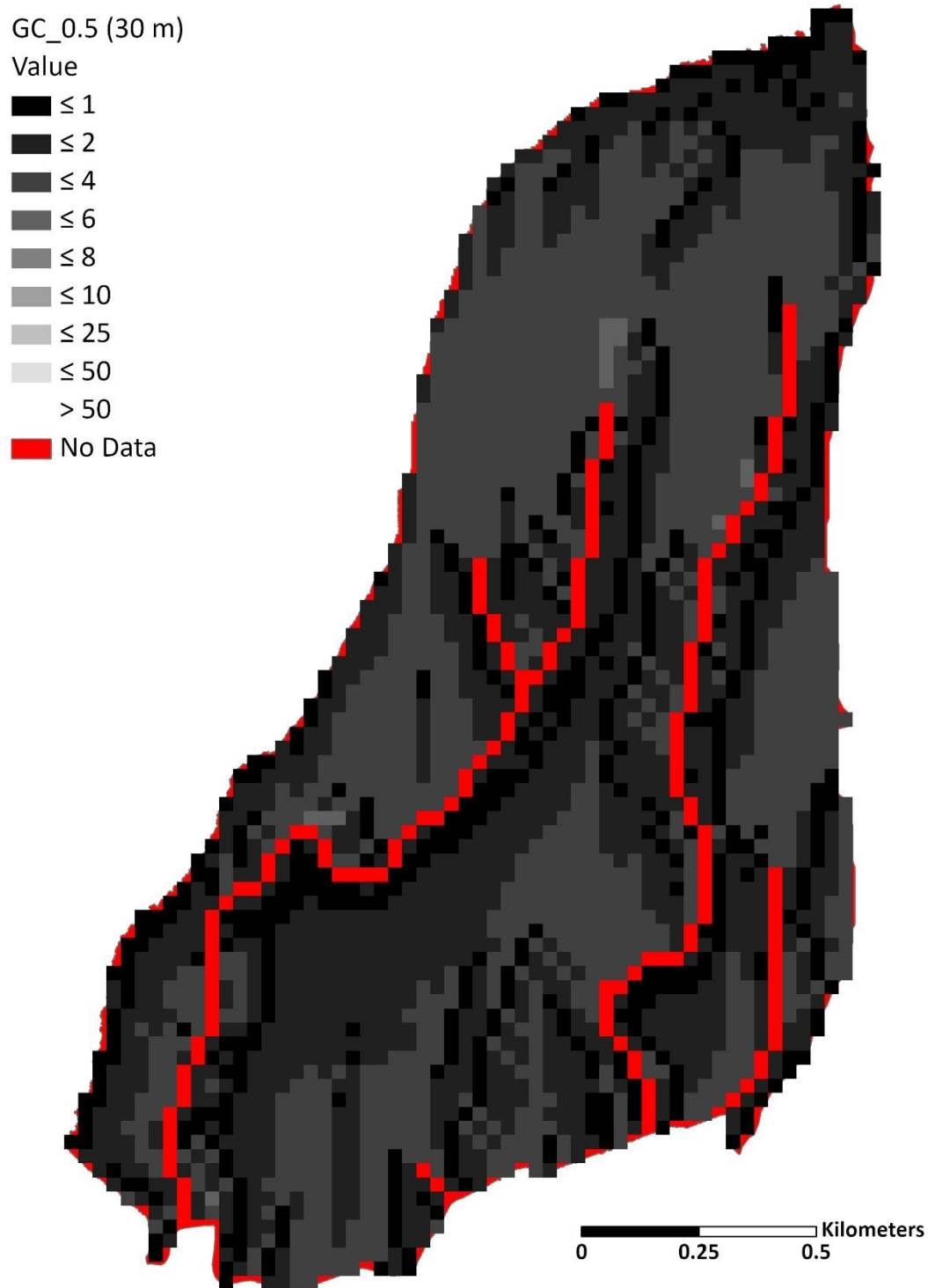


**Figure A4.** L factor with the GC Method with slope cutoff at 0.5 for Site A at 30 m.

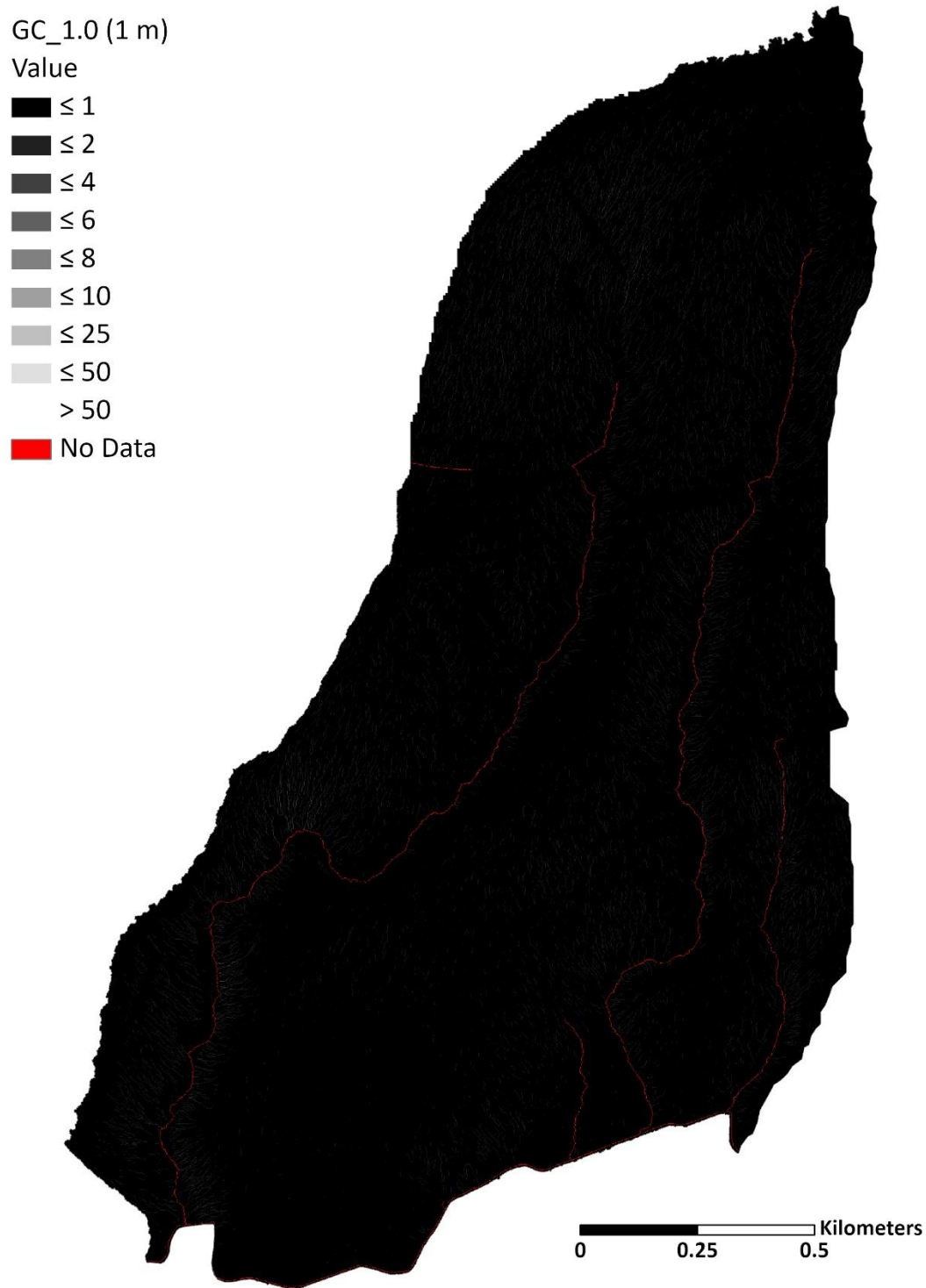


**Figure A5.** L factor with the GC Method without slope cutoff for Site A at 1 m.

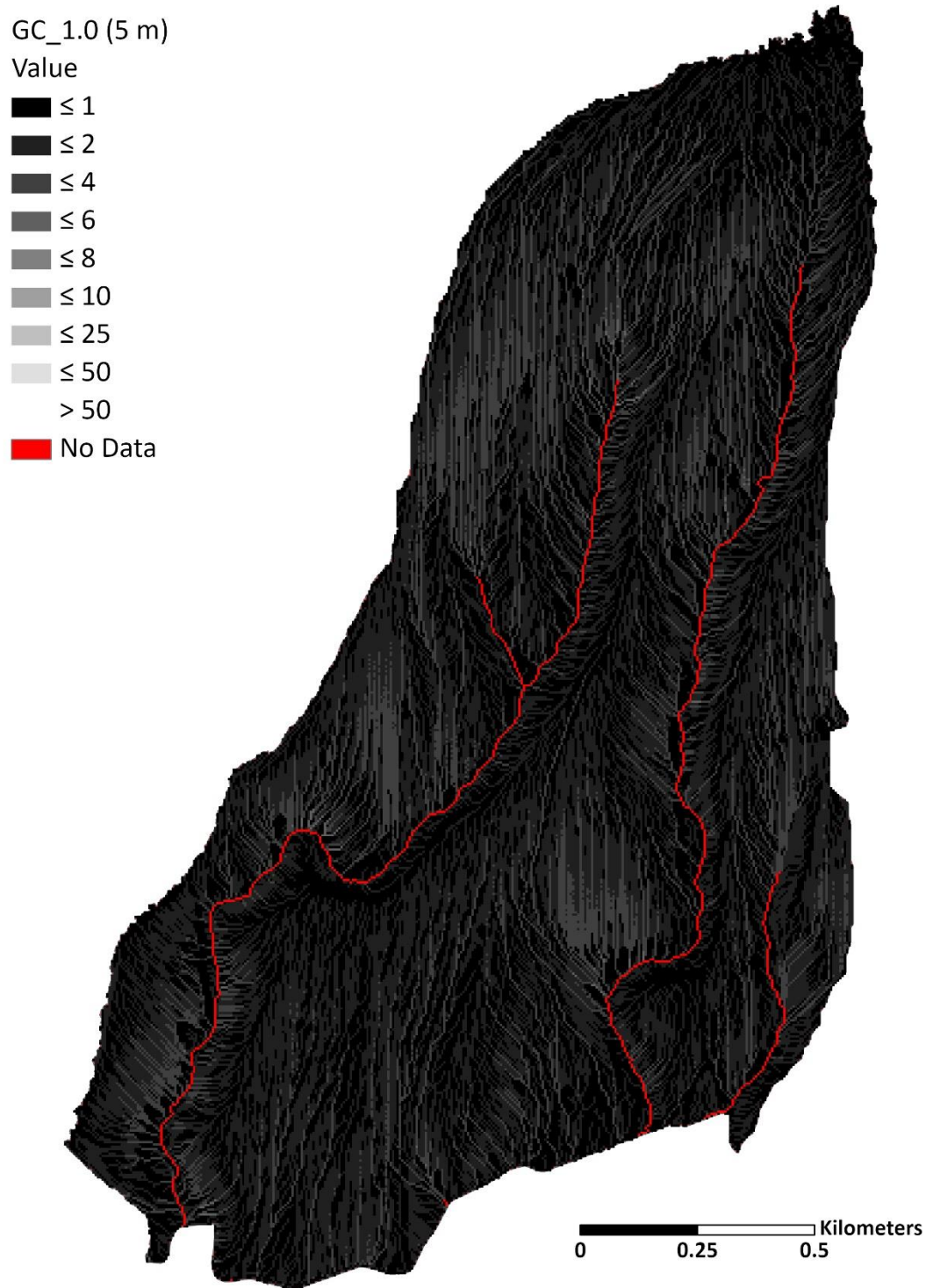


**Figure A6.** L factor with the GC Method without slope cutoff for Site A at 5 m.

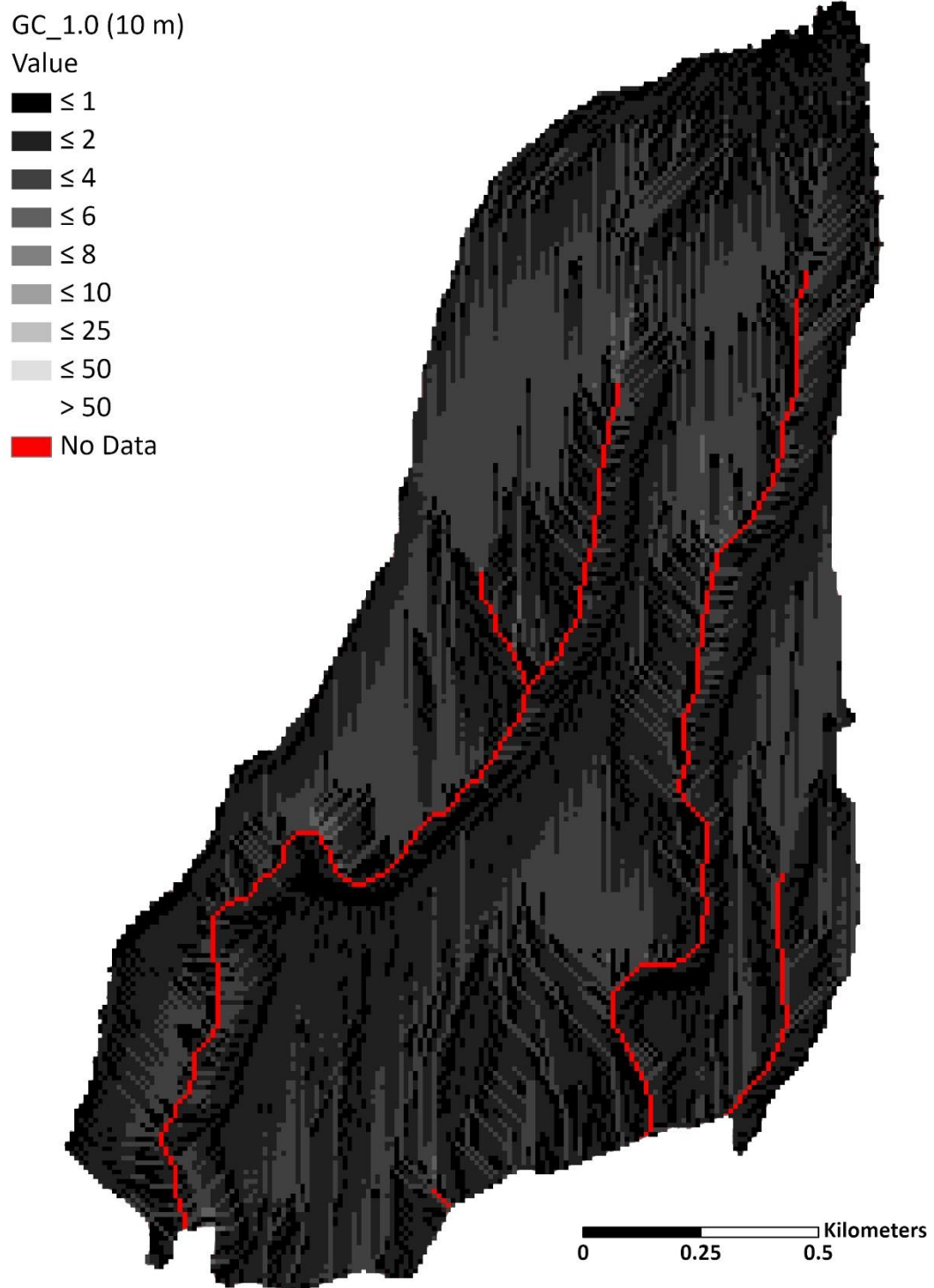


**Figure A7.** L factor with the GC Method without slope cutoff for Site A at 10 m.

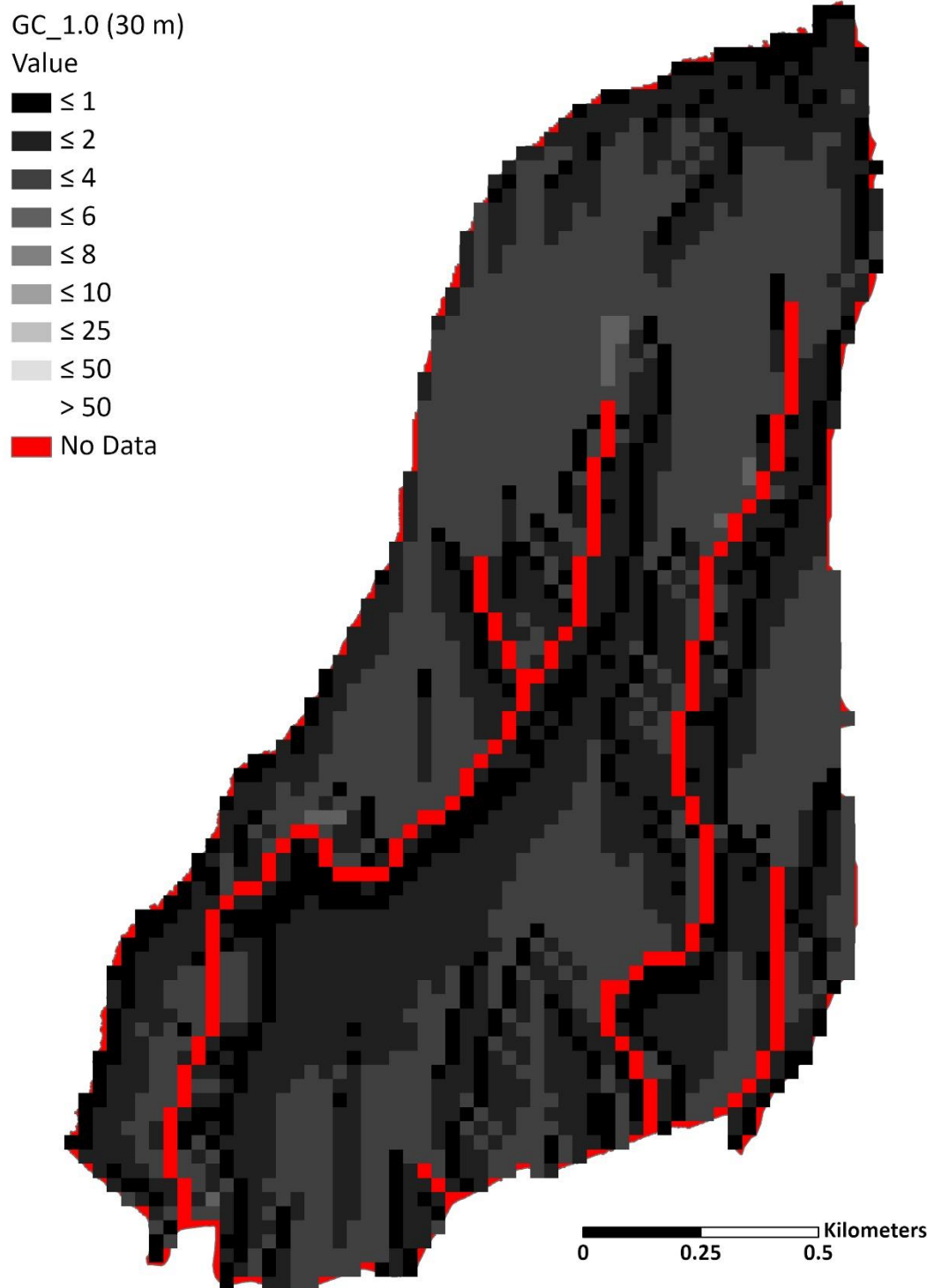


**Figure A8.** L factor with the GC Method without slope cutoff for Site A at 30 m.

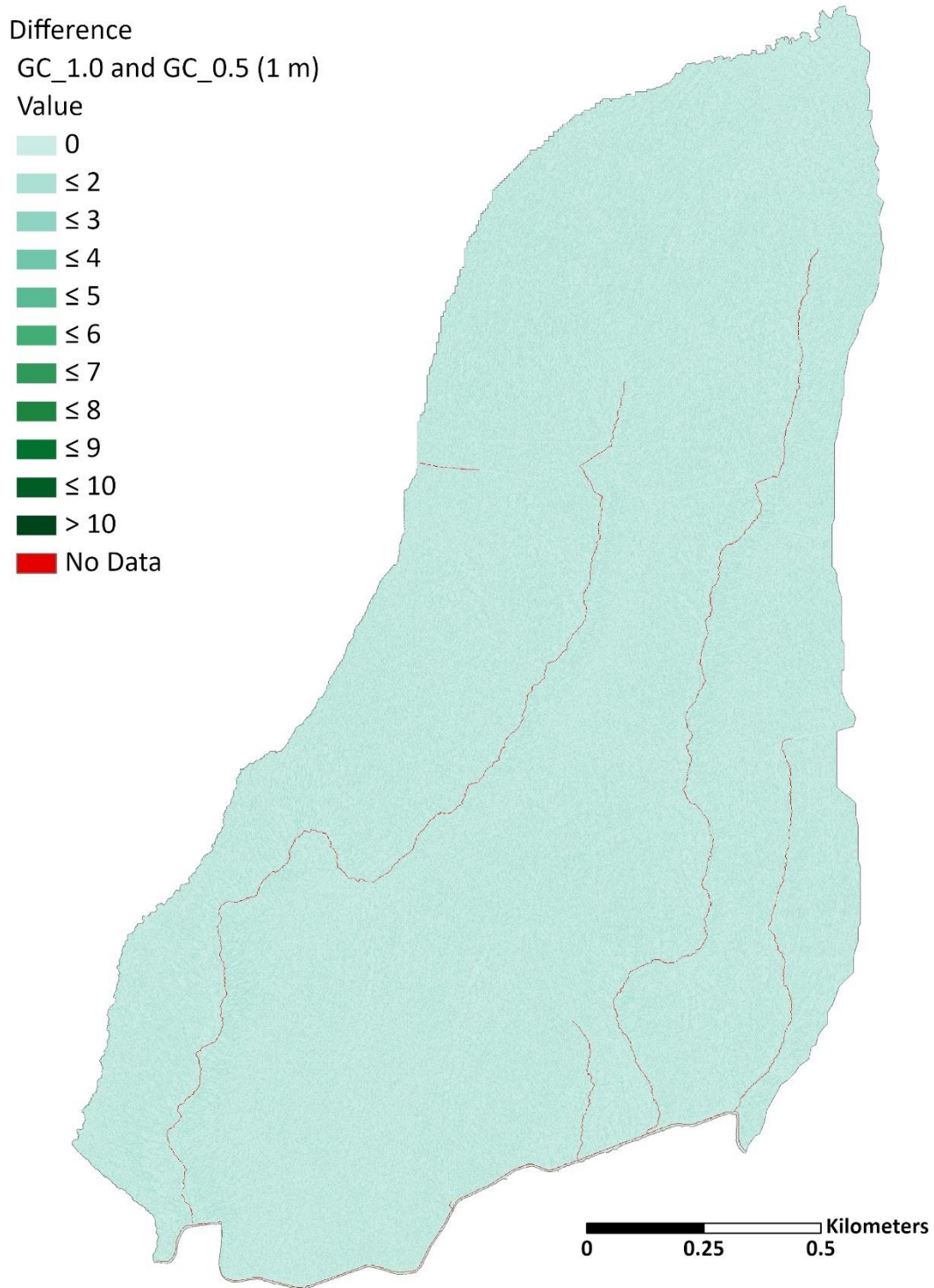


**Figure A9.** Site A difference raster (1 m) for the L Factor of the GC method with slope cutoff (GC\_0.5) subtracted from the GC method without slope cutoff (GC\_1.0).

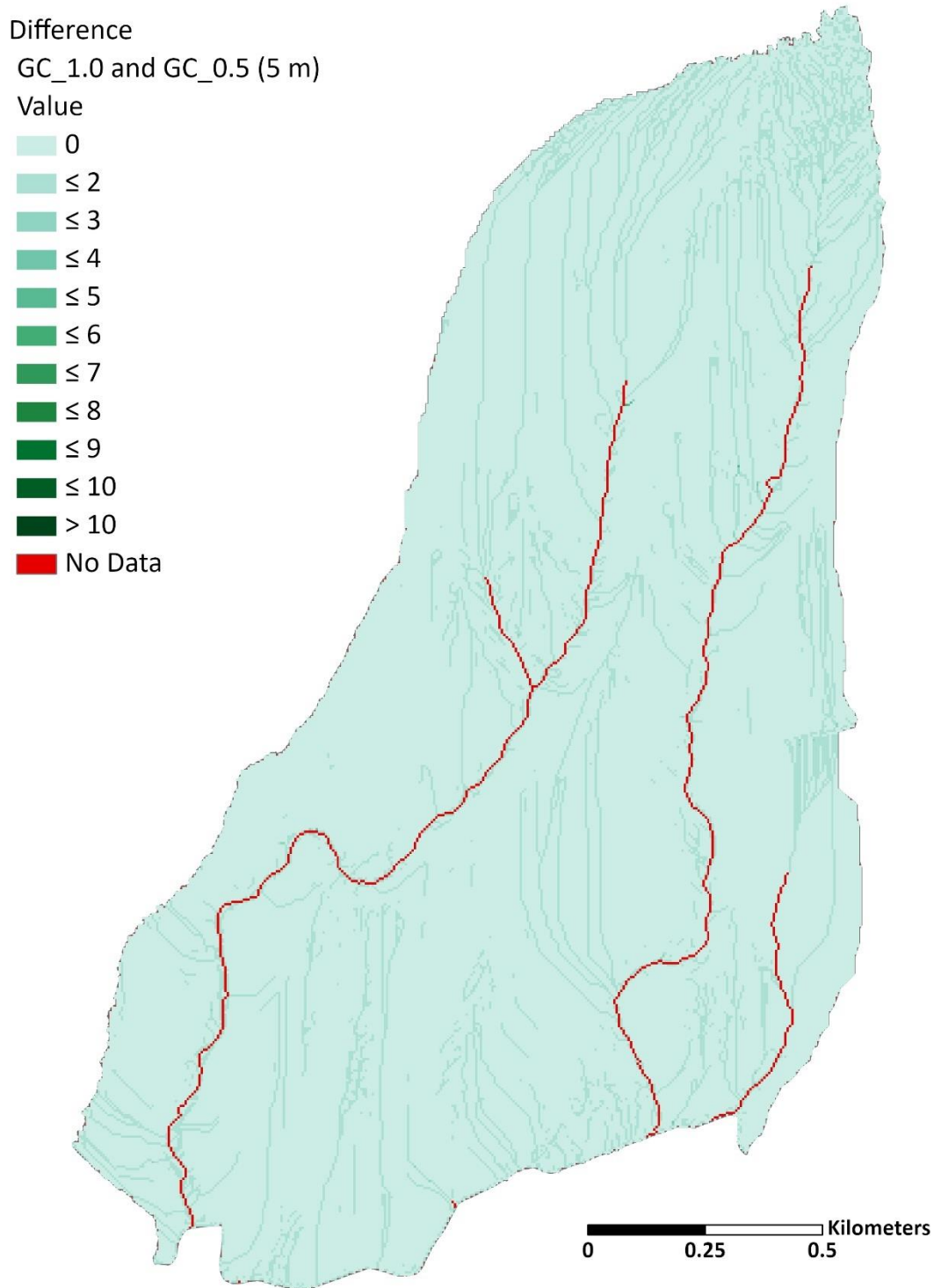


**Figure A10.** Site A difference raster (5 m) for the L Factor of the GC method with slope cutoff (GC\_0.5) subtracted from the GC method without slope cutoff (GC\_1.0).

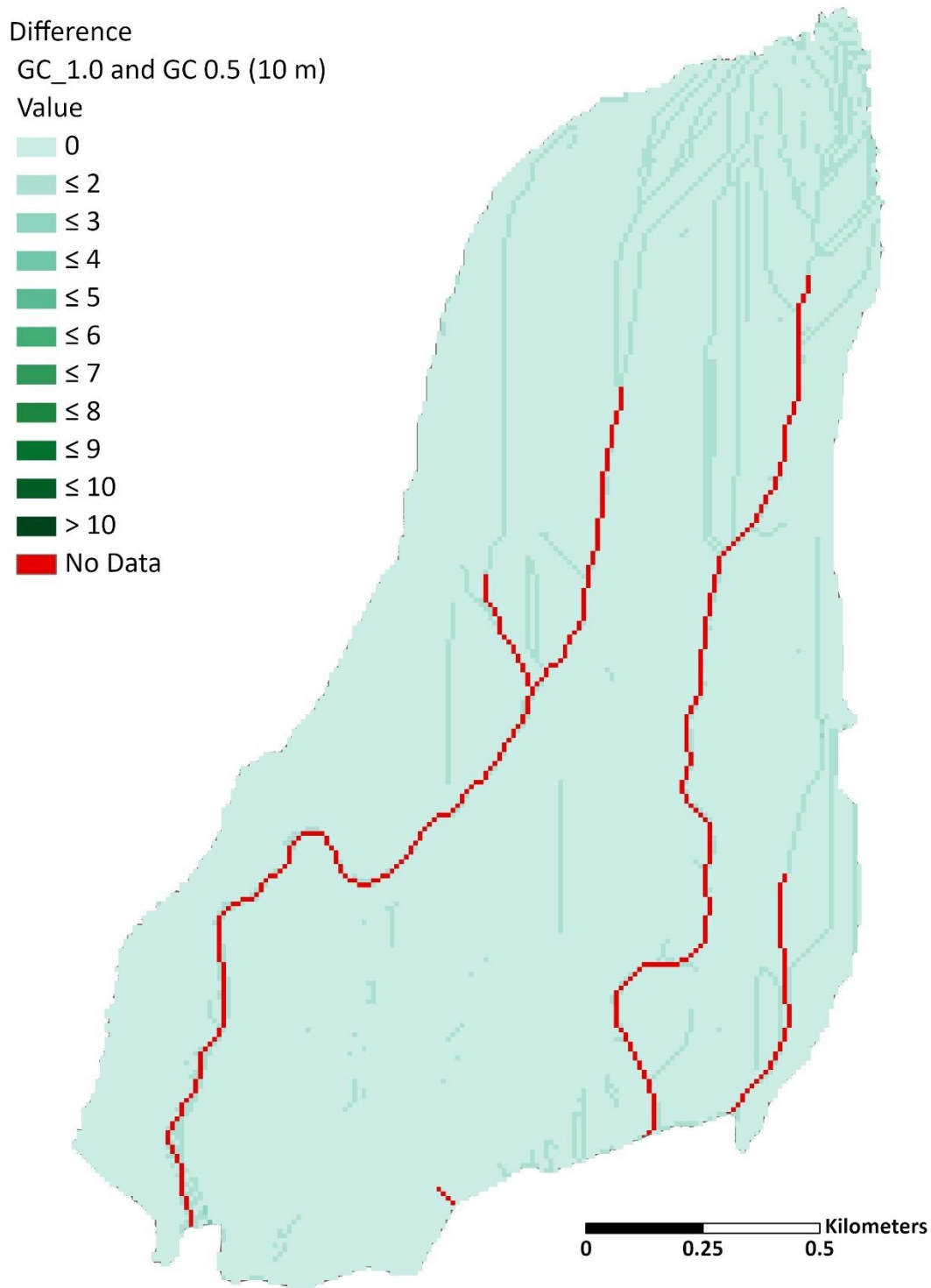


**Figure A11.** Site A difference raster (10 m) for the L Factor of the GC method with slope cutoff (GC\_0.5) subtracted from the GC method without slope cutoff (GC\_1.0).

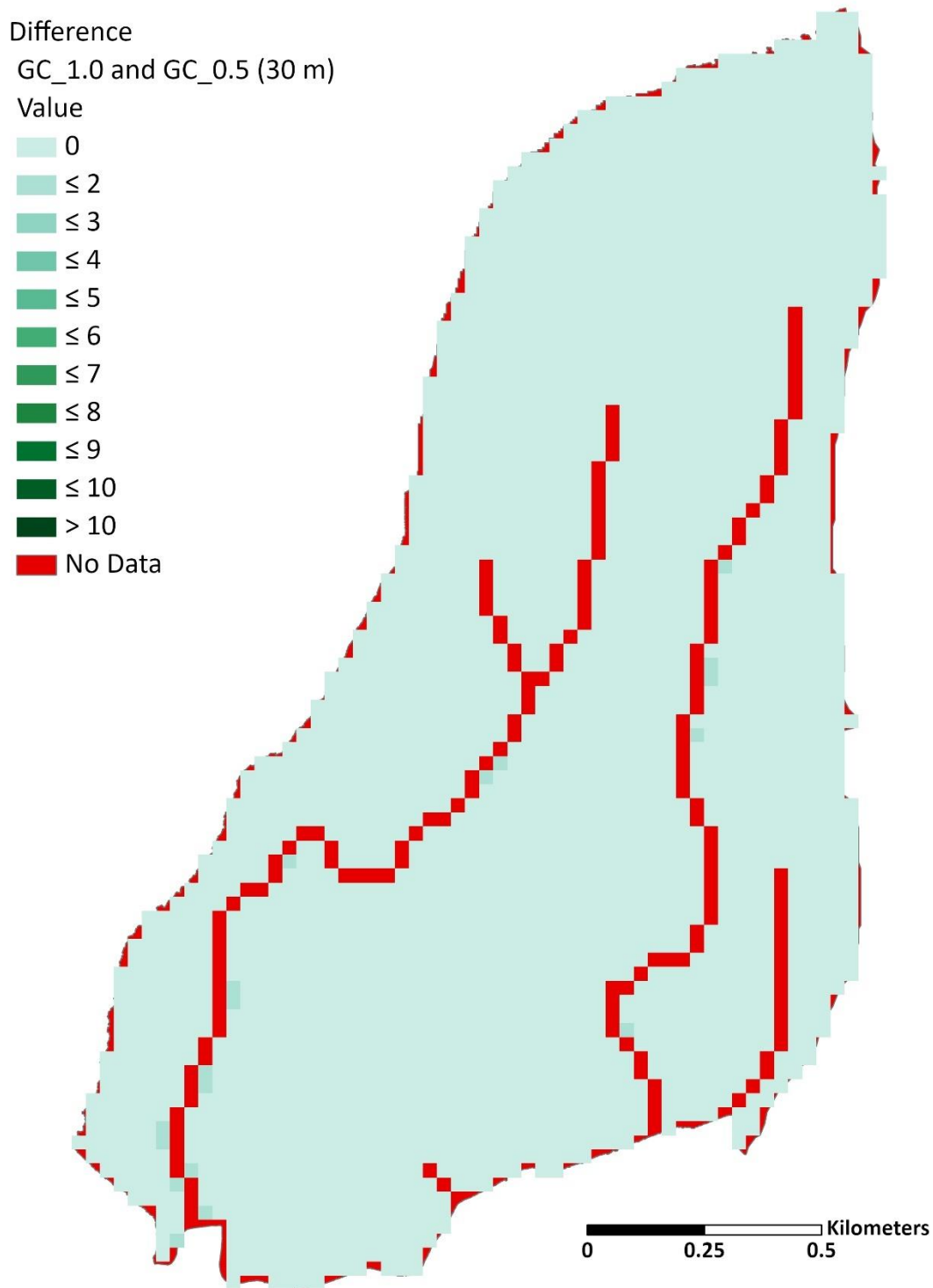


**Figure A12.** Site A difference raster (30 m) for the L Factor of the GC method with slope cutoff (GC\_0.5) subtracted from the GC method without slope cutoff (GC\_1.0).

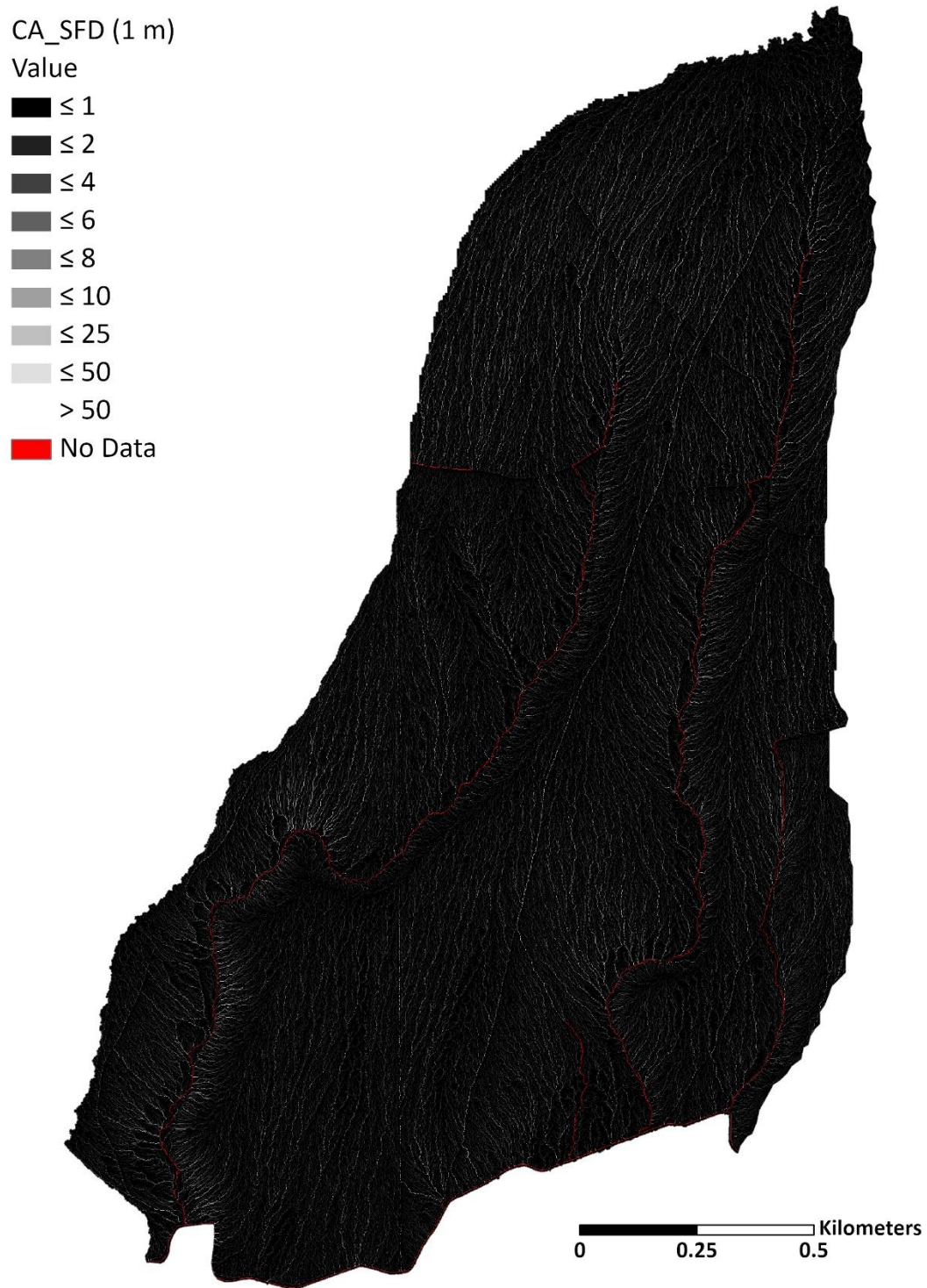


**Figure A13.** L factor with the CA method with a SFD algorithm for Site A at 1 m.

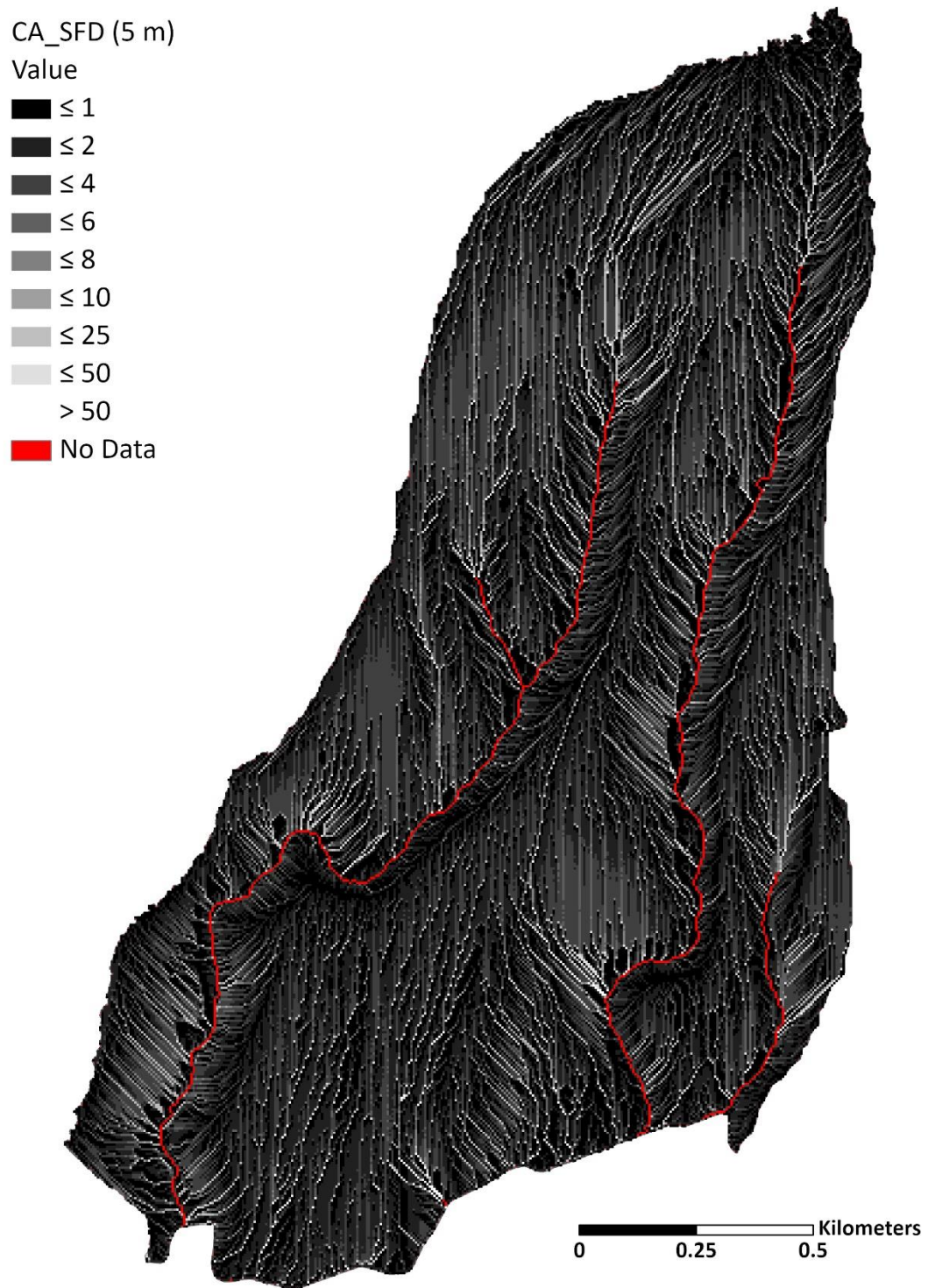


**Figure A14.** L factor with the CA method with a SFD algorithm for Site A at 5 m.

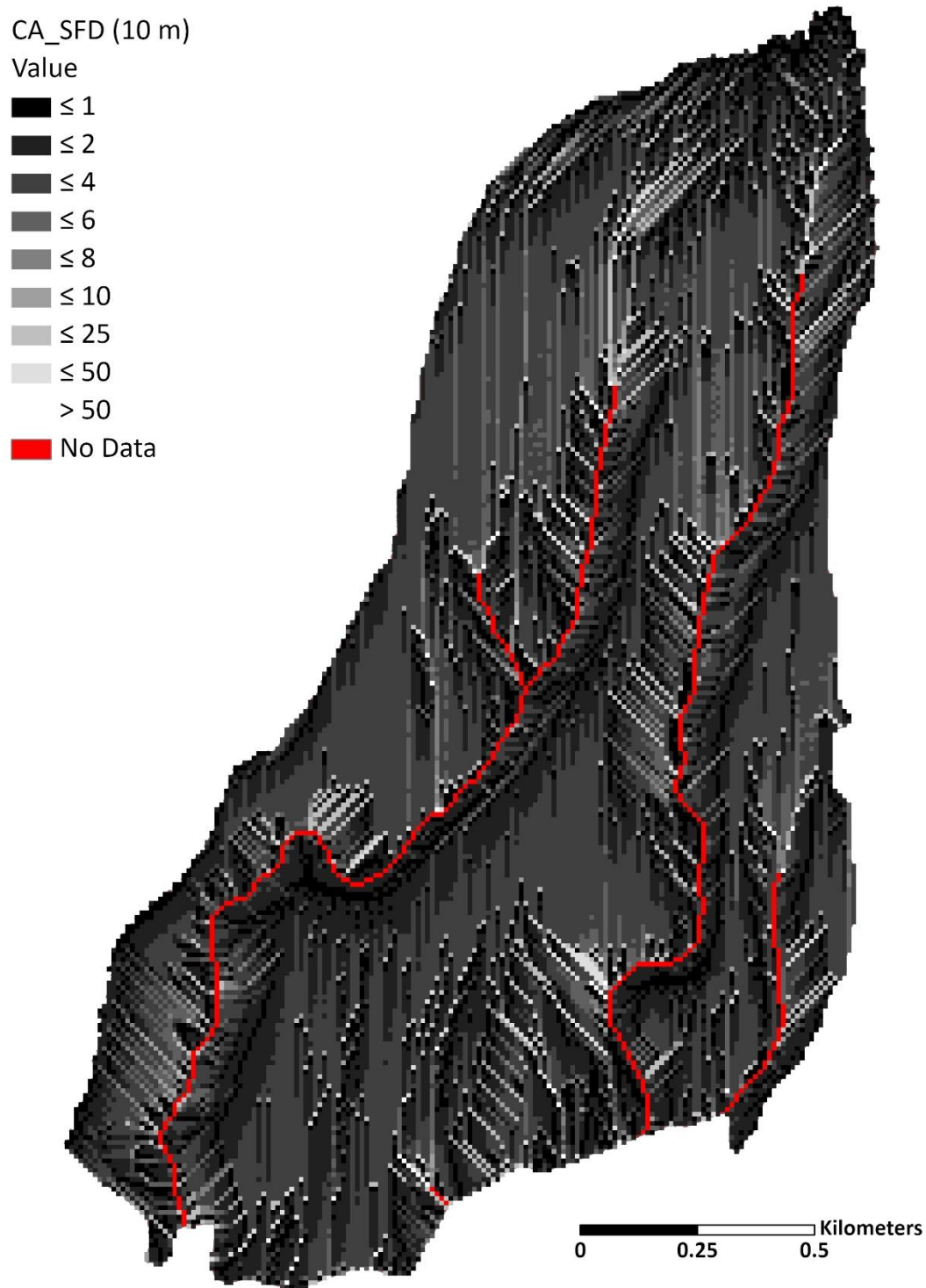


**Figure A15.** L factor with the CA method with a SFD algorithm for Site A at 10 m.

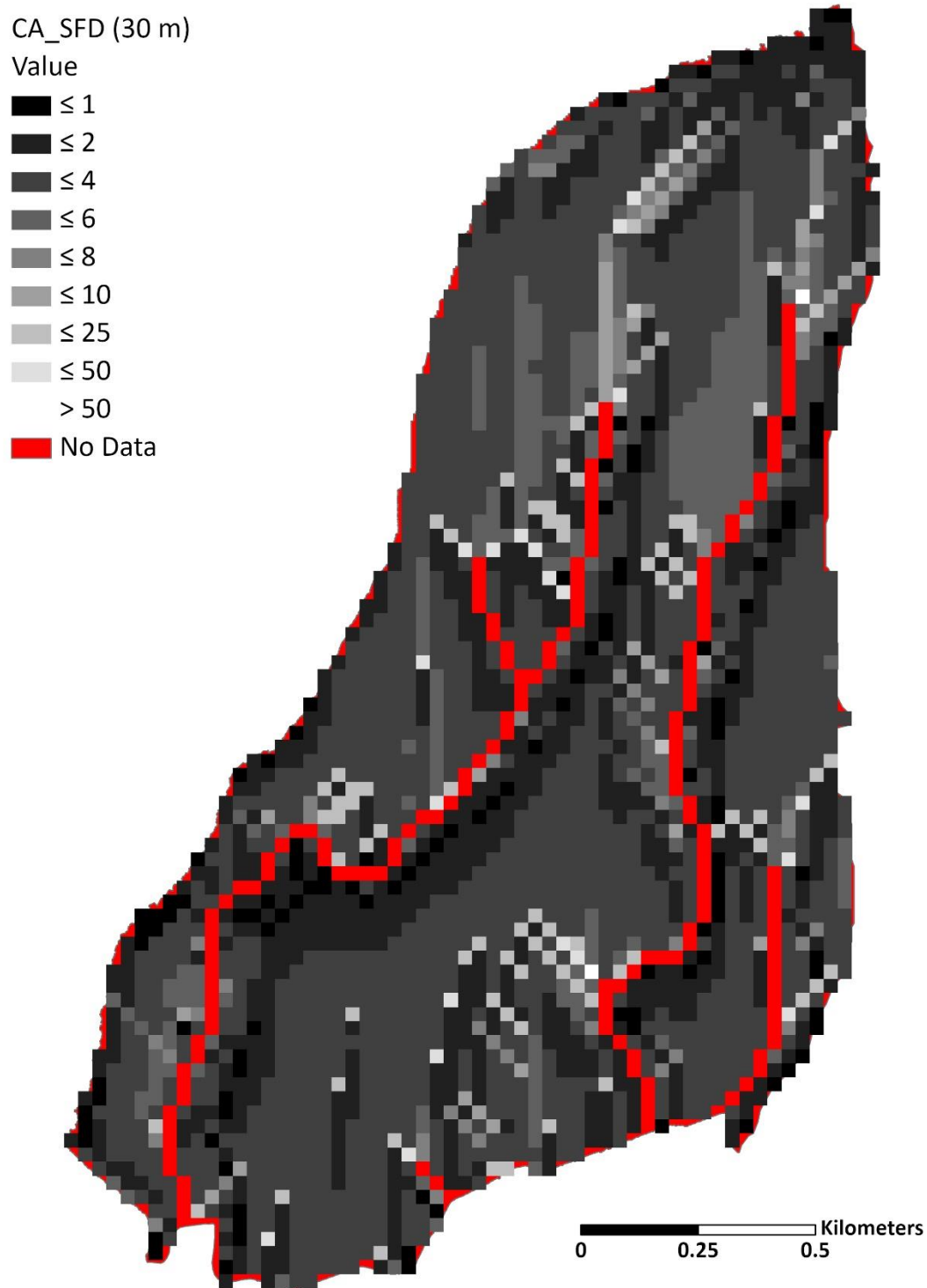


**Figure A16.** L factor with the CA method with a SFD algorithm for Site A at 30 m.

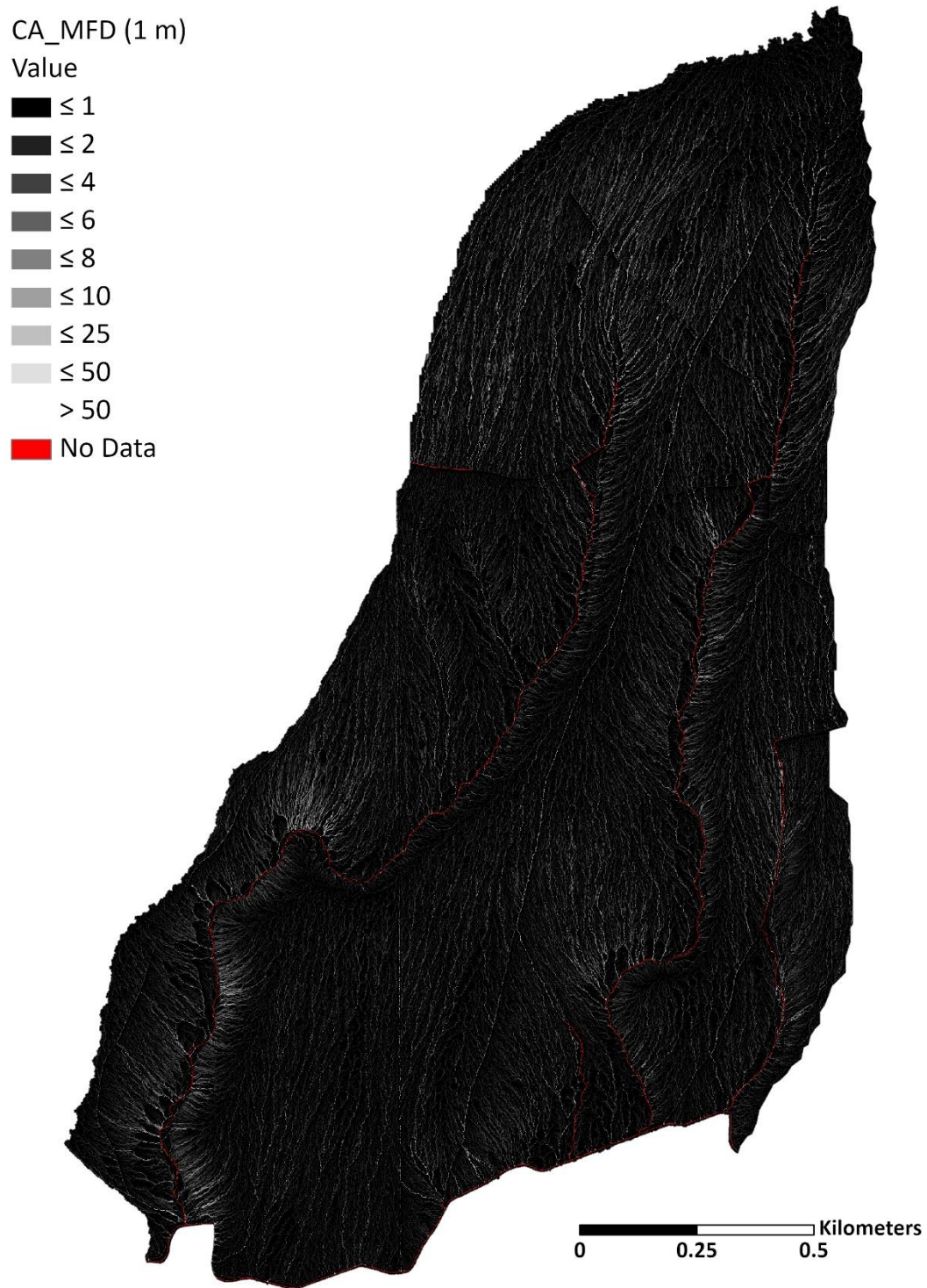


**Figure A17.** L factor with the CA method with a MFD algorithm for Site A at 1 m.

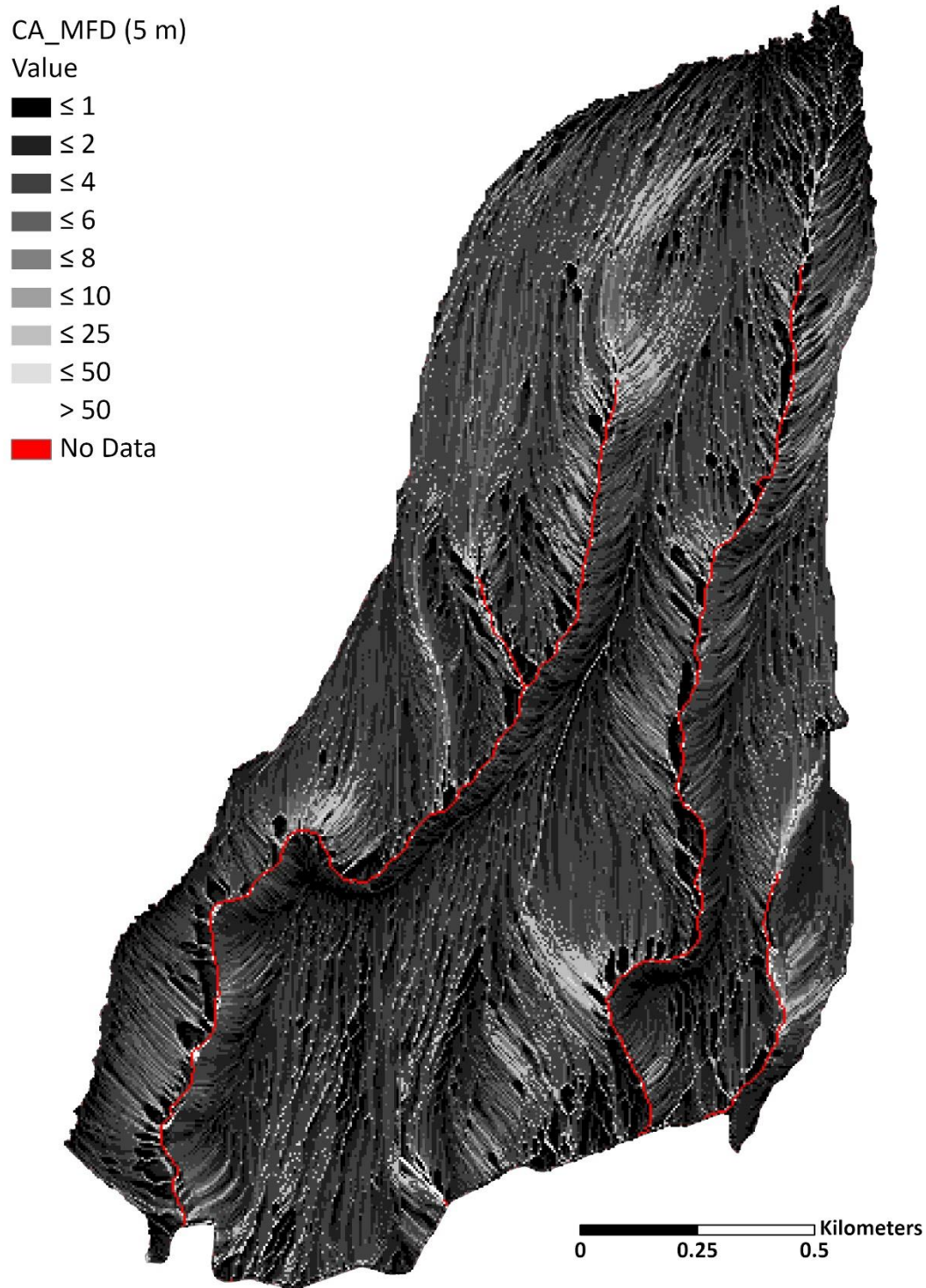


**Figure A18.** L factor with the CA method with a MFD algorithm for Site A at 5 m.

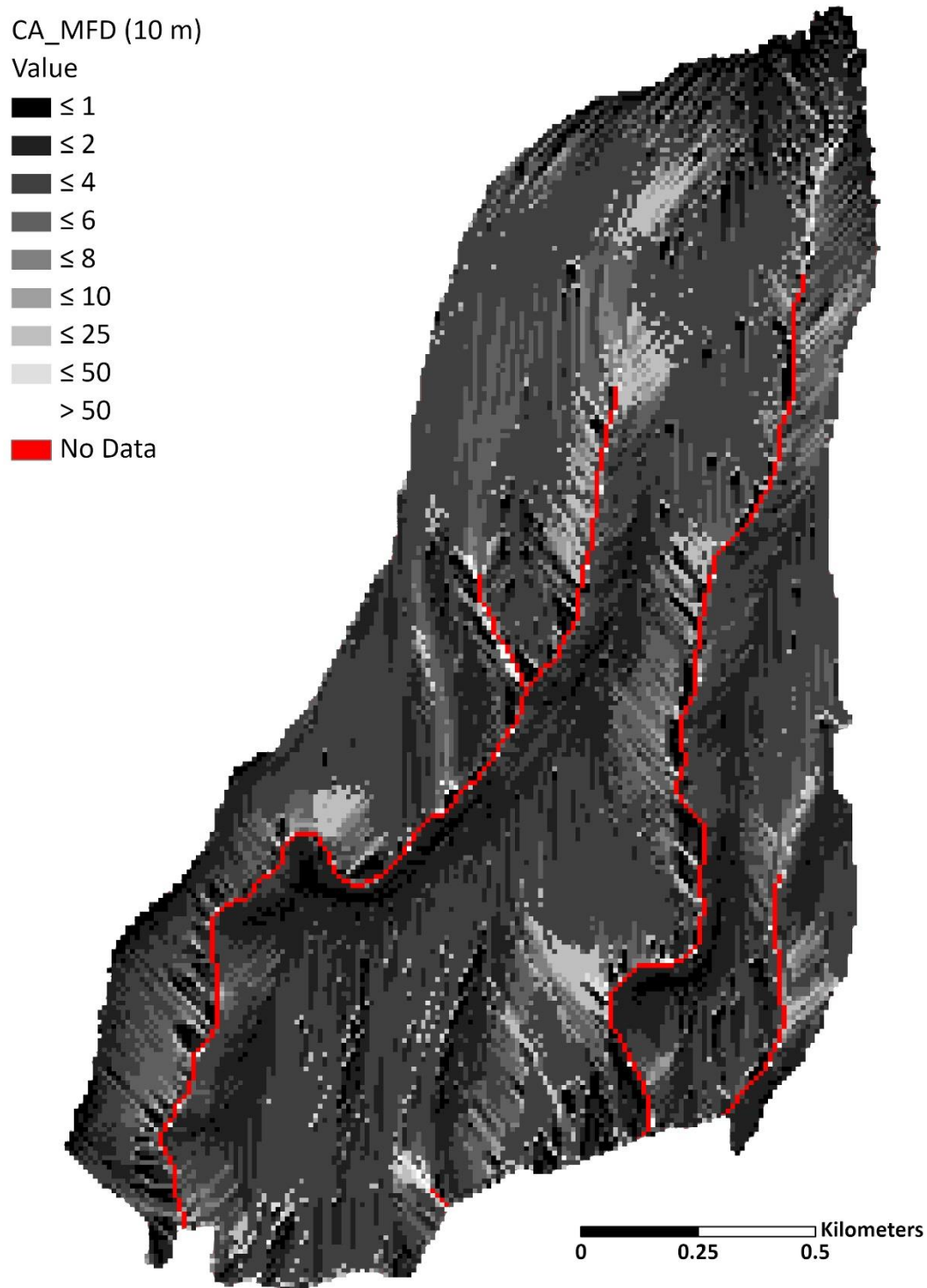


**Figure A19.** L factor with the CA method with a MFD algorithm for Site A at 10 m.

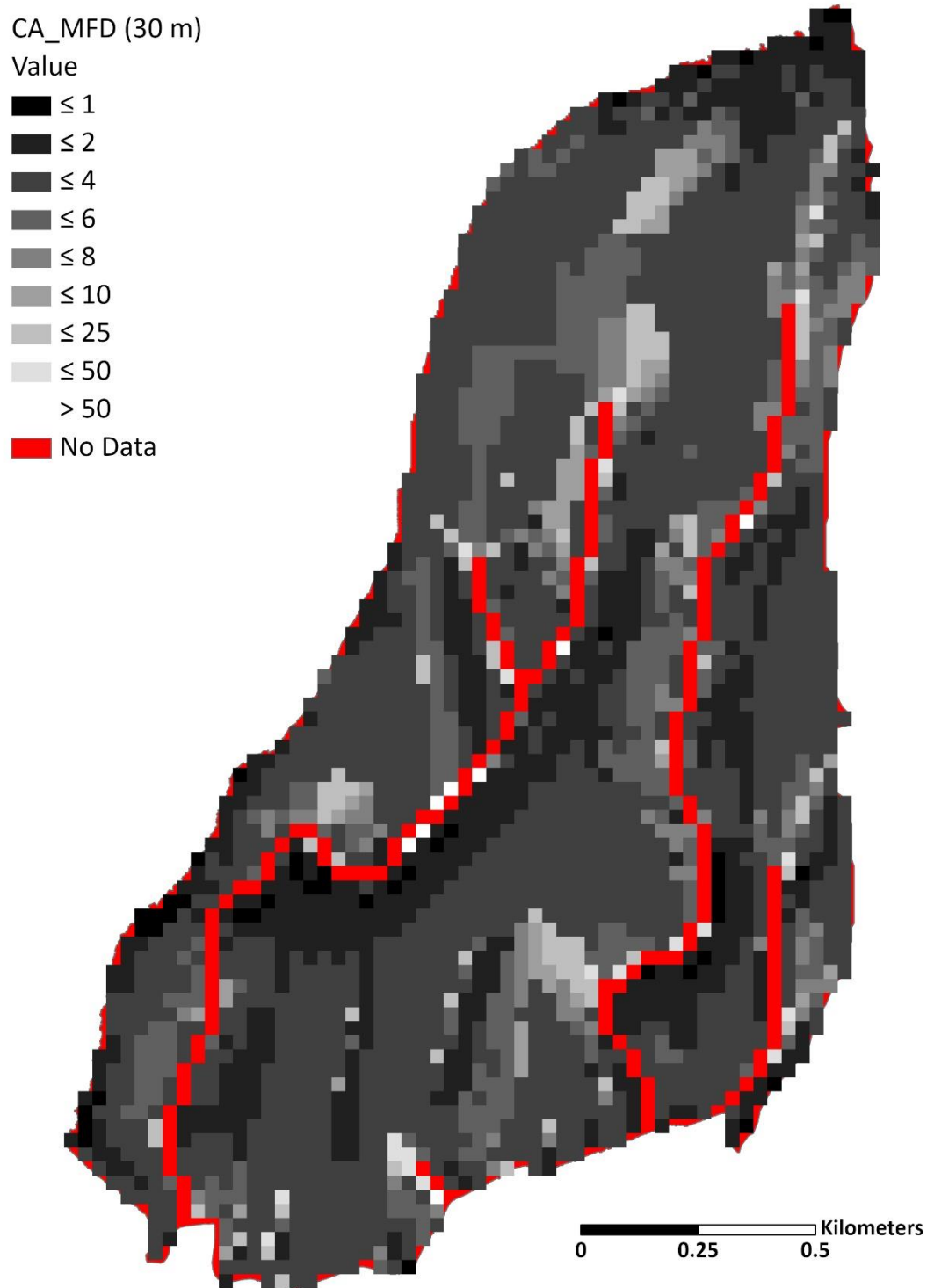


**Figure A20.** L factor with the CA method with a MFD algorithm for Site A at 30 m.

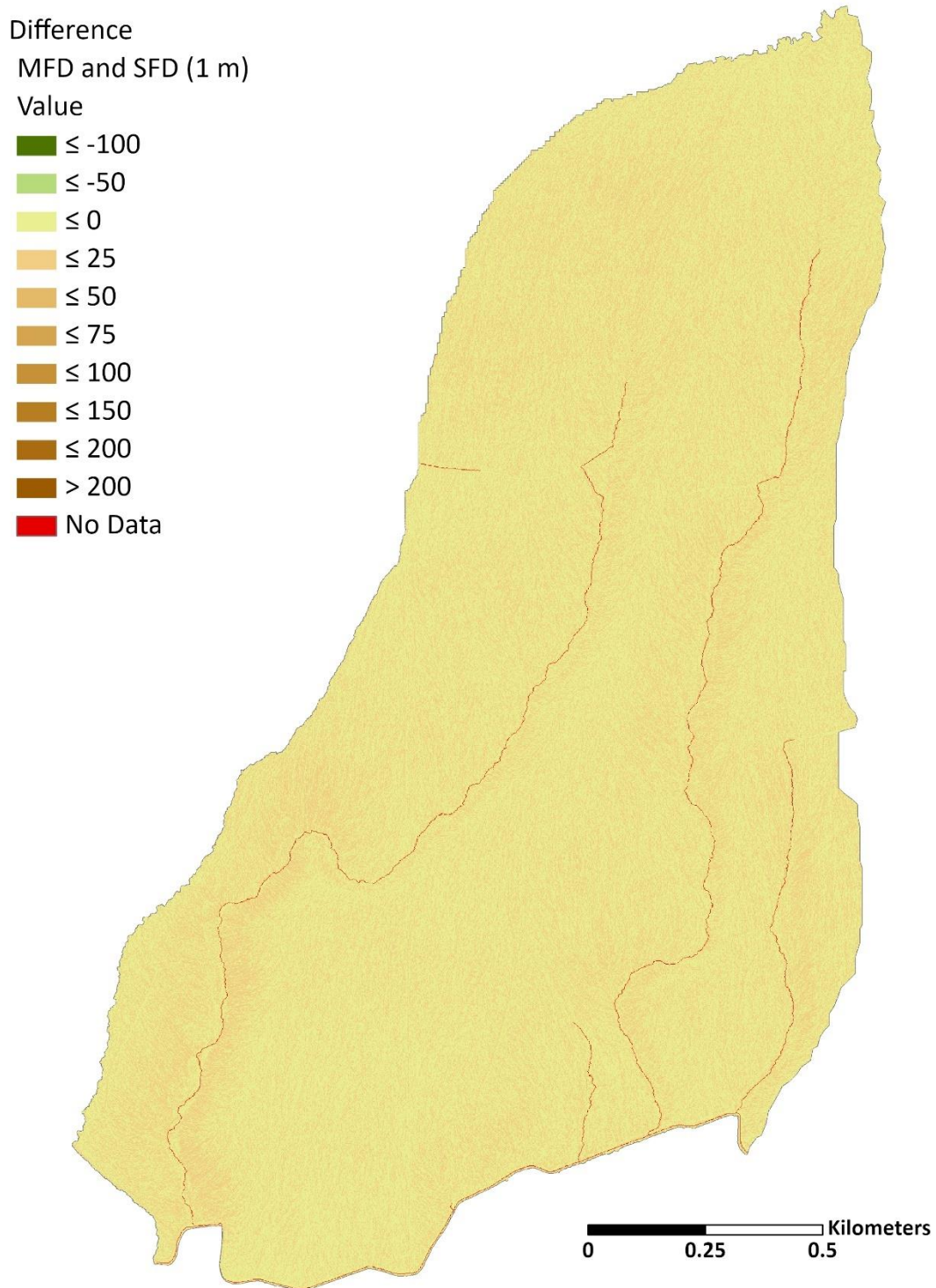


**Figure A21.** Site A difference raster (1 m) for the L Factor of the CA method using a SFD algorithm (SFD) subtracted from the CA method using a MFD algorithm (MFD).

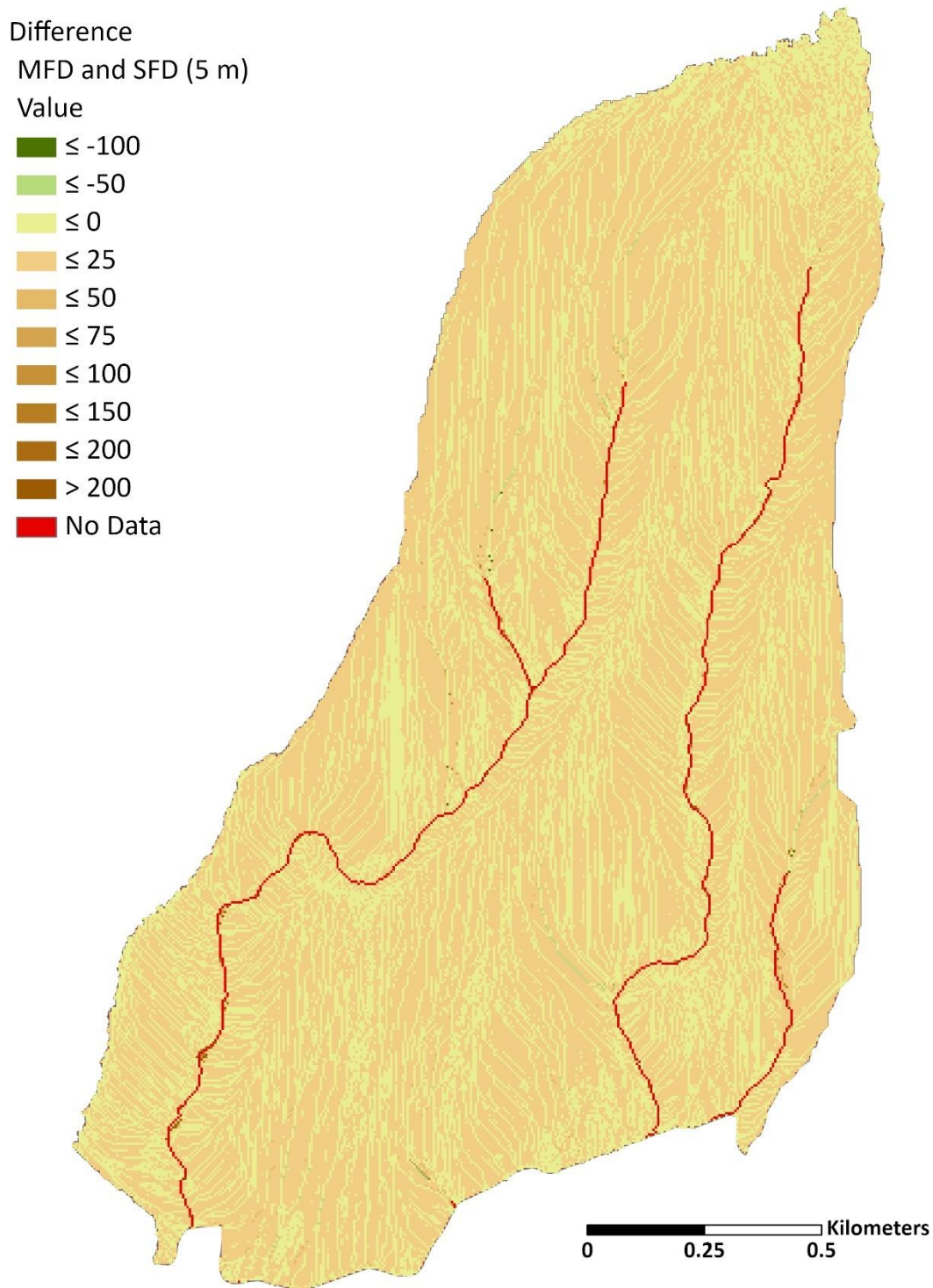


**Figure A22.** Site A difference raster (5 m) for the L Factor of the CA method using a SFD algorithm (SFD) subtracted from the CA method using a MFD algorithm (MFD).

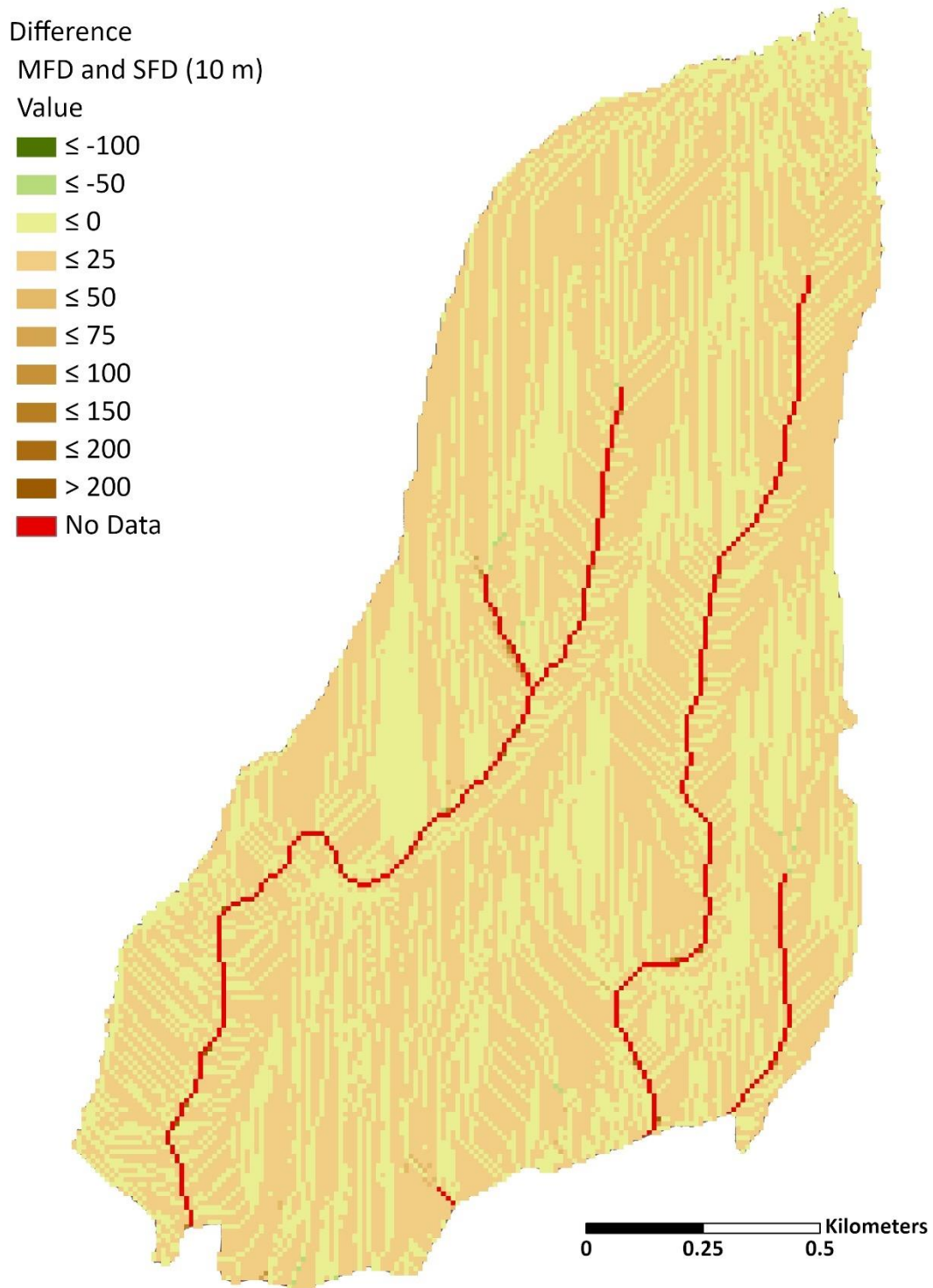


**Figure A23.** Site A difference raster (10 m) for the L Factor of the CA method using a SFD algorithm (SFD) subtracted from the CA method using a MFD algorithm (MFD).

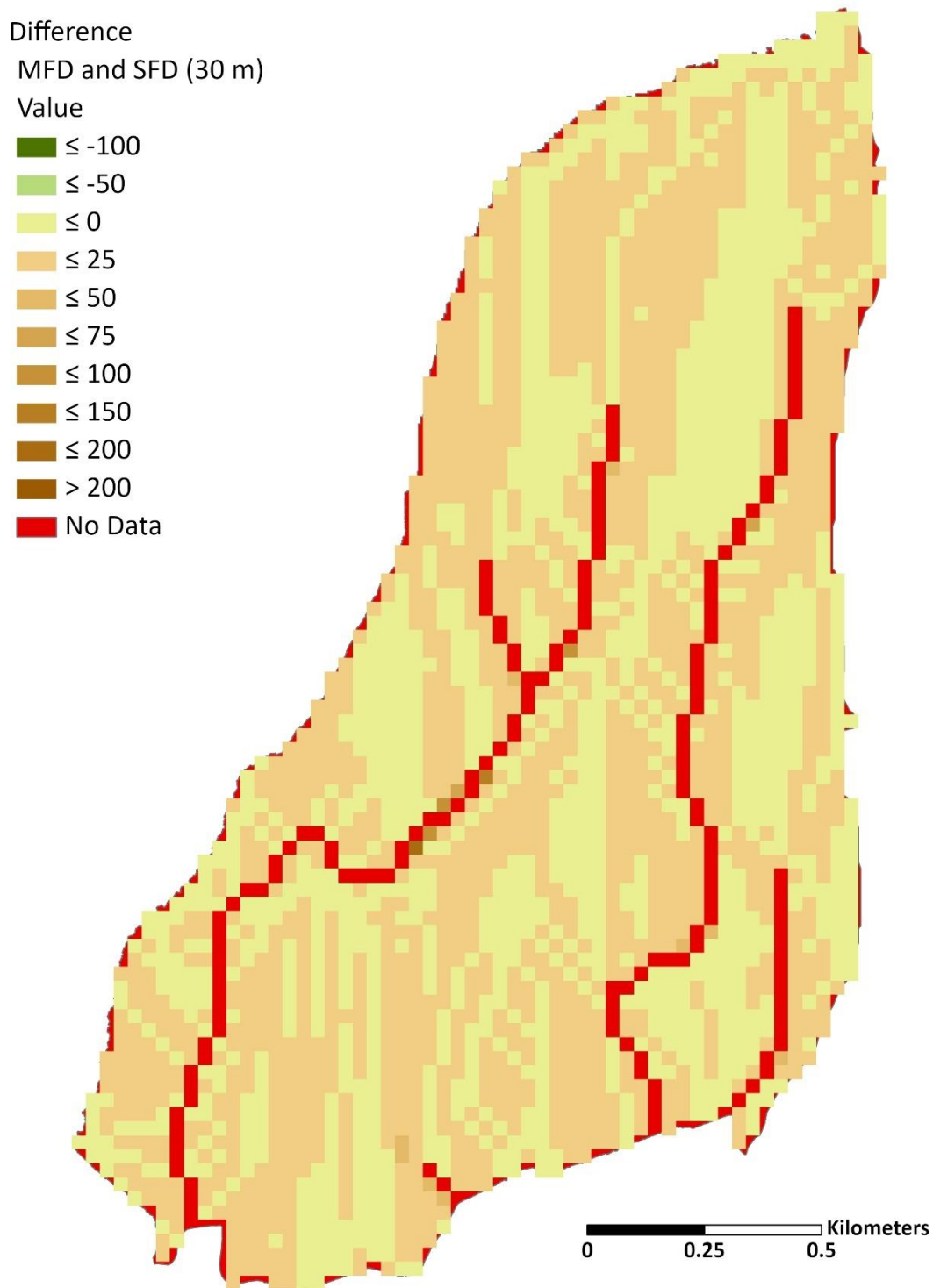


**Figure A24.** Site A difference raster (30 m) for the L Factor of the CA method using a SFD algorithm (SFD) subtracted from the CA method using a MFD algorithm (MFD).

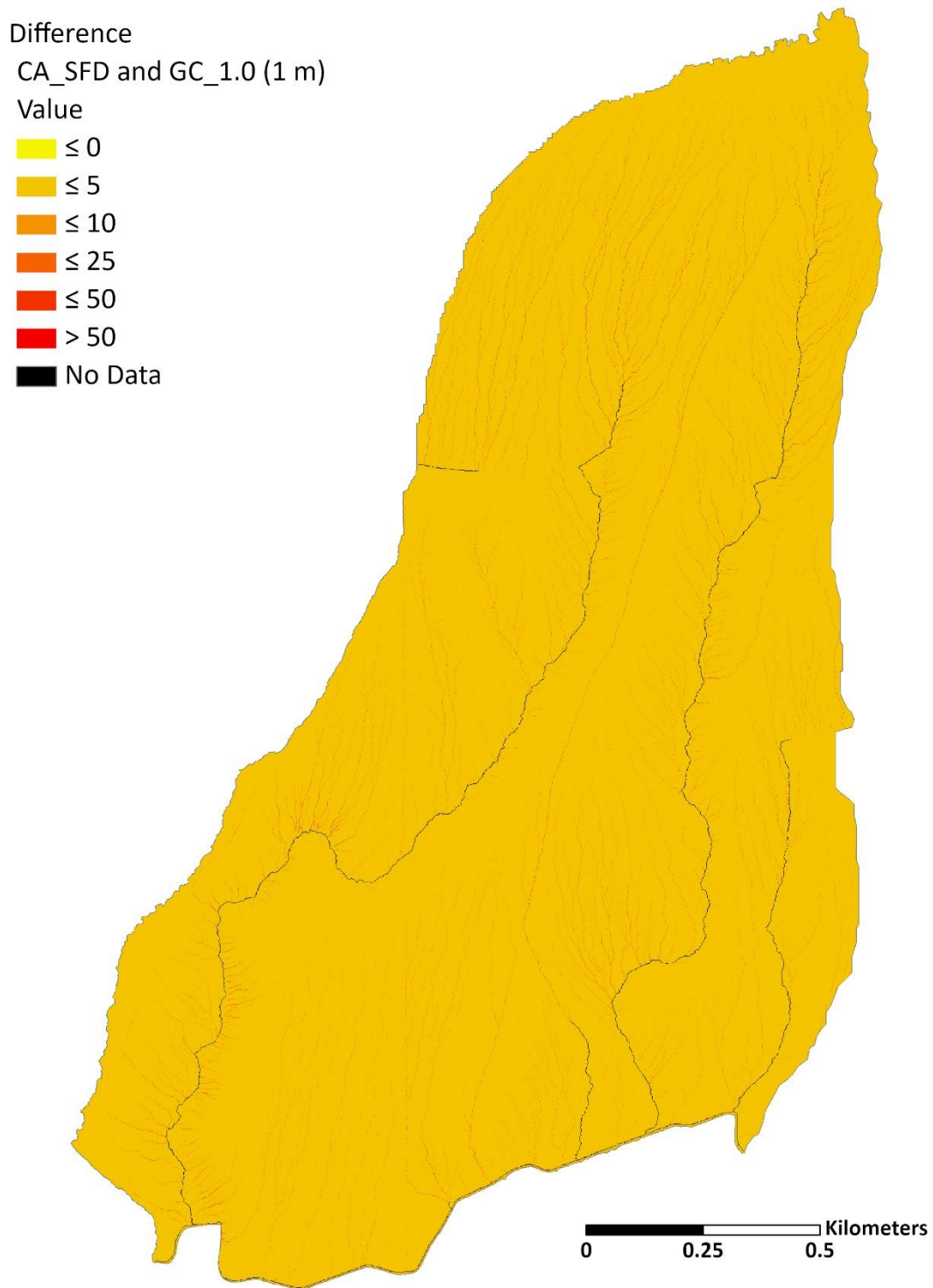


**Figure A25.** Site A difference raster (1 m) for the L Factor of the CA method using a SFD algorithm (CA\_SFD) and the GC method without slope cutoff (GC\_1.0).

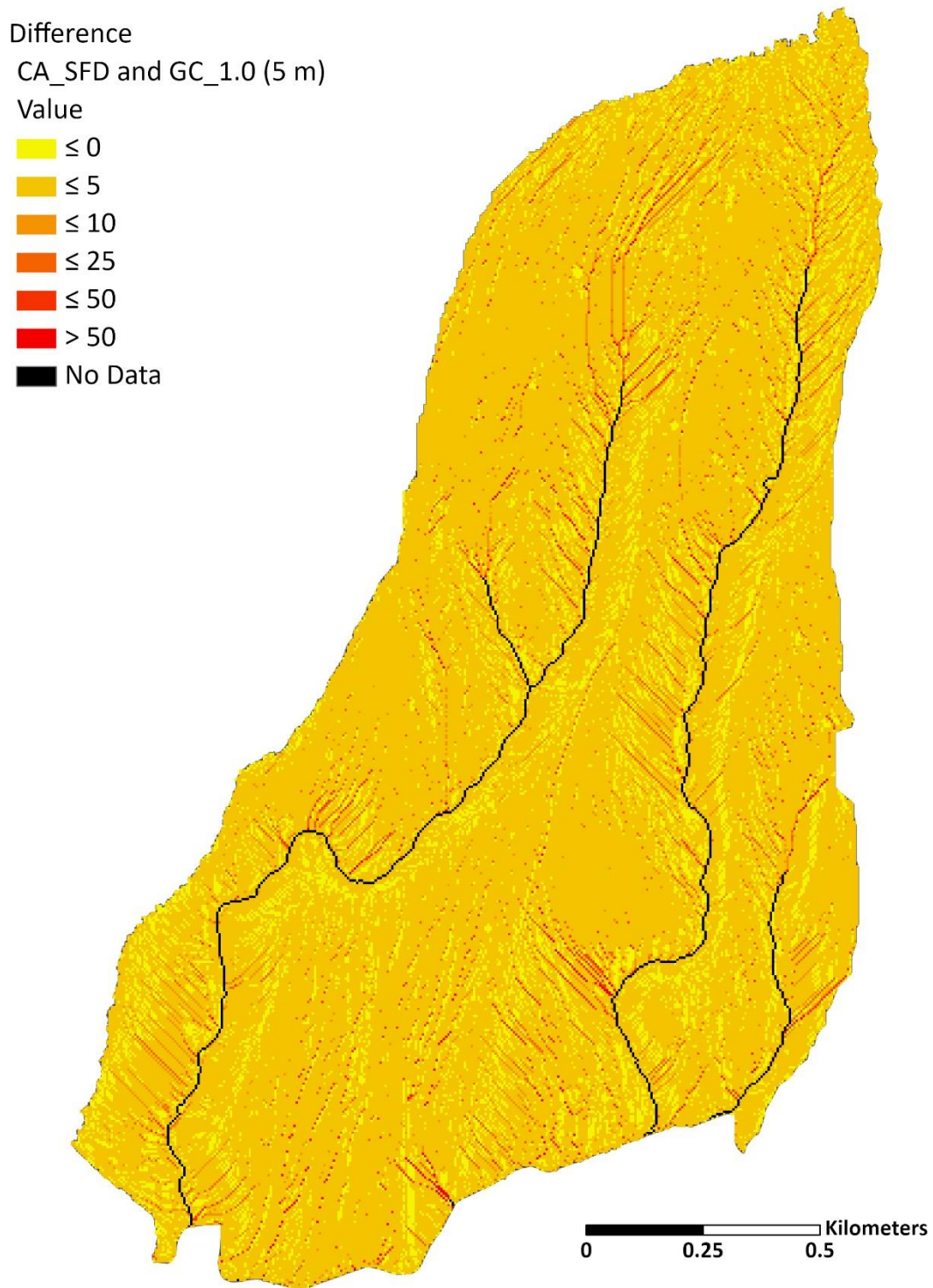


**Figure A26.** Site A difference raster (5 m) for the L Factor of the CA method using a SFD algorithm (CA\_SFD) and the GC method without slope cutoff (GC\_1.0).

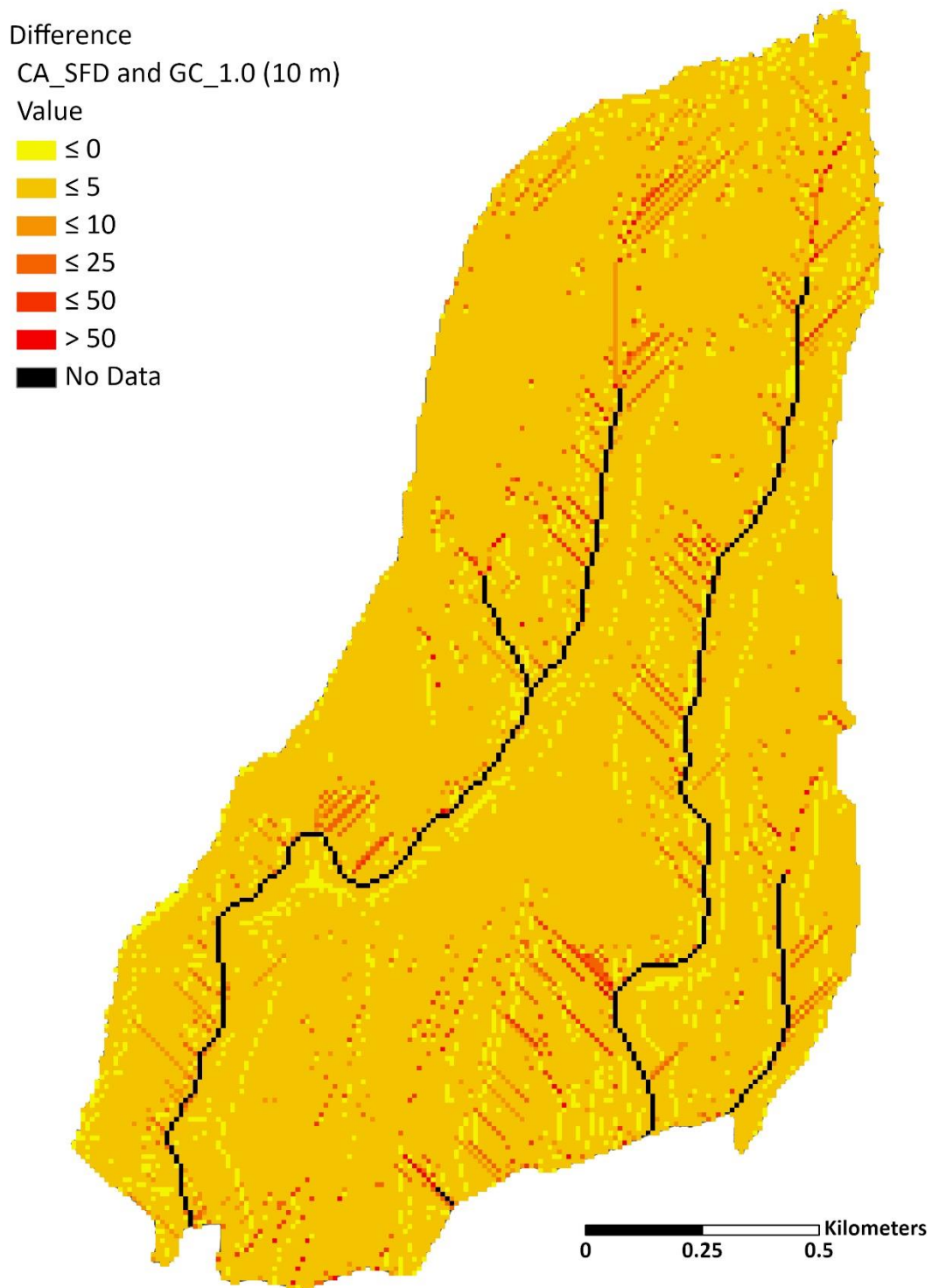


**Figure A27.** Site A difference raster (10 m) for the L Factor of the CA method using a SFD algorithm (CA\_SFD) and the GC method without slope cutoff (GC\_1.0).

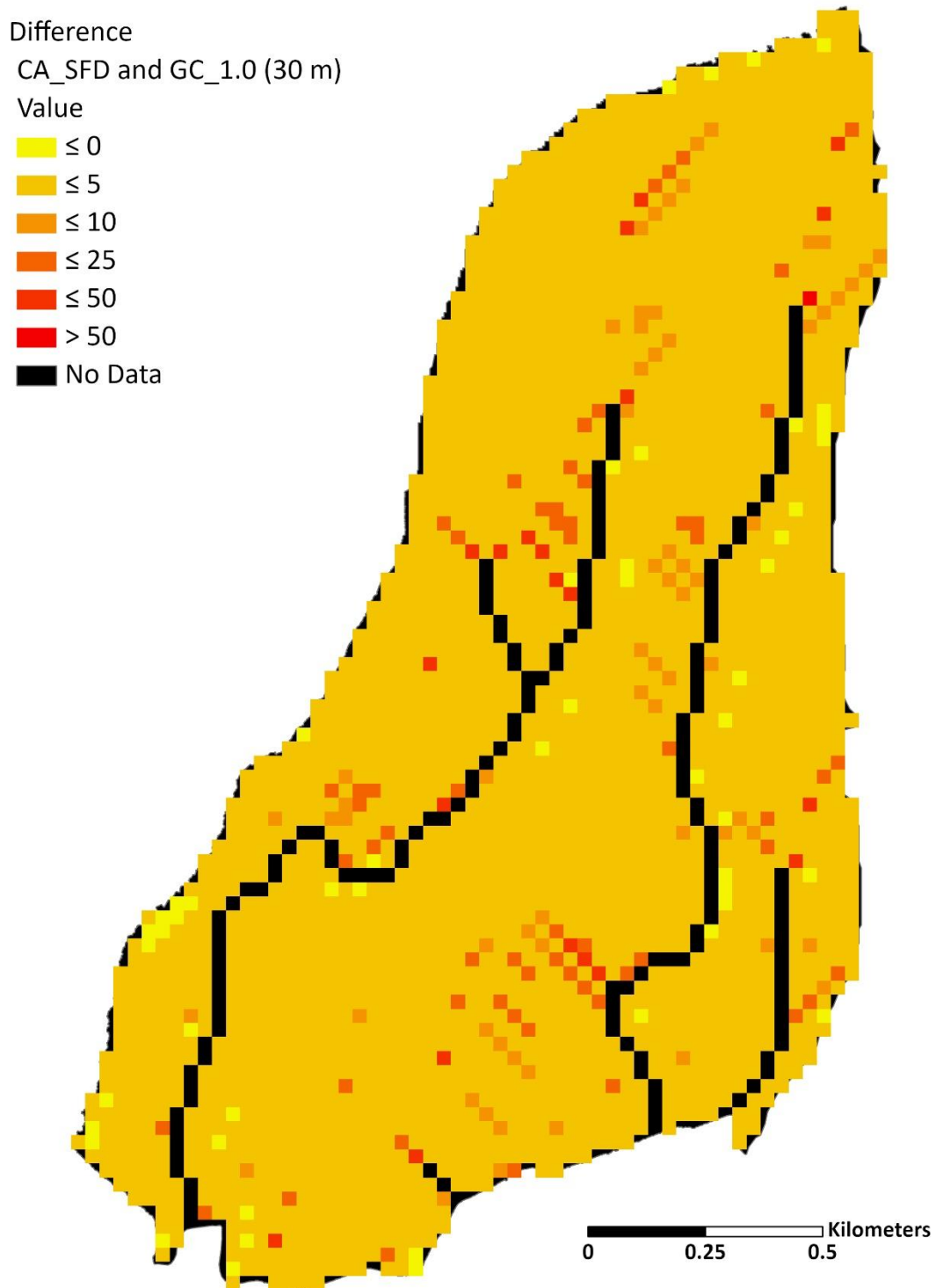


**Figure A28.** Site A difference raster (30 m) for the L Factor of the CA method using a SFD algorithm (CA\_SFD) and the GC method without slope cutoff (GC\_1.0).

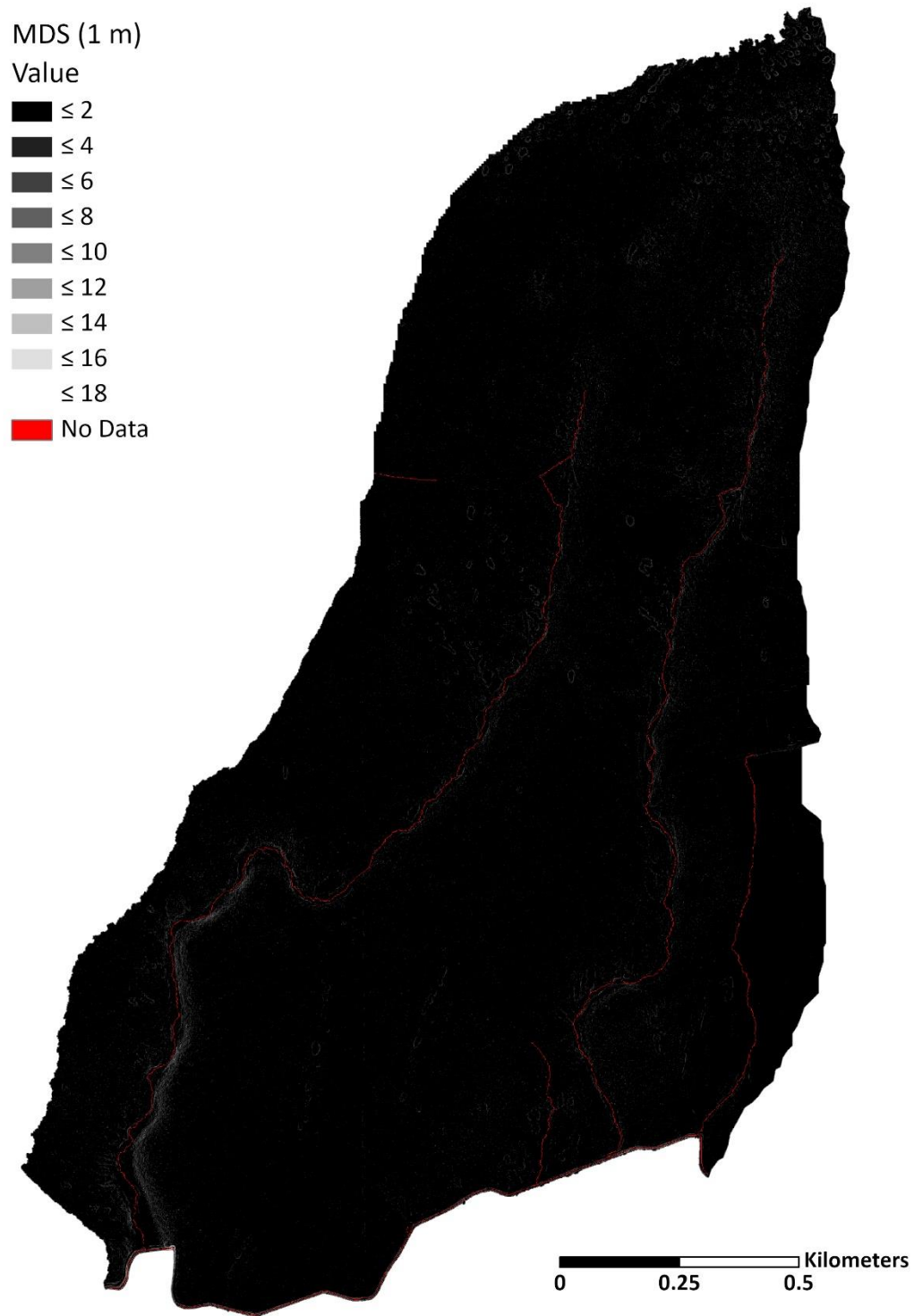


**Figure A29.** S factor with the MDS method for Site A at 1 m.

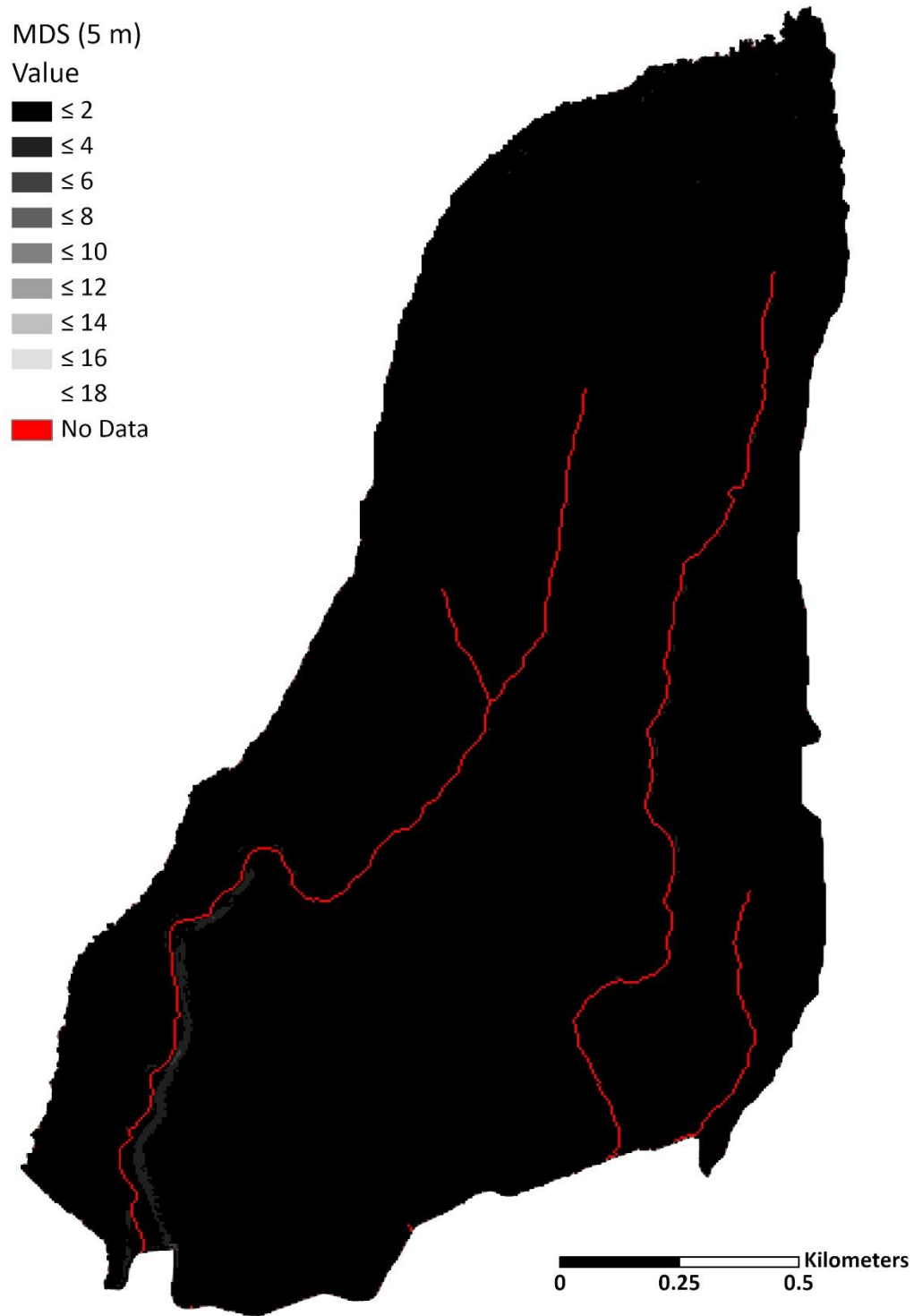


**Figure A30.** S factor with the MDS method for Site A at 5 m.

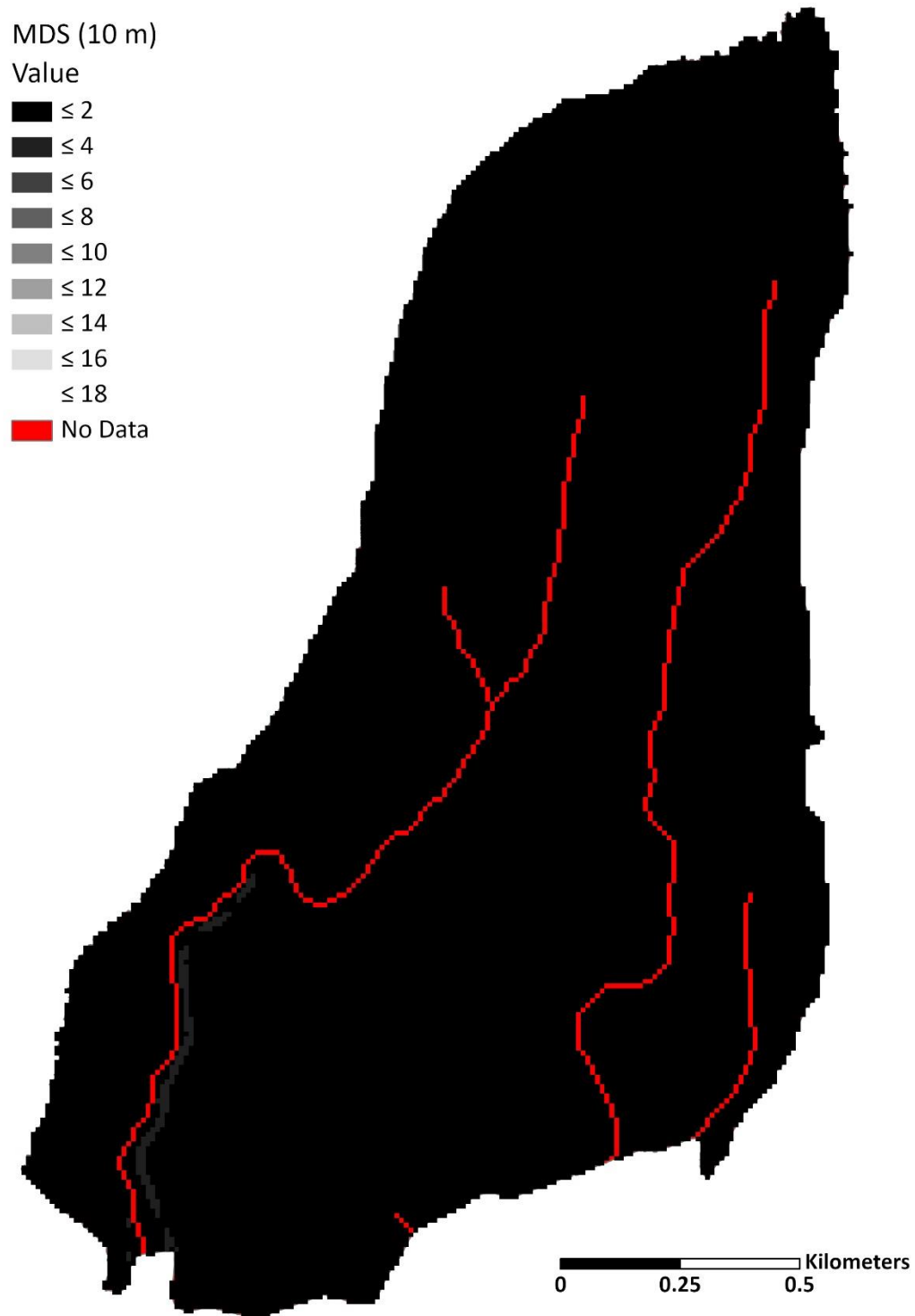


**Figure A31.** S factor with the MDS method for Site A at 10 m.

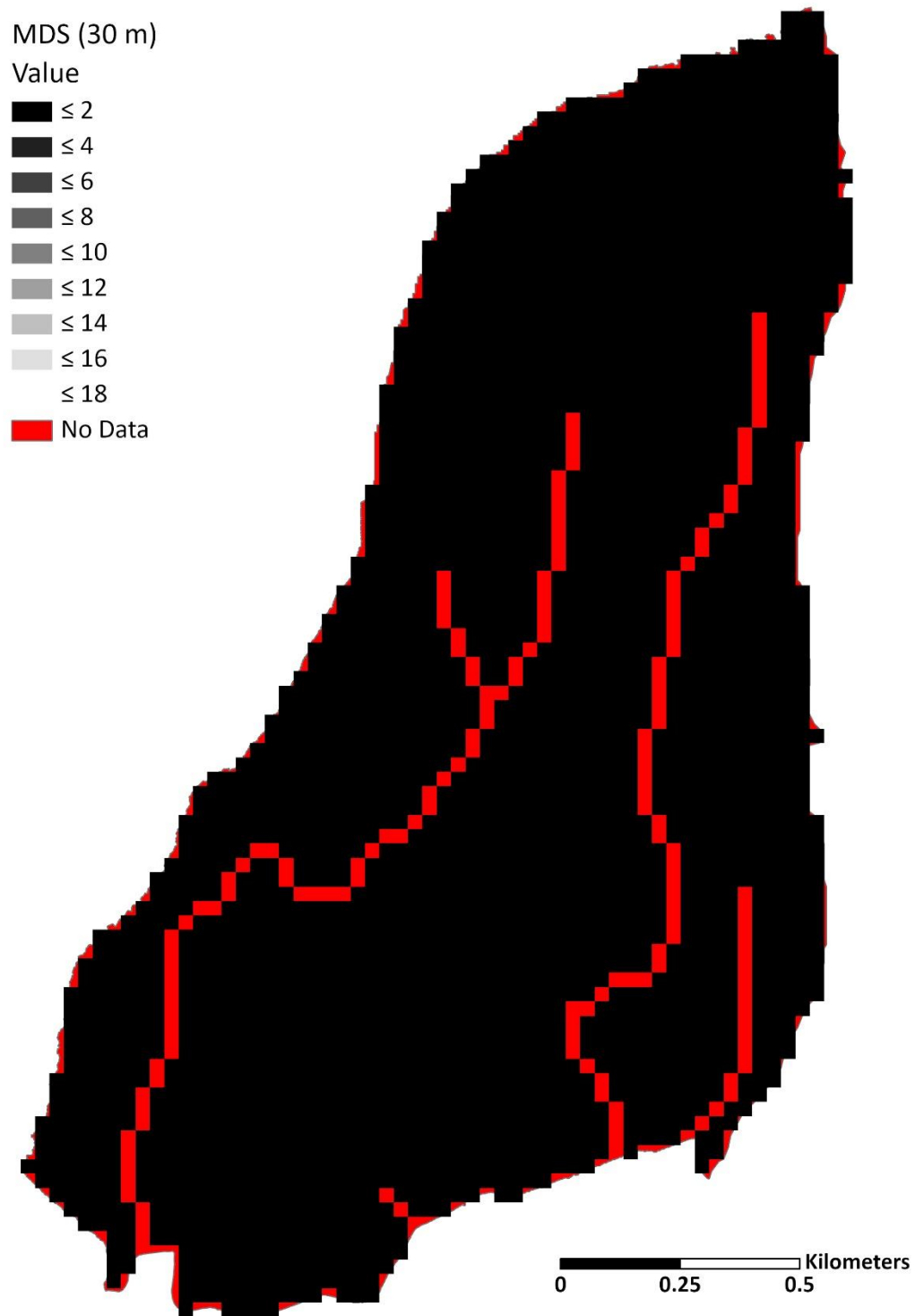


**Figure A32.** S factor with the MDS method for Site A at 30 m.

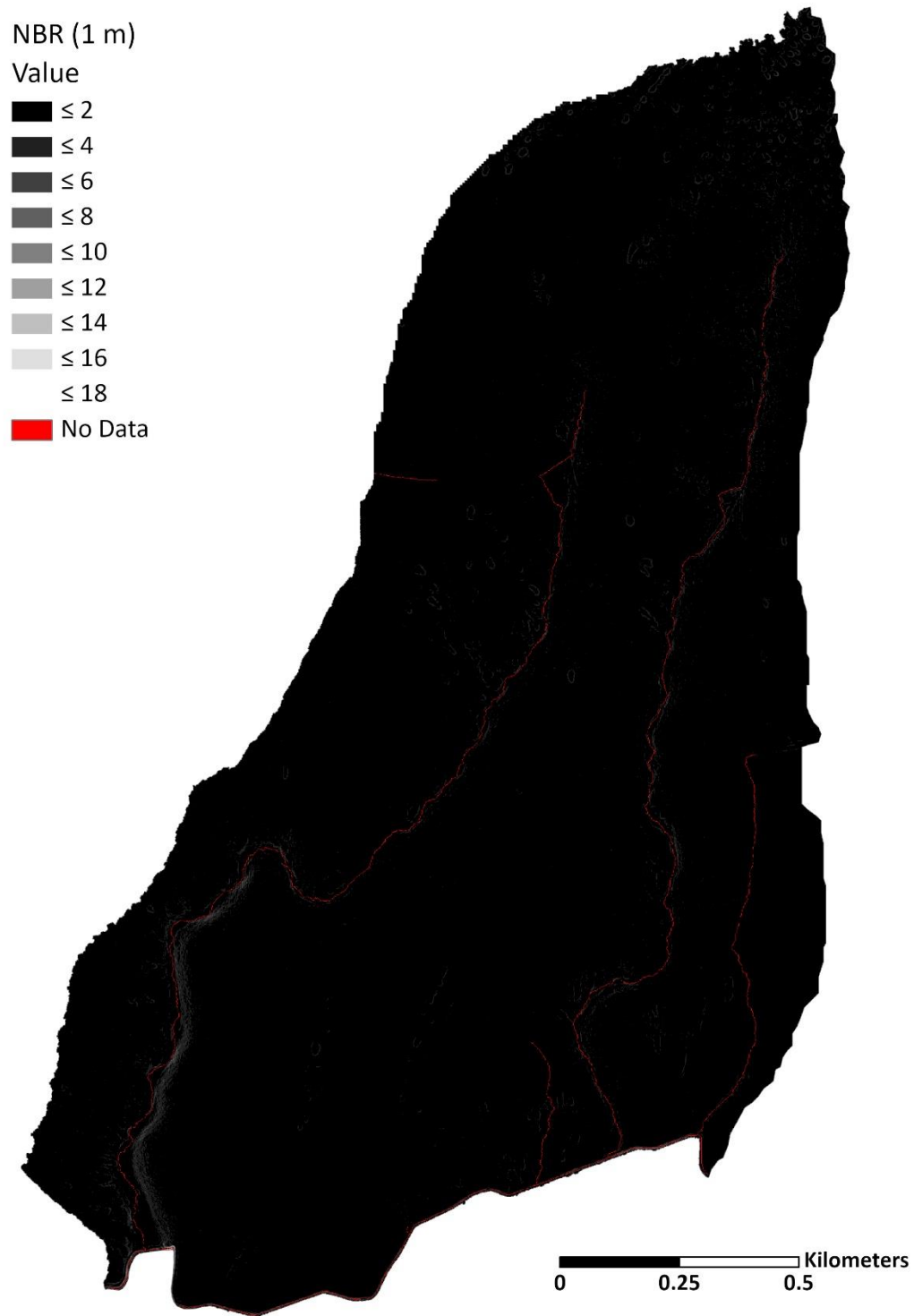


**Figure A33.** S factor with the NBR method for Site A at 1 m.

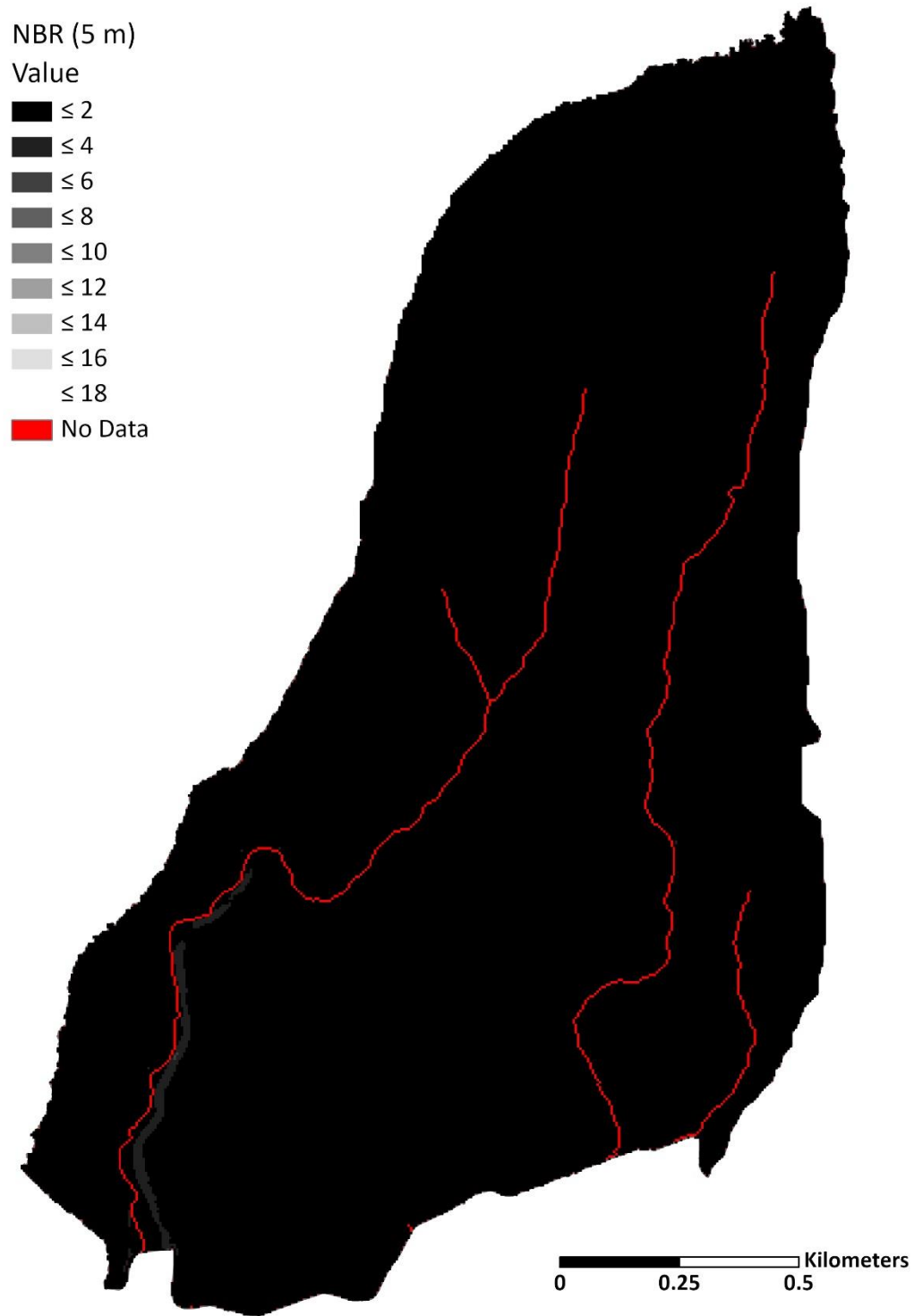


**Figure A34.** S factor with the NBR method for Site A at 5 m.

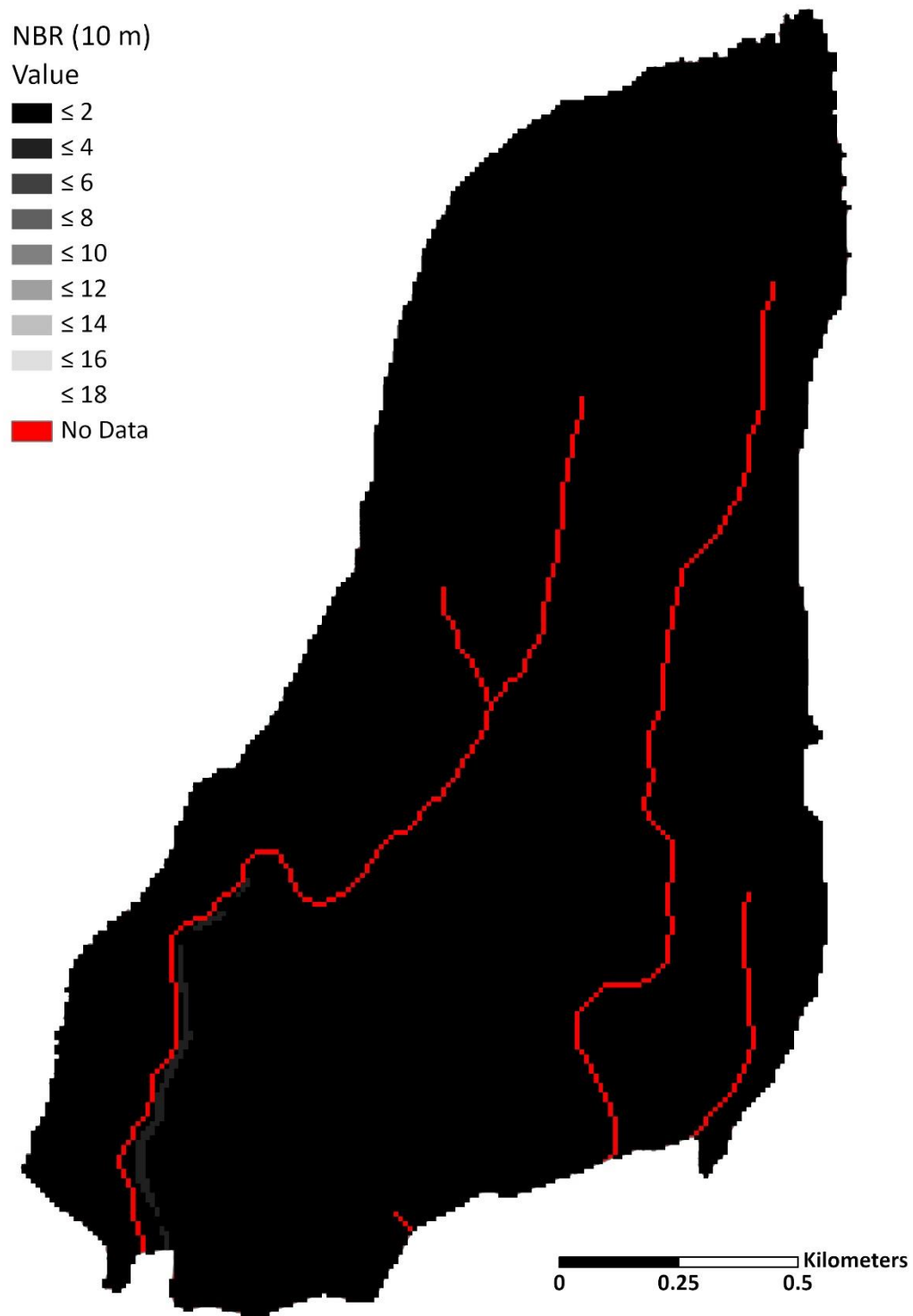


**Figure A35.** S factor with the NBR method for Site A at 10 m.

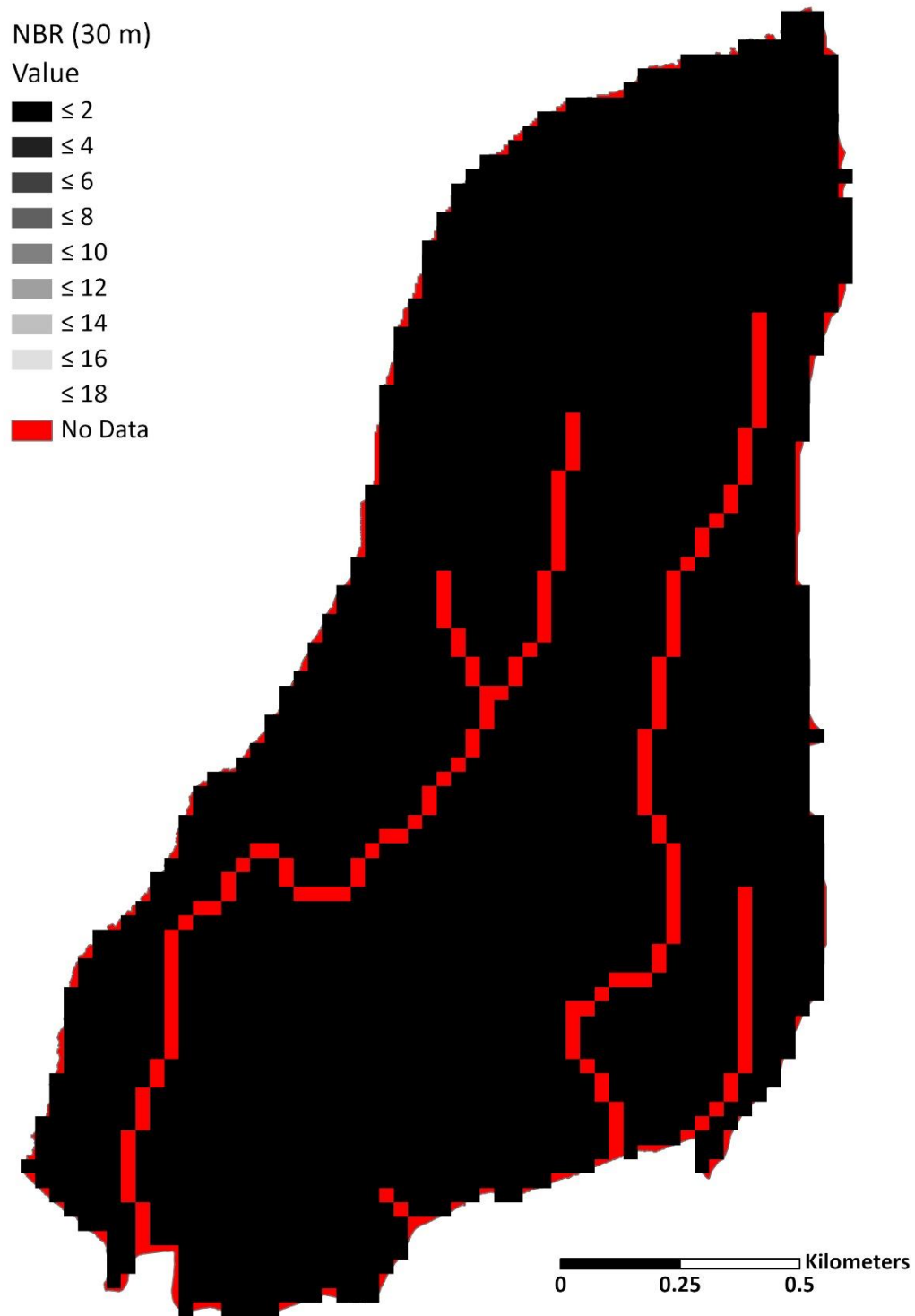


**Figure A36.** S factor with the NBR method for Site A at 30 m.

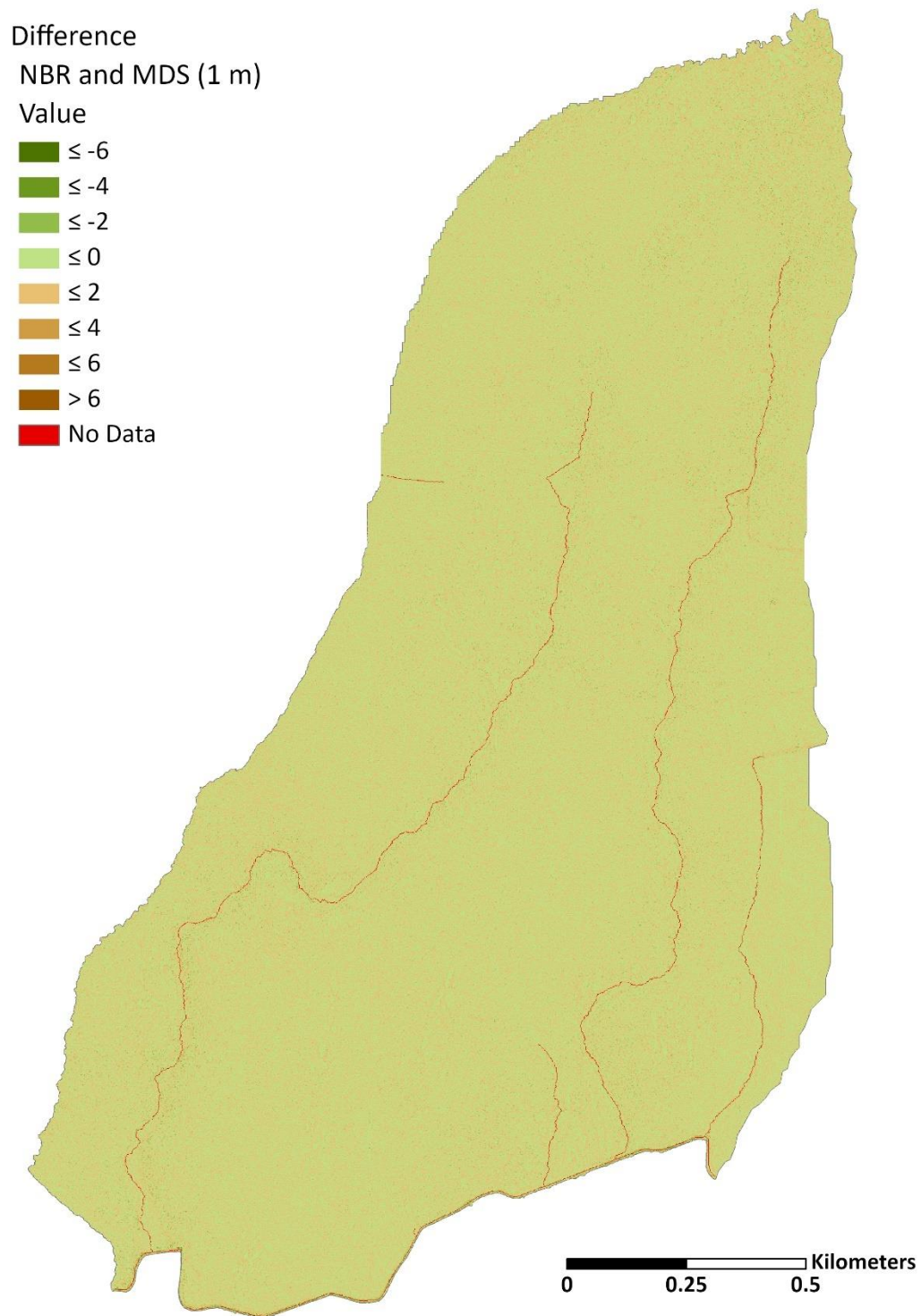


**Figure A37.** Site A difference raster (1 m) for the S Factor of the MDS method subtracted from the NBR method.

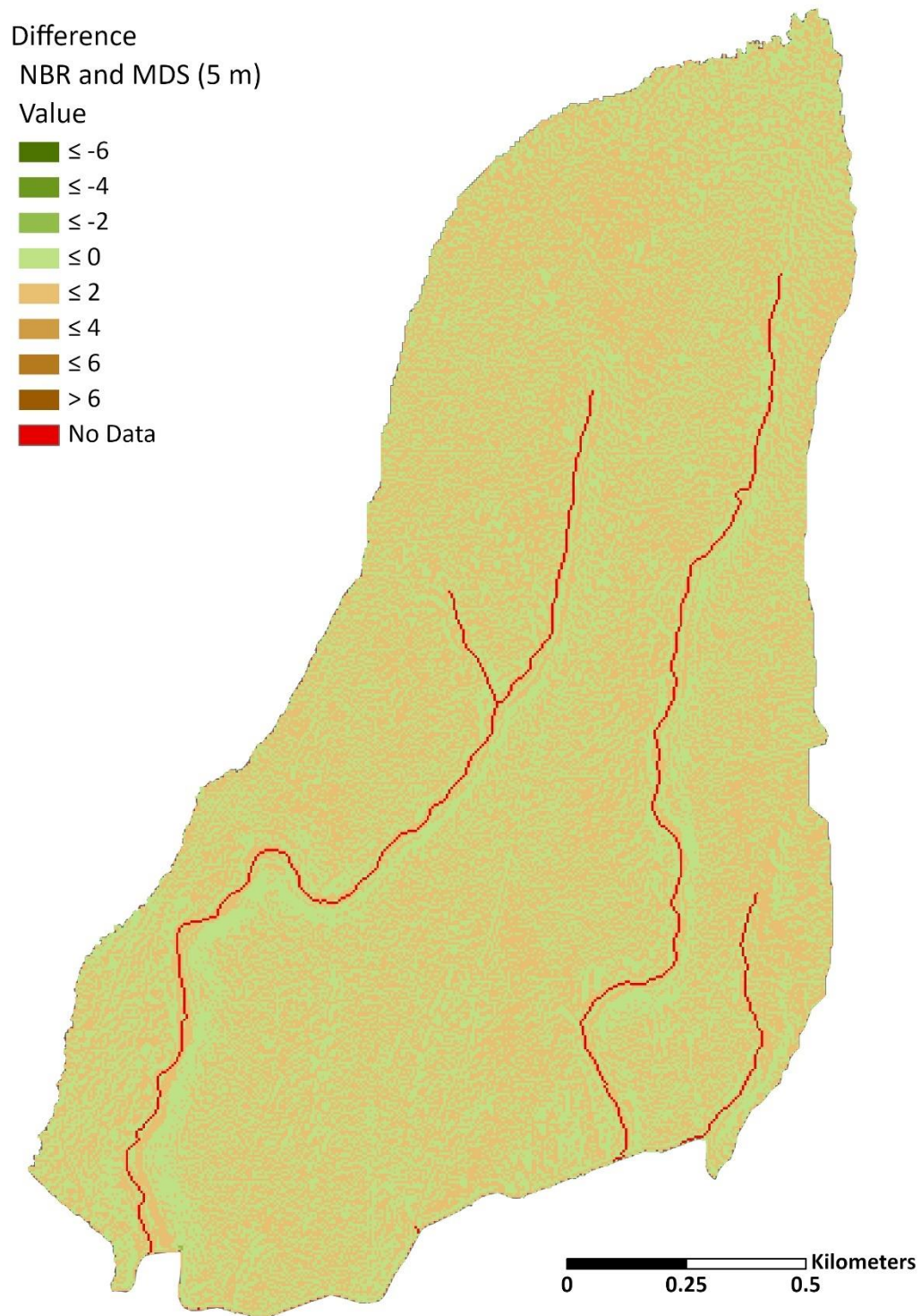


**Figure A38.** Site A difference raster (5 m) for the S Factor of the MDS method subtracted from the NBR method.

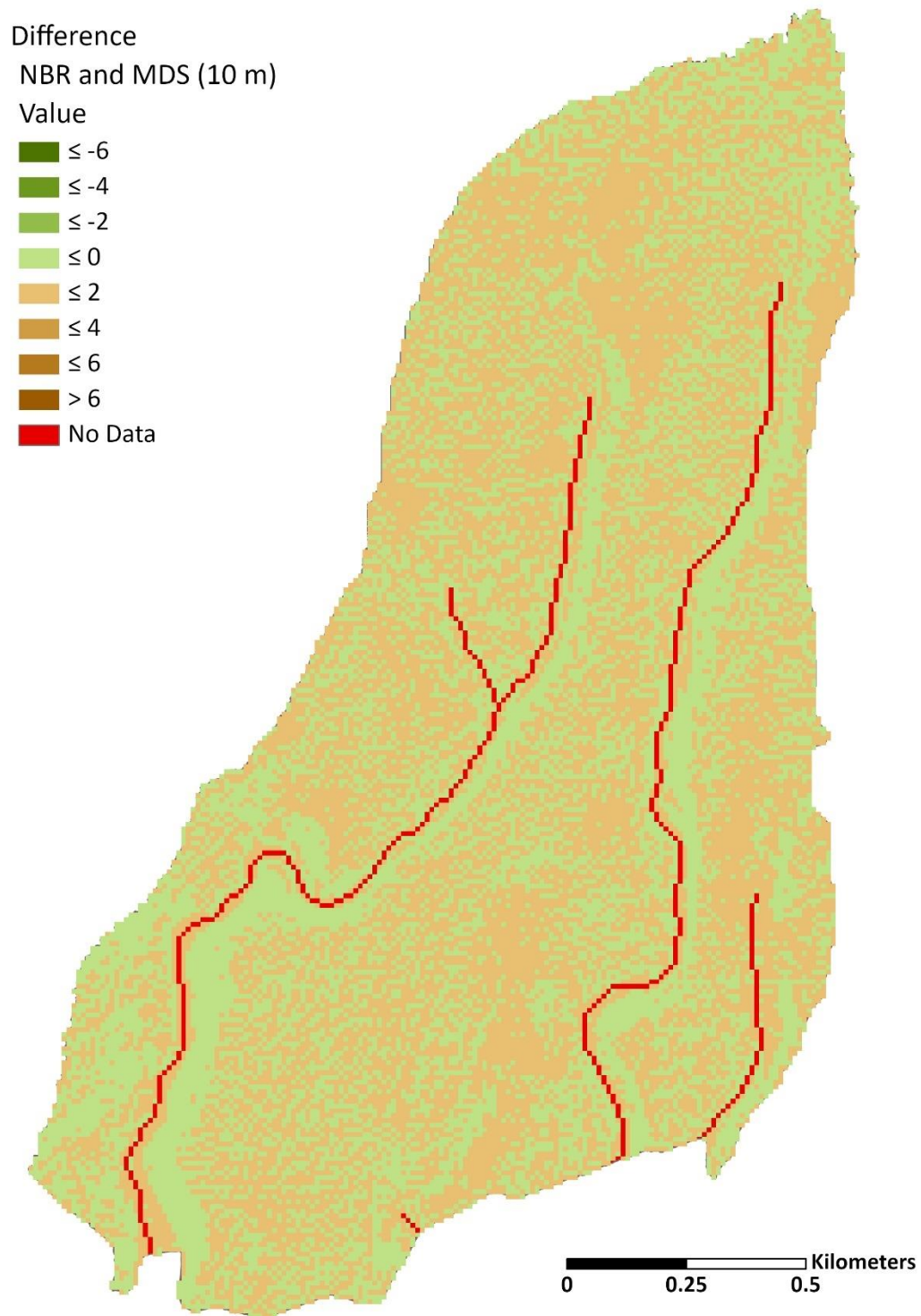


**Figure A39.** Site A difference raster (10 m) for the S Factor of the MDS method subtracted from the NBR method.

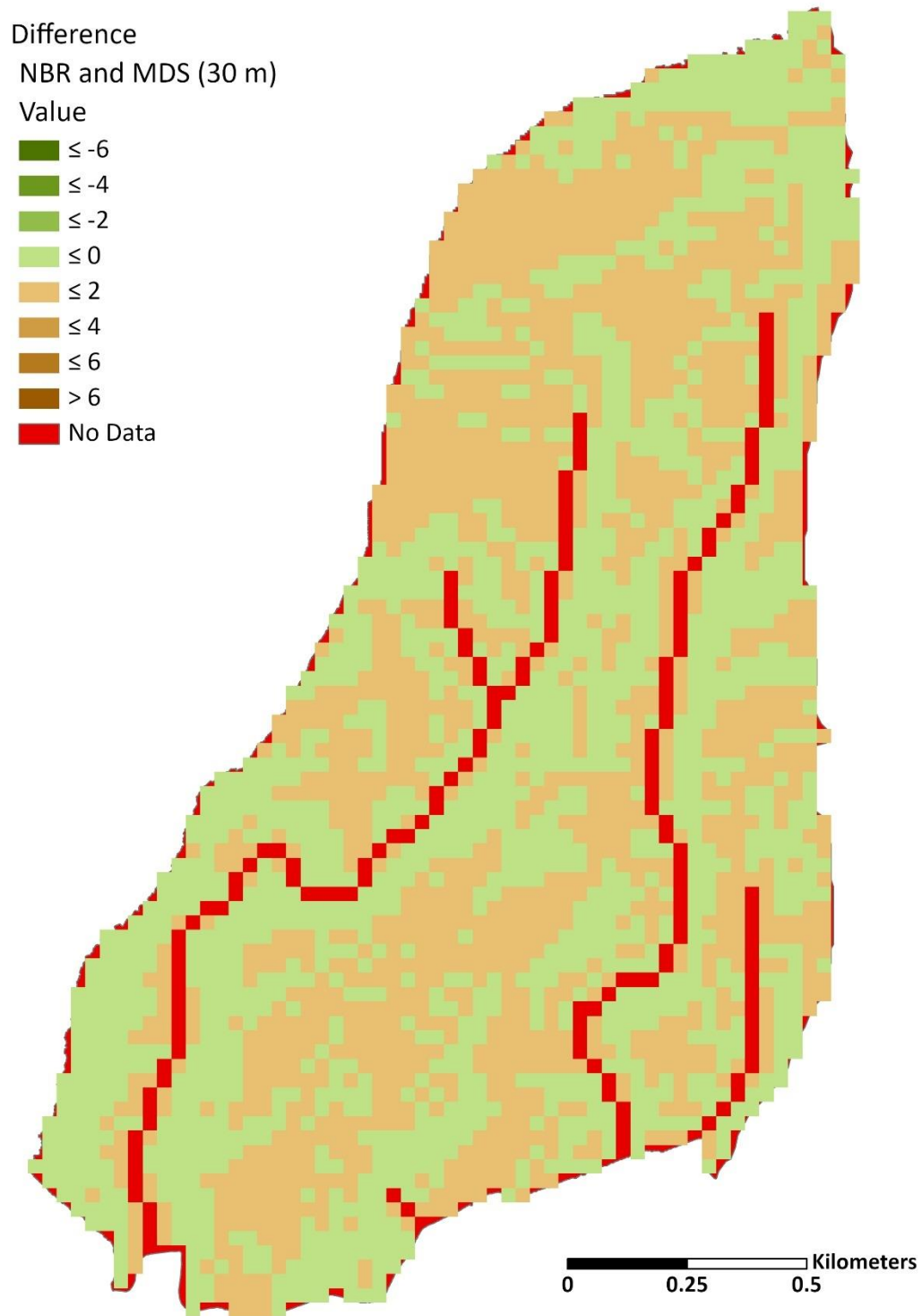


**Figure A40.** Site A difference raster (30 m) for the S Factor of the MDS method subtracted from the NBR method.

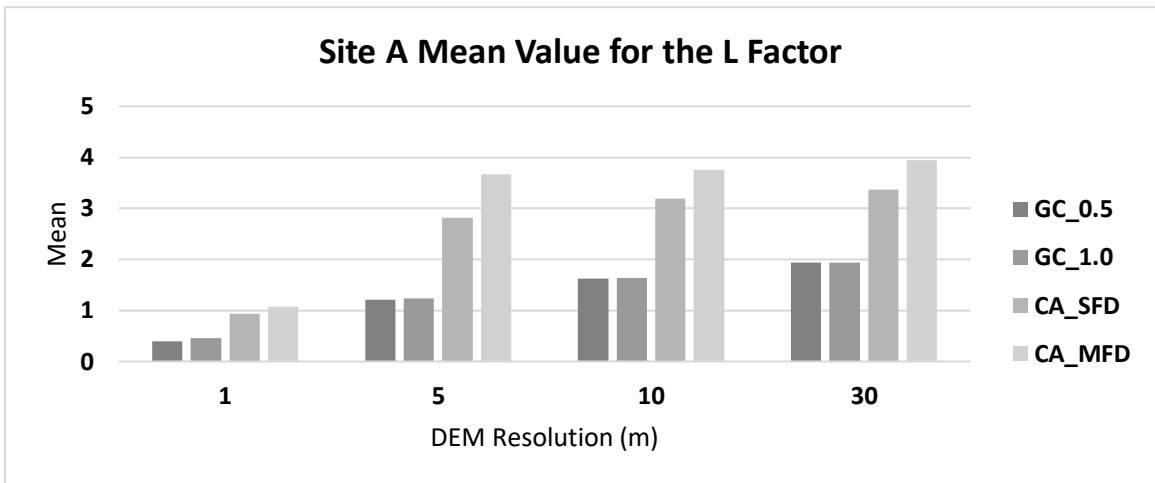


**Figure A41.** Mean value of L factor for Site A where GC\_0.5 is the GC method with slope cutoff set to 0.5, GC\_1.0 is the GC method without slope cutoff, CA\_SFD is the CA method using a SFD algorithm, and CA\_MFD is the CA method using a MFD algorithm.

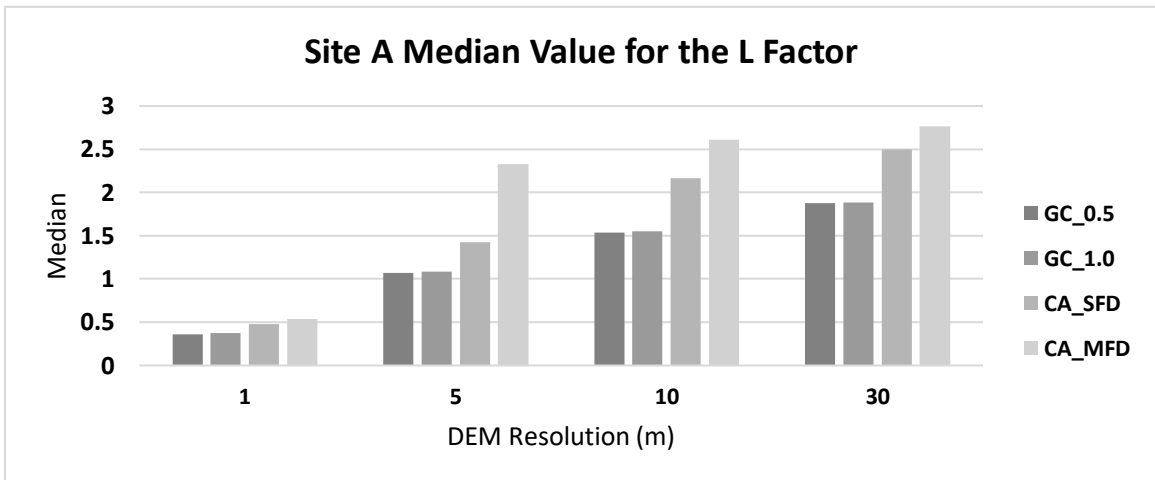


**Figure A42.** Median value of L factor for Site A where GC\_0.5 is the GC method with slope cutoff set to 0.5, GC\_1.0 is the GC method without slope cutoff, CA\_SFD is the CA method using a SFD algorithm, and CA\_MFD is the CA method using a MFD algorithm.

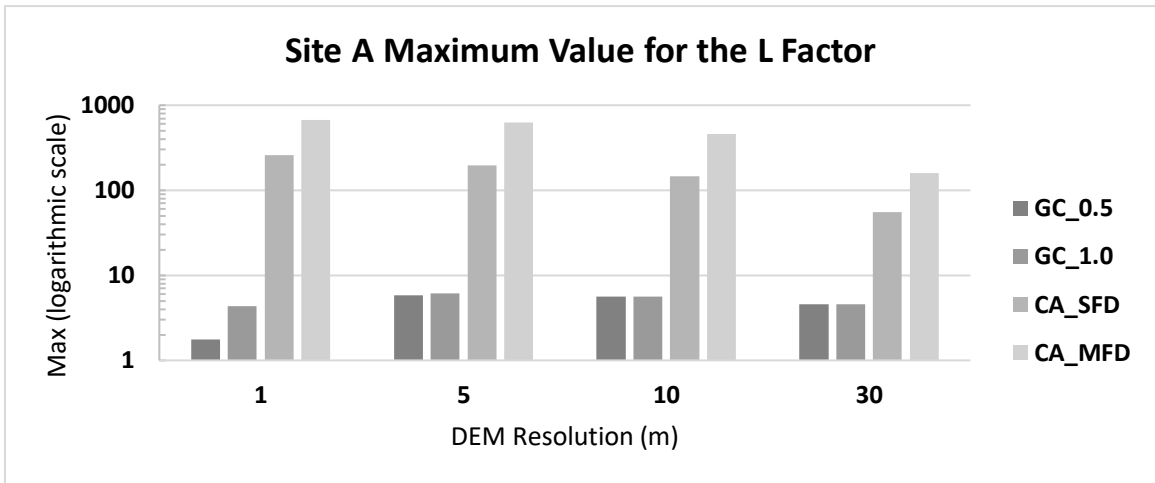


**Figure A43.** Maximum value of L factor for Site A where GC\_0.5 is the GC method with slope cutoff set to 0.5, GC\_1.0 is the GC method without slope cutoff, CA\_SFD is the CA method using a SFD algorithm, and CA\_MFD is the CA method using a MFD algorithm.

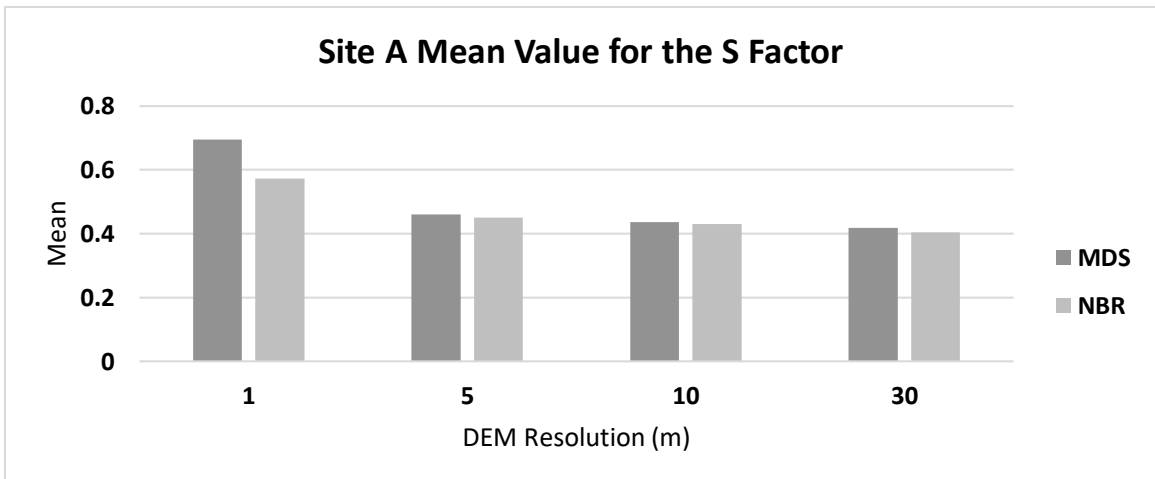


**Figure A44.** Mean value of S factor for Site A.

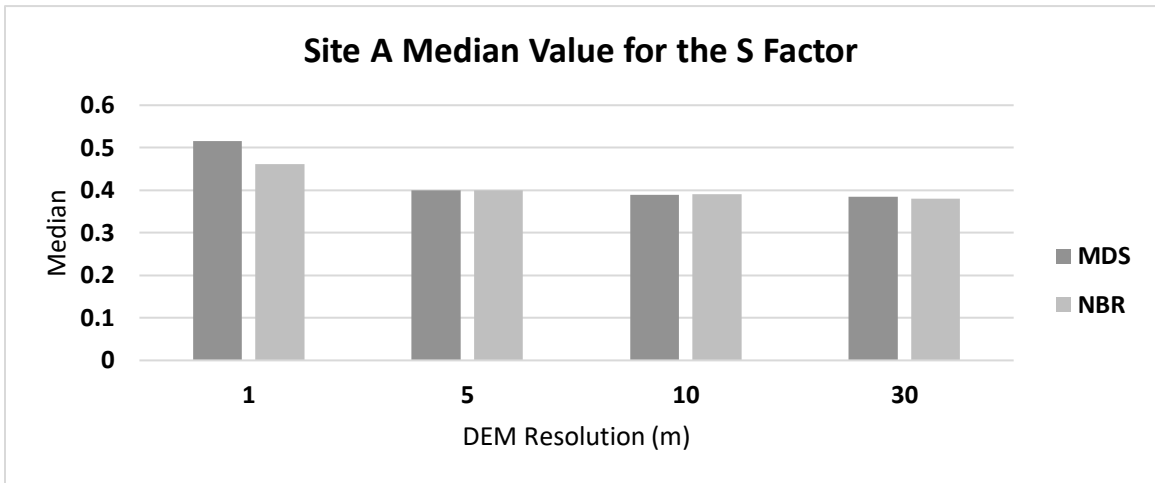


**Figure A45.** Median value of S factor for Site A.

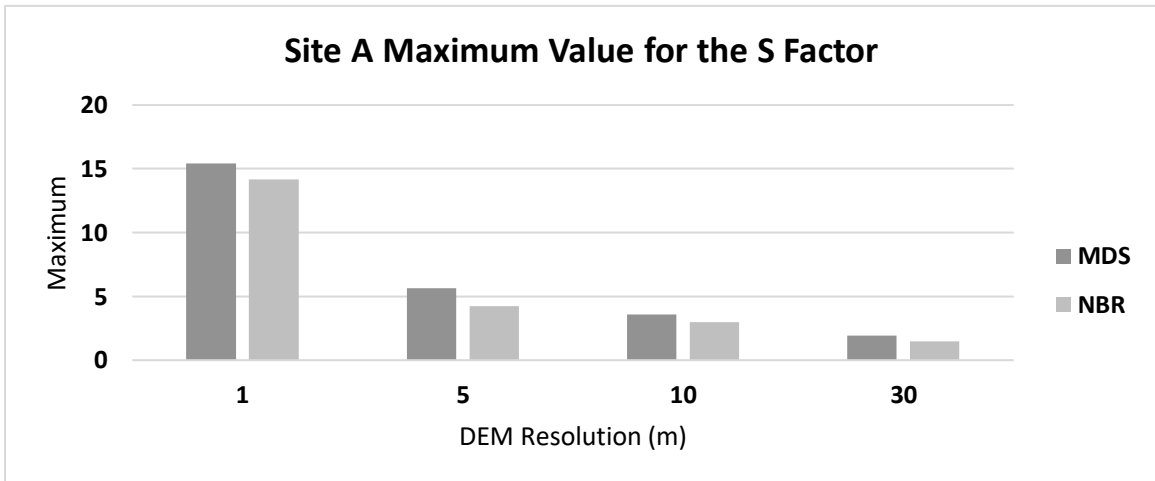


**Figure A46.** Maximum value of S factor for Site A.

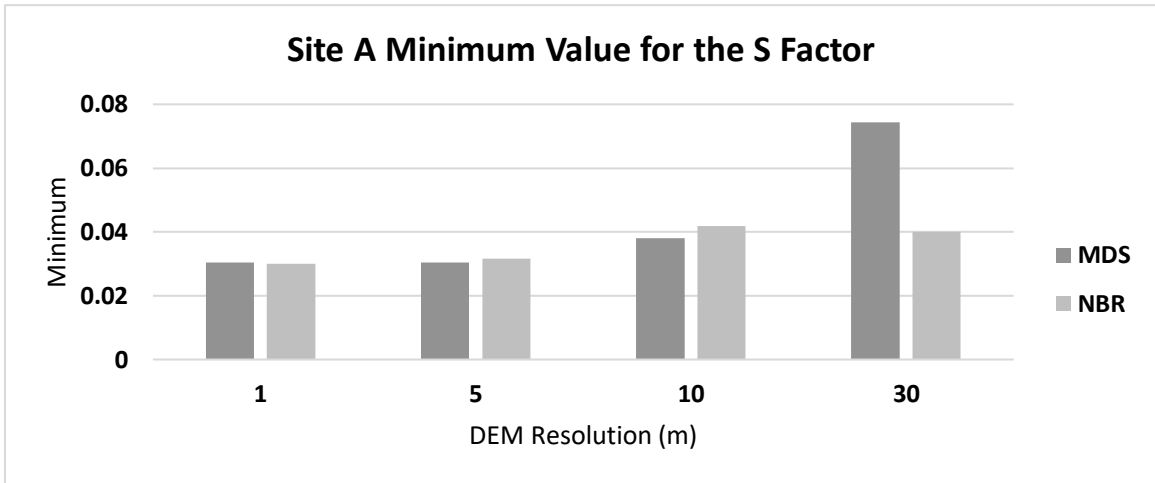
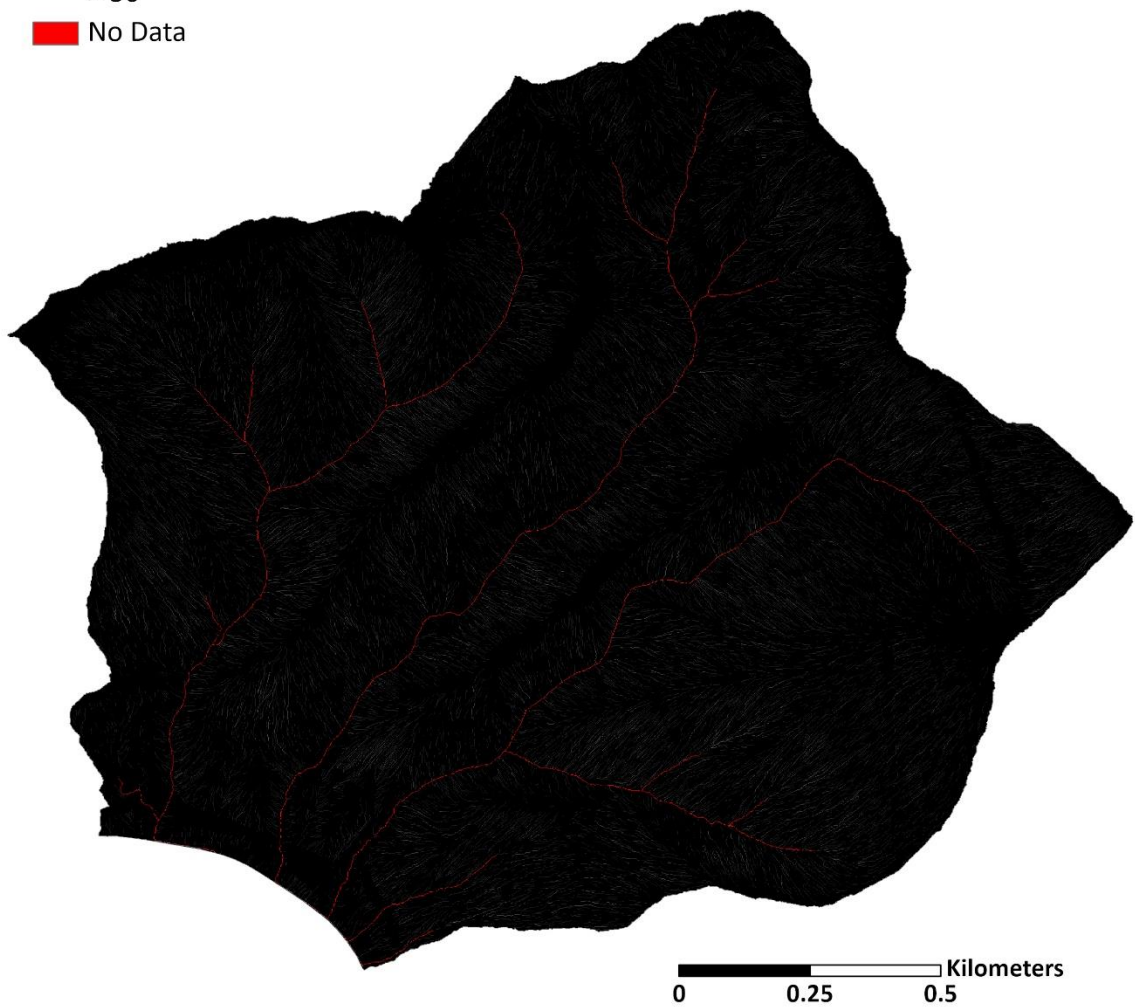
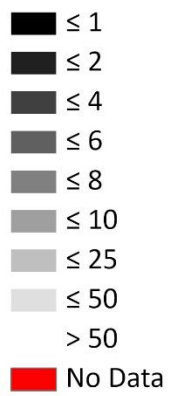


Figure A47. Minimum value of S factor for Site A.

Site B outputs:

GC\_0.5 (1 m)

Value



**Figure B1.** L factor with the GC Method with slope cutoff at 0.5 for Site B at 1 m.

GC\_0.5 (5 m)

Value

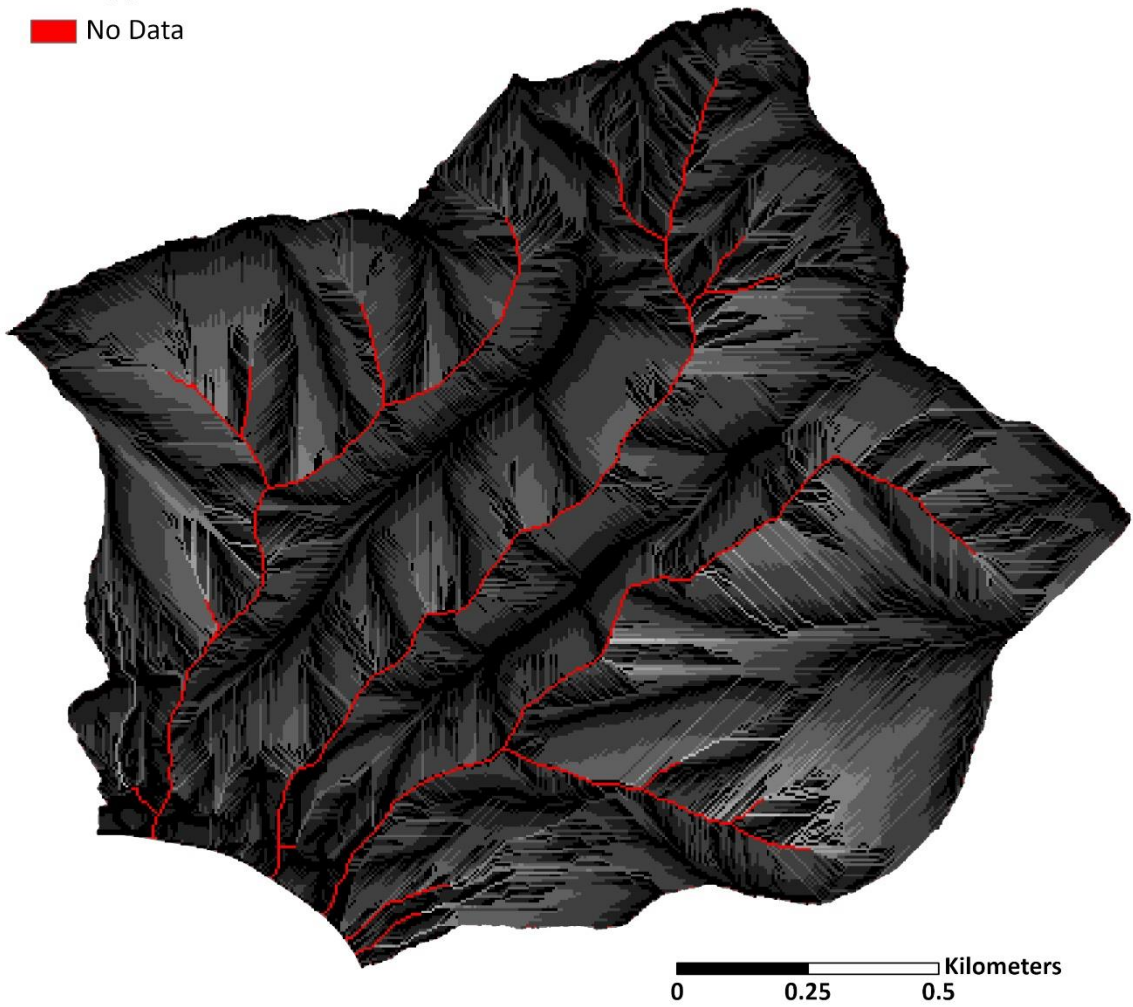


**Figure B2.** L factor with the GC Method with slope cutoff at 0.5 for Site B at 5 m.

GC\_0.5 (10 m)

Value

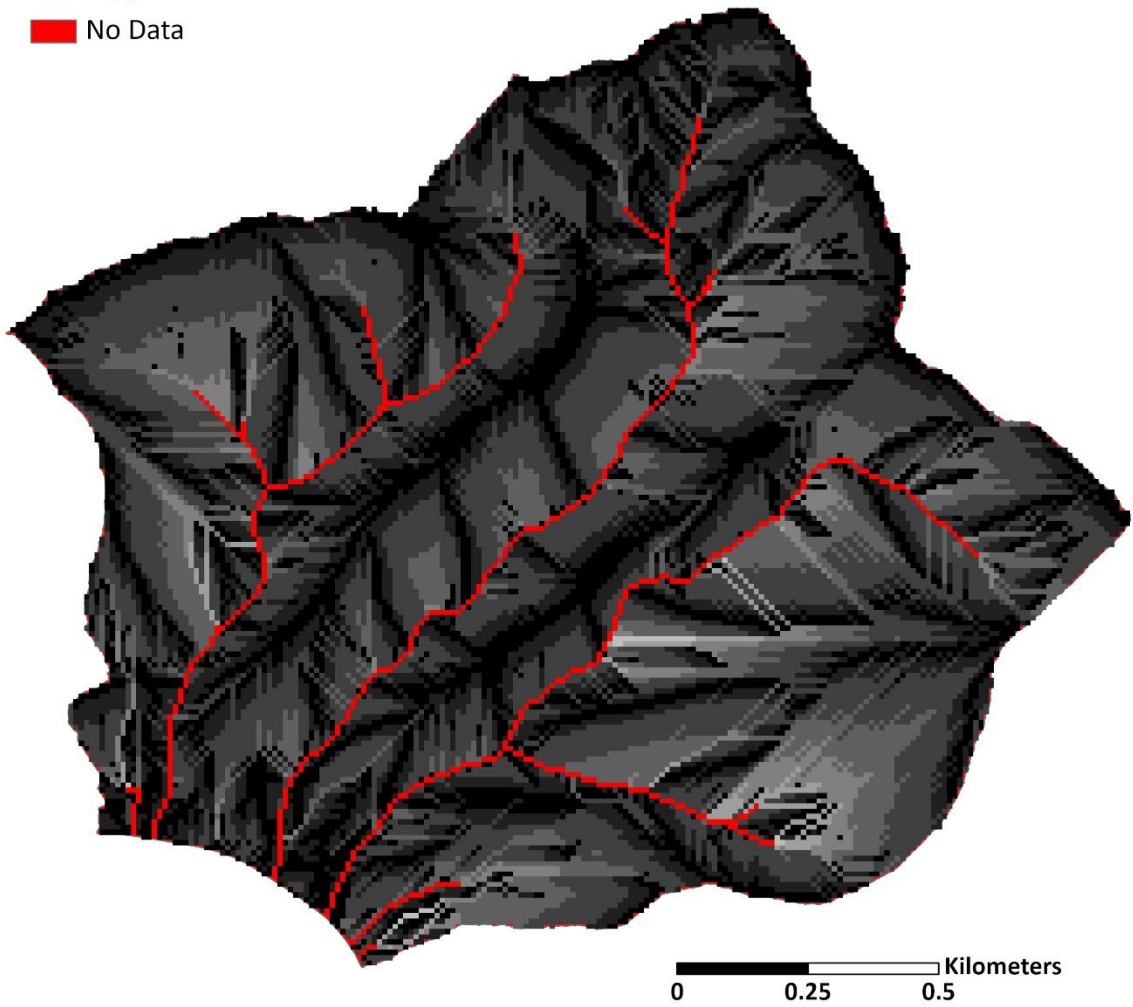


**Figure B3.** L factor with the GC Method with slope cutoff at 0.5 for Site B at 10 m.

GC\_0.5 (30 m)

Value

■ ≤ 1

■ ≤ 2

■ ≤ 4

■ ≤ 6

■ ≤ 8

■ ≤ 10

■ ≤ 25

■ ≤ 50

> 50

■ No Data

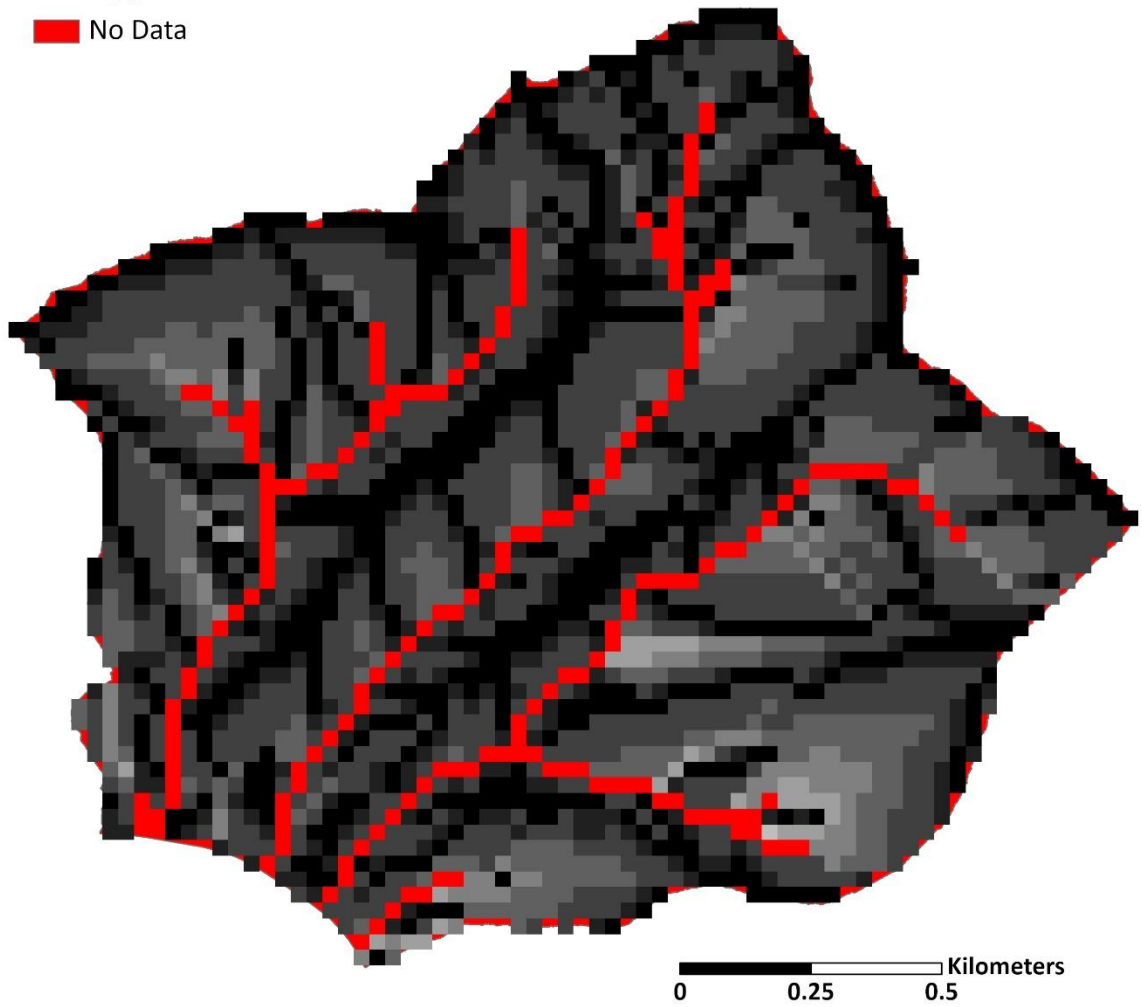


**Figure B4.** L factor with the GC Method with slope cutoff at 0.5 for Site B at 30 m.

GC\_1.0 (1 m)

Value

■ ≤ 1

■ ≤ 2

■ ≤ 4

■ ≤ 6

■ ≤ 8

■ ≤ 10

■ ≤ 25

■ ≤ 50

> 50

■ No Data

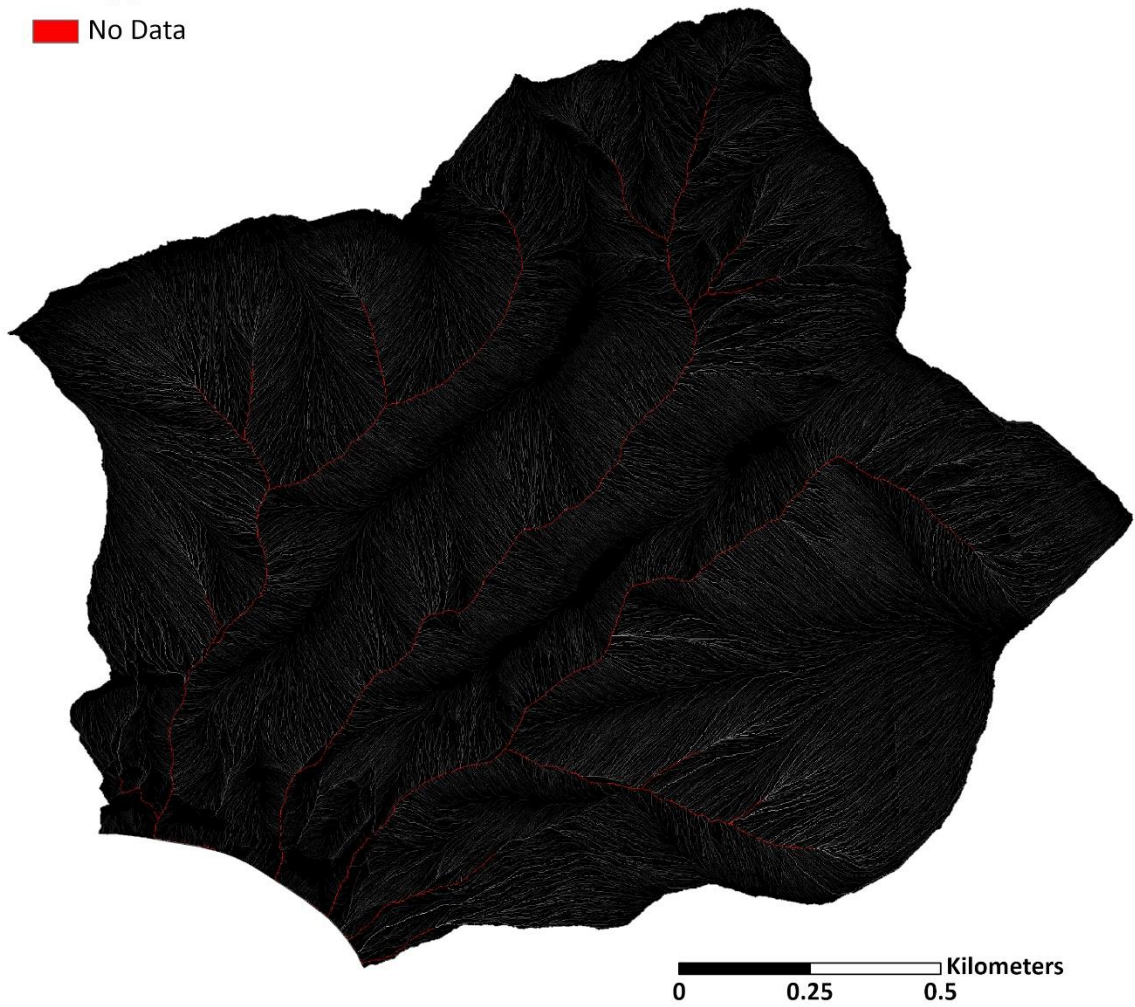


**Figure B5.** L factor with the GC Method without slope cutoff for Site B at 1 m resolution.

GC\_1.0 (5 m)

Value

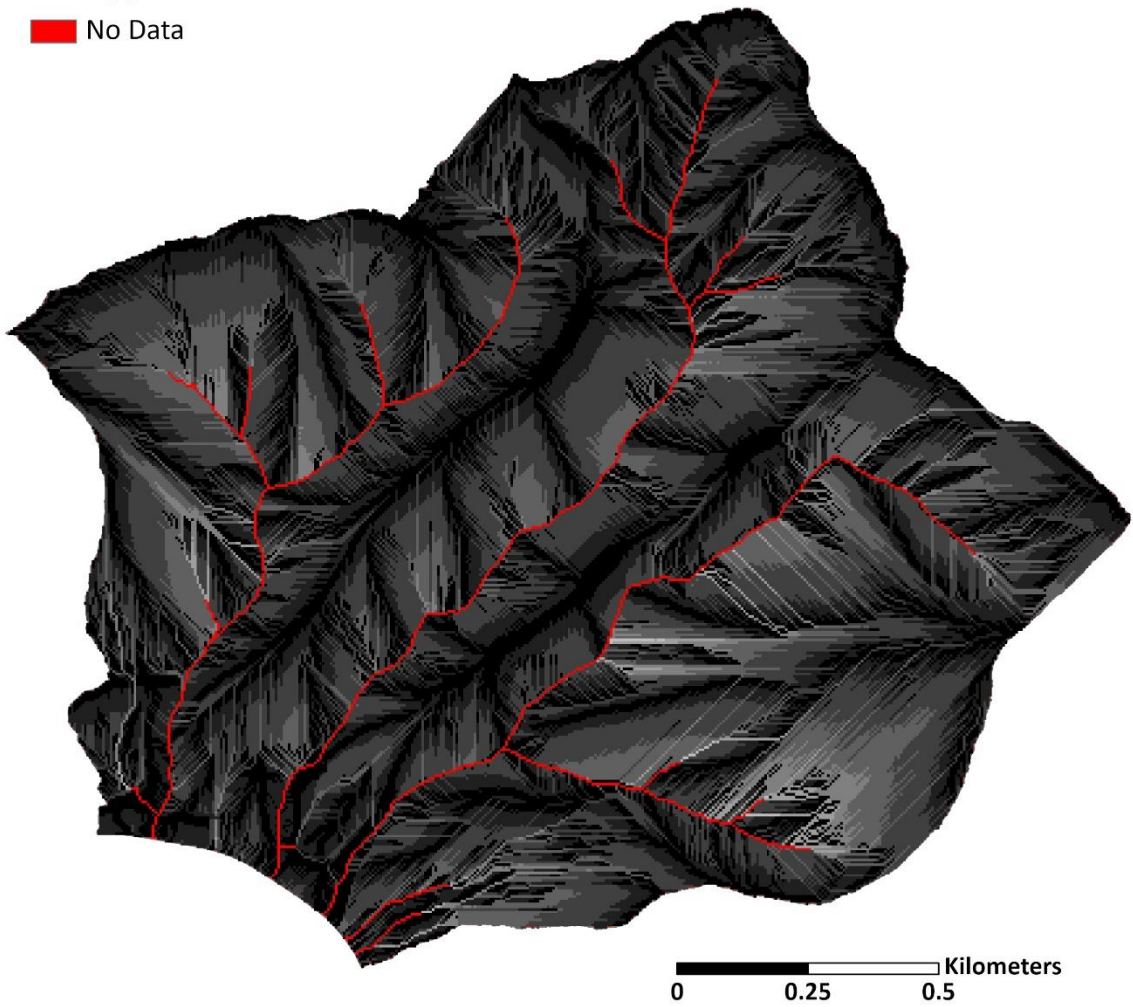


**Figure B6.** L factor with the GC Method without slope cutoff for Site B at 5 m.

GC\_1.0 (10 m)

Value

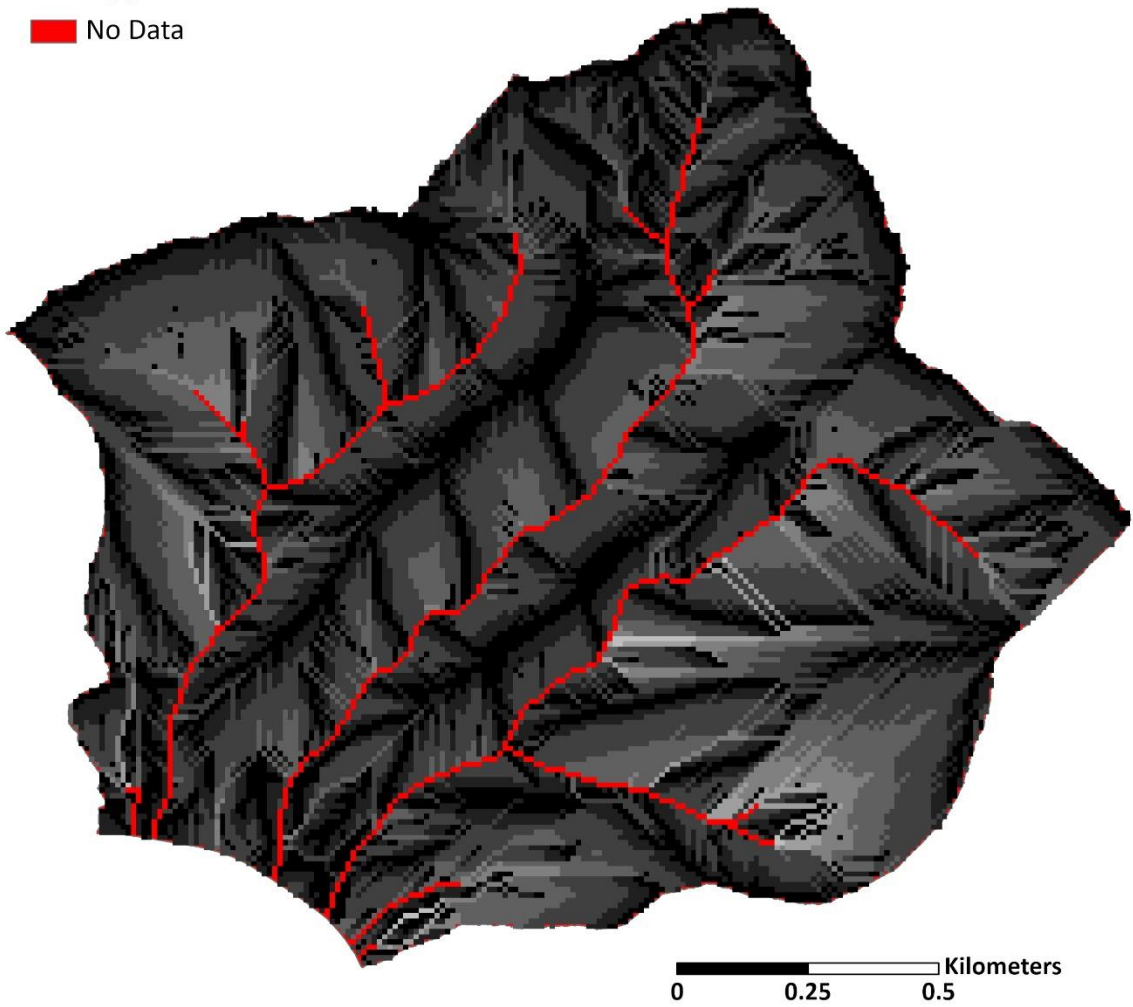


**Figure B7.** L factor with the GC Method without slope cutoff for Site B at 10 m.

GC\_1.0 (30 m)

Value

■ ≤ 1

■ ≤ 2

■ ≤ 4

■ ≤ 6

■ ≤ 8

■ ≤ 10

■ ≤ 25

■ ≤ 50

> 50

■ No Data

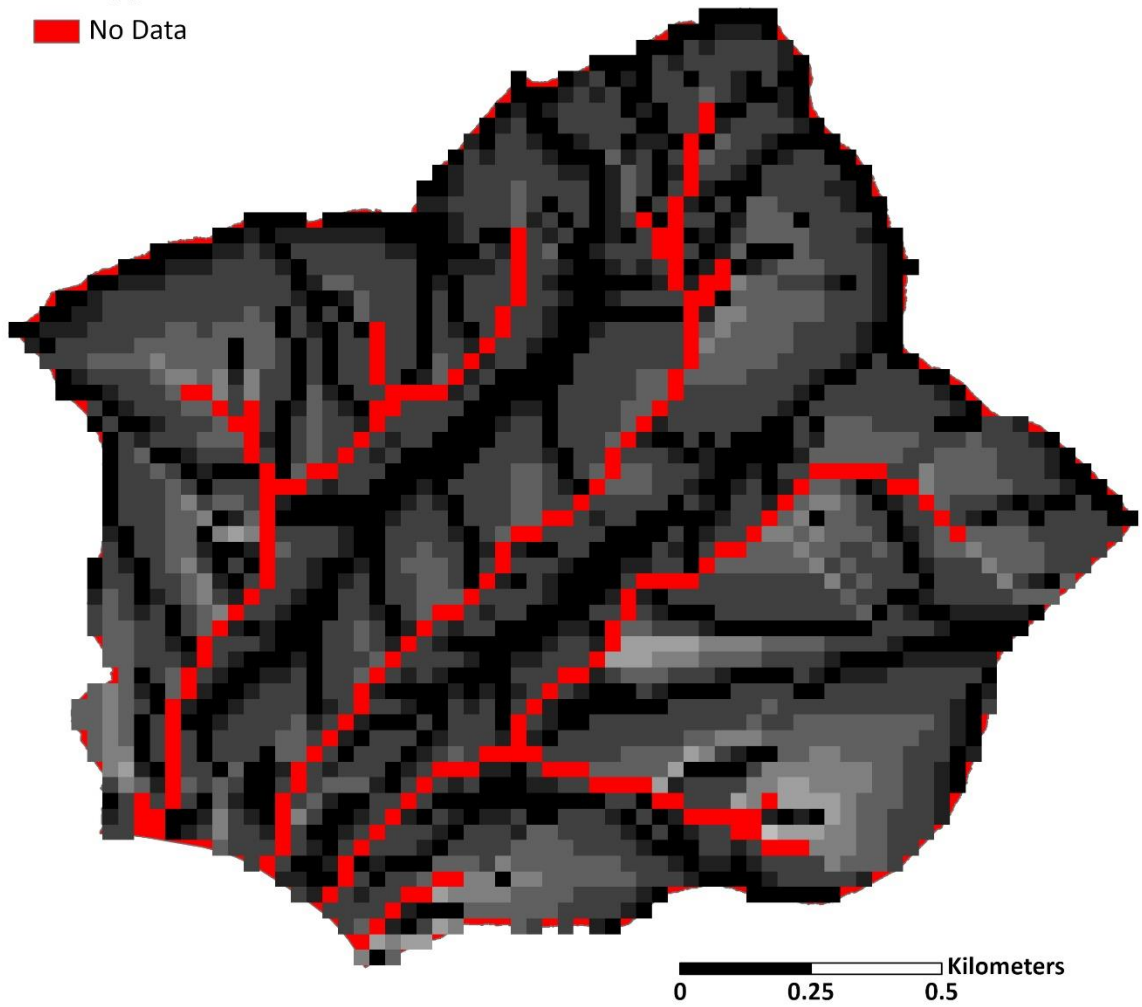


**Figure B8.** L factor with the GC Method without slope cutoff for Site B at 30 m.

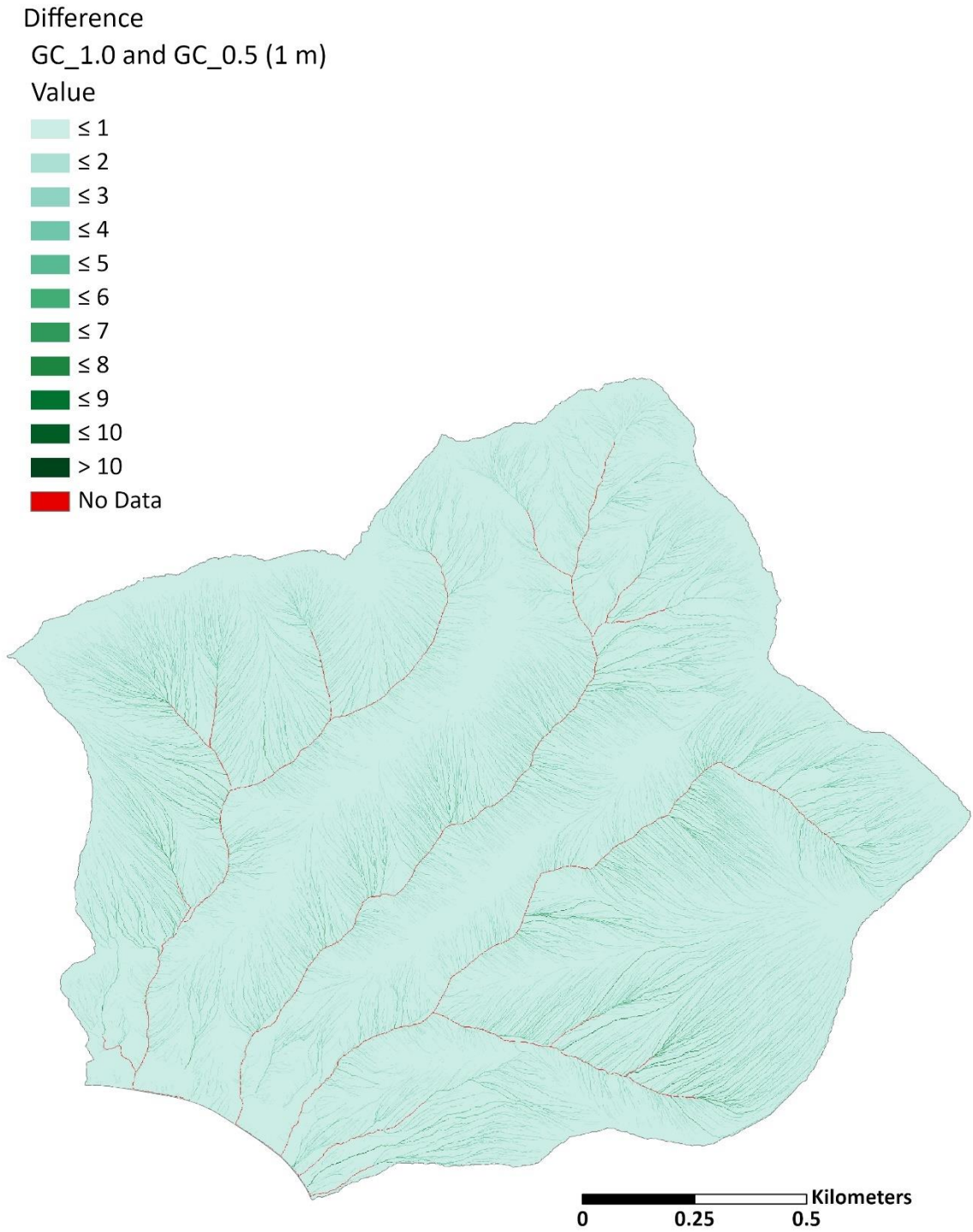


**Figure B9.** Site B difference raster (1 m) for the L Factor of the GC method with slope cutoff (GC\_0.5) subtracted from the GC method without slope cutoff (GC\_1.0).

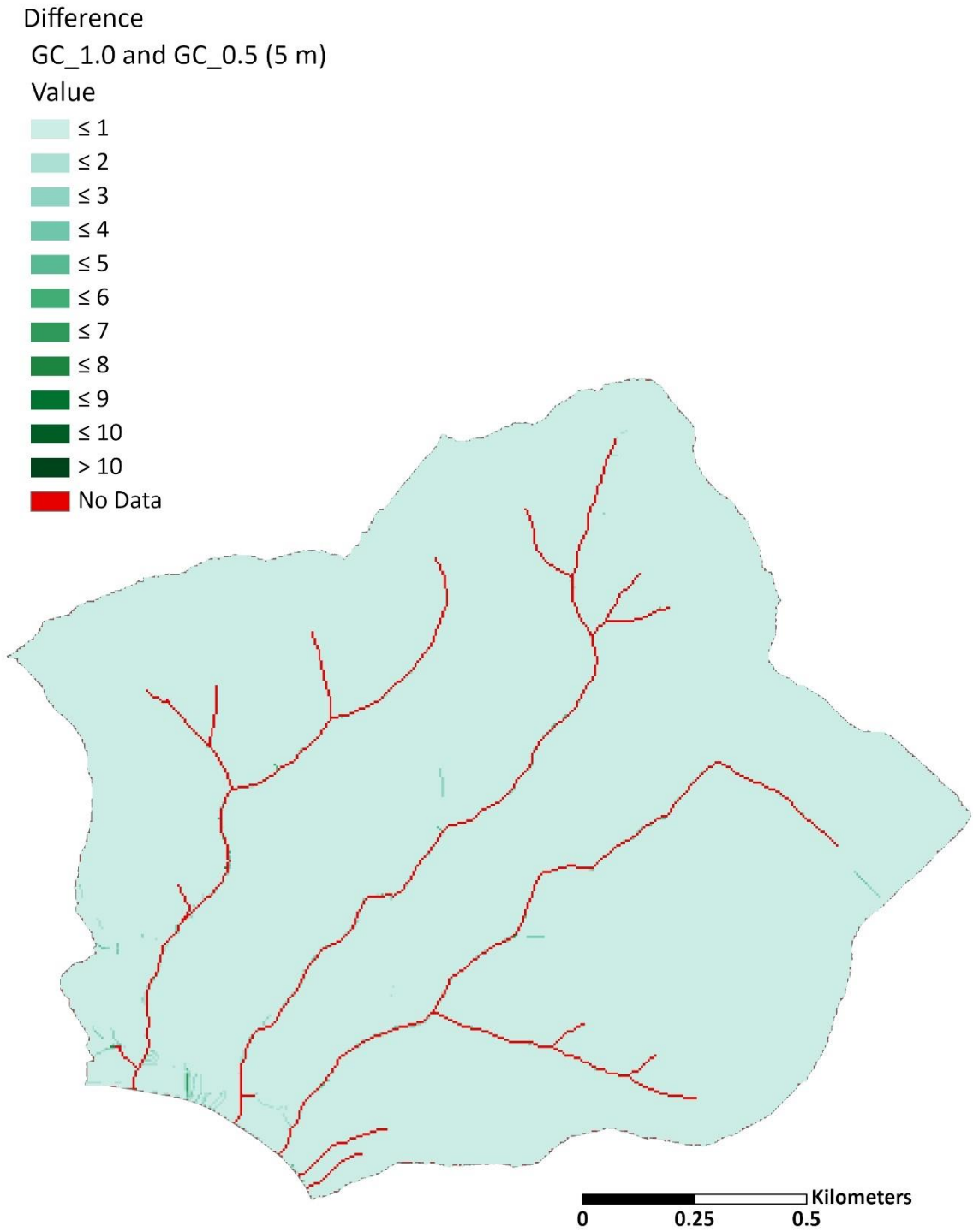


**Figure B10.** Site B difference raster (5 m) for the L Factor of the GC method with slope cutoff (GC\_0.5) subtracted from the GC method without slope cutoff (GC\_1.0).

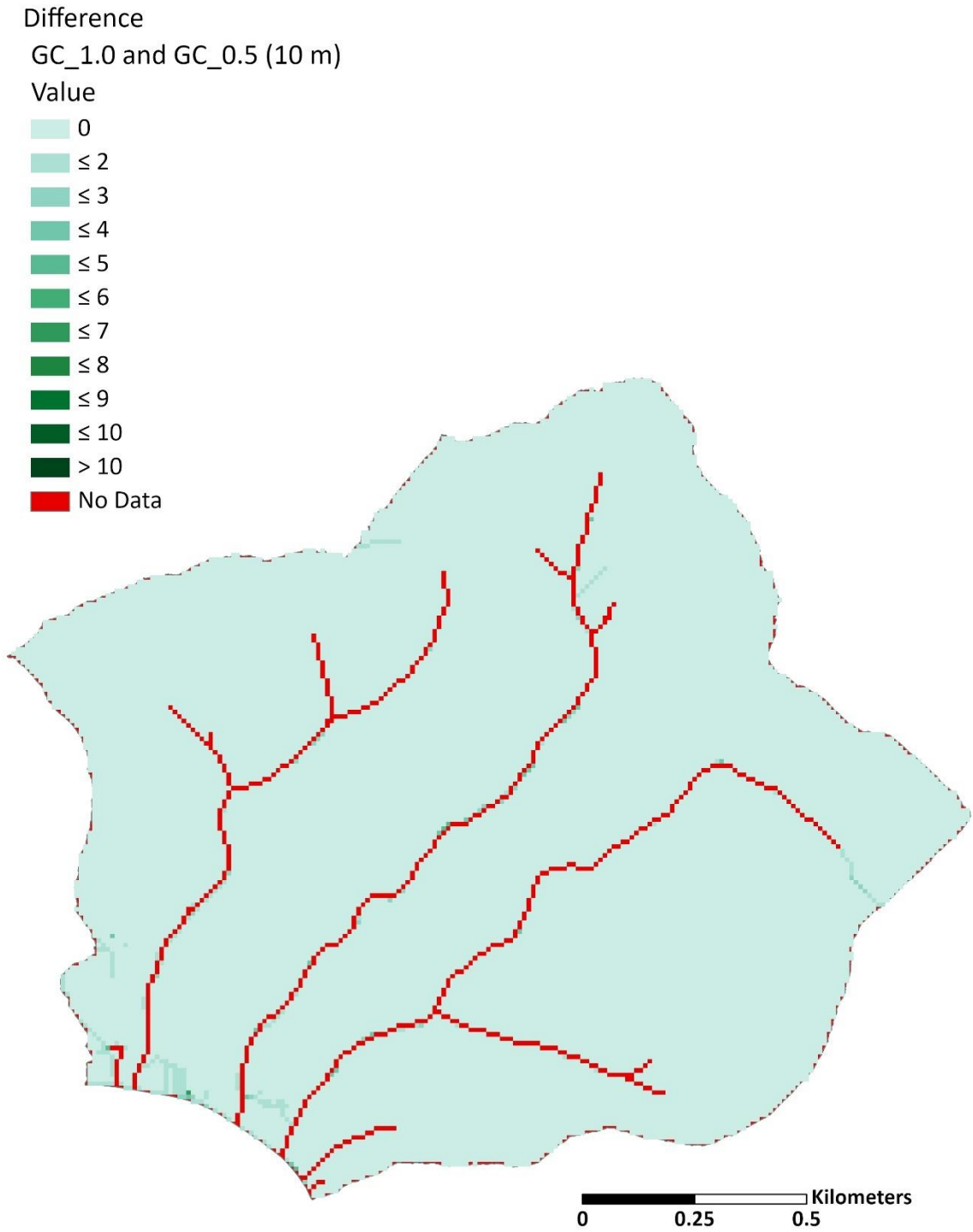


**Figure B11.** Site B difference raster (10 m) for the L Factor of the GC method with slope cutoff (GC\_0.5) subtracted from the GC method without slope cutoff (GC\_1.0).

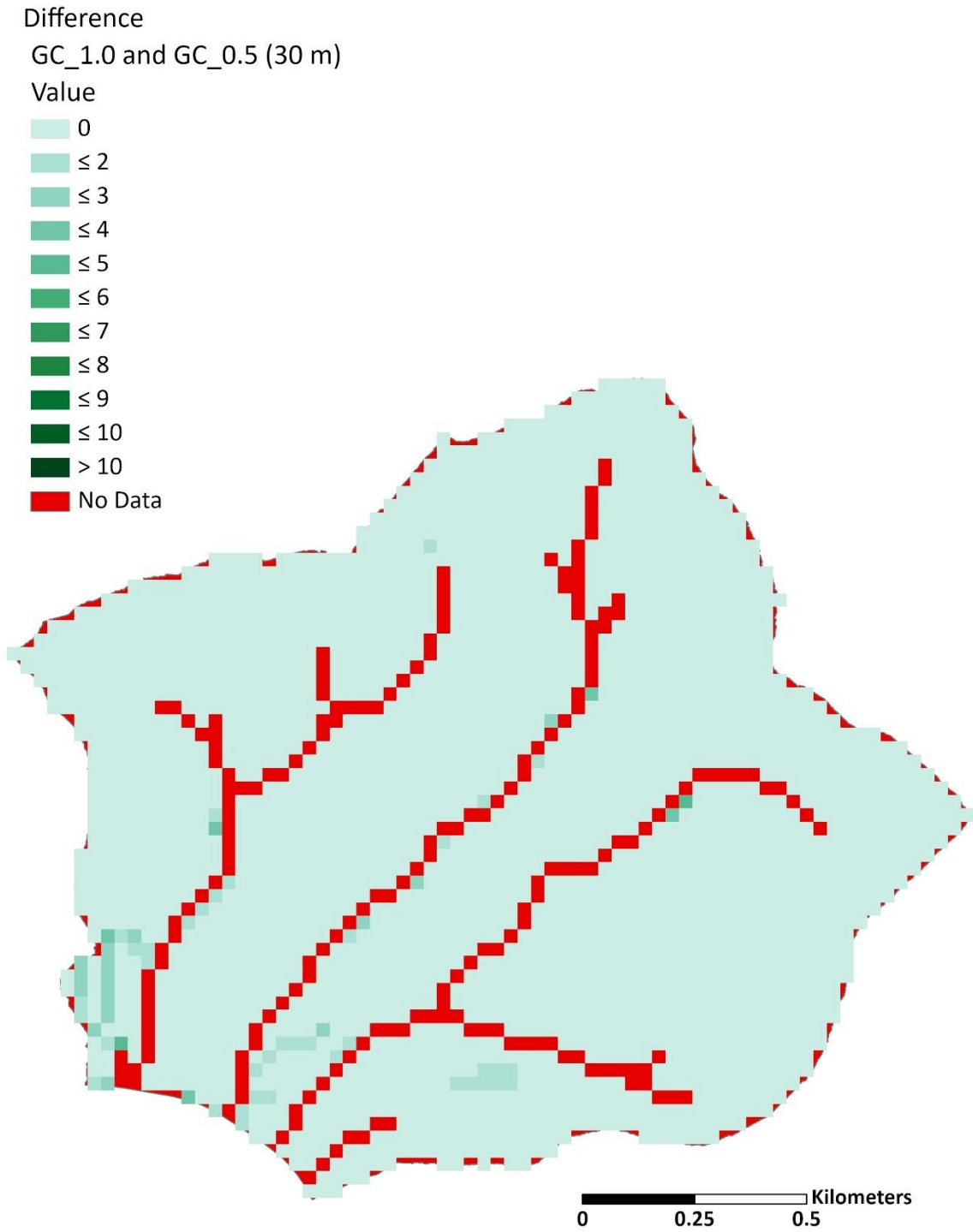


**Figure B12.** Site B difference raster (30 m) for the L Factor of the GC method with slope cutoff (GC\_0.5) subtracted from the GC method without slope cutoff (GC\_1.0).

CA\_SFD (1 m)

Value

■ ≤ 1

■ ≤ 2

■ ≤ 4

■ ≤ 6

■ ≤ 8

■ ≤ 10

■ ≤ 25

■ ≤ 50

> 50

■ No Data

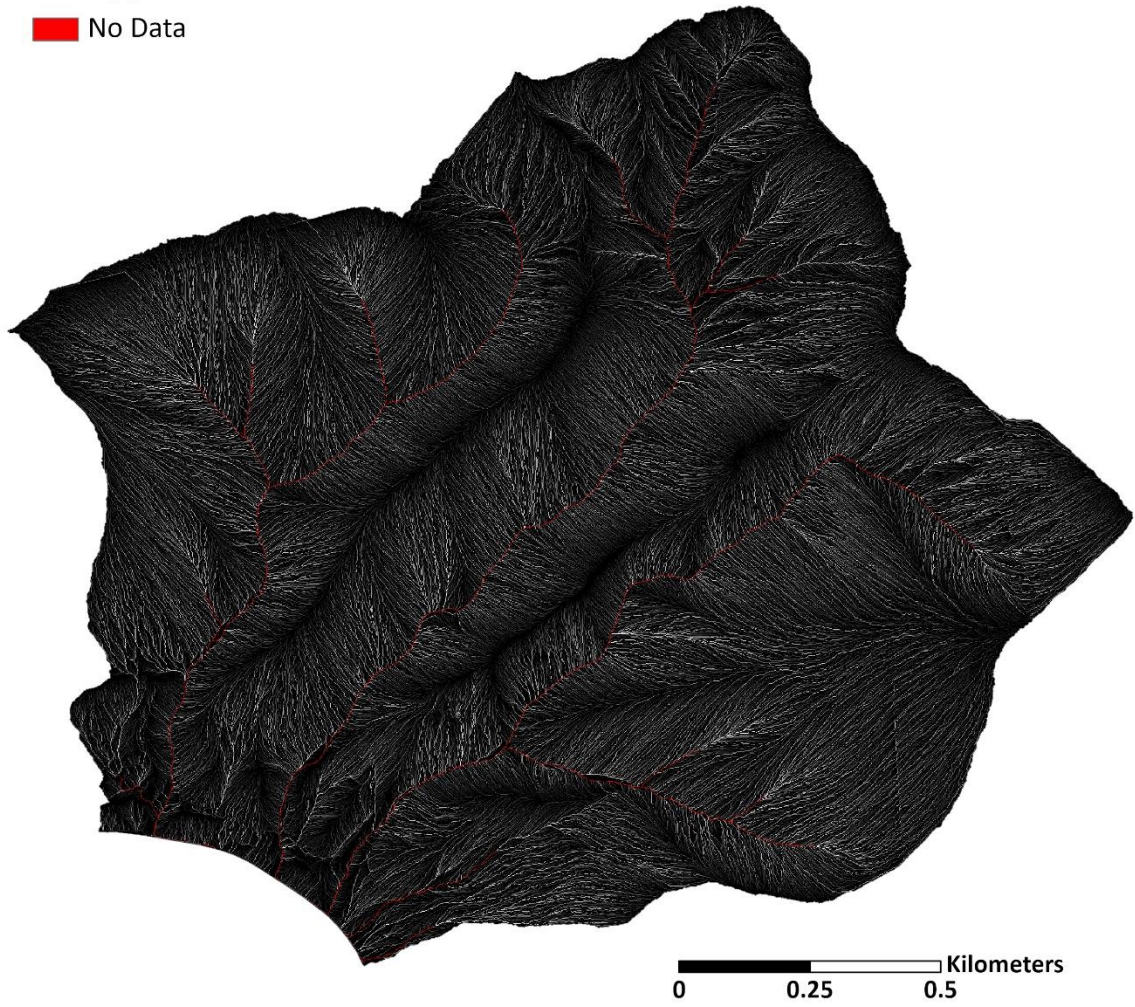


**Figure B13.** L factor with the CA method with a SFD algorithm for Site B at 1 m.

CA\_SFD (5 m)

Value

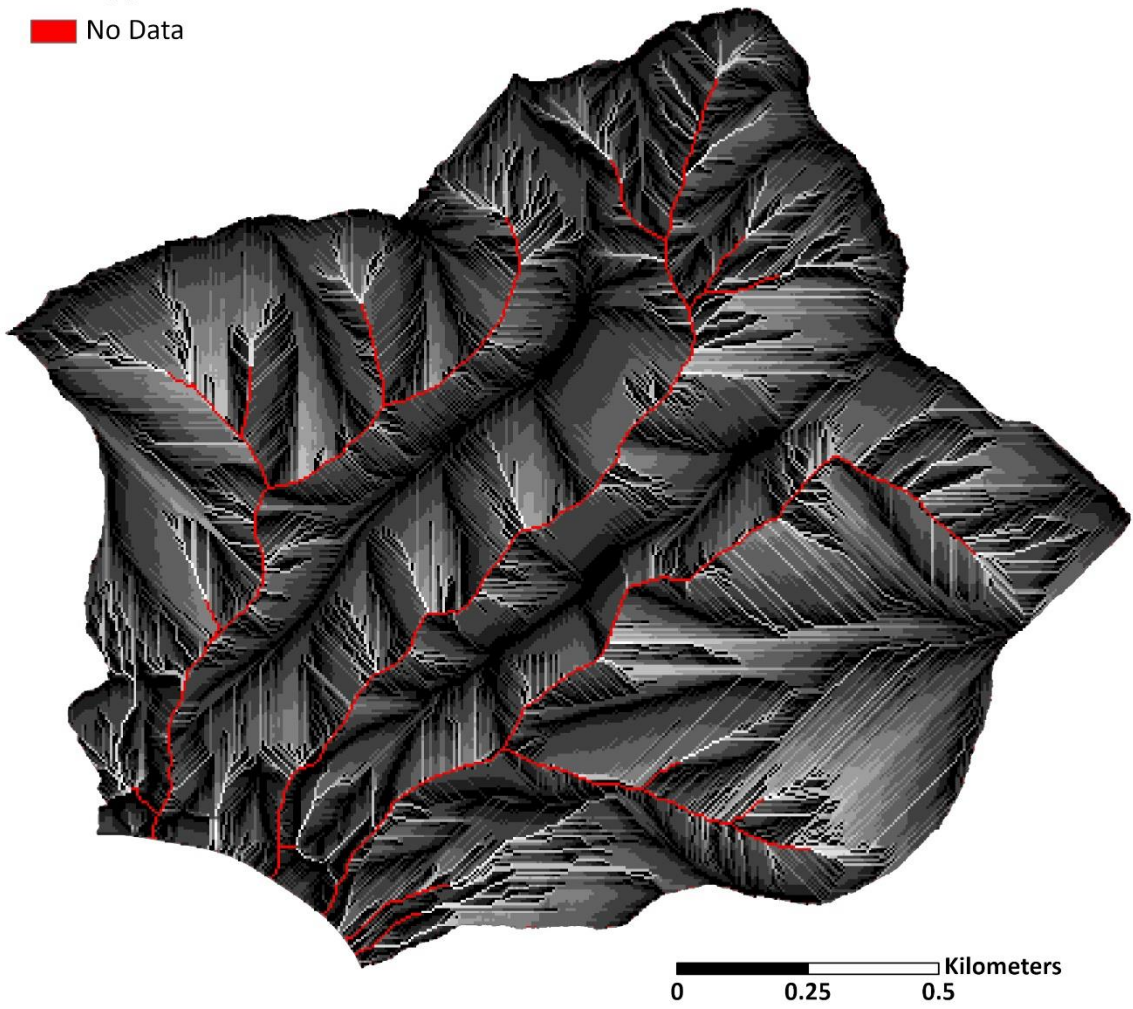


**Figure B14.** L factor with the CA method with a SFD algorithm for Site B at 5 m.

CA\_SFD (10 m)

Value

■ ≤ 1

■ ≤ 2

■ ≤ 4

■ ≤ 6

■ ≤ 8

■ ≤ 10

■ ≤ 25

■ ≤ 50

> 50

■ No Data

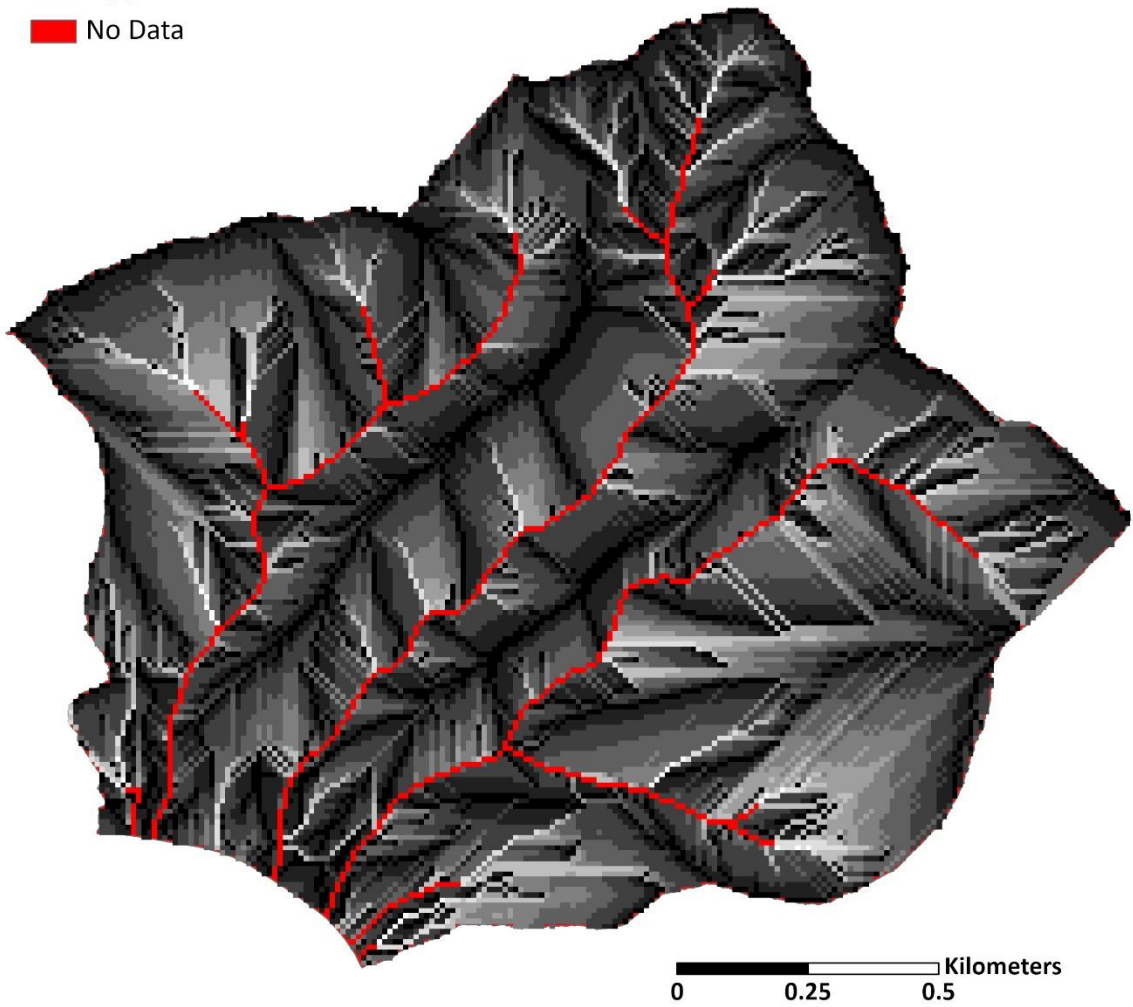


**Figure B15.** L factor with the CA method with a SFD algorithm for Site B at 10 m.

CA\_SFD (30 m)

Value

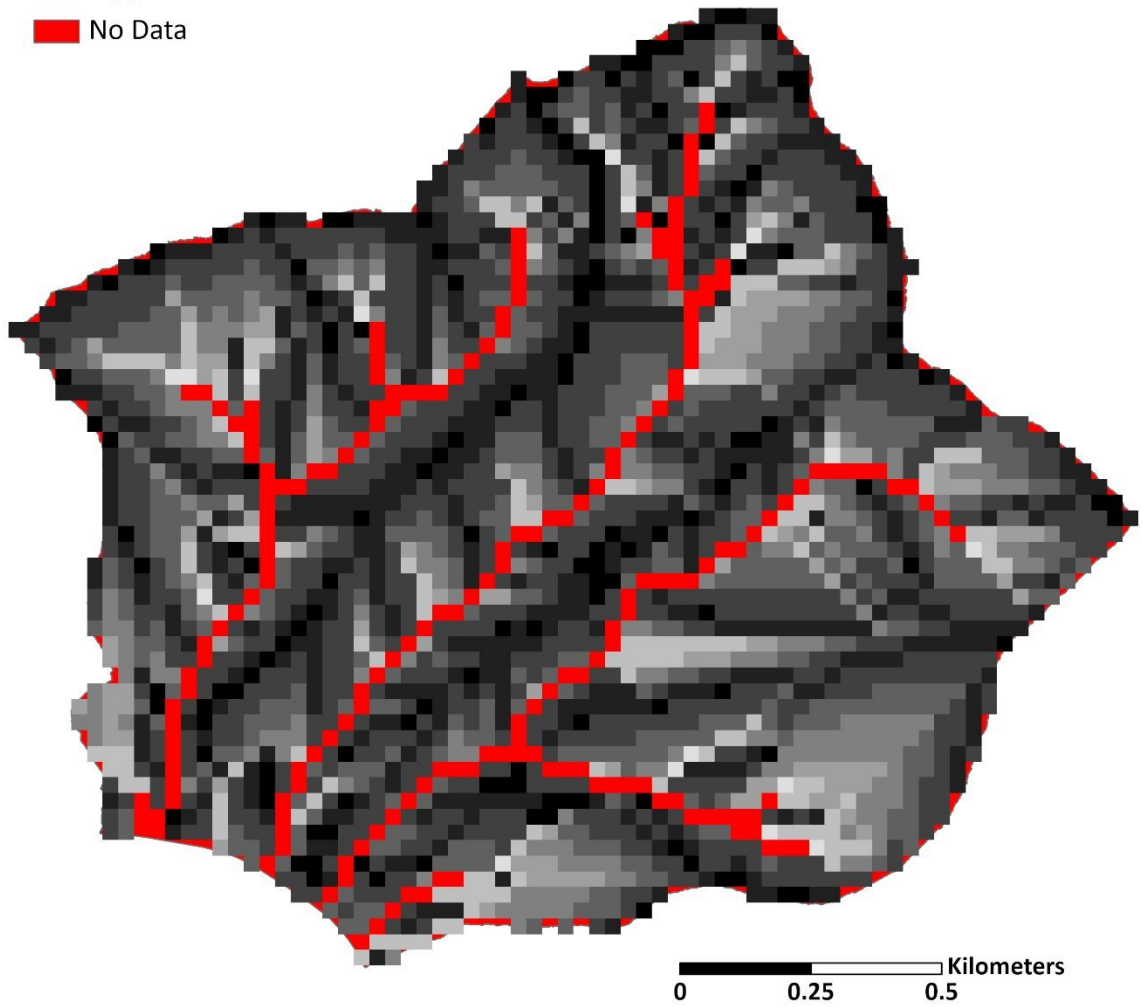
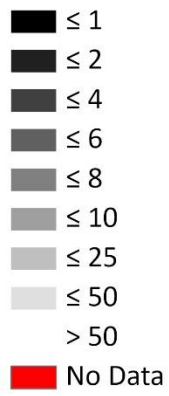


**Figure B16.** L factor with the CA method with a SFD algorithm for Site B at 30 m.

CA\_MFD (1 m)

Value

■ ≤ 1

■ ≤ 2

■ ≤ 4

■ ≤ 6

■ ≤ 8

■ ≤ 10

■ ≤ 25

■ ≤ 50

> 50

■ No Data

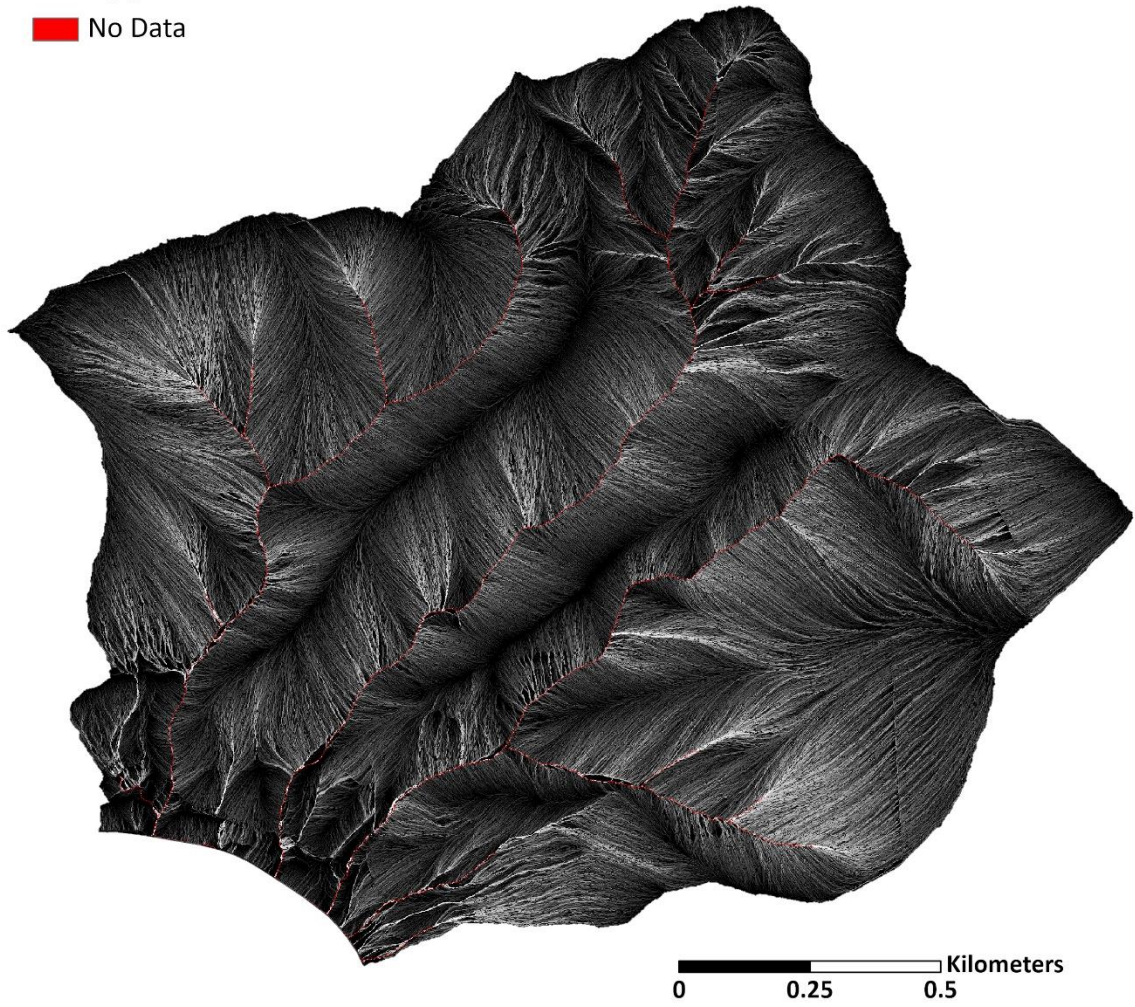


**Figure B17.** L factor with the CA method with a MFD algorithm for Site B at 1 m.

CA\_MFD (5 m)

Value

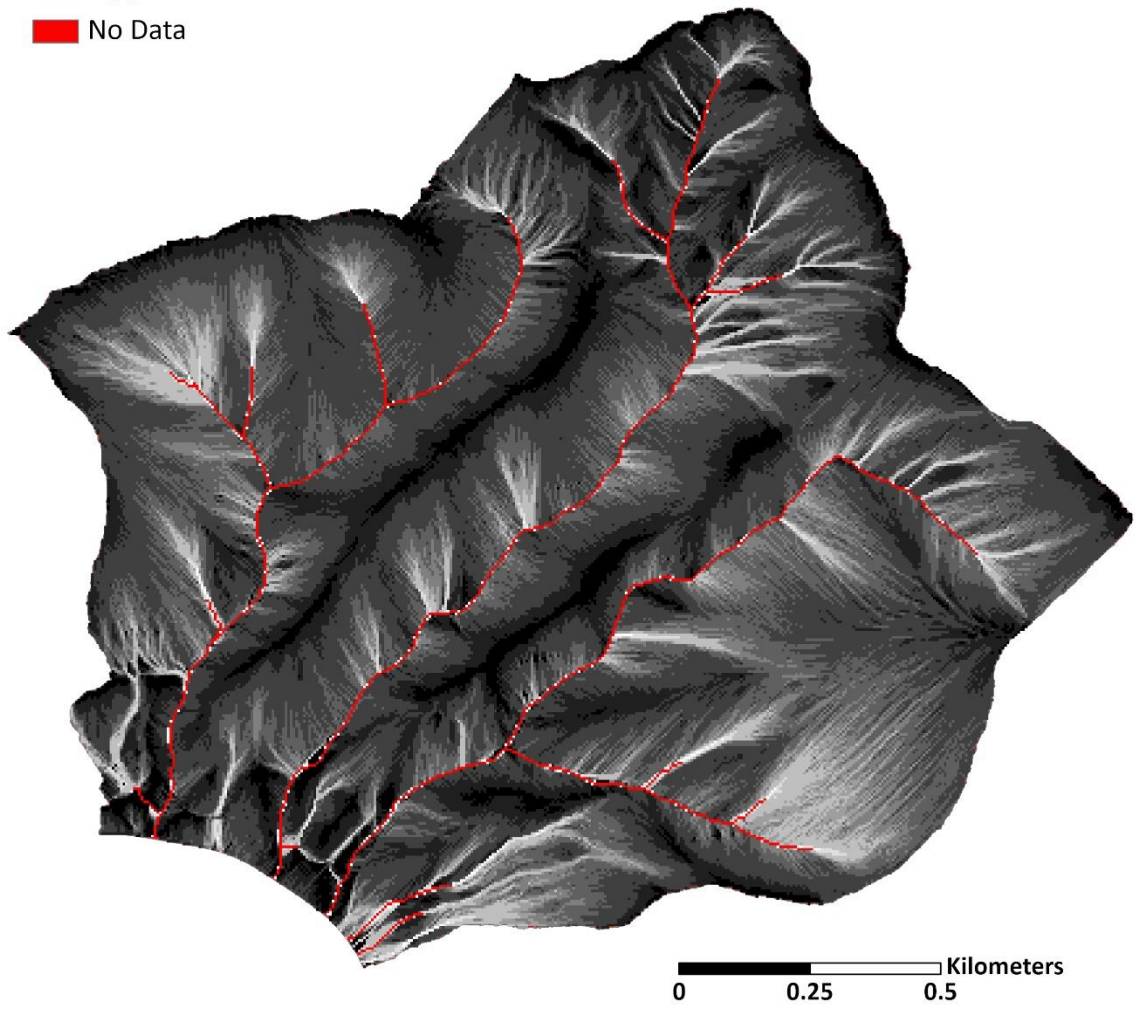


**Figure B18.** L factor with the CA method with a MFD algorithm for Site B at 5 m.

CA\_MFD (10 m)

Value

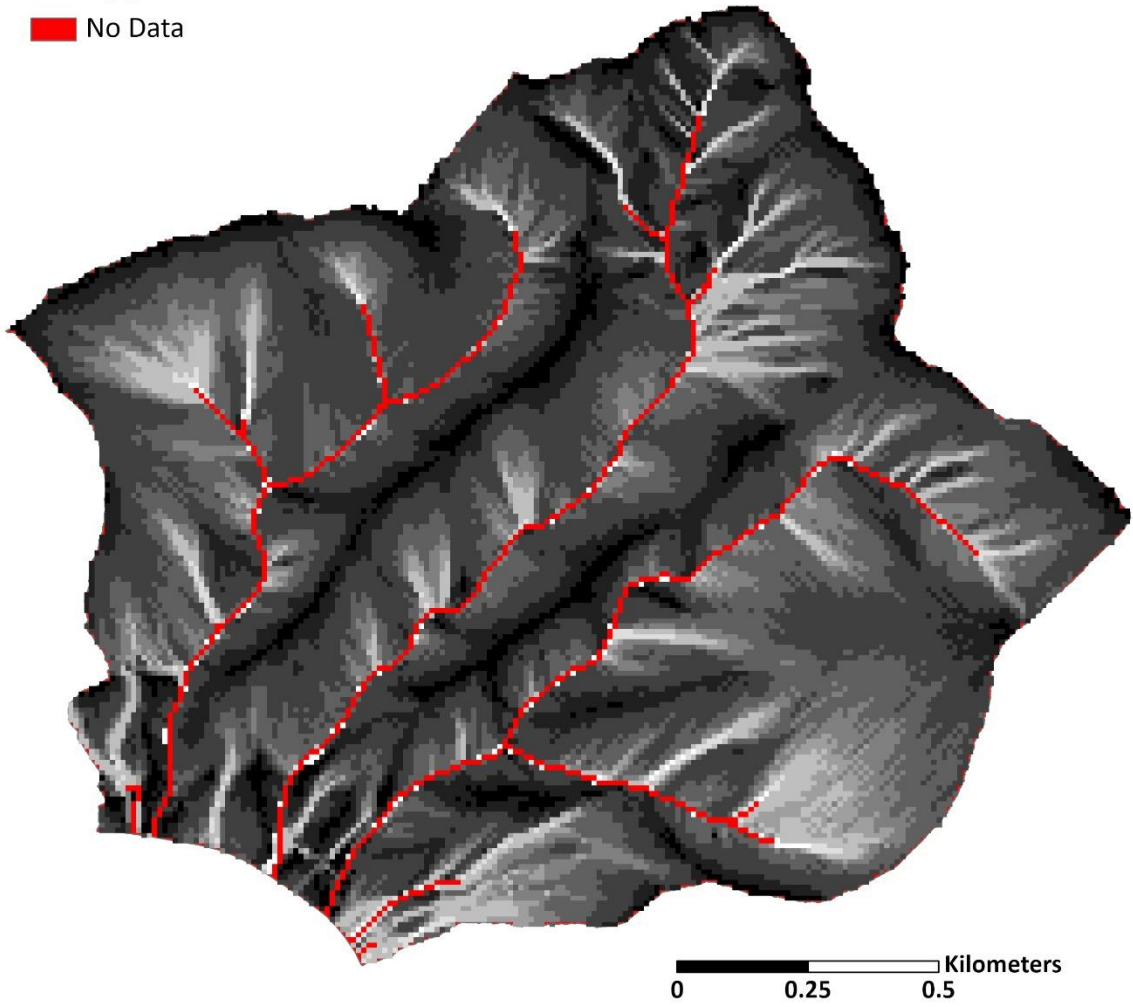
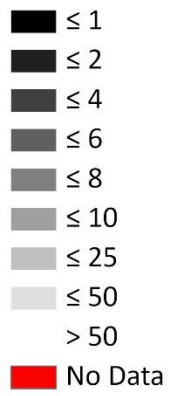


**Figure B19.** L factor with the CA method with a MFD algorithm for Site B at 10 m.

CA\_MFD (30 m)

Value

■ ≤ 1

■ ≤ 2

■ ≤ 4

■ ≤ 6

■ ≤ 8

■ ≤ 10

■ ≤ 25

■ ≤ 50

> 50

■ No Data

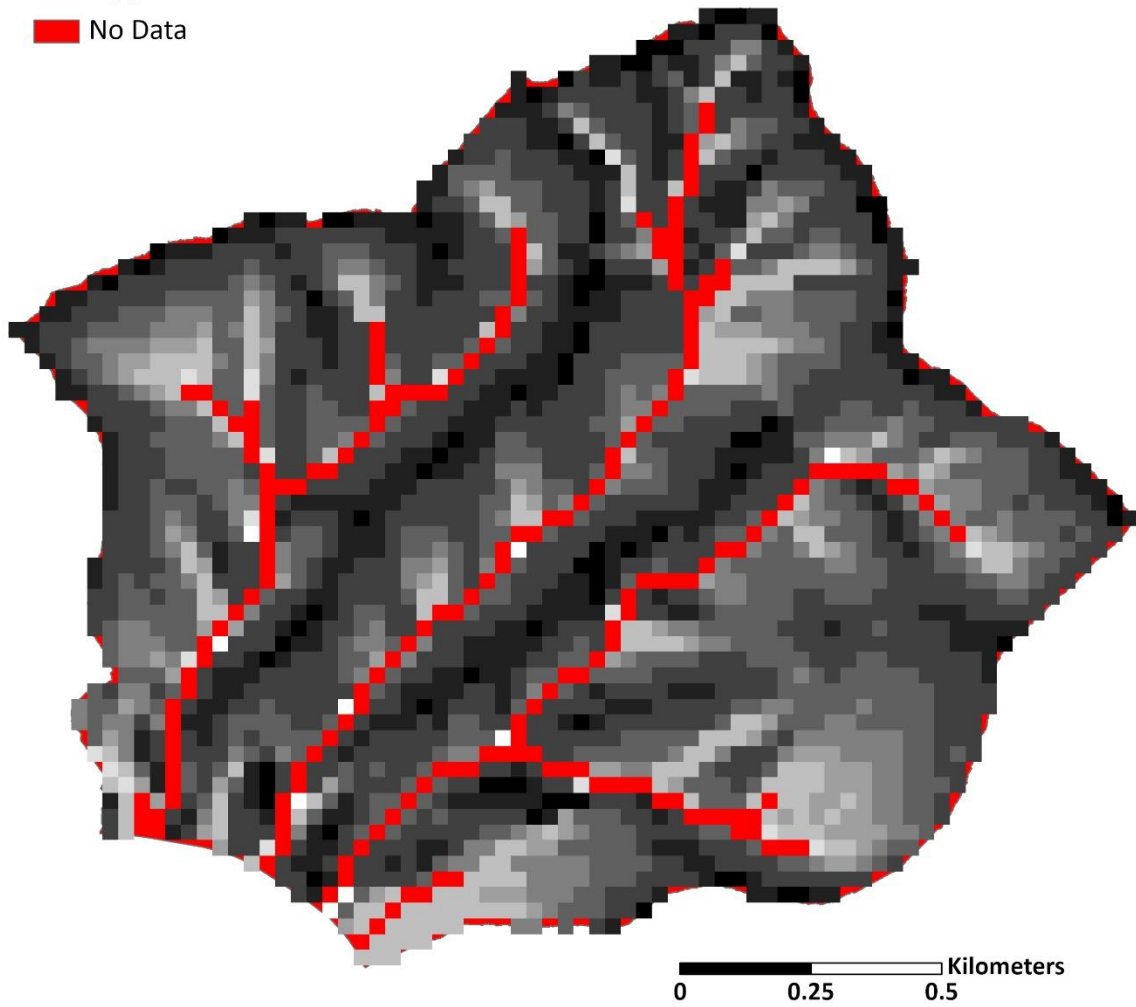


**Figure B20.** L factor with the CA method with a MFD algorithm for Site B at 30 m.

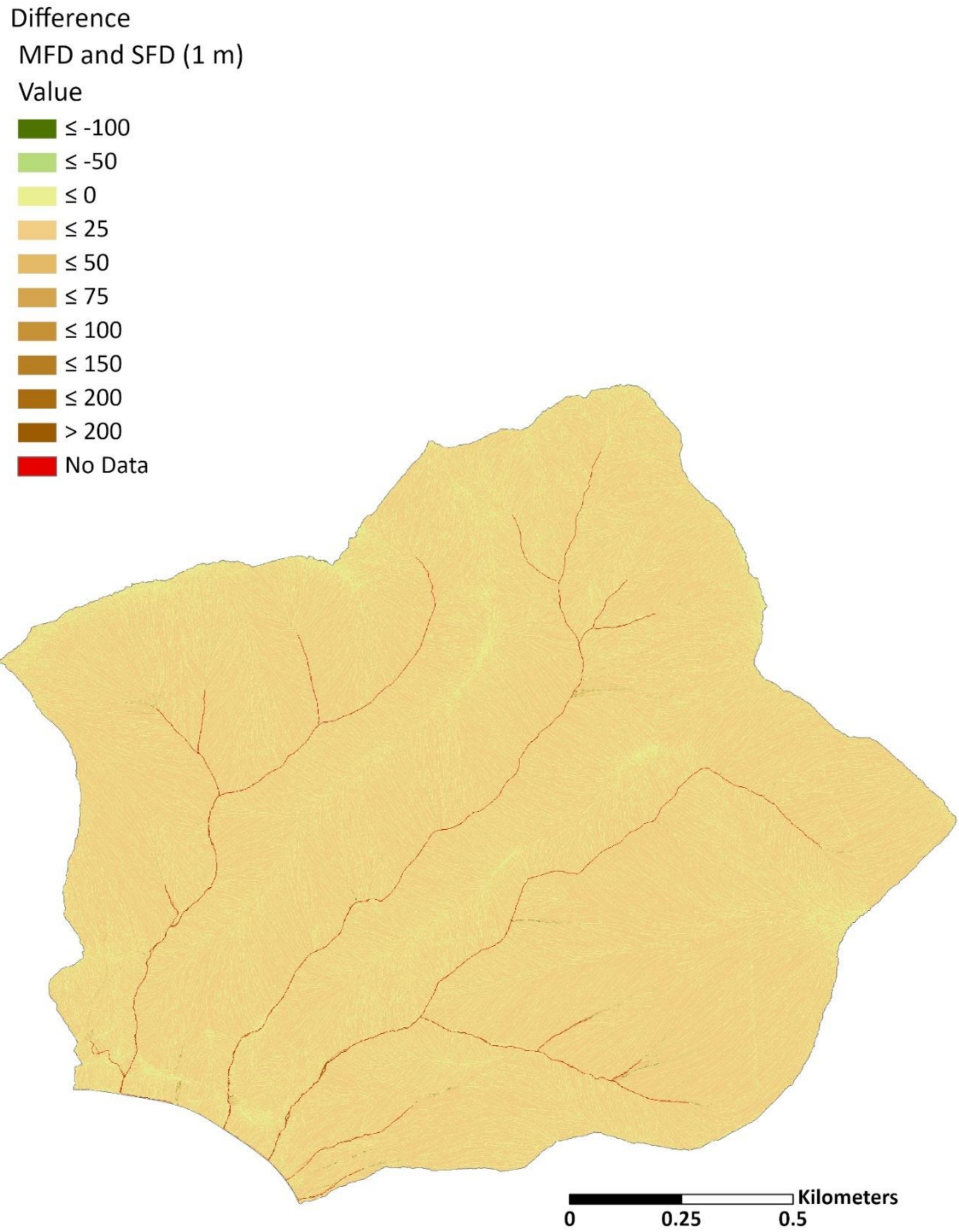


**Figure B21.** Site B difference raster (1 m) for the L Factor of the CA method using a SFD algorithm (SFD) subtracted from the CA method using a MFD algorithm (MFD).

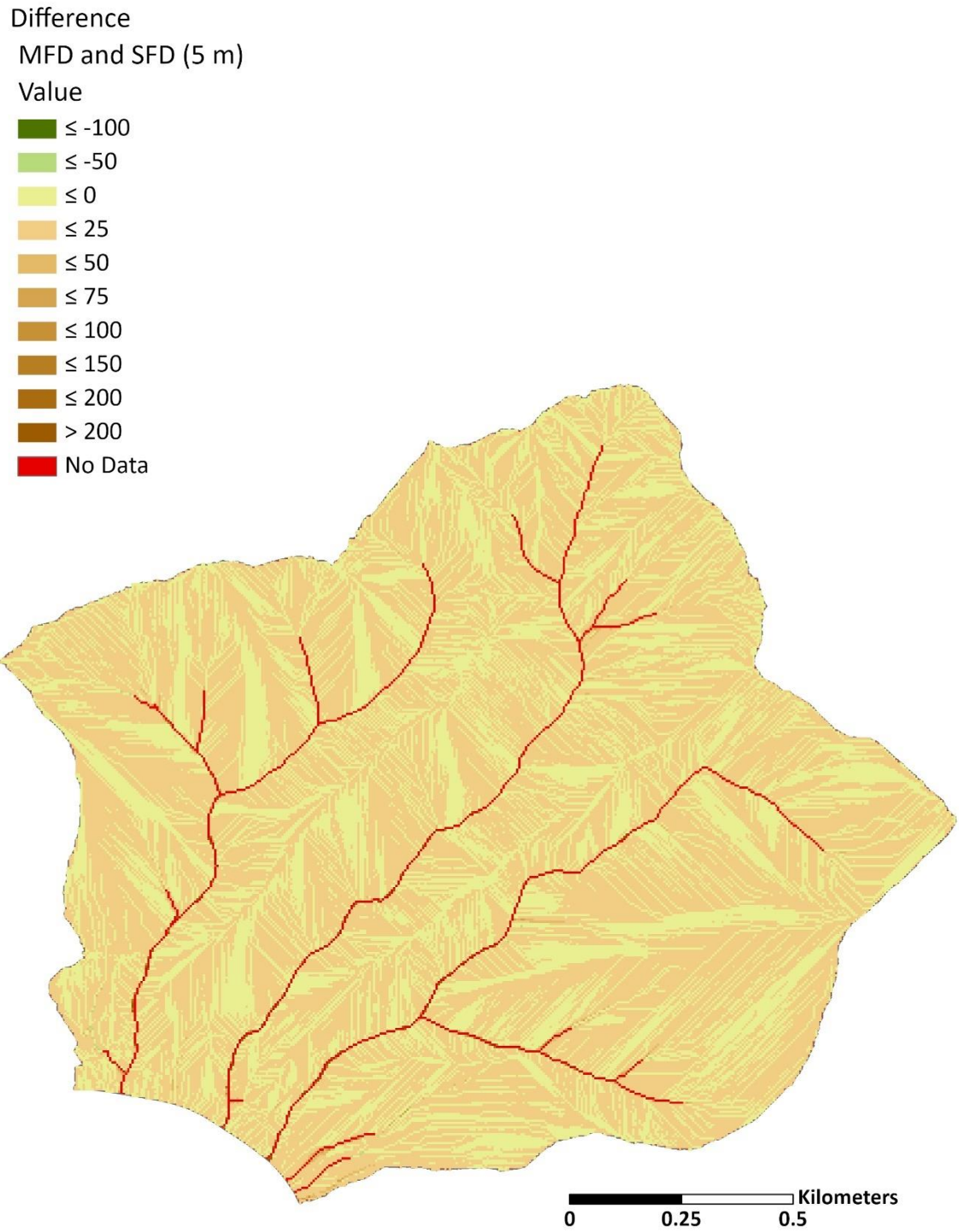


**Figure B22.** Site B difference raster (5 m) for the L Factor of the CA method using a SFD algorithm (SFD) subtracted from the CA method using a MFD algorithm (MFD).

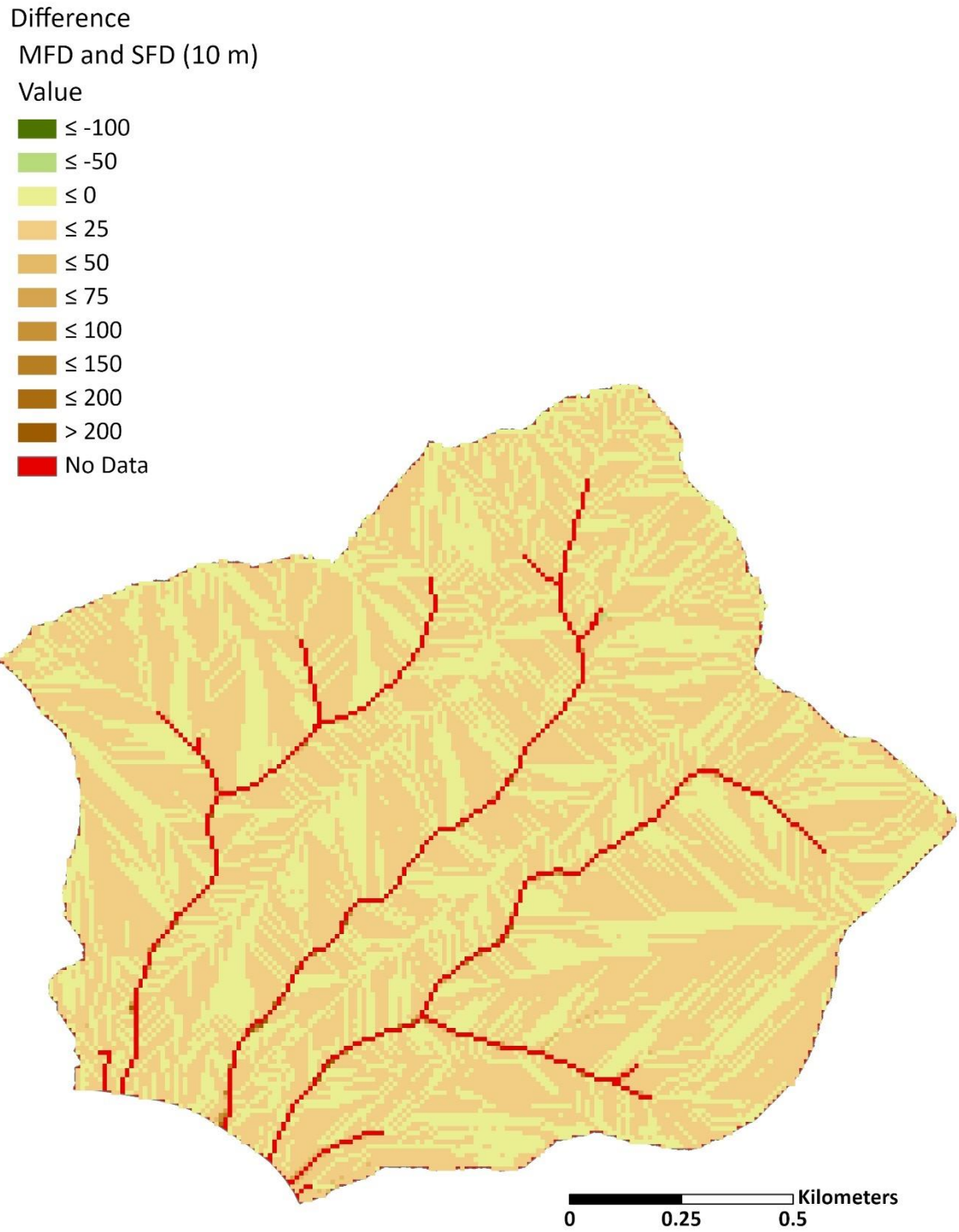


**Figure B23.** Site B difference raster (10 m) for the L Factor of the CA method using a SFD algorithm (SFD) subtracted from the CA method using a MFD algorithm (MFD).

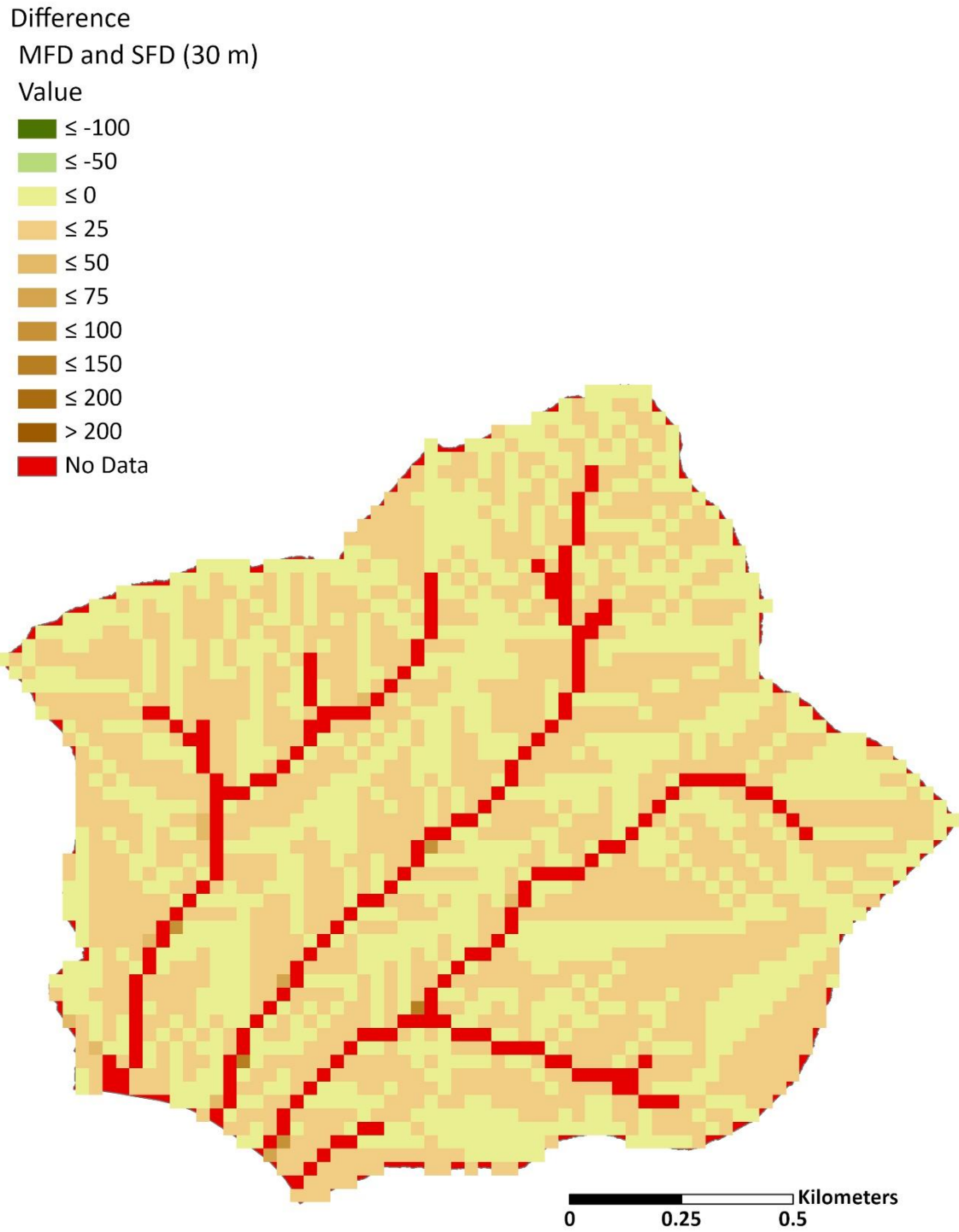


**Figure B24.** Site B difference raster (30 m) for the L Factor of the CA method using a SFD algorithm (SFD) subtracted from the CA method using a MFD algorithm (MFD).

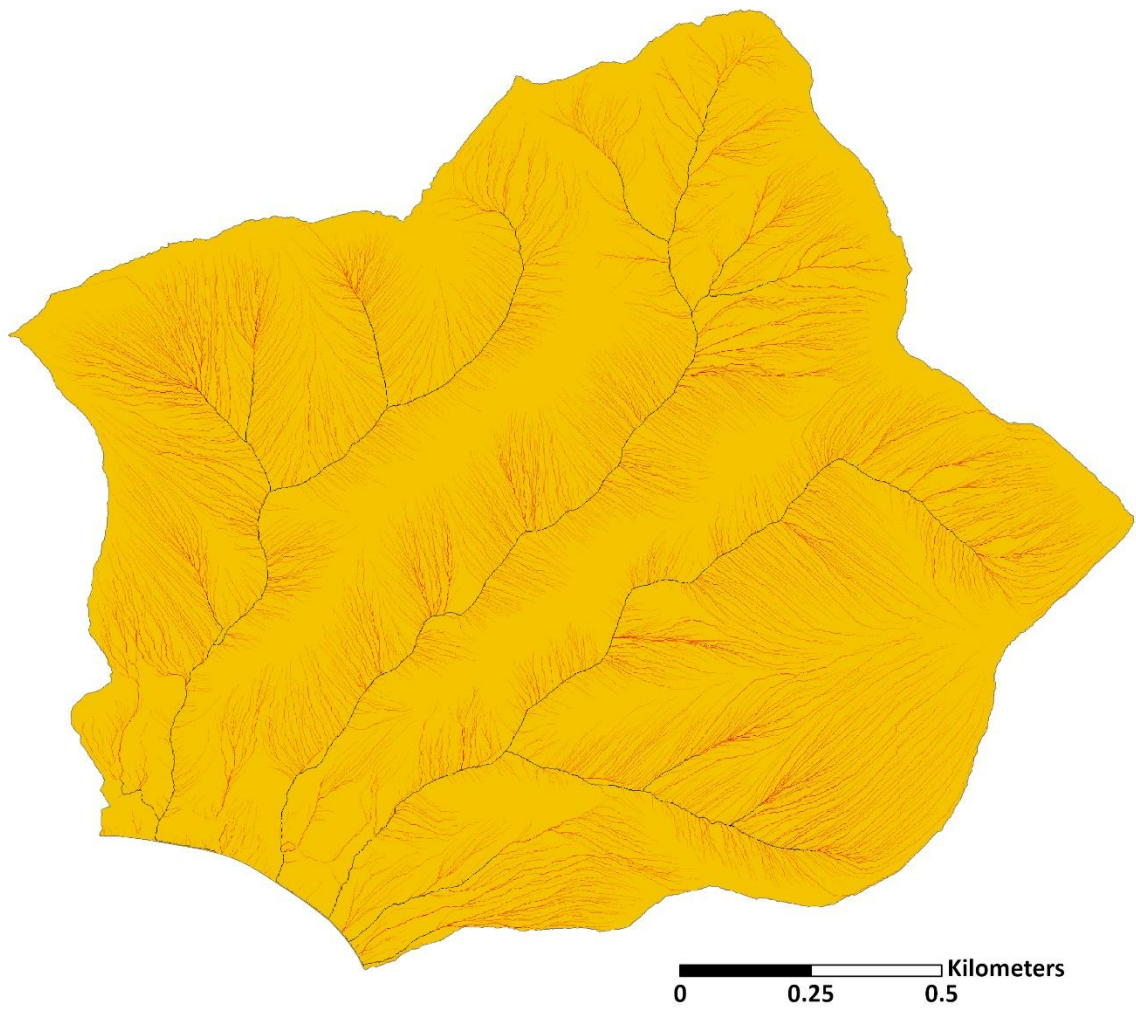
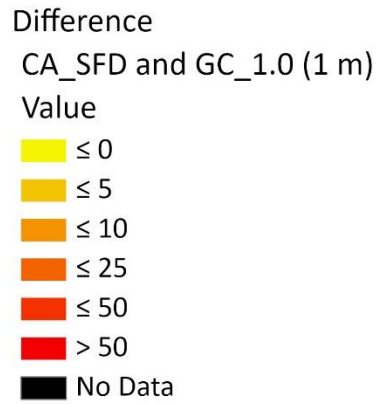


**Figure B25.** Site B difference raster (1 m) for the L Factor of the CA method using a SFD algorithm (CA\_SFD) and the GC method without slope cutoff (GC\_1.0).

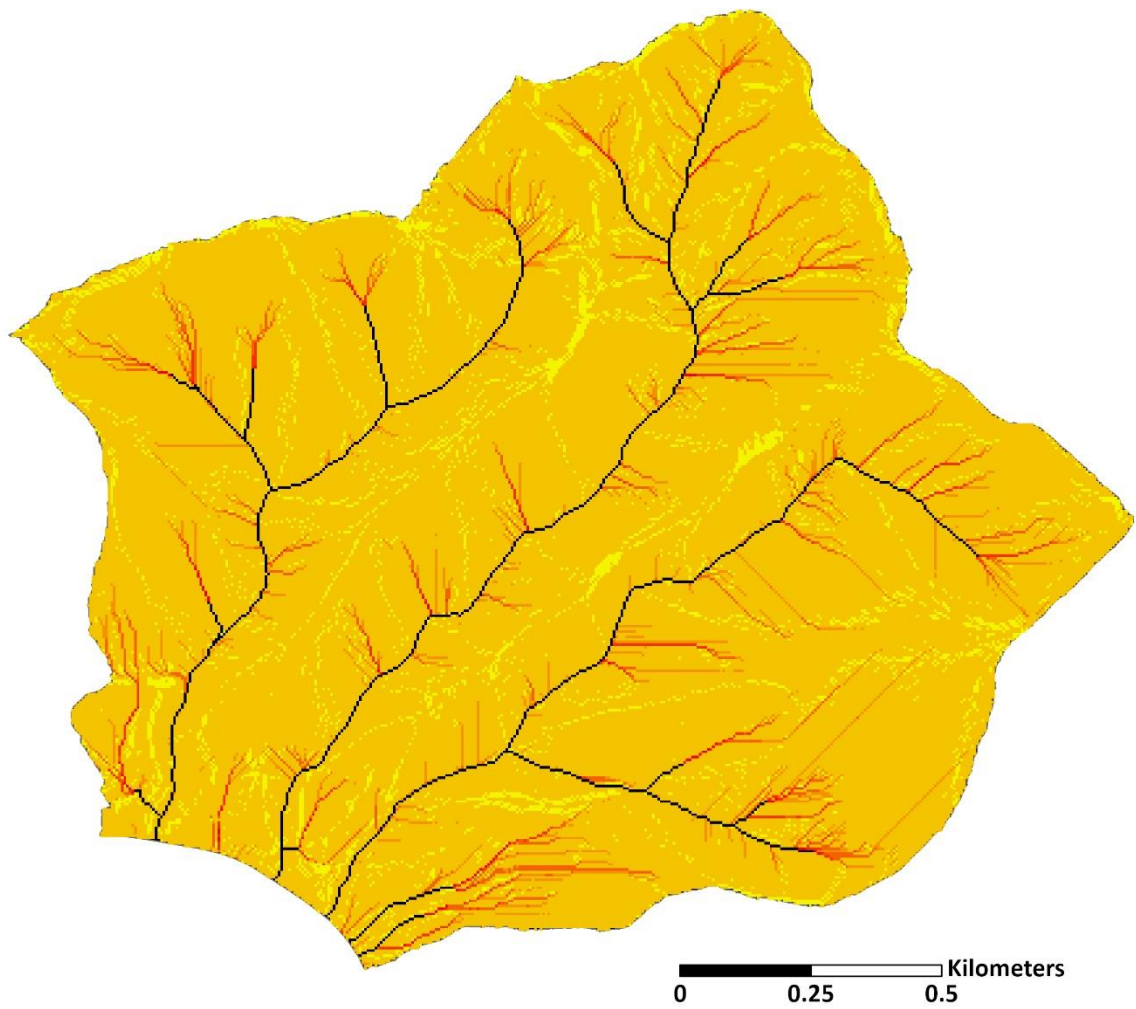
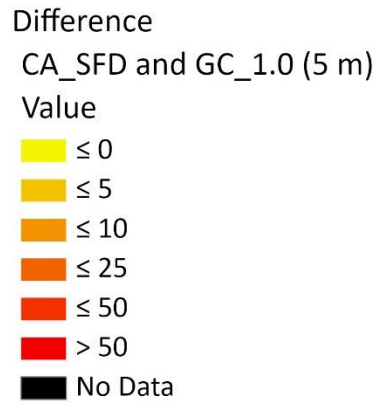


**Figure B26.** Site B difference raster (5 m) for the L Factor of the CA method using a SFD algorithm (CA\_SFD) and the GC method without slope cutoff (GC\_1.0).

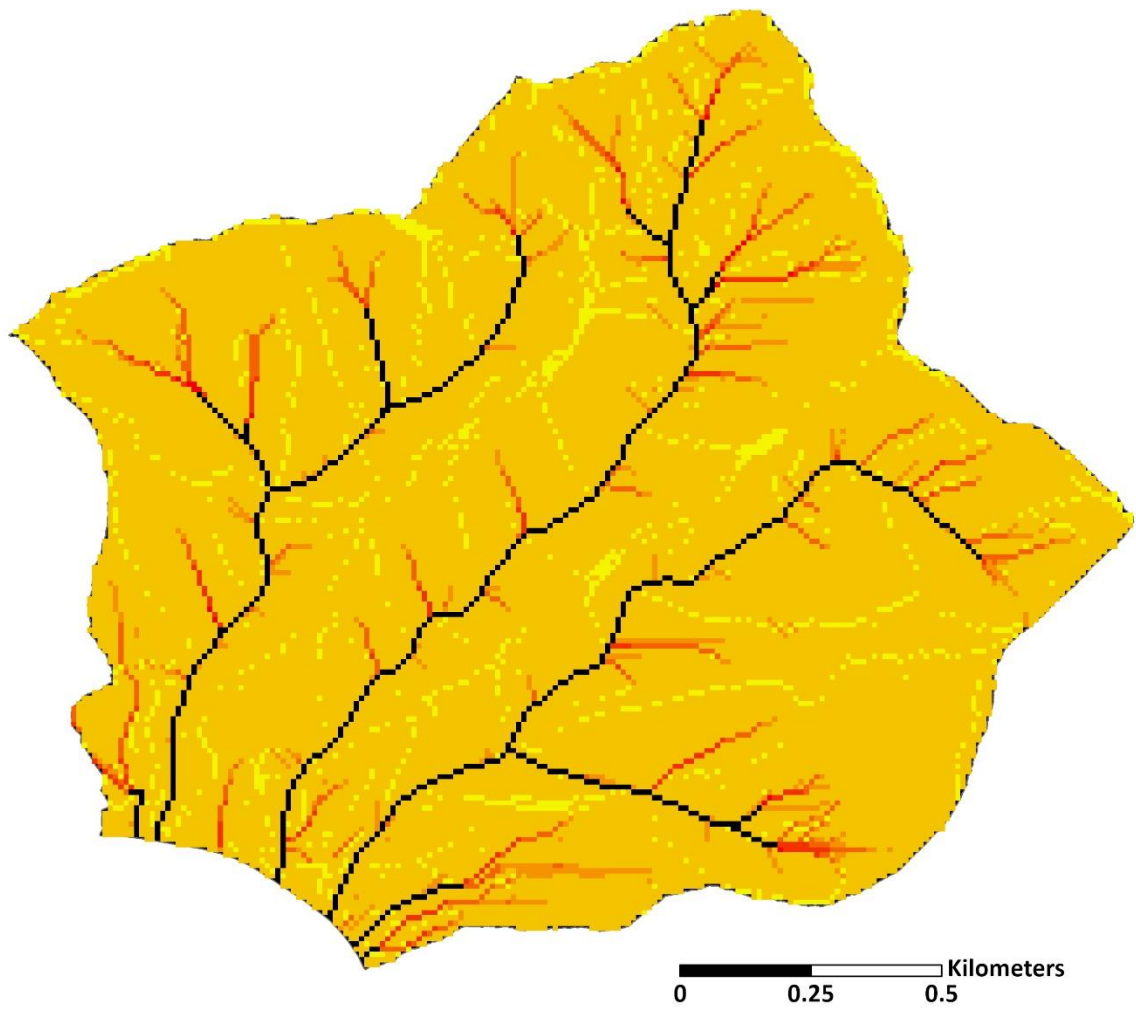


**Figure B27.** Site B difference raster (10 m) for the L Factor of the CA method using a SFD algorithm (CA\_SFD) and the GC method without slope cutoff (GC\_1.0).

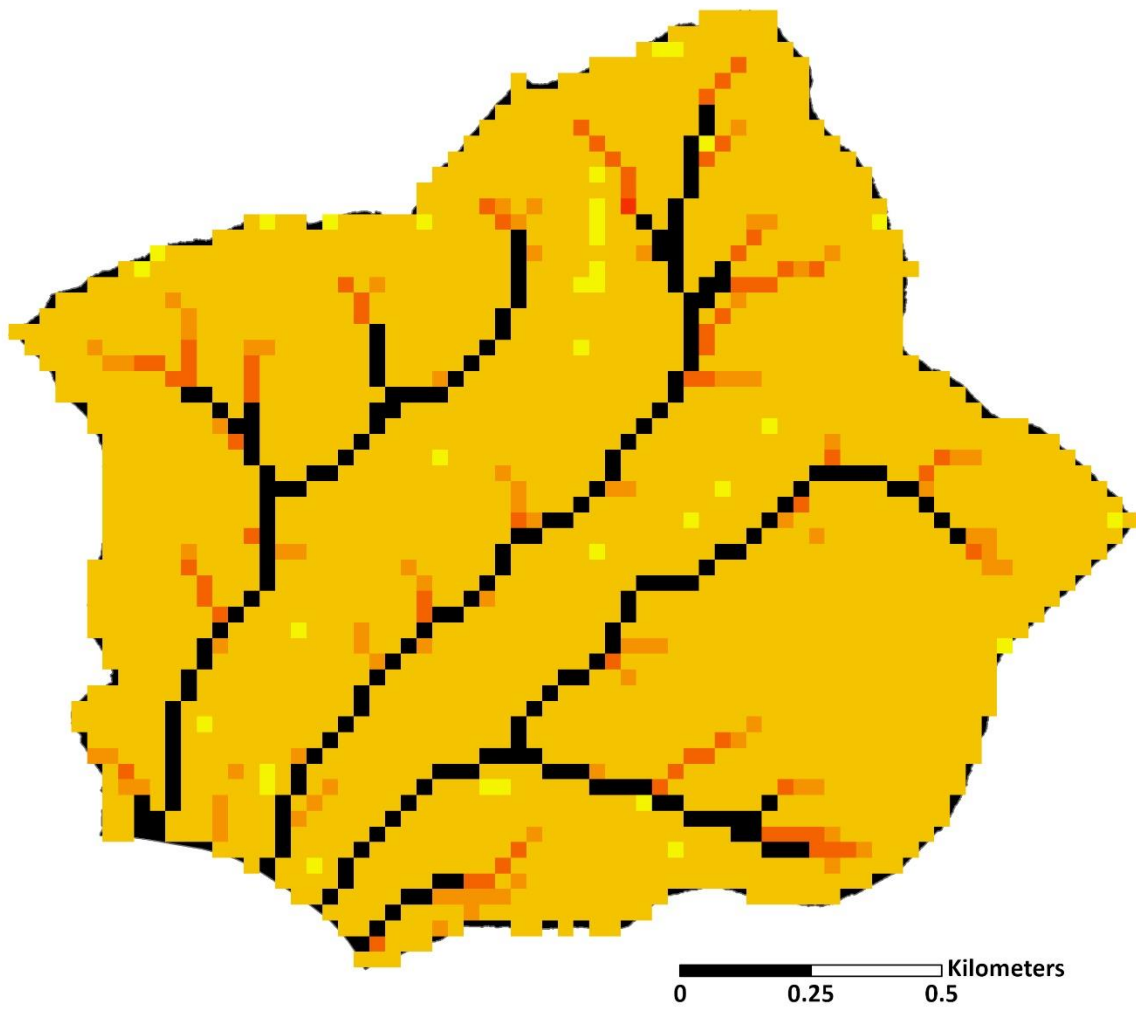


**Figure B28.** Site B difference raster (30 m) for the L Factor of the CA method using a SFD algorithm (CA\_SFD) and the GC method without slope cutoff (GC\_1.0).

MDS (1 m)

Value

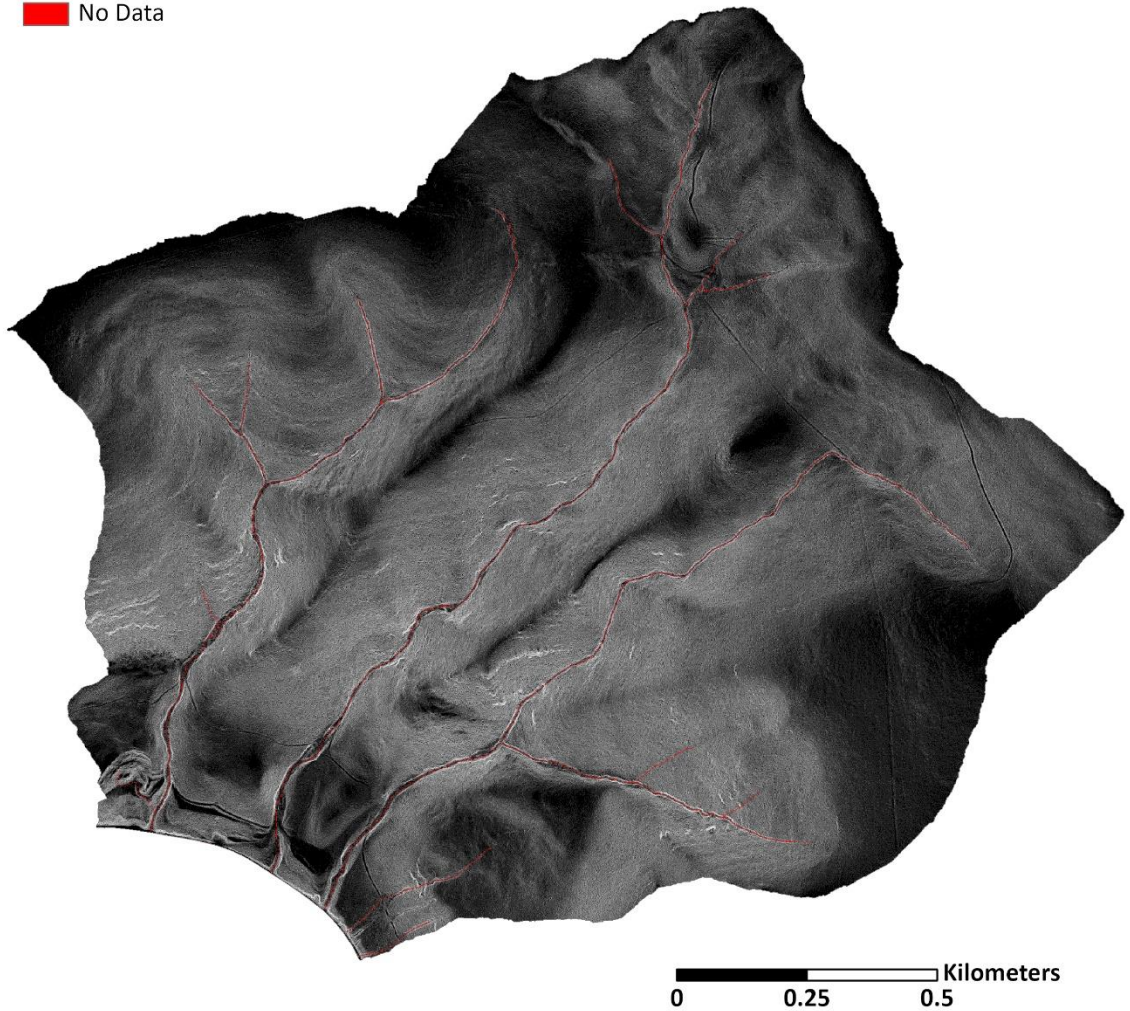
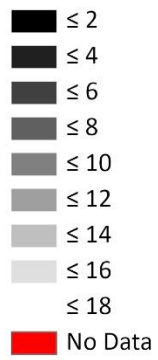


**Figure B298.** S factor with the MDS method for Site B at 1 m.

MDS (5 m)

Value

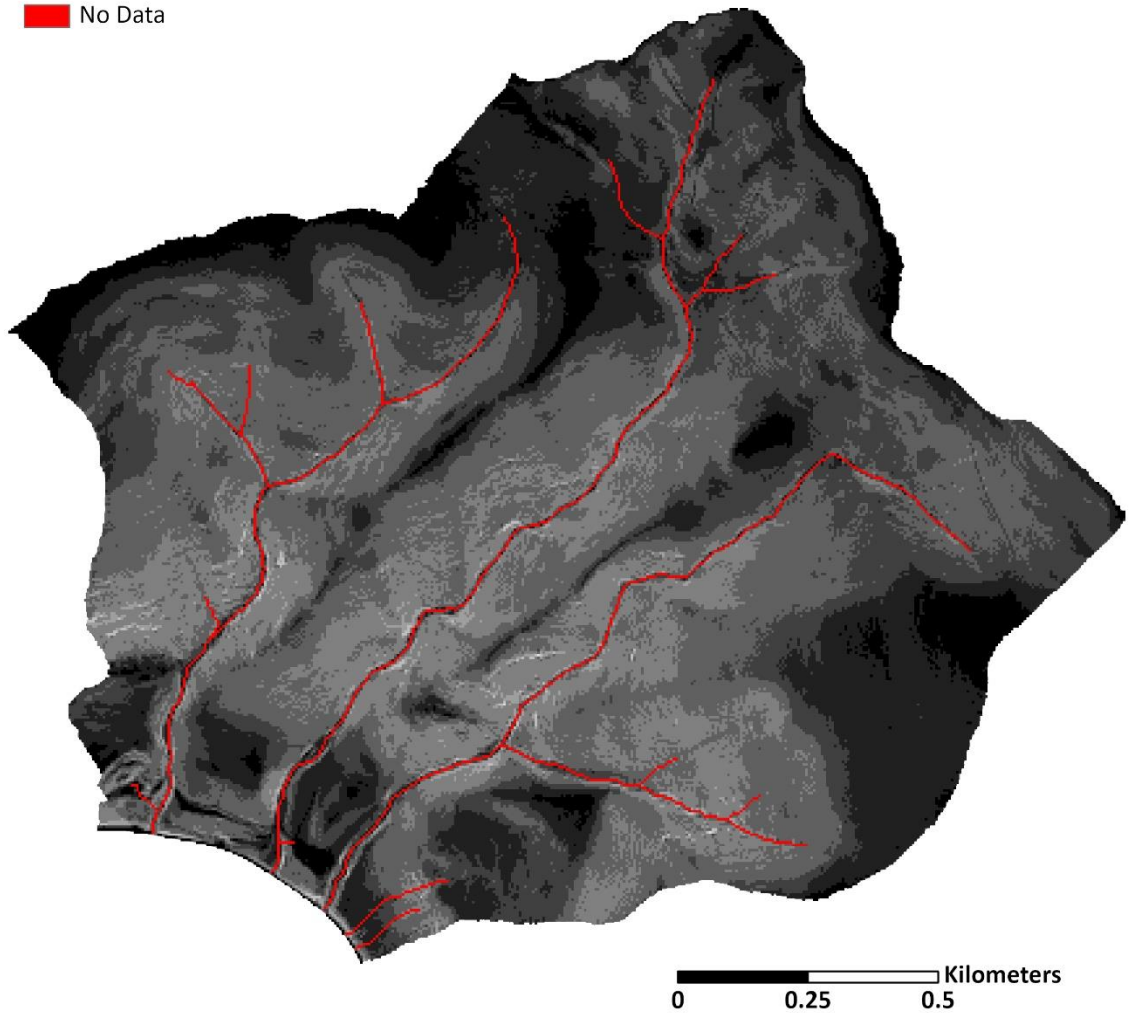
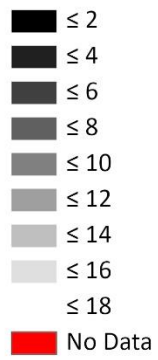


**Figure B30.** S factor with the MDS method for Site B at 5 m.

MDS (10 m)

Value

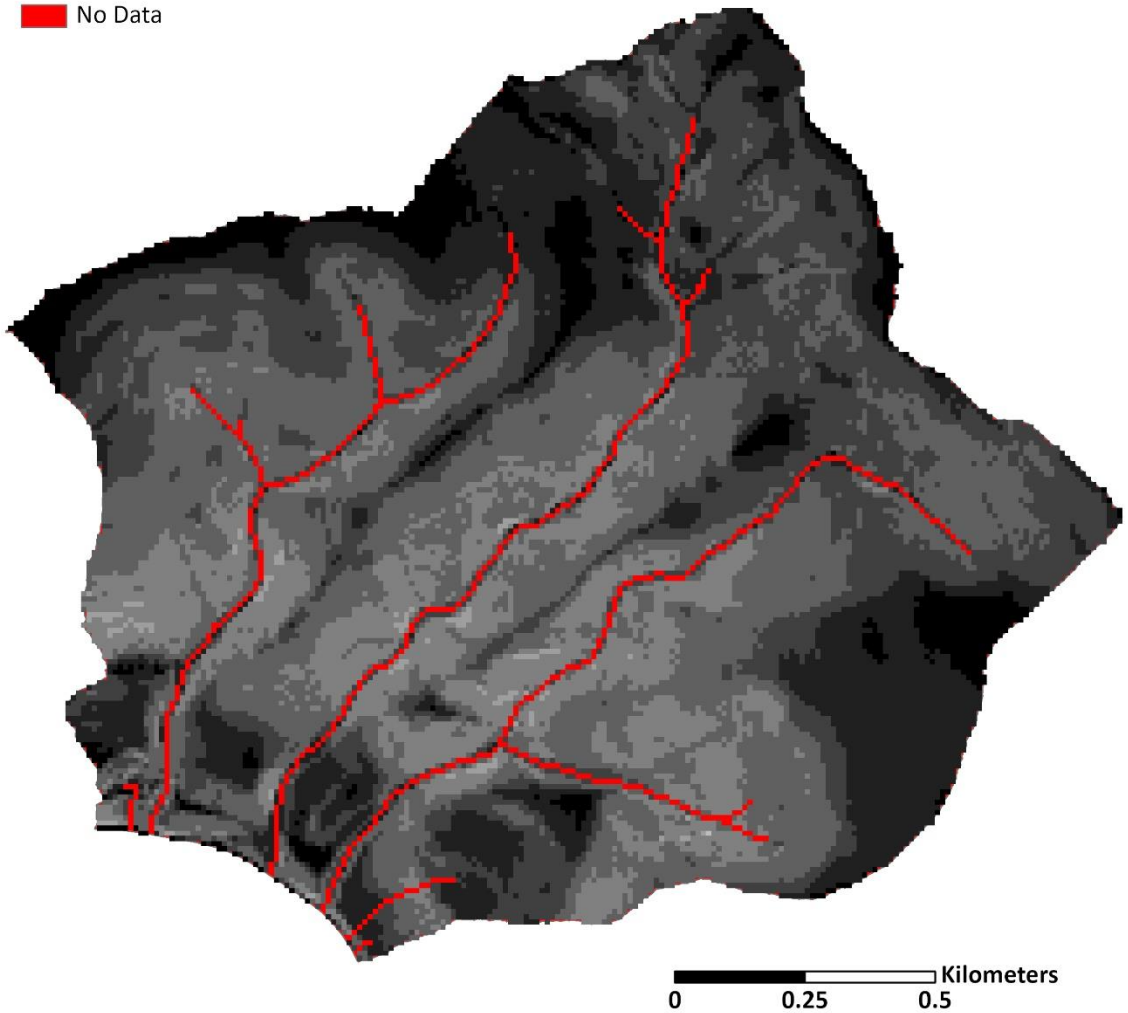
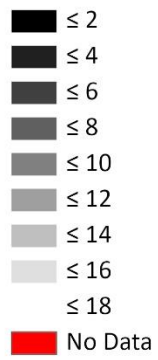


**Figure B31.** S factor with the MDS method for Site B at 10 m.

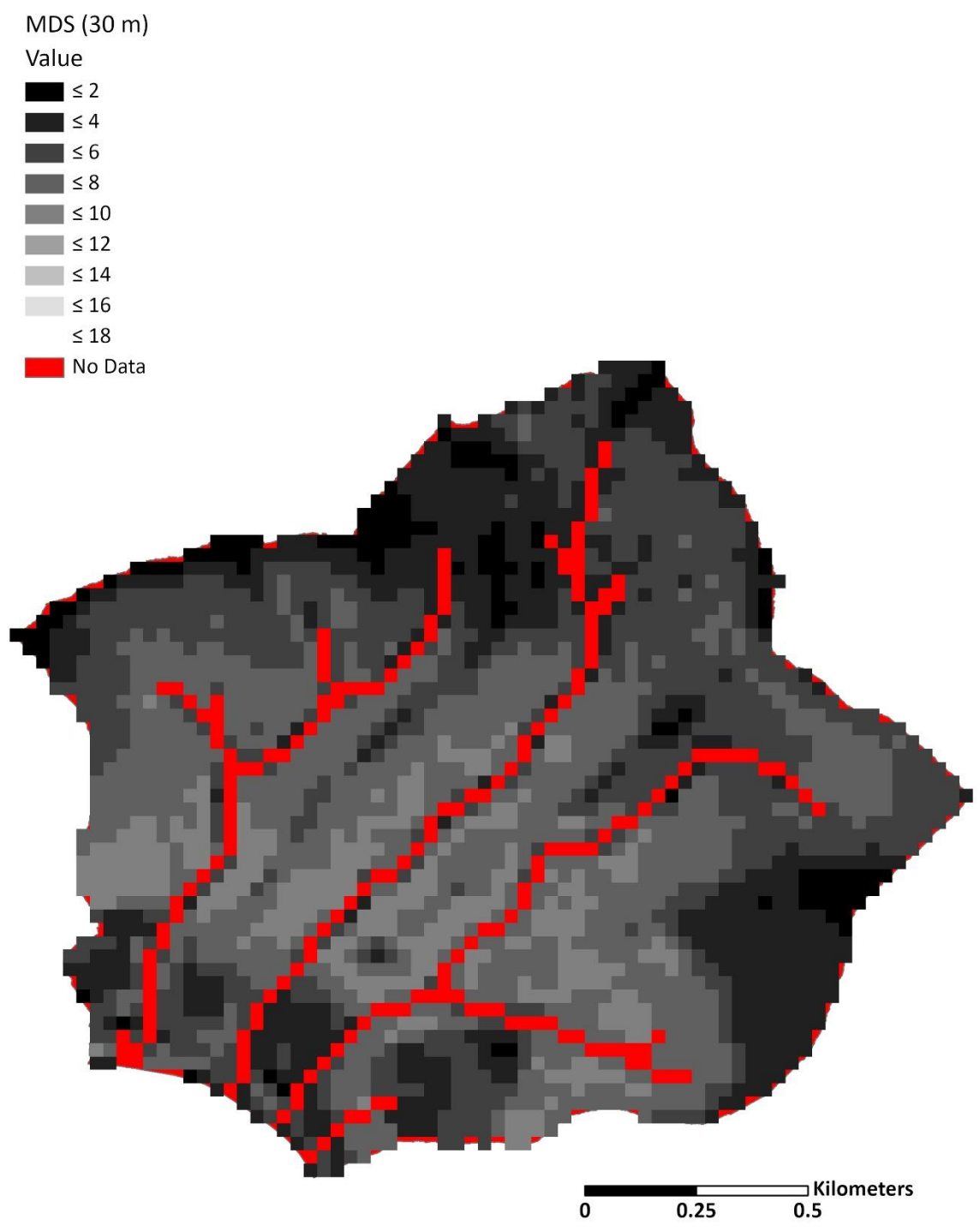


**Figure B32.** S factor with the MDS method for Site B at 30 m.

NBR (1 m)

Value

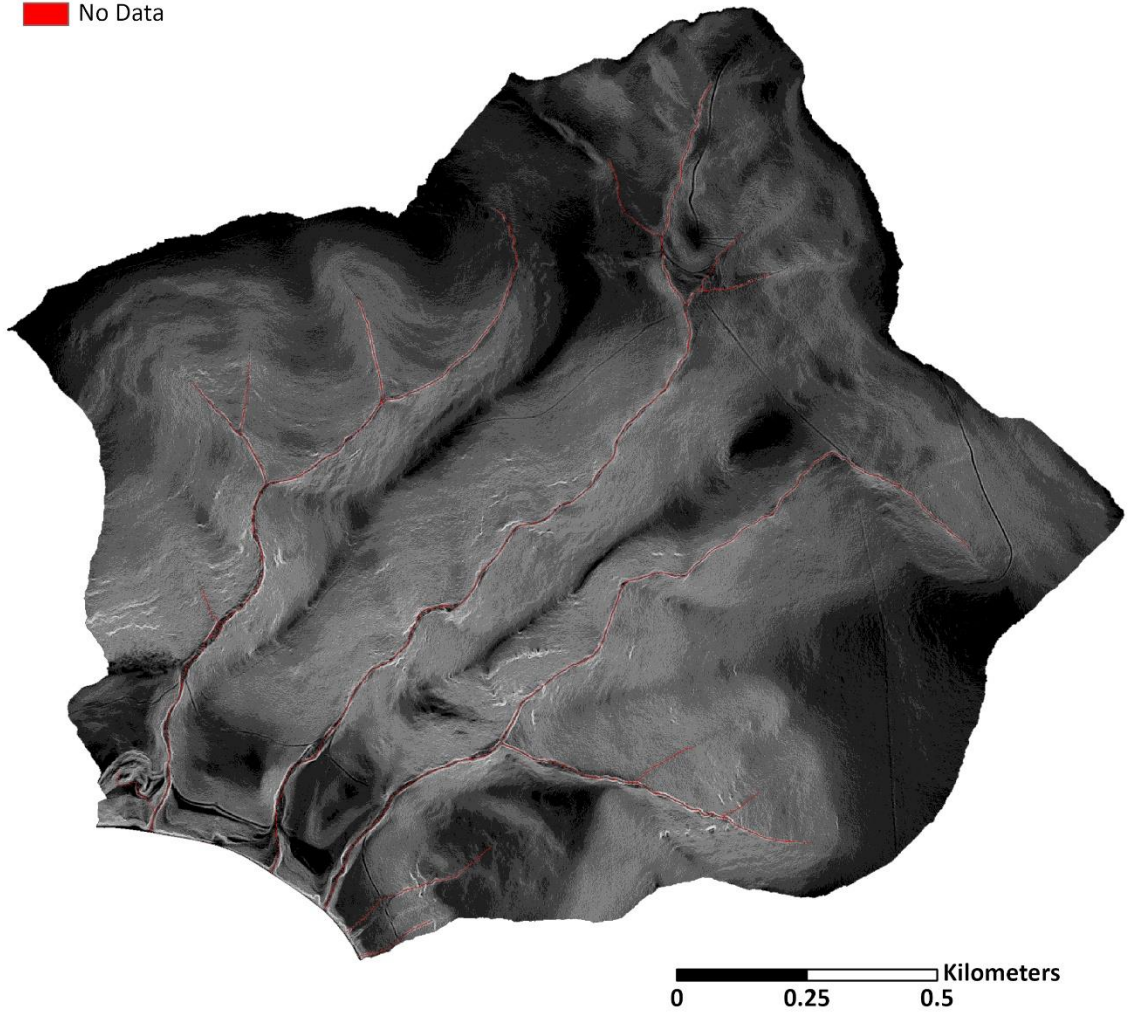
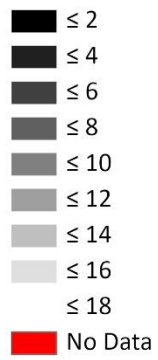


**Figure B33.** S factor with the NBR method for Site B at 1 m.

NBR (5 m)

Value

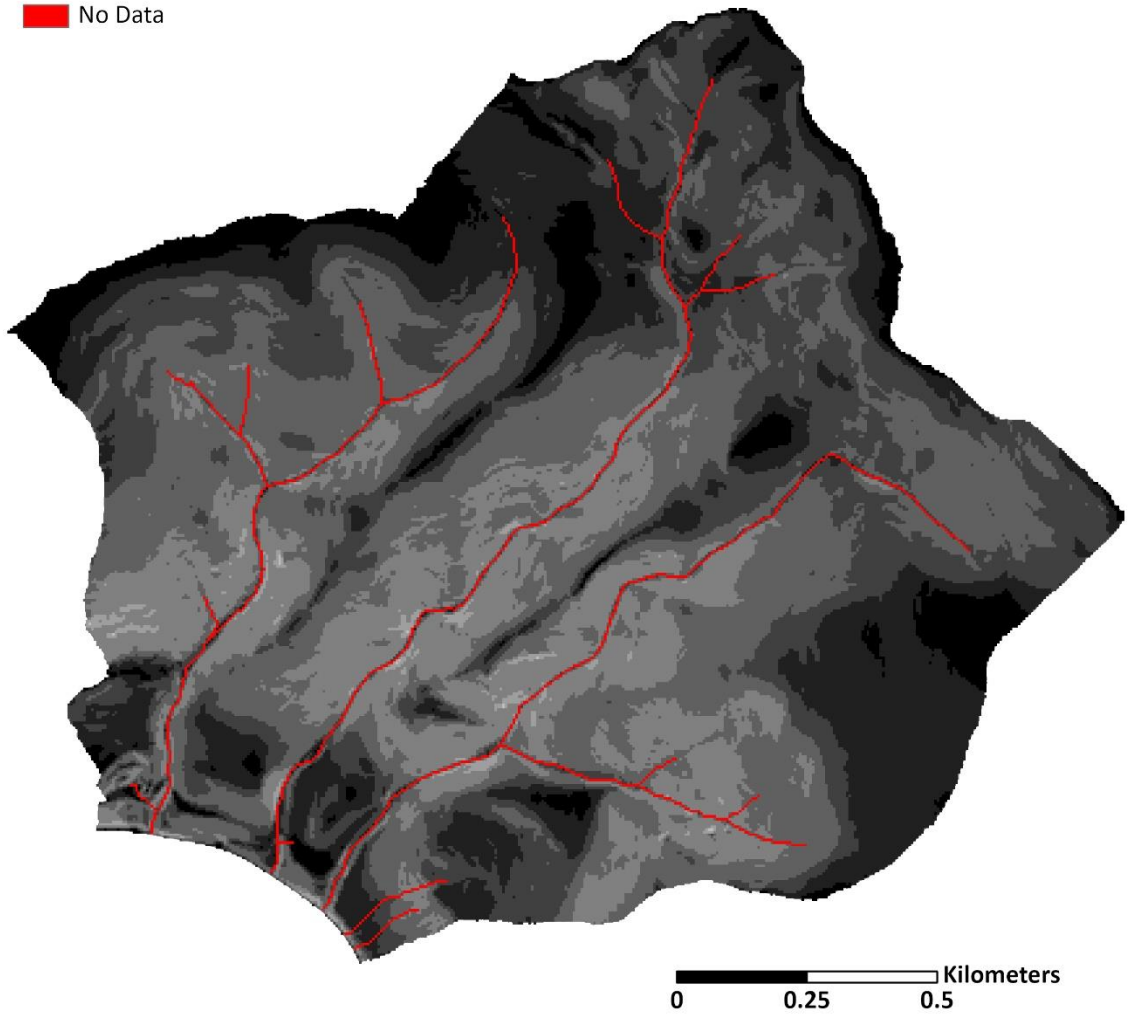
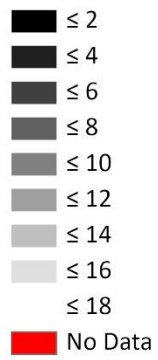


**Figure B34.** S factor with the NBR method for Site B at 5 m.

NBR (10 m)

Value

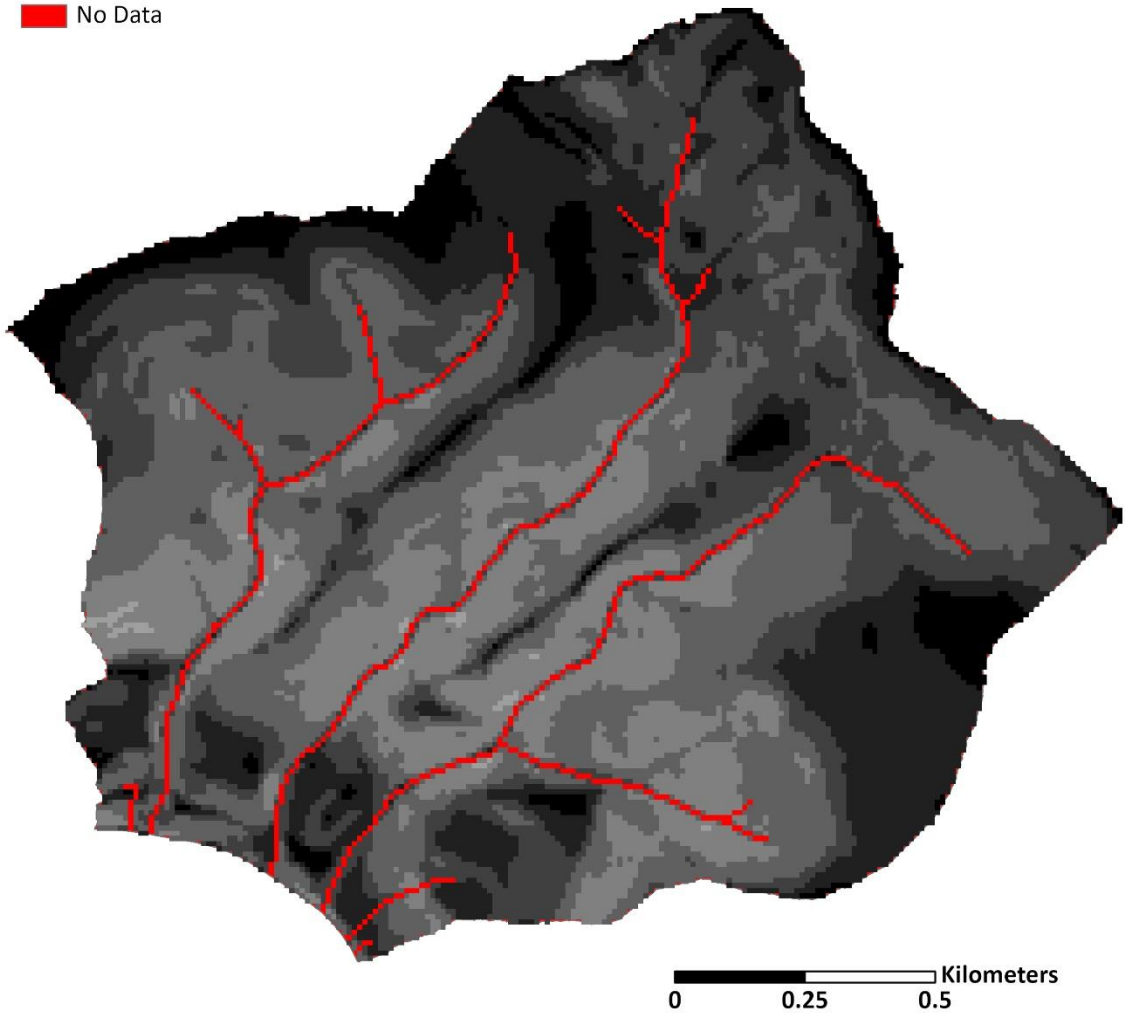
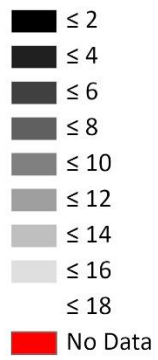


**Figure B35.** S factor with the NBR method for Site B at 10 m.

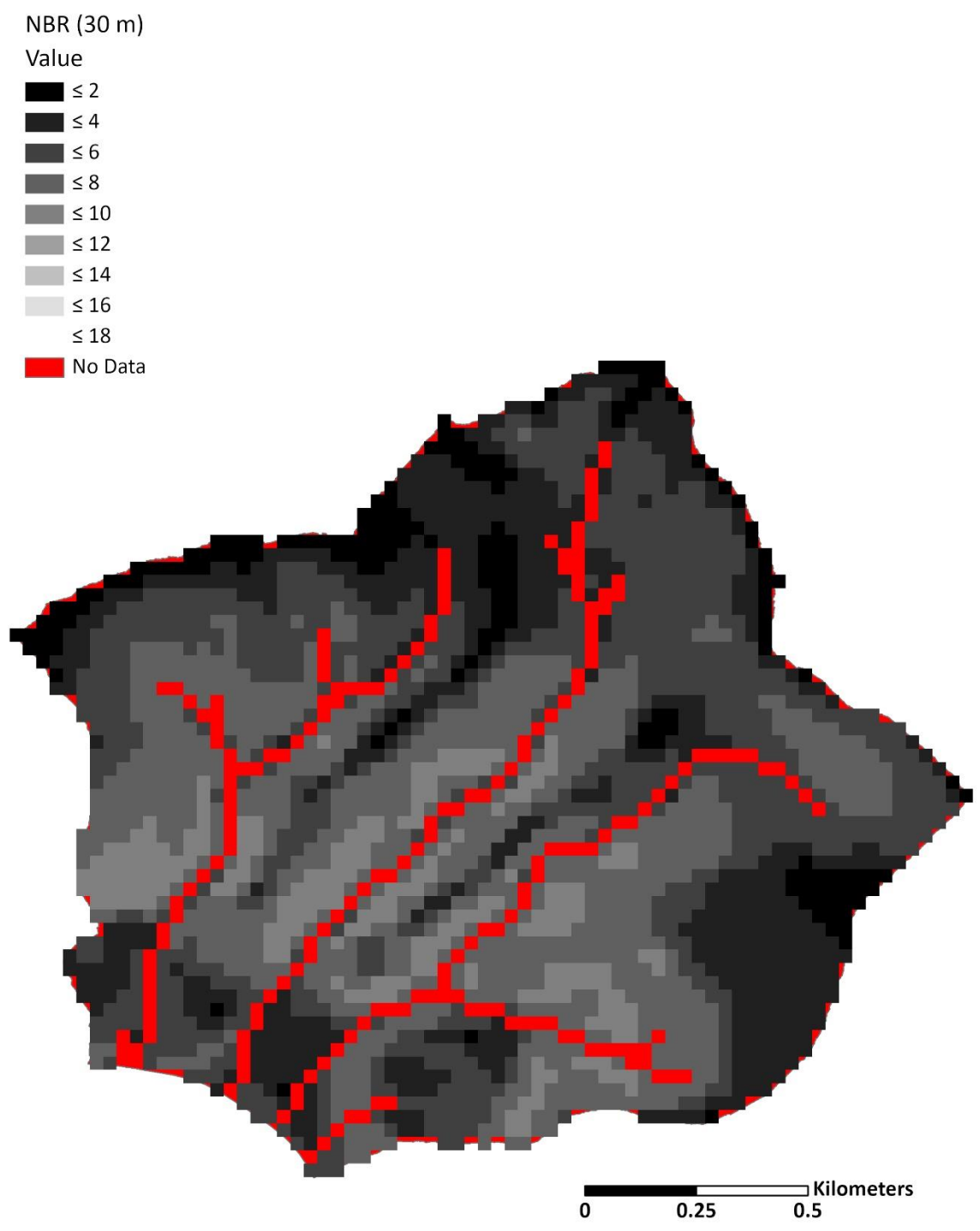


**Figure B36.** S factor with the NBR method for Site B at 30 m.

Difference  
NBR and MDS (1 m)

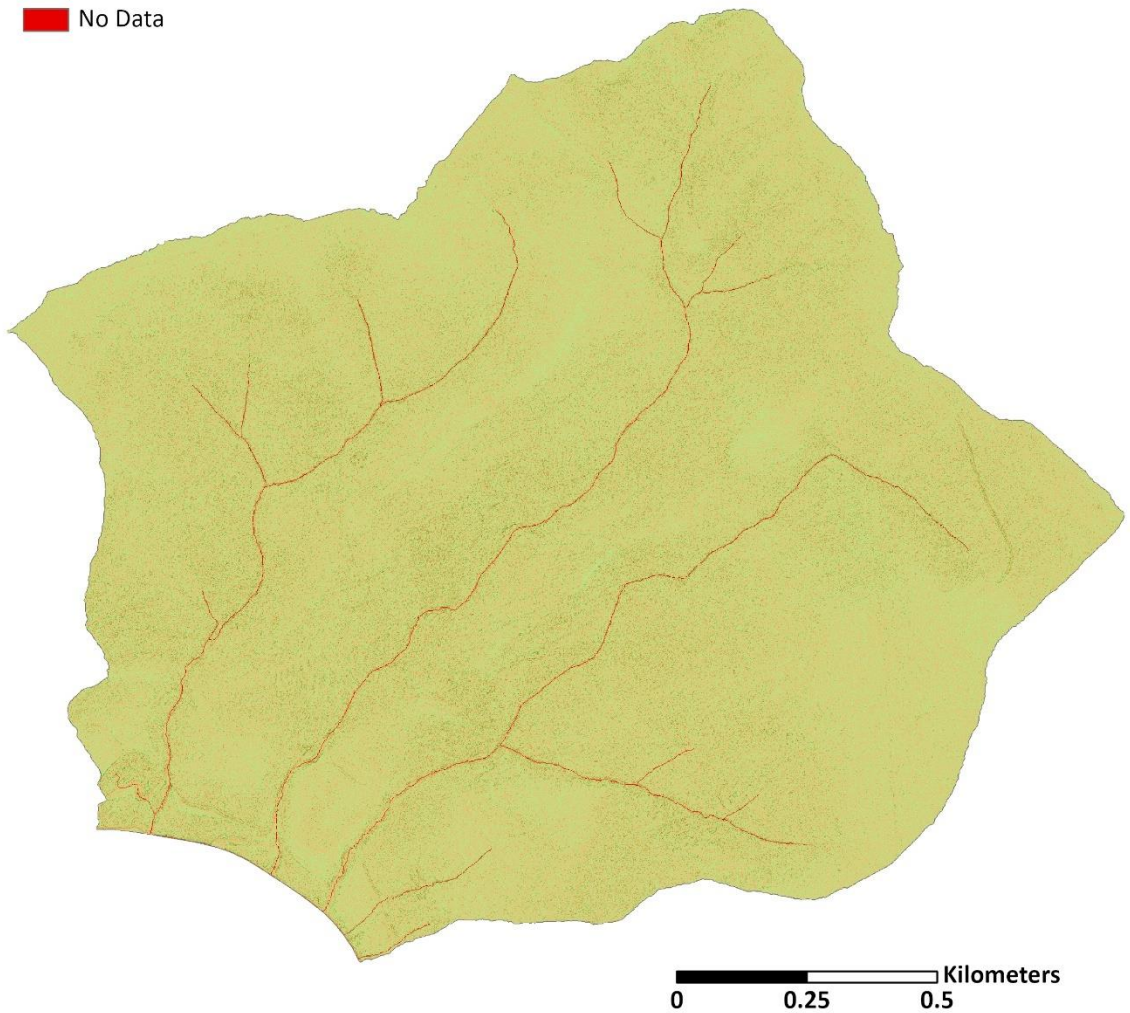
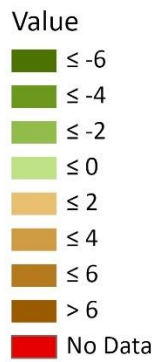


**Figure B37.** Site B difference raster (1 m) for the S Factor of the MDS method subtracted from the NBR method.

Difference  
NBR and MDS (5 m)

Value

■  $\leq -6$

■  $\leq -4$

■  $\leq -2$

■  $\leq 0$

■  $\leq 2$

■  $\leq 4$

■  $\leq 6$

■  $> 6$

■ No Data

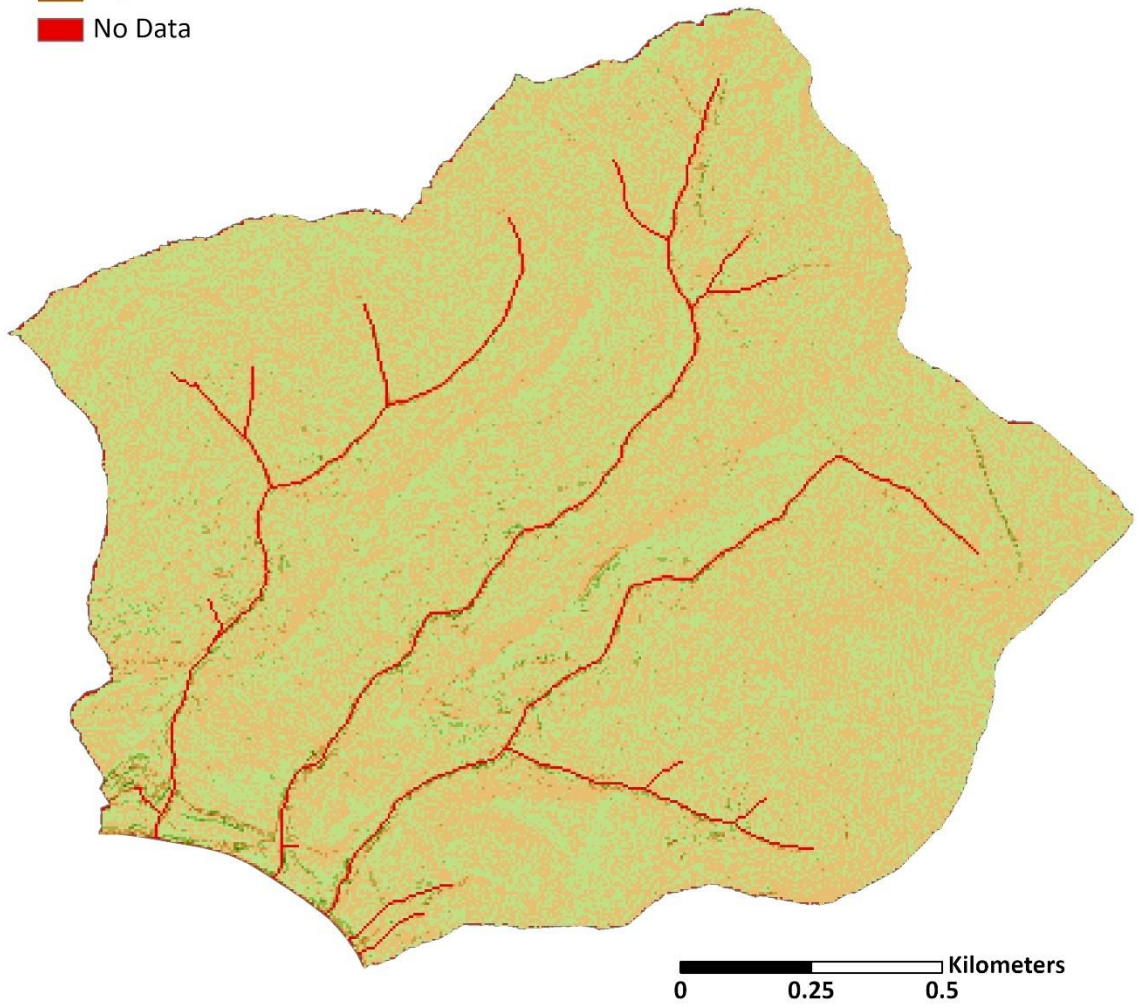


**Figure B38.** Site B difference raster (5 m) for the S Factor of the MDS method subtracted from the NBR method.

Difference  
NBR and MDS (10 m)

Value

■  $\leq -6$

■  $\leq -4$

■  $\leq -2$

■  $\leq 0$

■  $\leq 2$

■  $\leq 4$

■  $\leq 6$

■  $> 6$

■ No Data

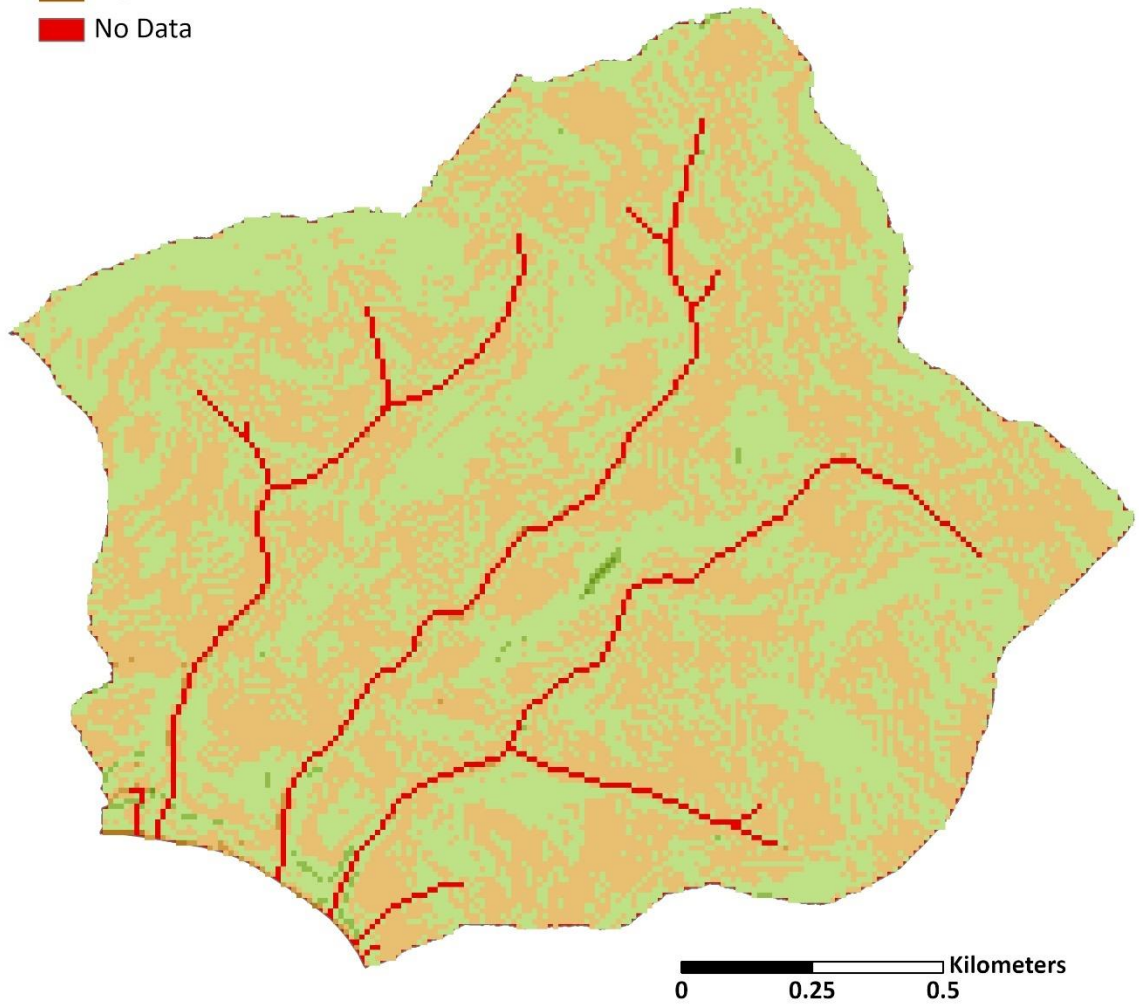


**Figure B39.** Site B difference raster (10 m) for the S Factor of the MDS method subtracted from the NBR method.

Difference  
NBR and MDS (30 m)

Value

■  $\leq -6$

■  $\leq -4$

■  $\leq -2$

■  $\leq 0$

■  $\leq 2$

■  $\leq 4$

■  $\leq 6$

■  $> 6$

■ No Data

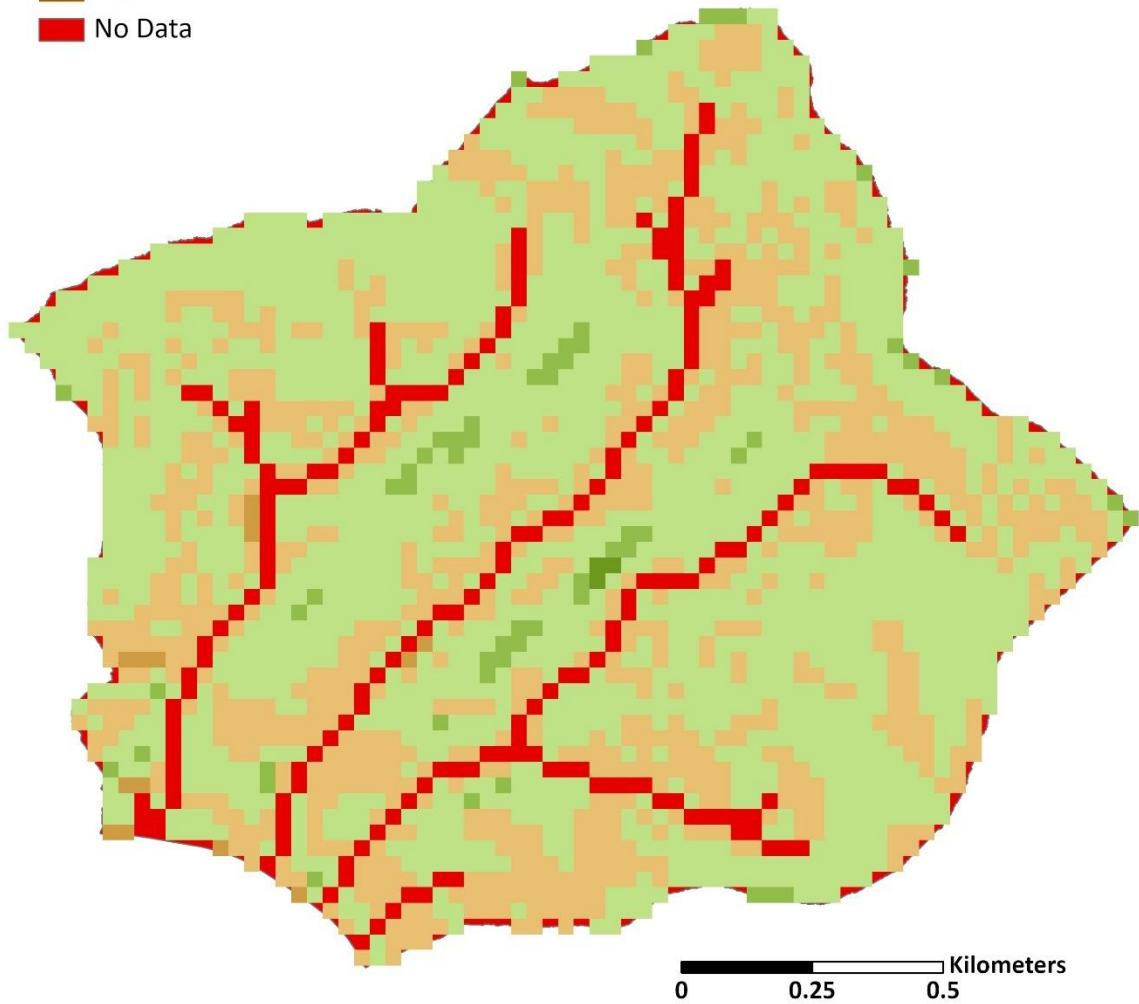


**Figure B40.** Site B difference raster (30 m) for the S Factor of the MDS method subtracted from the NBR method.

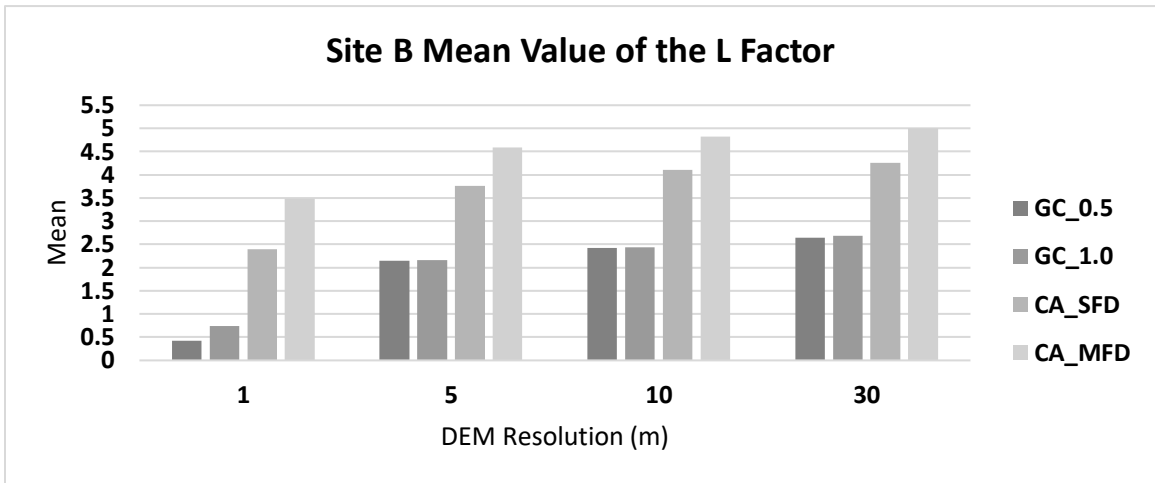


**Figure B41.** Mean value of L factor for Site B where GC\_0.5 is the GC method with slope cutoff set to 0.5, GC\_1.0 is the GC method without slope cutoff, CA\_SFD is the CA method using a SFD algorithm, and CA\_MFD is the CA method using a MFD algorithm.

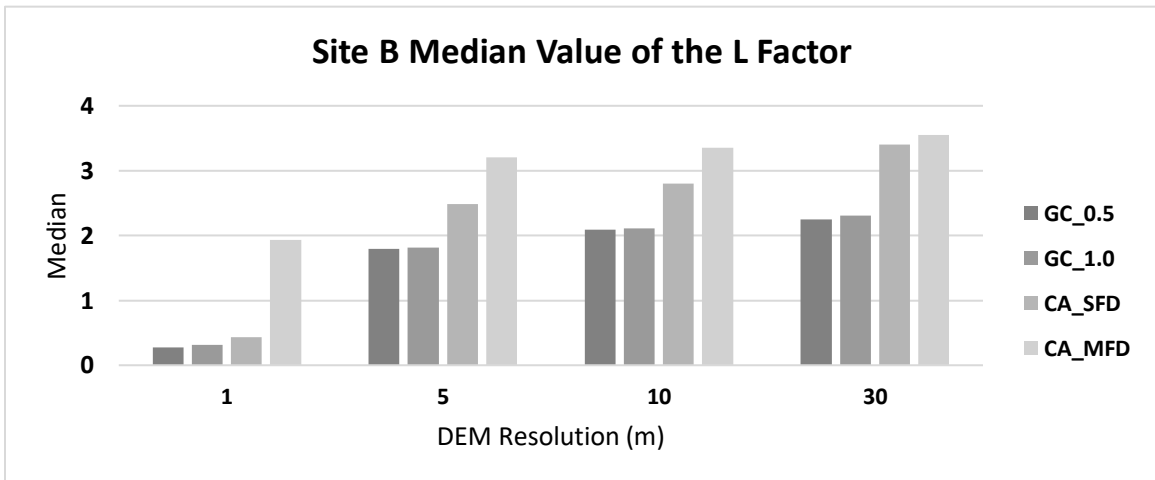


**Figure B42.** Median value of L factor for Site B where GC\_0.5 is the GC method with slope cutoff set to 0.5, GC\_1.0 is the GC method without slope cutoff, CA\_SFD is the CA method using a SFD algorithm, and CA\_MFD is the CA method using a MFD algorithm.

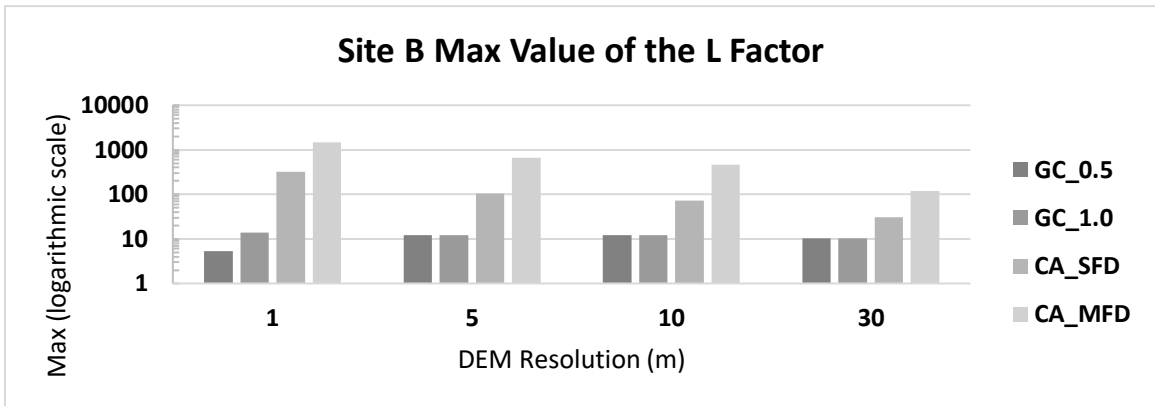


**Figure B43.** Maximum value of L factor for Site B where GC\_0.5 is the GC method with slope cutoff set to 0.5, GC\_1.0 is the GC method without slope cutoff, CA\_SFD is the CA method using a SFD algorithm, and CA\_MFD is the CA method using a MFD algorithm.

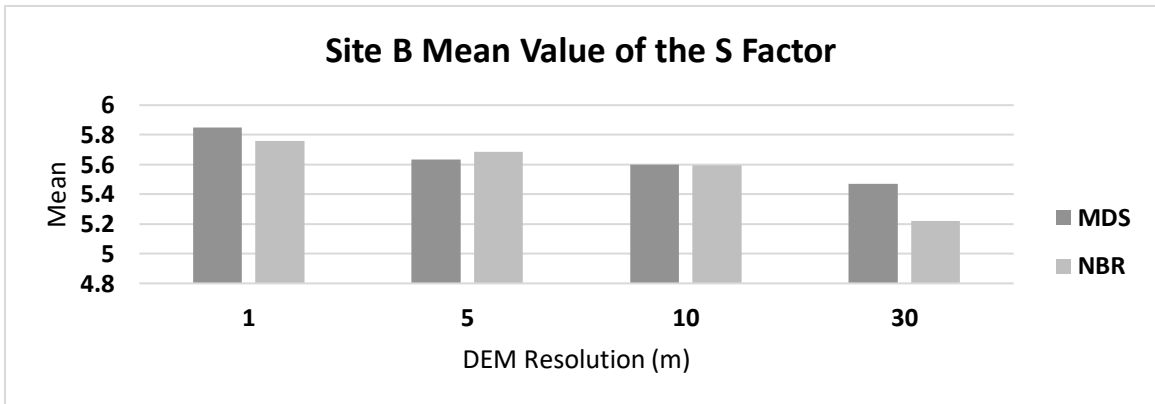


**Figure B44.** Mean value of S factor for Site B.

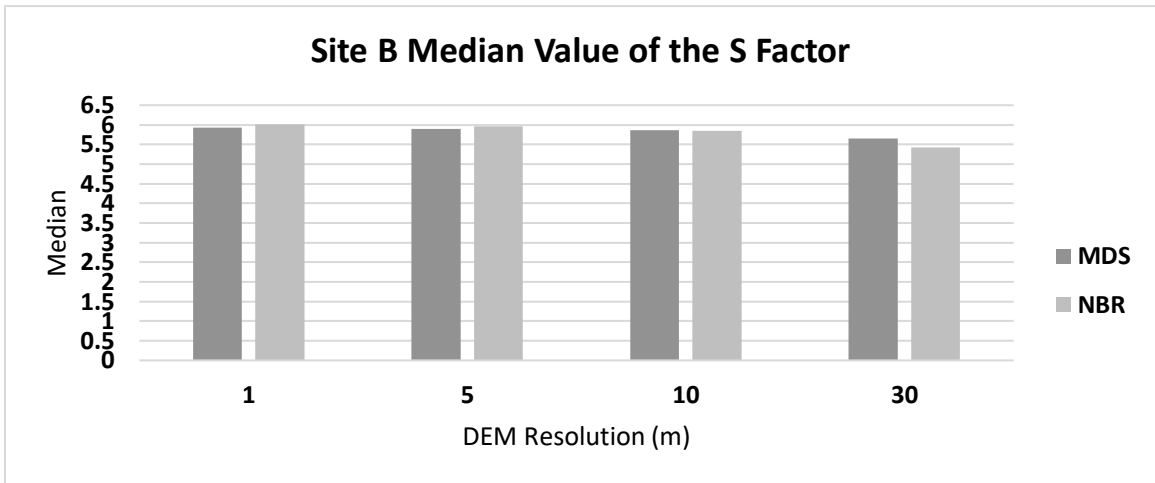


**Figure B45.** Median value of S factor for Site B.

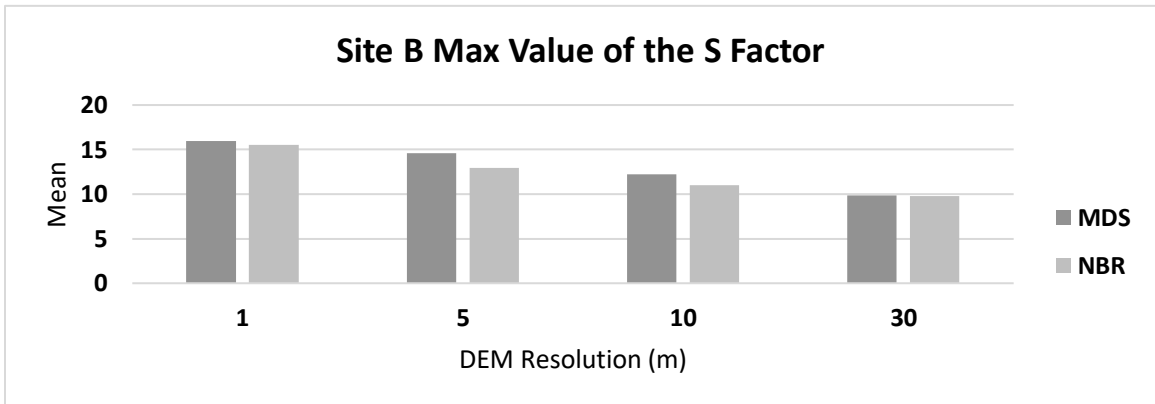


**Figure B46.** Maximum value of S factor for Site B.

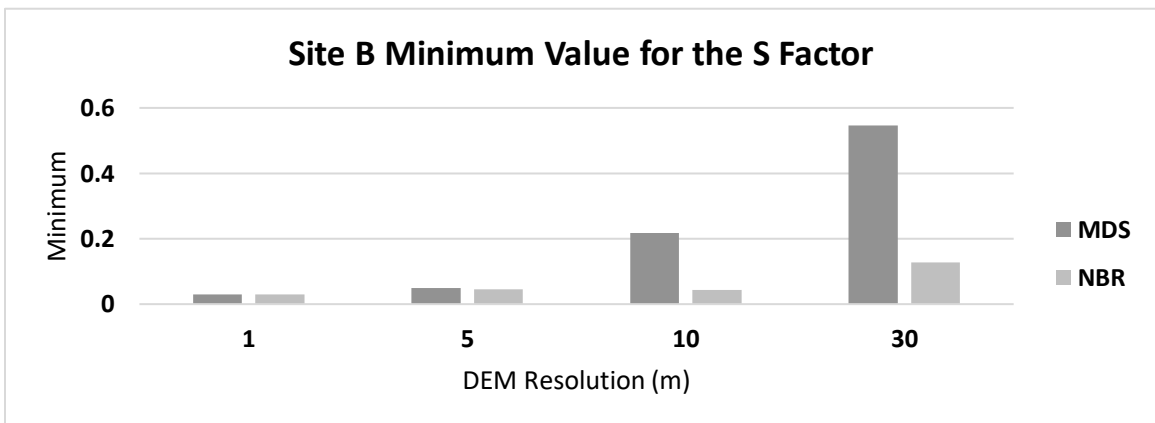


**Figure B47.** Minimum value of S factor for Site B.

Site C outputs:

GC\_0.5 (1 m)

Value

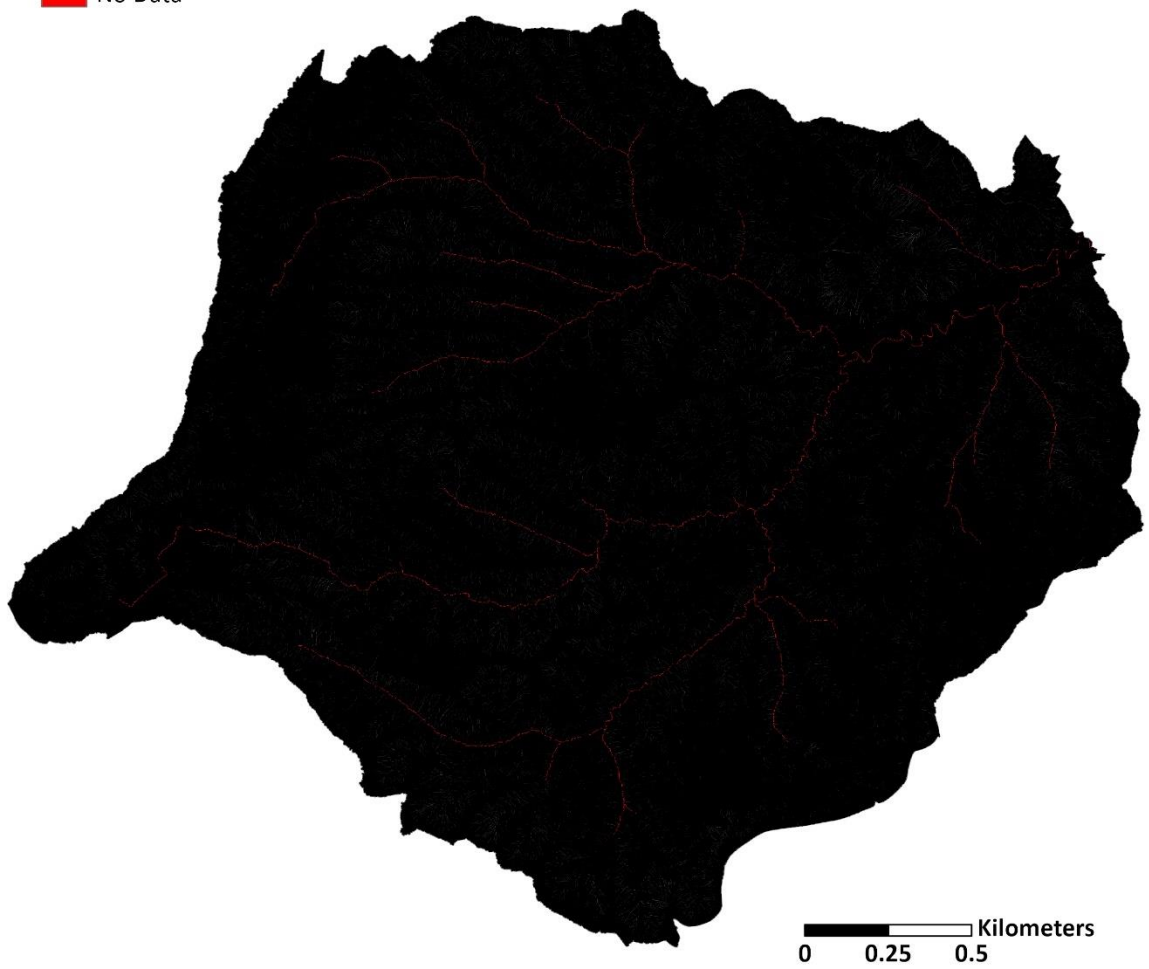
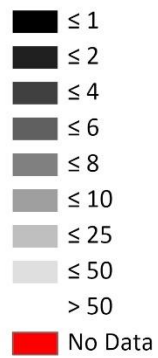


**Figure C1.** L factor with the GC Method with slope cutoff at 0.5 for Site C at 1 m resolution.

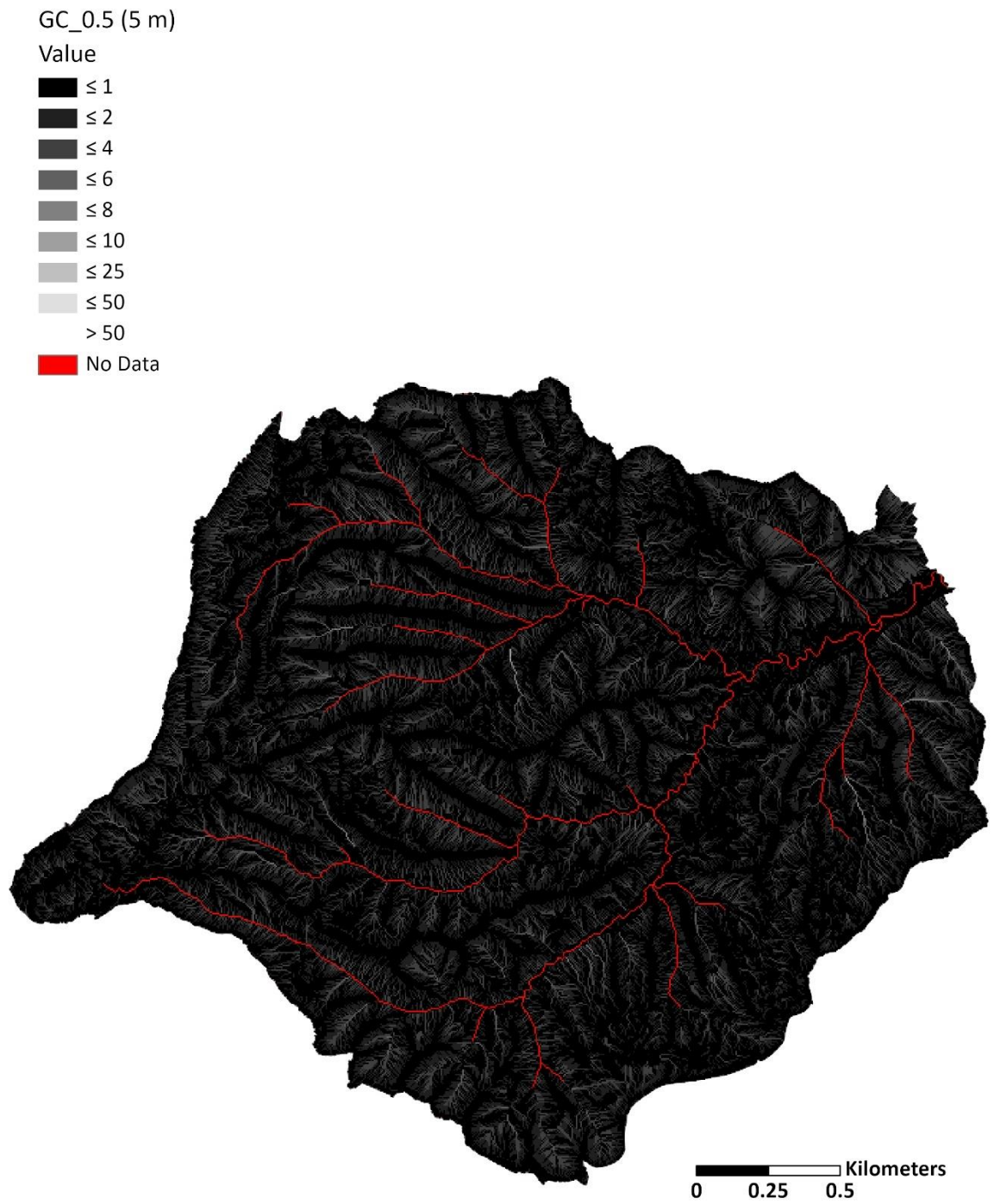


**Figure C2.** L factor with the GC Method with slope cutoff at 0.5 for Site C at 5 m.

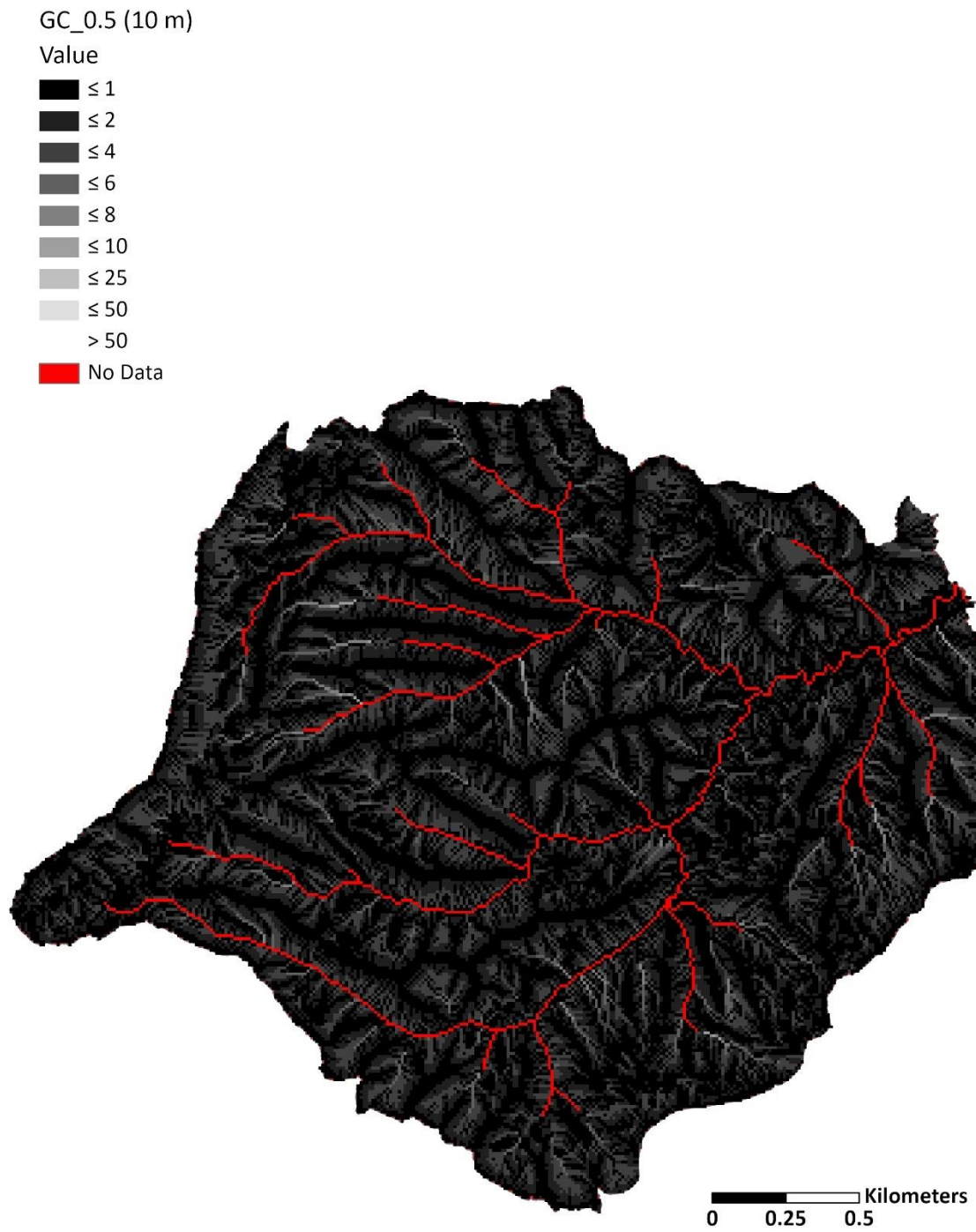


**Figure C3.** L factor with the GC Method with slope cutoff at 0.5 for Site C at 10 m.

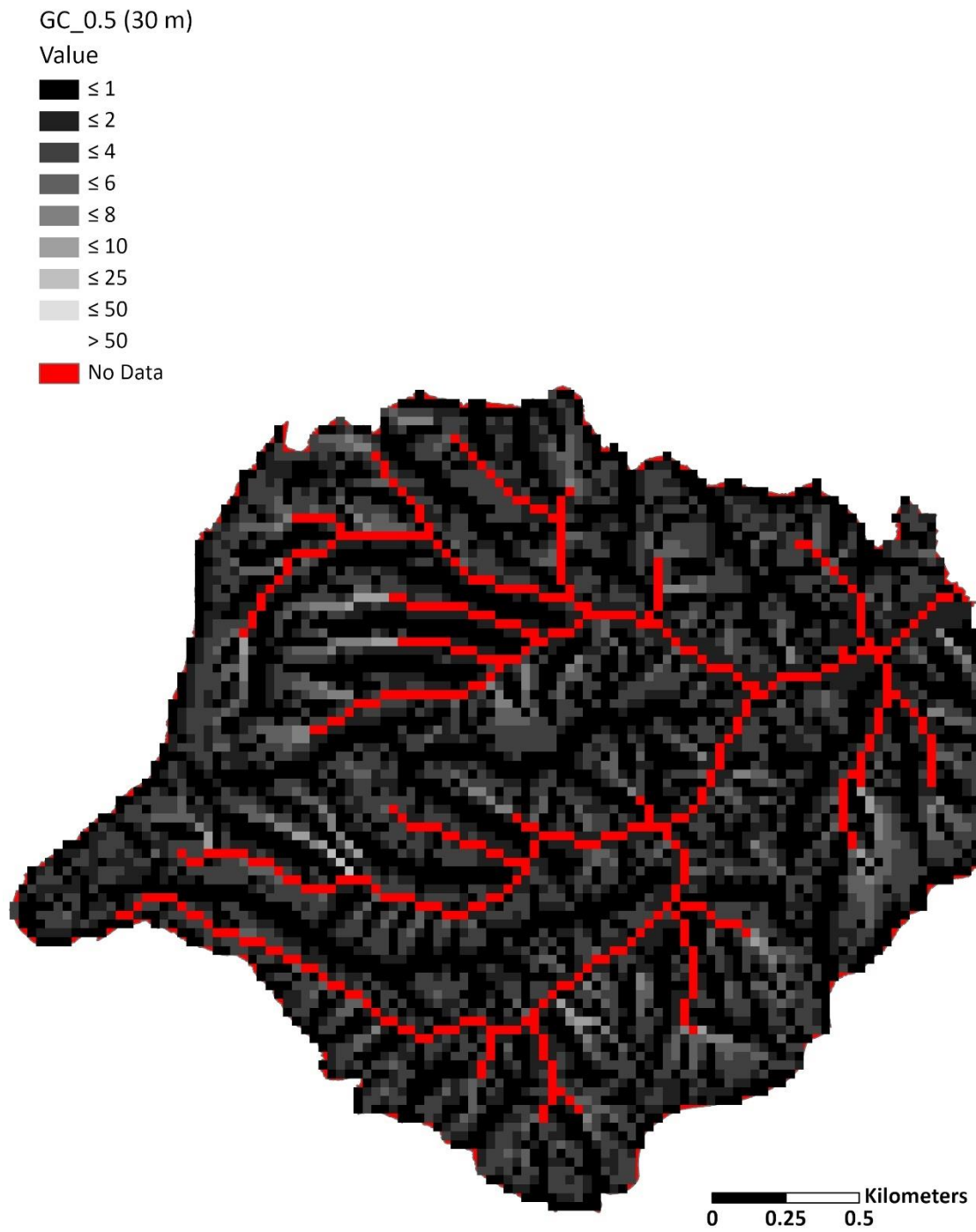


**Figure C4.** L factor with the GC Method with slope cutoff at 0.5 for Site C at 30 m.

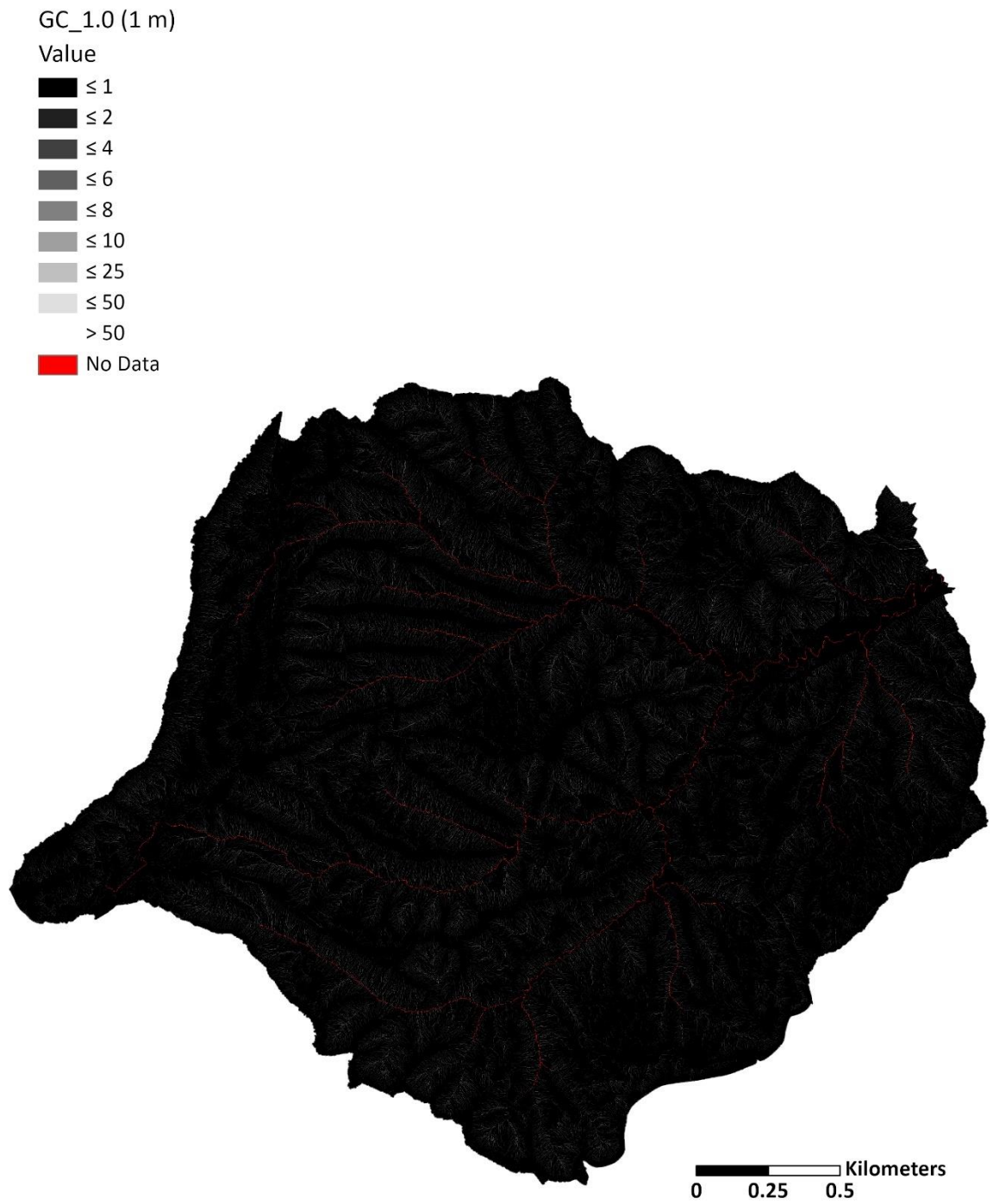


**Figure C5.** L factor with the GC Method without slope cutoff for Site C at 1 m resolution.

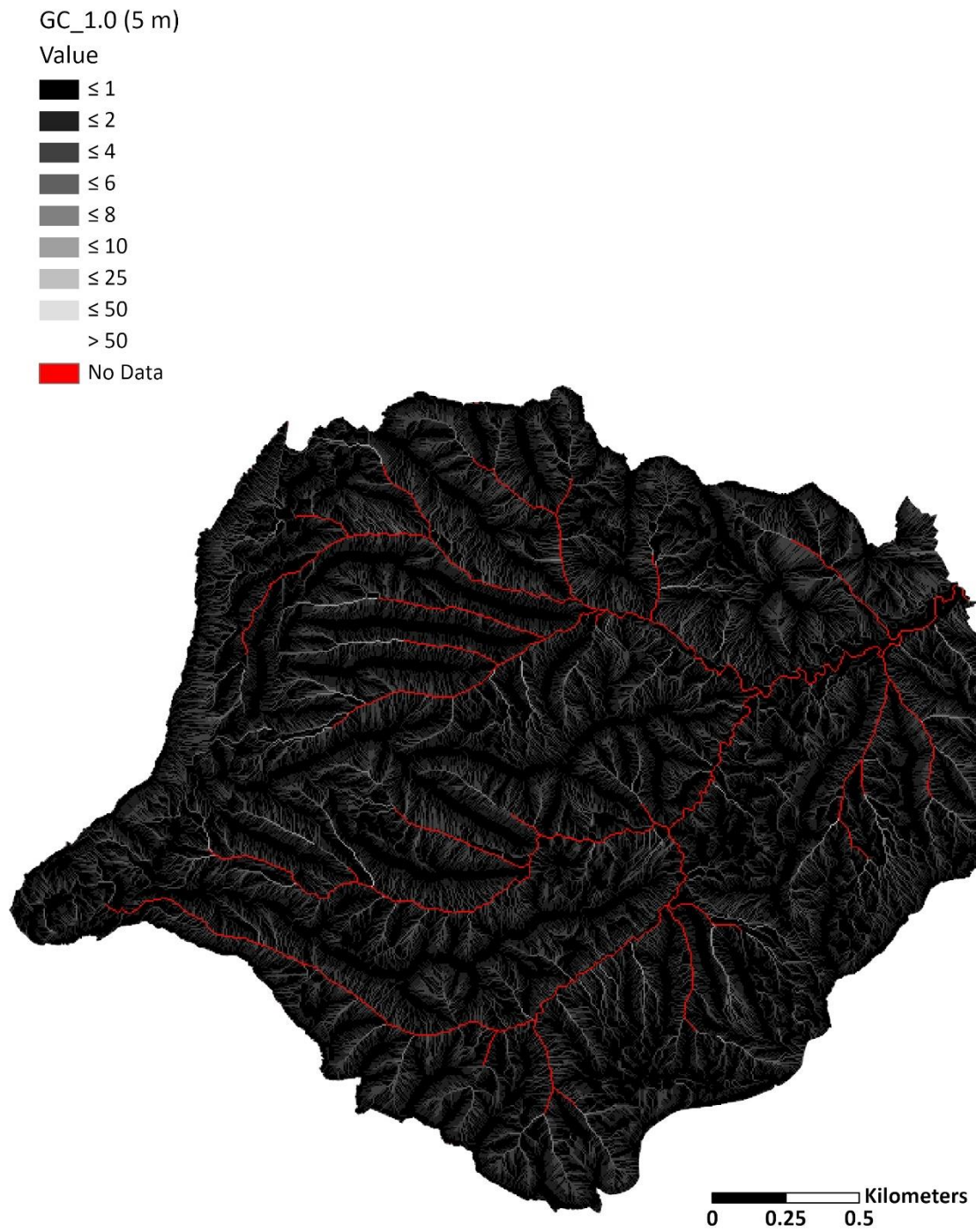


**Figure C6.** L factor with the GC Method without slope cutoff for Site C at 5 m.

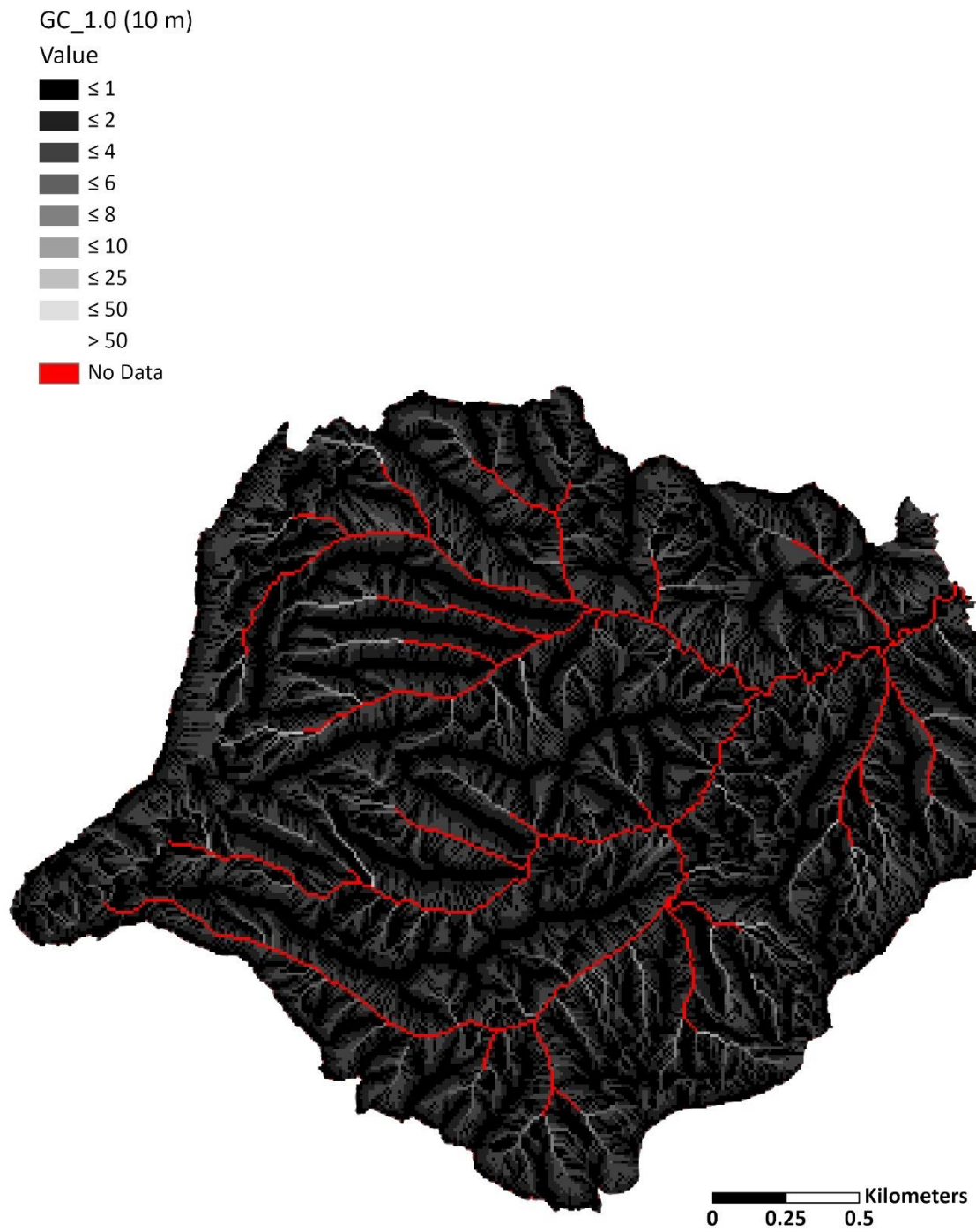


**Figure C7.** L factor with the GC Method without slope cutoff for Site C at 10 m.

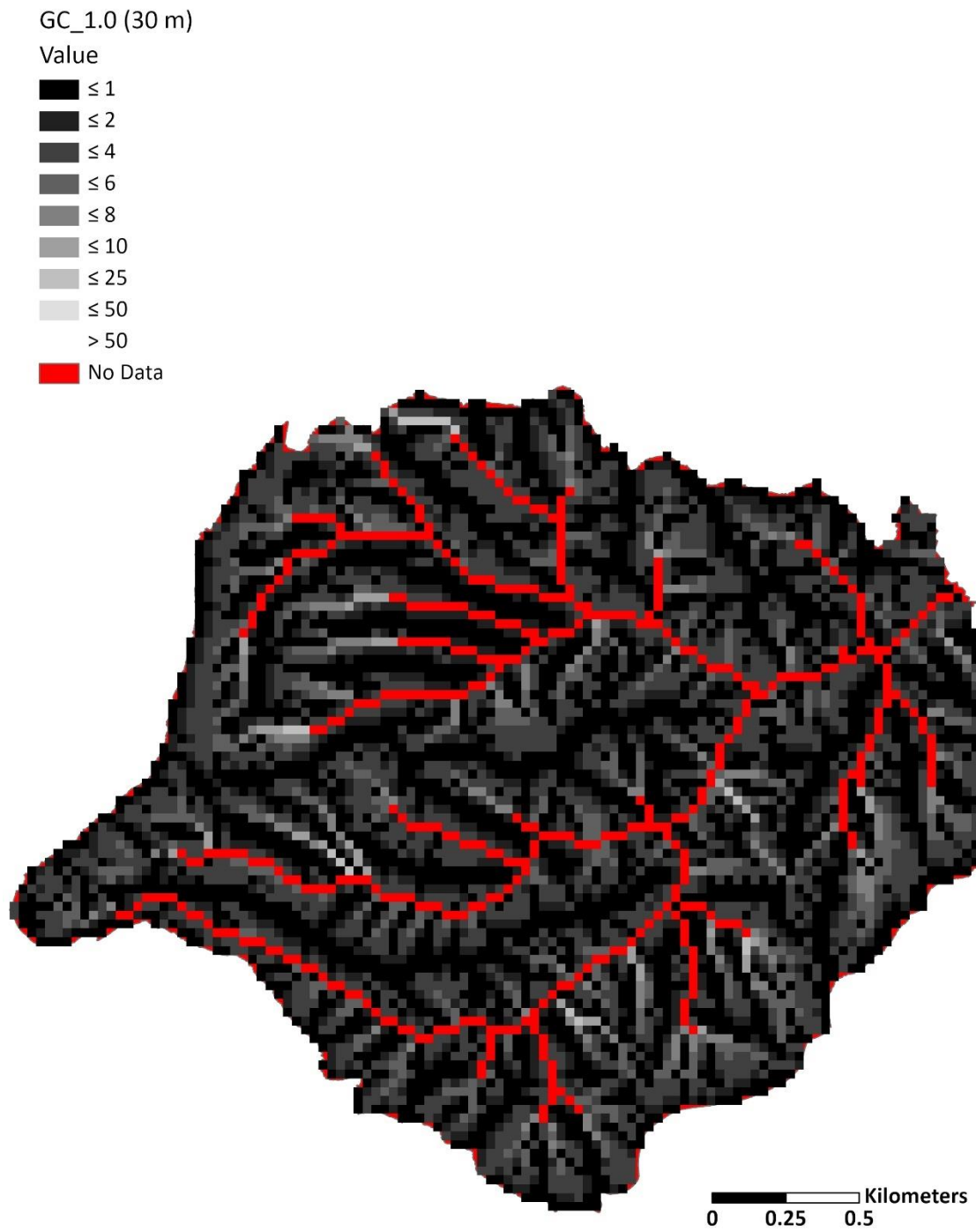


**Figure C8.** L factor with the GC Method without slope cutoff for Site C at 30 m.

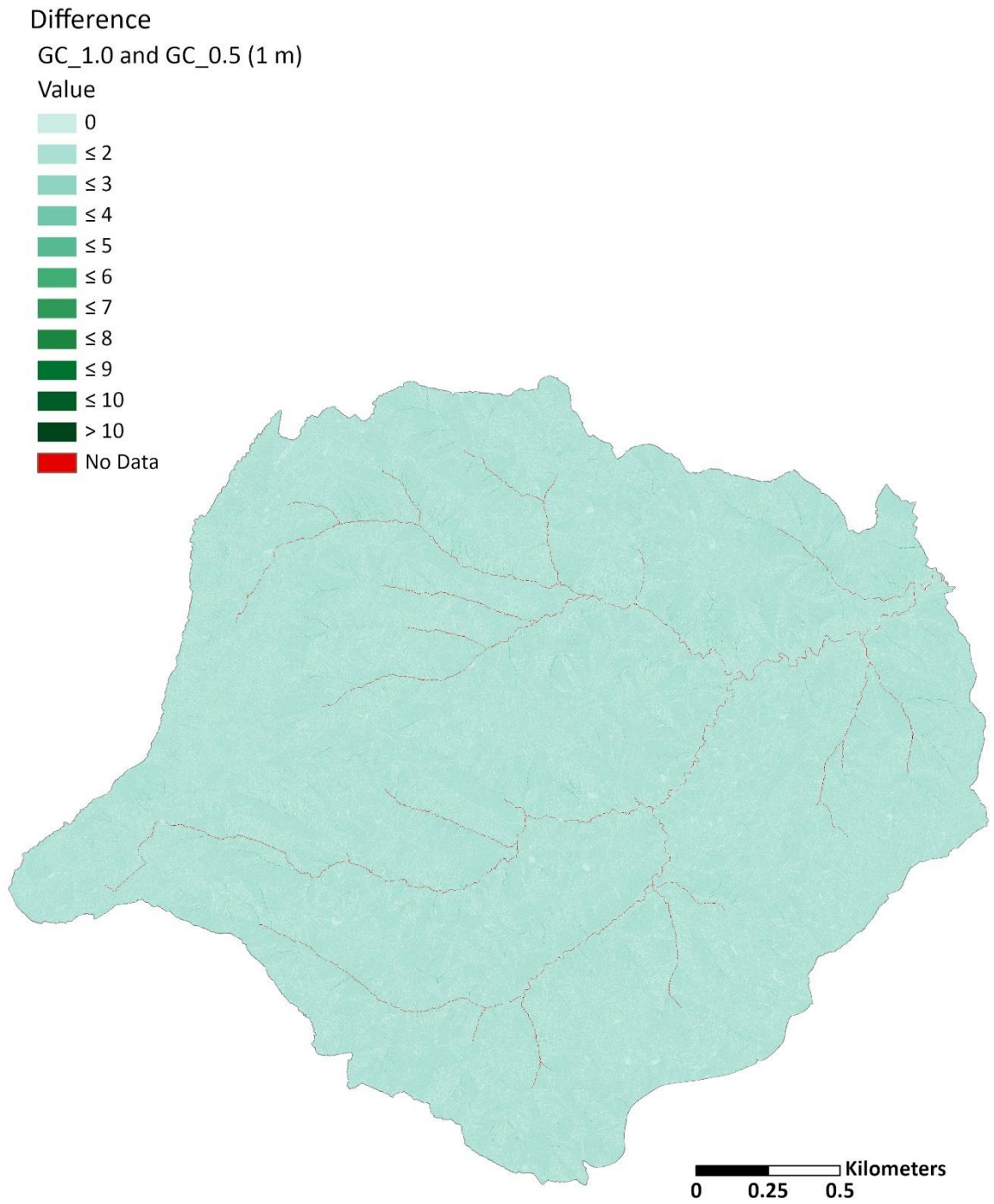


**Figure C9.** Site C difference raster (1 m) for the L Factor of the GC method with slope cutoff (GC\_0.5) subtracted from the GC method without slope cutoff (GC\_1.0).

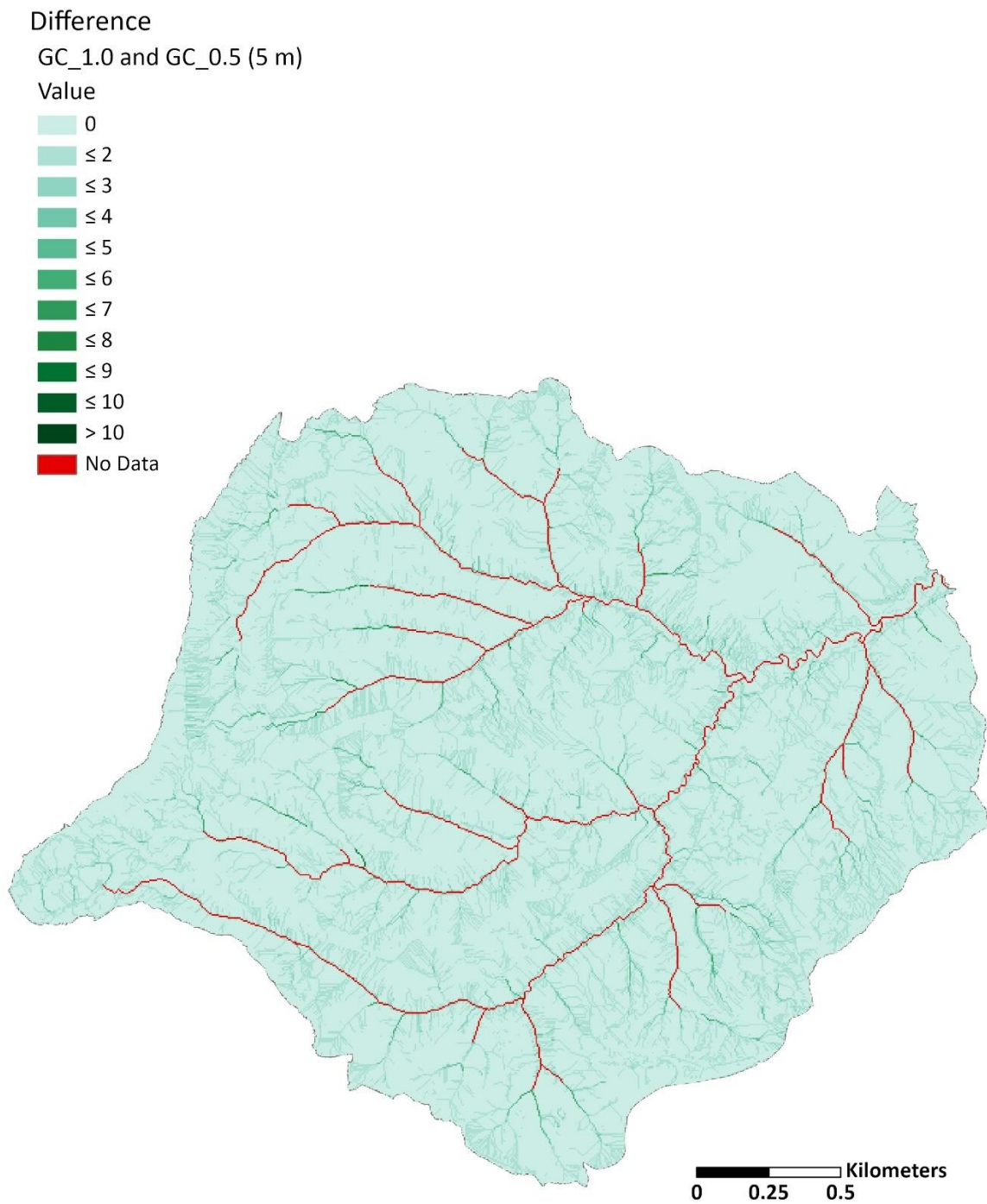


**Figure C10.** Site C difference raster (5 m) for the L Factor of the GC method with slope cutoff (GC\_0.5) subtracted from the GC method without slope cutoff (GC\_1.0).

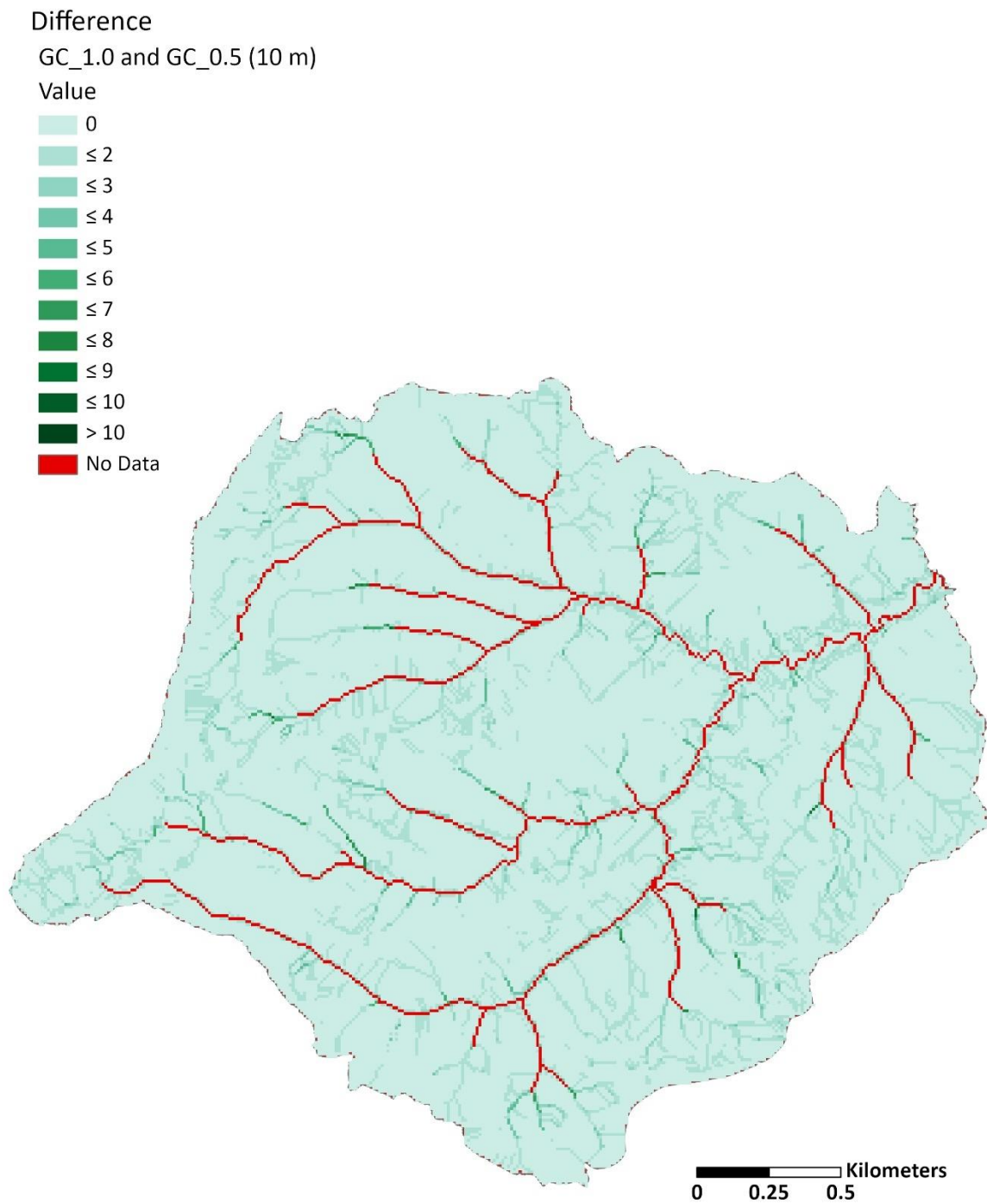


**Figure C11.** Site C difference raster (10 m) for the L Factor of the GC method with slope cutoff (GC\_0.5) subtracted from the GC method without slope cutoff (GC\_1.0).

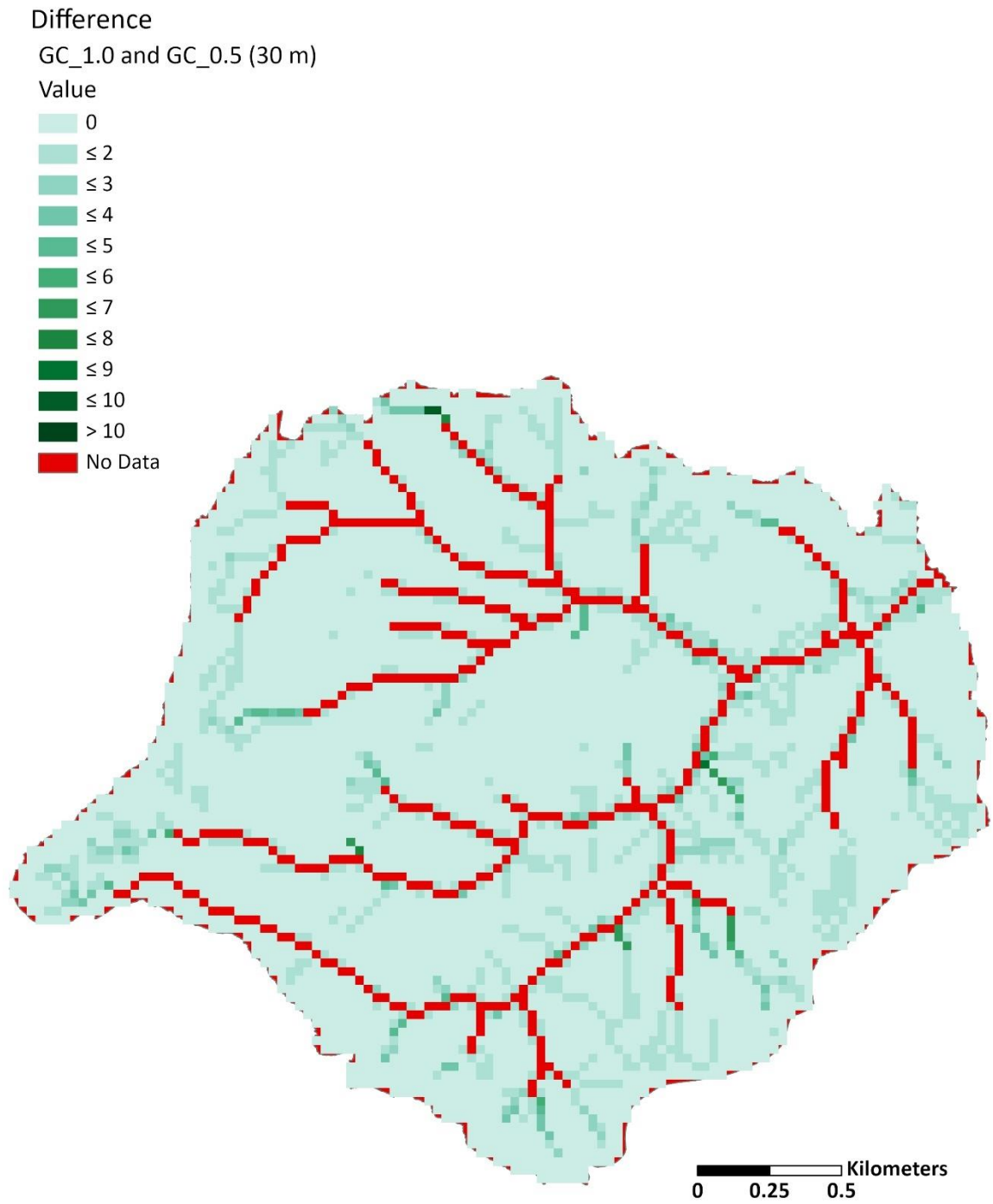


**Figure C12.** Site C difference raster (30 m) for the L Factor of the GC method with slope cutoff (GC\_0.5) subtracted from the GC method without slope cutoff (GC\_1.0).

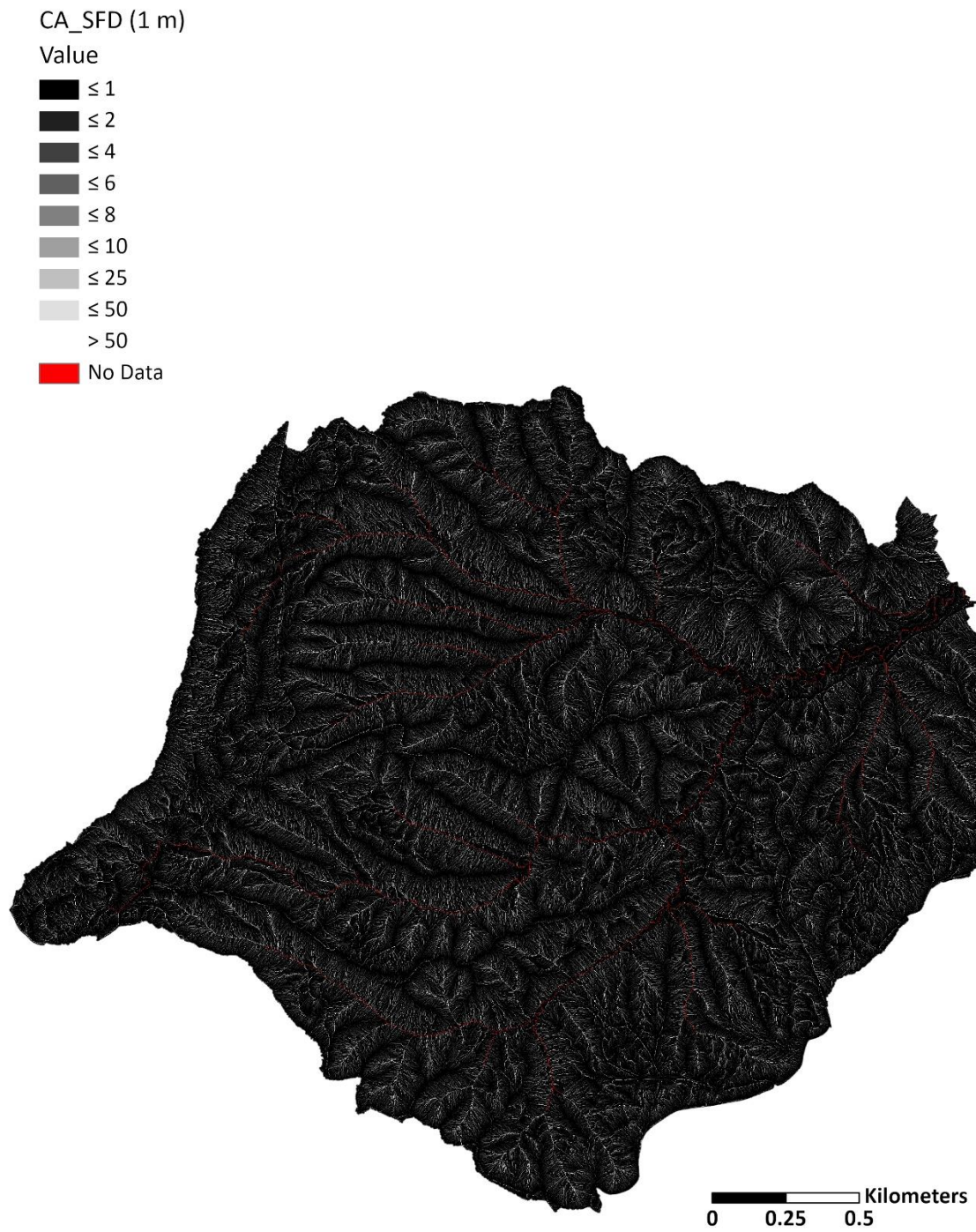


**Figure C13.** L factor with the CA method with a SFD algorithm for Site C at 1 m.

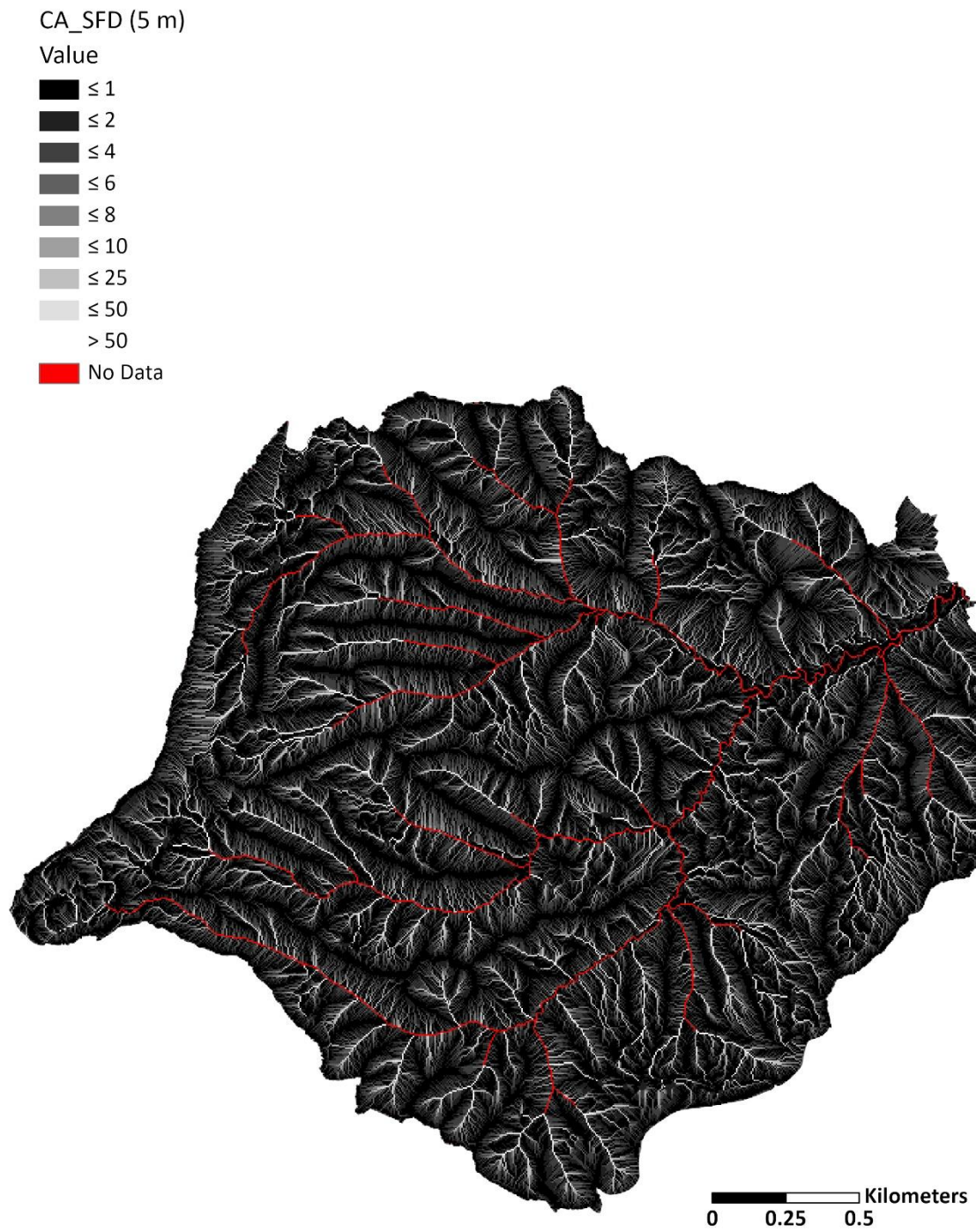


**Figure C14.** L factor with the CA method with a SFD algorithm for Site C at 5 m.

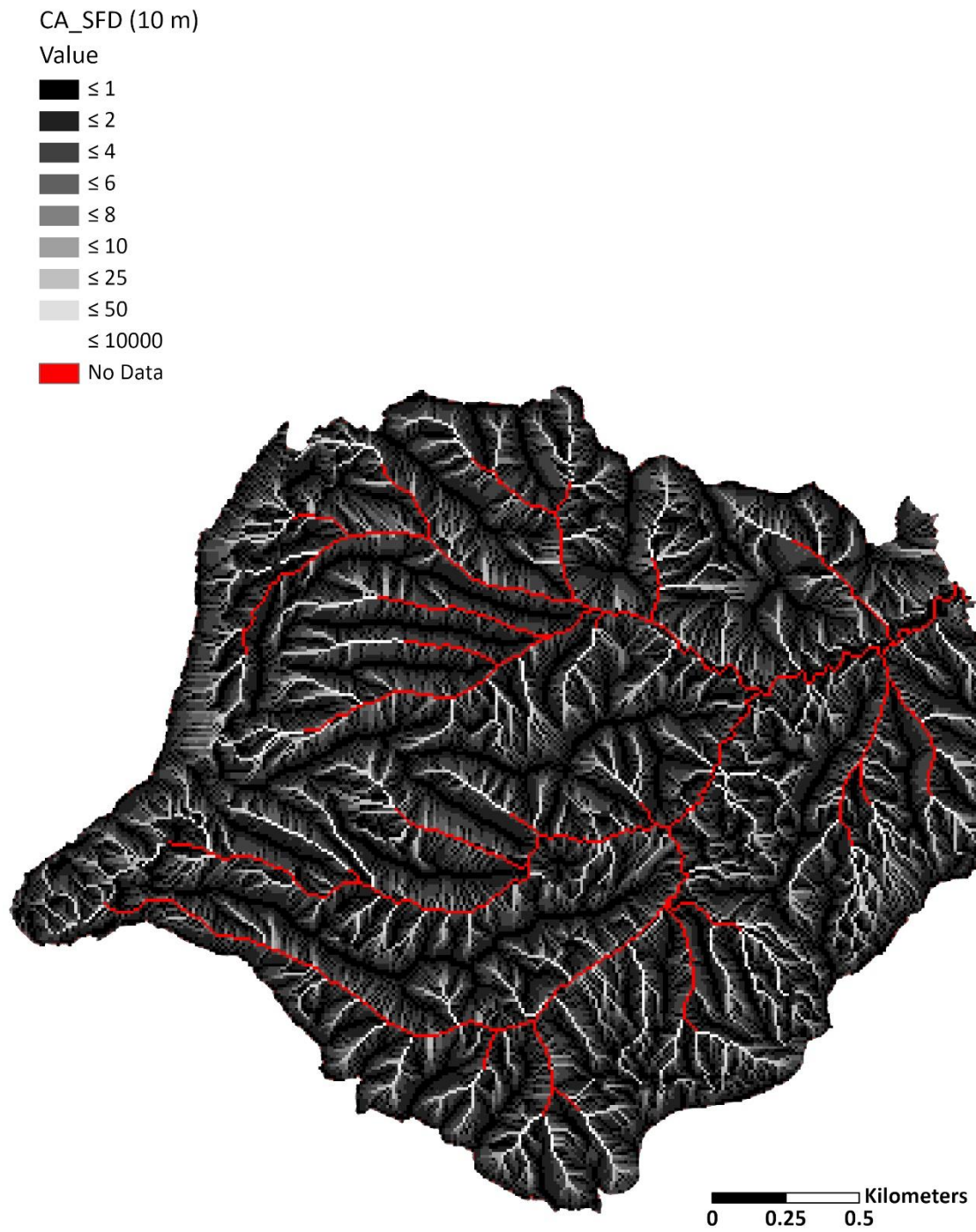


**Figure C15.** L factor with the CA method with a SFD algorithm for Site C at 10 m.

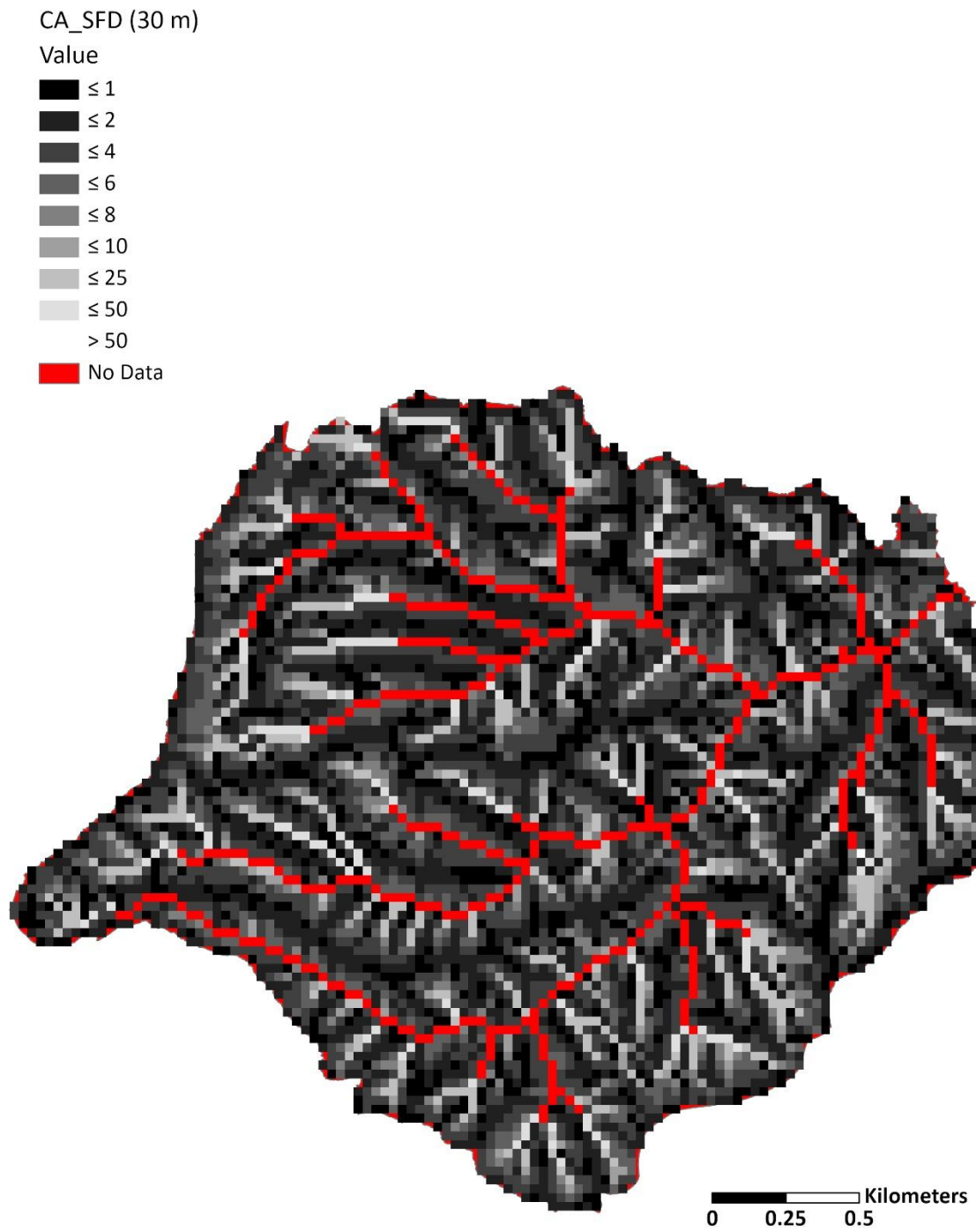


**Figure C16.** L factor with the CA method with a SFD algorithm for Site C at 30 m.

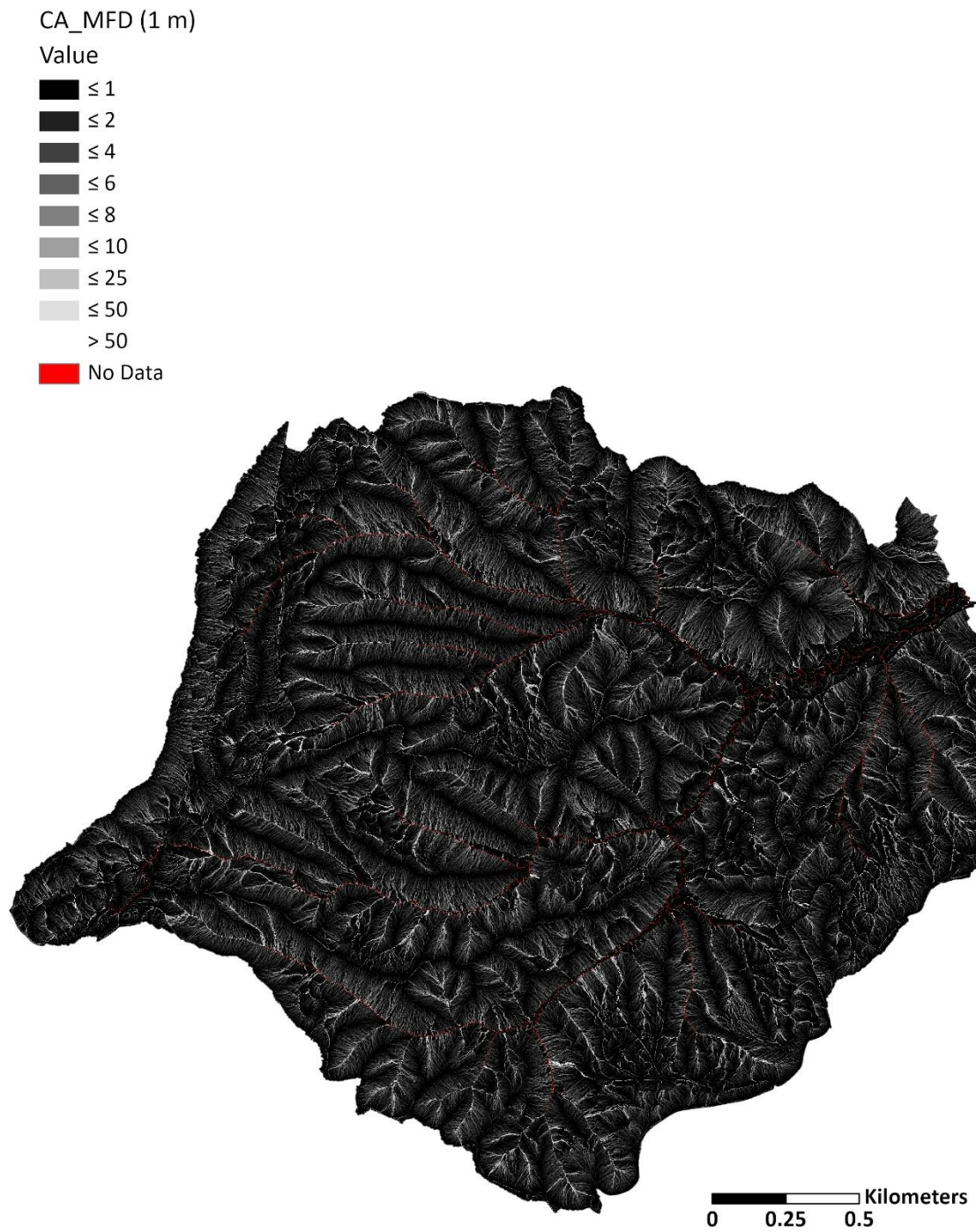


**Figure C17.** L factor with the CA method with a MFD algorithm for Site C at 1 m.

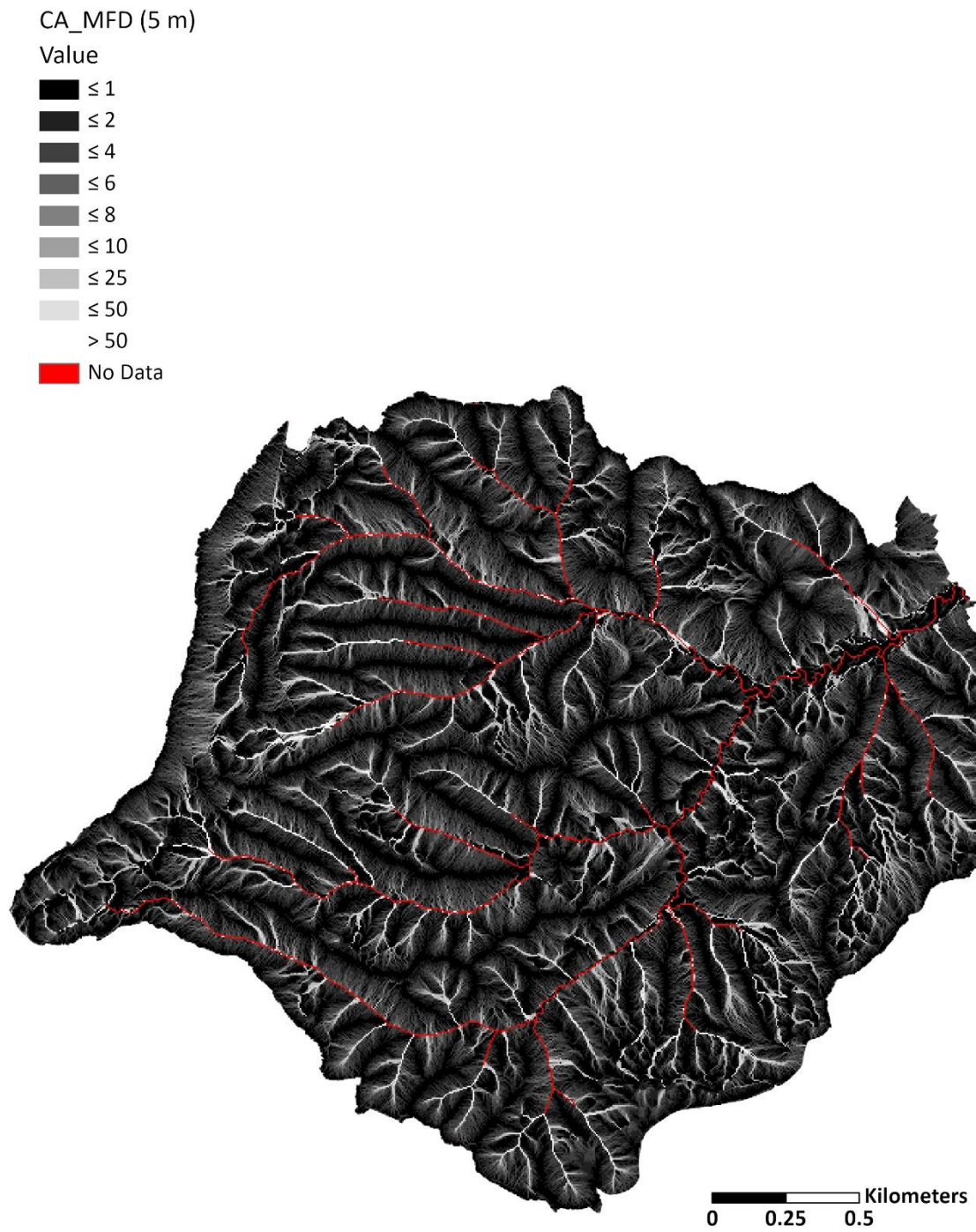


**Figure C18.** L factor with the CA method with a MFD algorithm for Site C at 5 m.

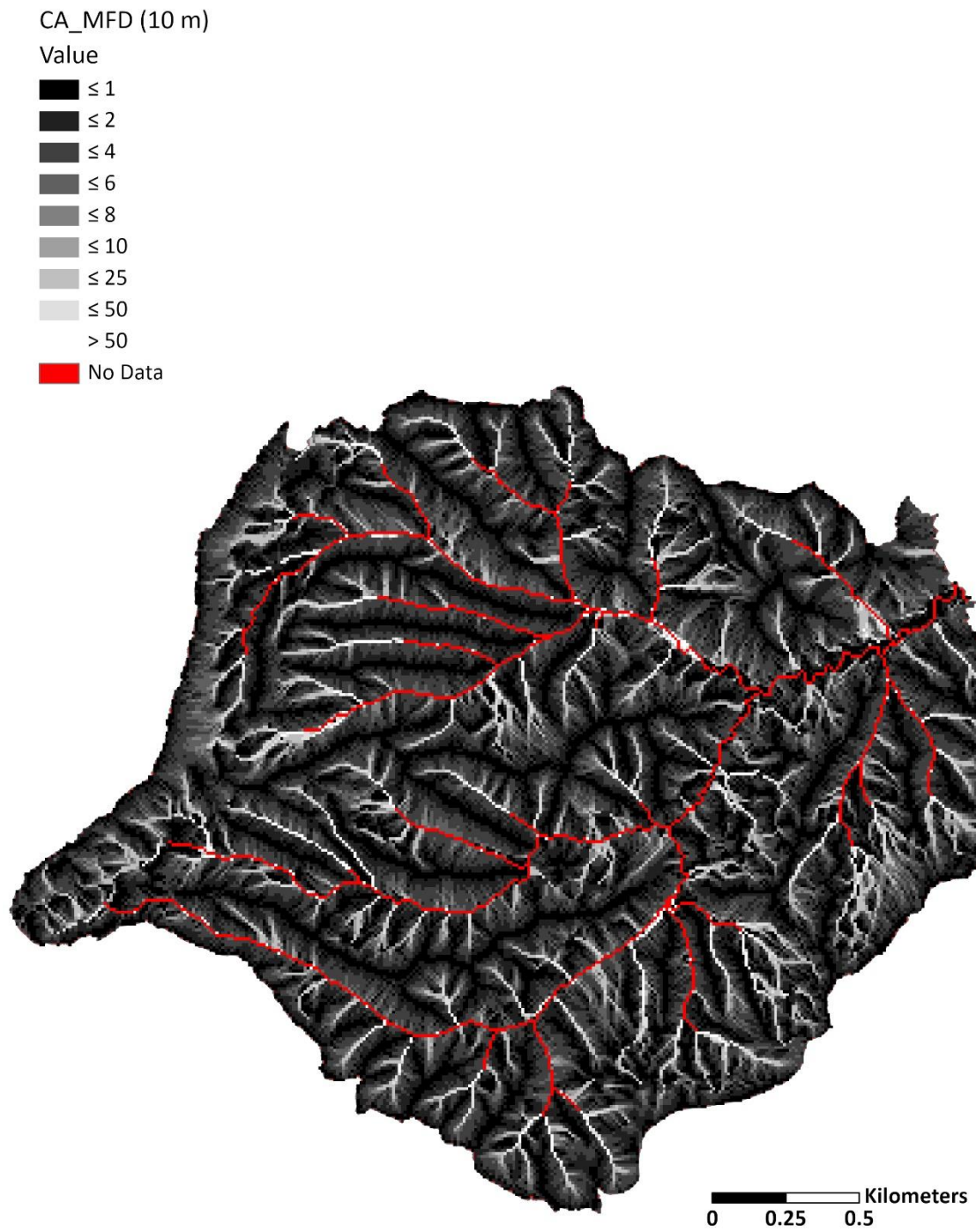


**Figure C19.** L factor with the CA method with a MFD algorithm for Site C at 10 m.

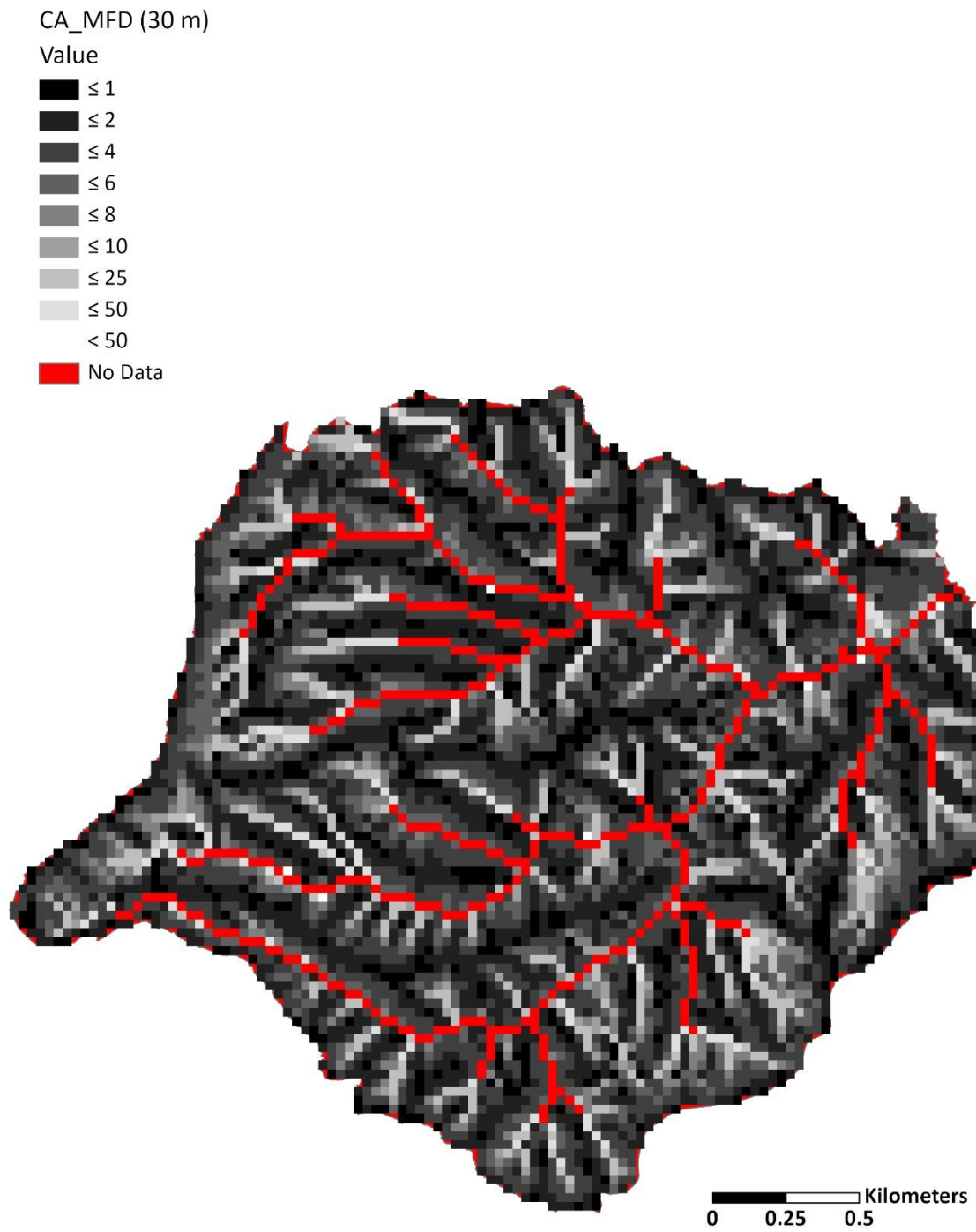


**Figure C20.** L factor with the CA method with a MFD algorithm for Site C at 30 m.

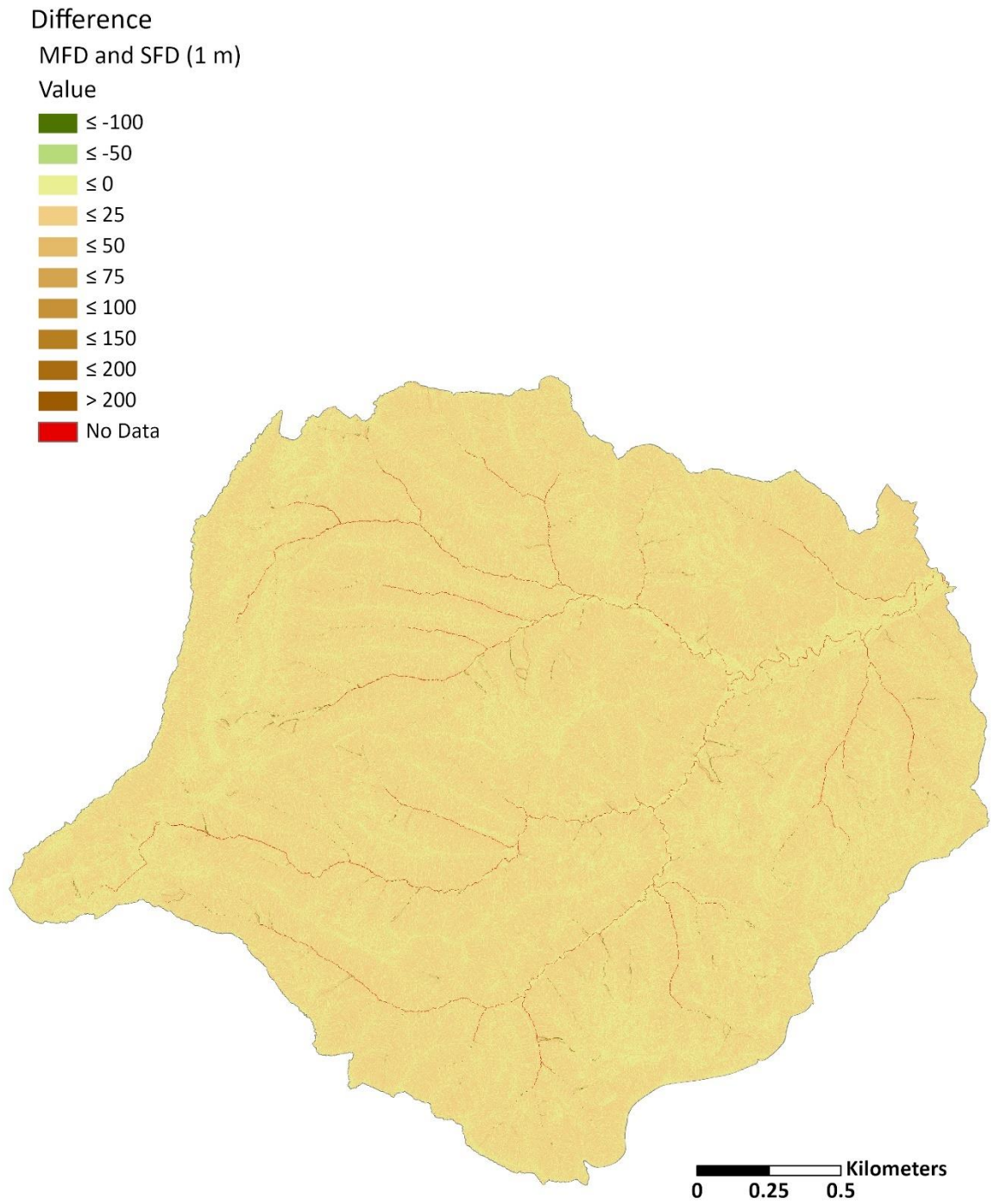


**Figure C21.** Site C difference raster (1 m) for the L Factor of the CA method using a SFD algorithm (SFD) subtracted from the CA method using a MFD algorithm (MFD).

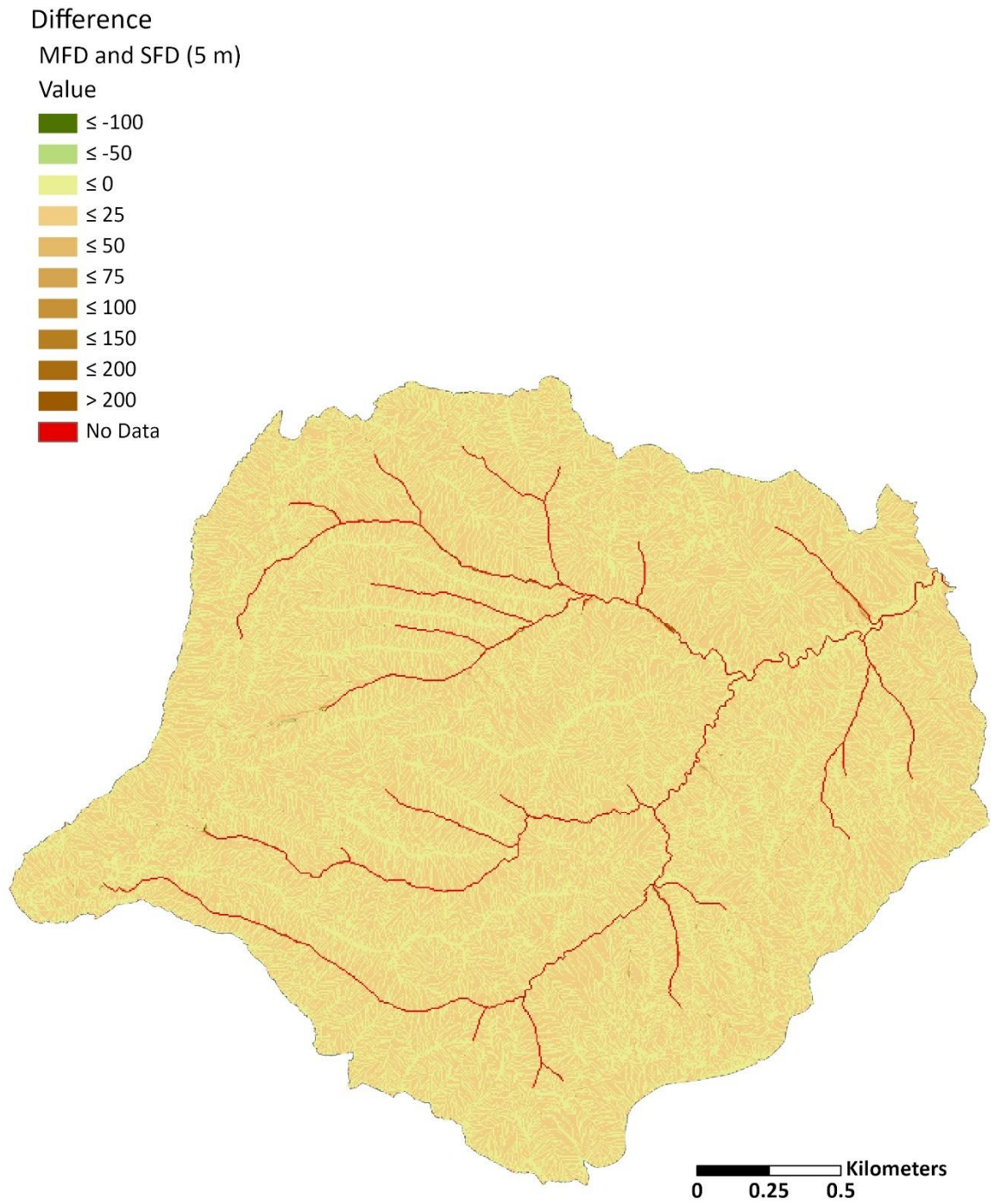


**Figure C22.** Site C difference raster (5 m) for the L Factor of the CA method using a SFD algorithm (SFD) subtracted from the CA method using a MFD algorithm (MFD).

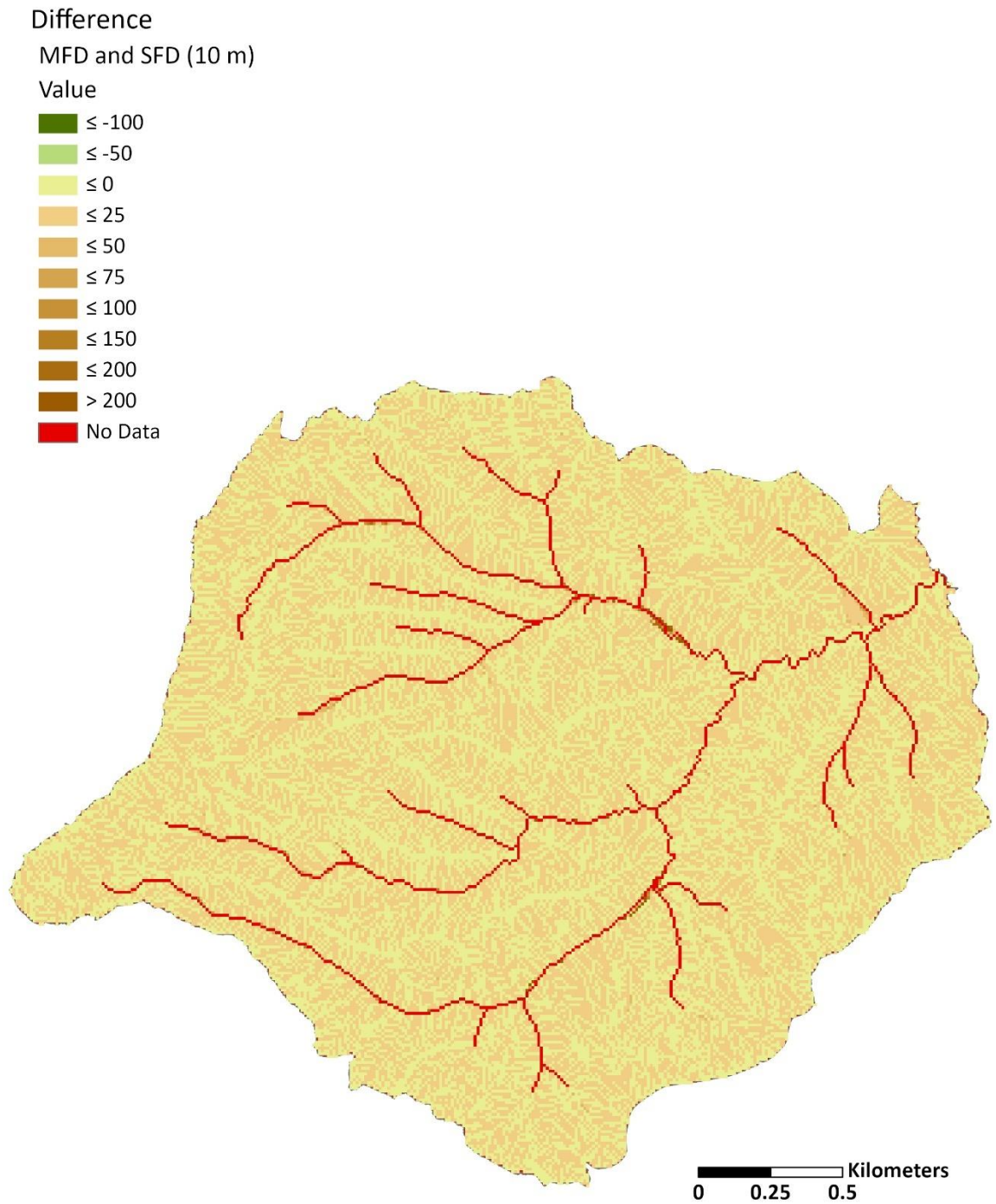


**Figure C23.** Site C difference raster (10 m) for the L Factor of the CA method using a SFD algorithm (SFD) subtracted from the CA method using a MFD algorithm (MFD).

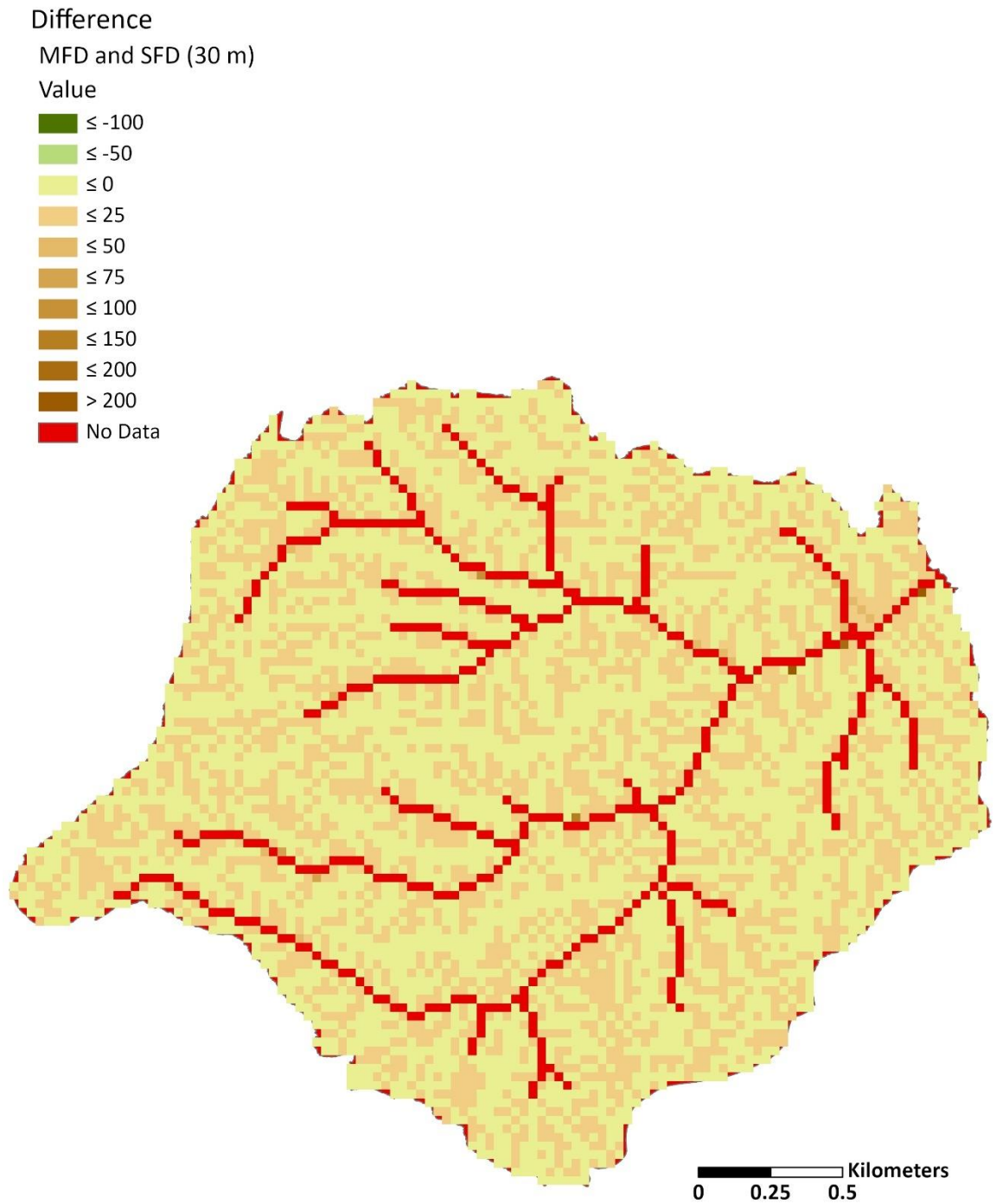


**Figure C24.** Site C difference raster (30 m) for the L Factor of the CA method using a SFD algorithm (SFD) subtracted from the CA method using a MFD algorithm (MFD).

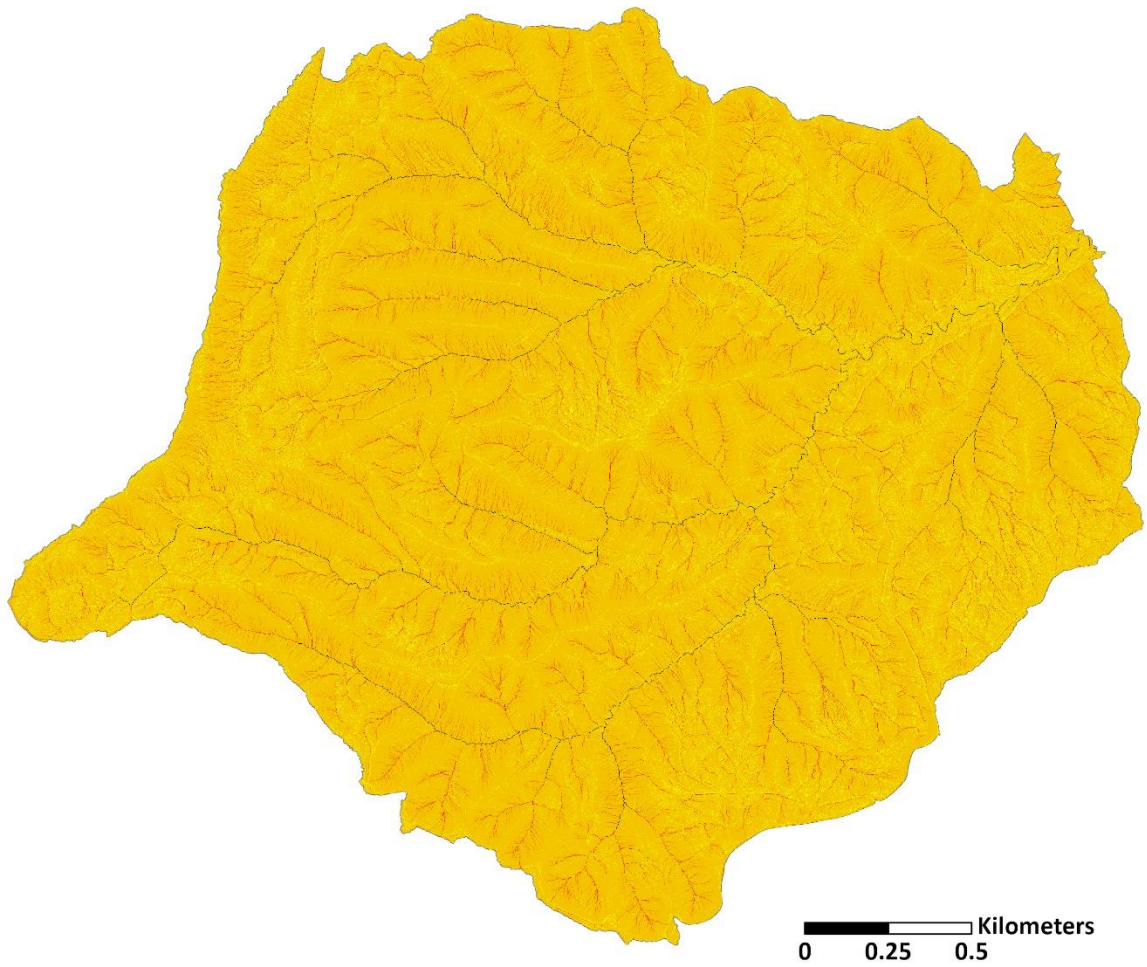
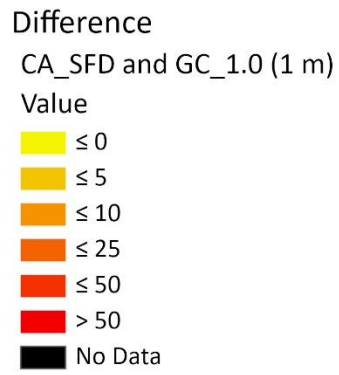


**Figure C25.** Site C difference raster (1 m) for the L Factor of the CA method using a SFD algorithm (CA\_SFD) and the GC method without slope cutoff (GC\_1.0).

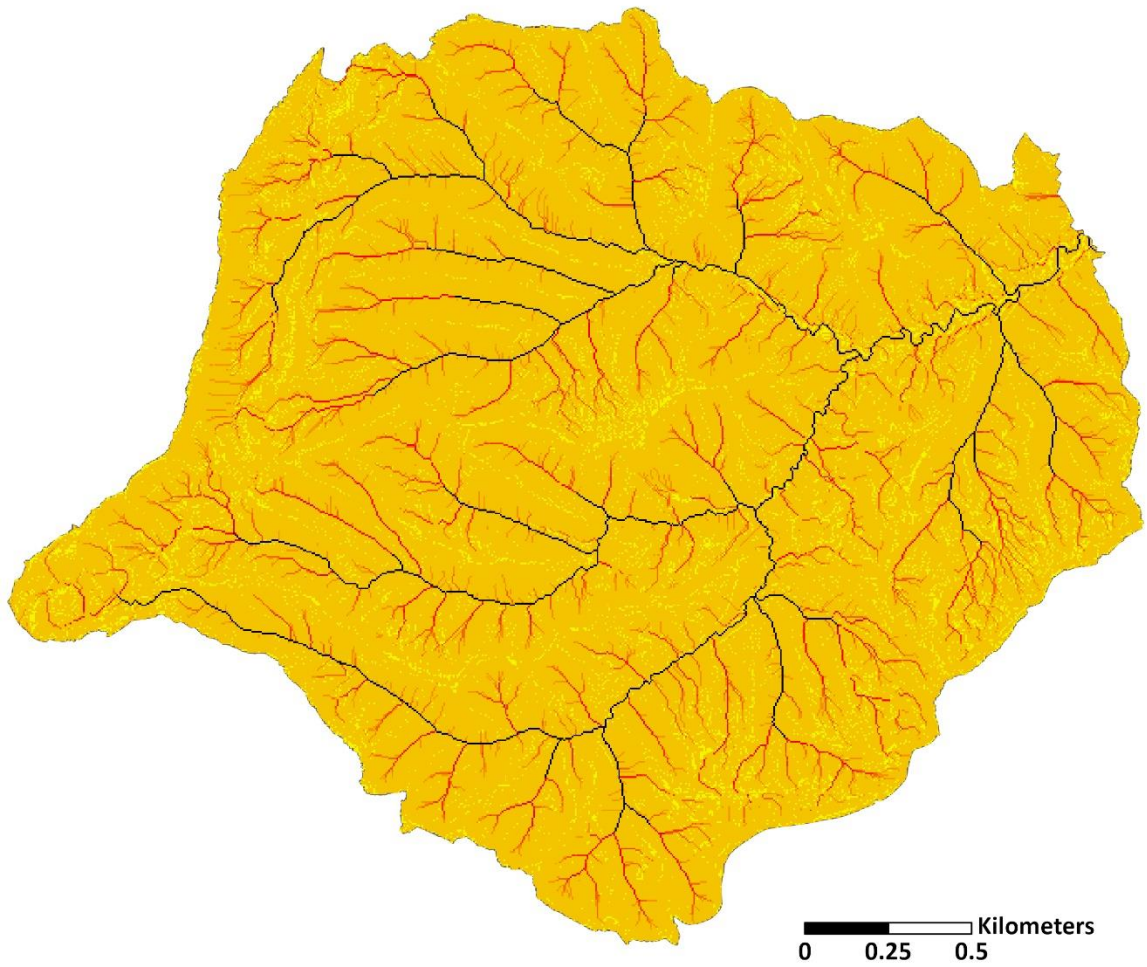
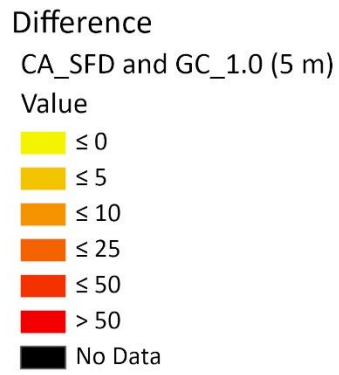


**Figure C26.** Site C difference raster (5 m) for the L Factor of the CA method using a SFD algorithm (CA\_SFD) and the GC method without slope cutoff (GC\_1.0).

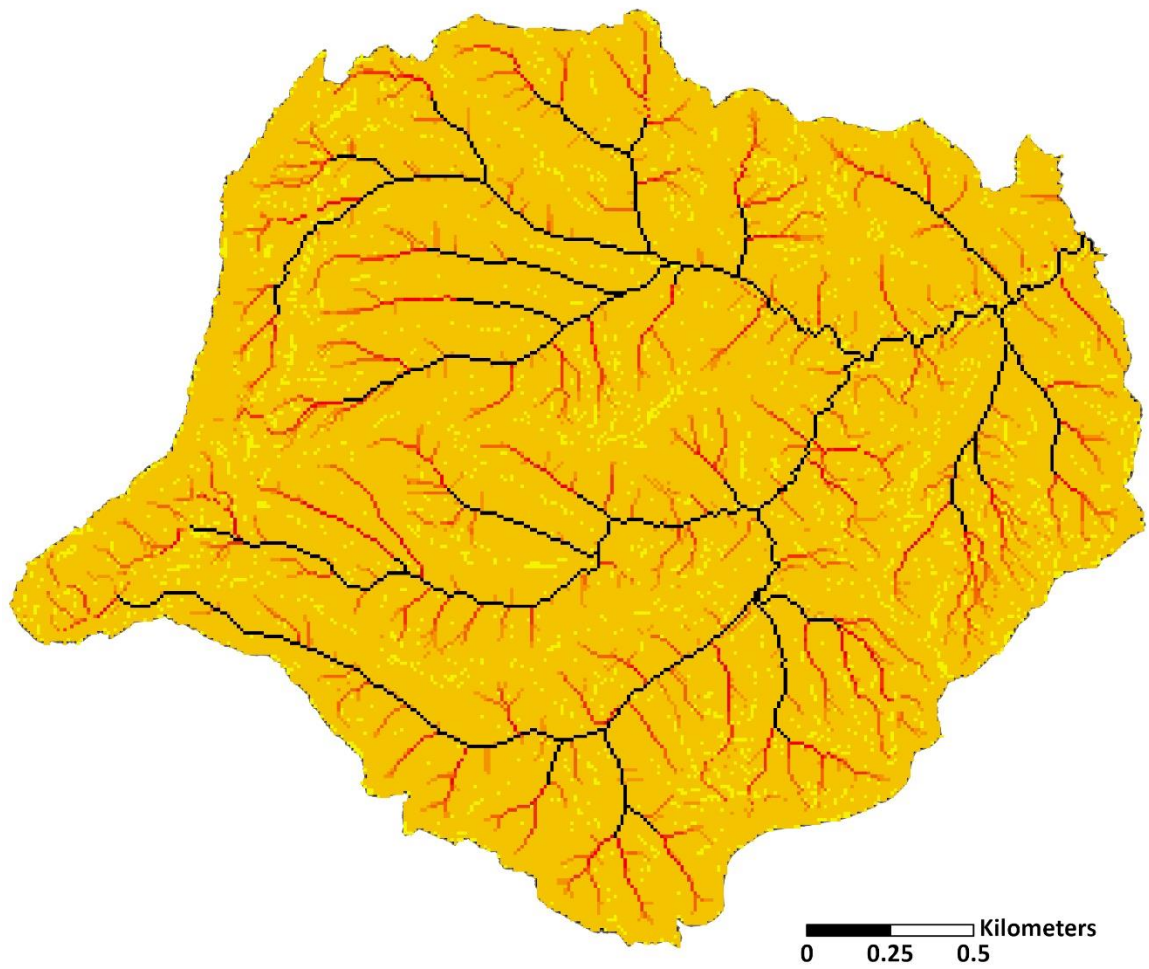
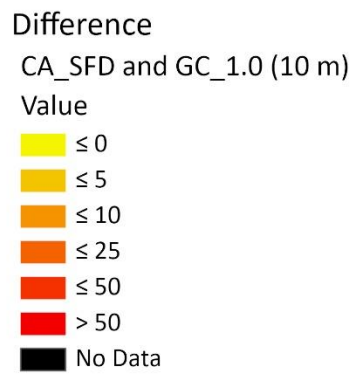


**Figure C27.** Site C difference raster (10 m) for the L Factor of the CA method using a SFD algorithm (CA\_SFD) and the GC method without slope cutoff (GC\_1.0).

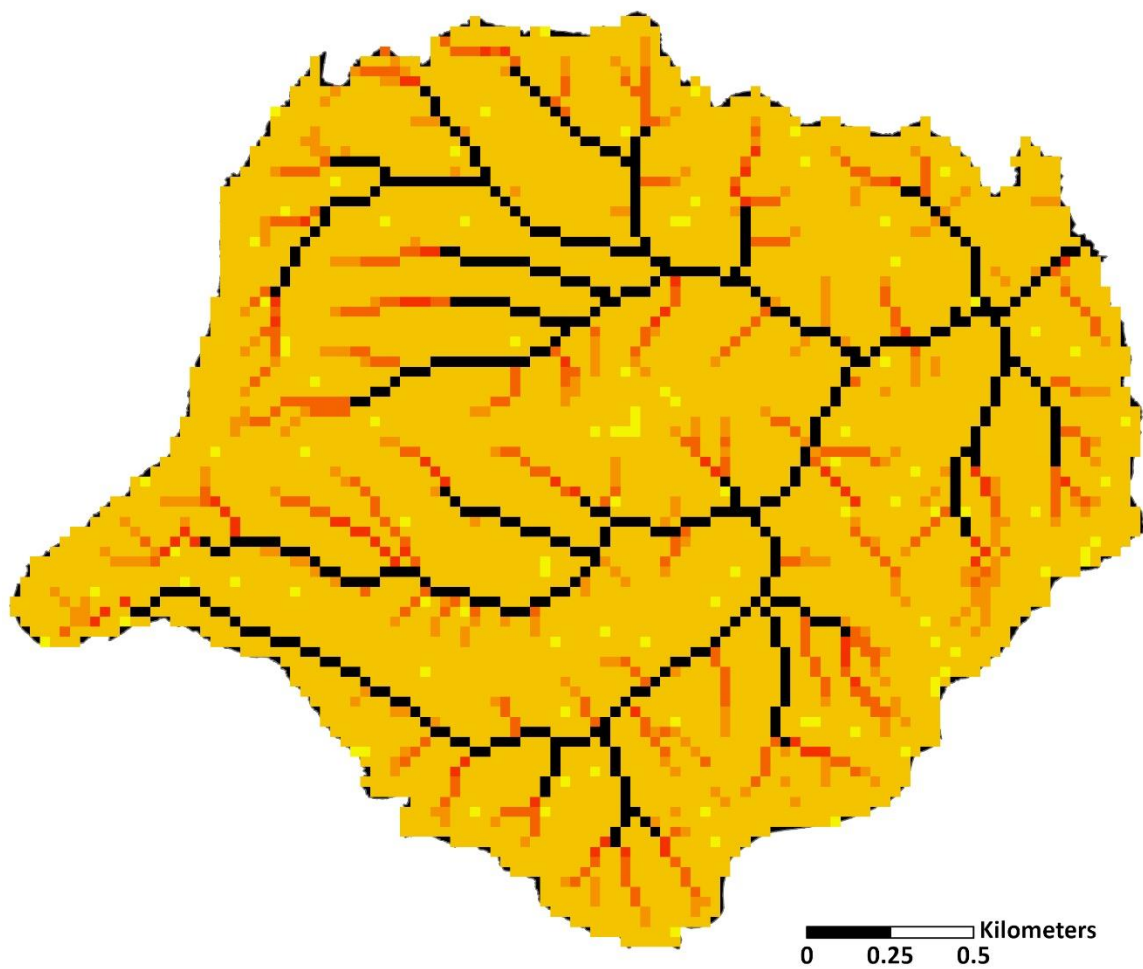
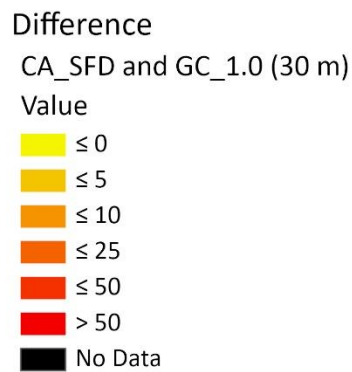


**Figure C28.** Site C difference raster (30 m) for the L Factor of the CA method using a SFD algorithm (CA\_SFD) and the GC method without slope cutoff (GC\_1.0).

MDS (1 m)

Value

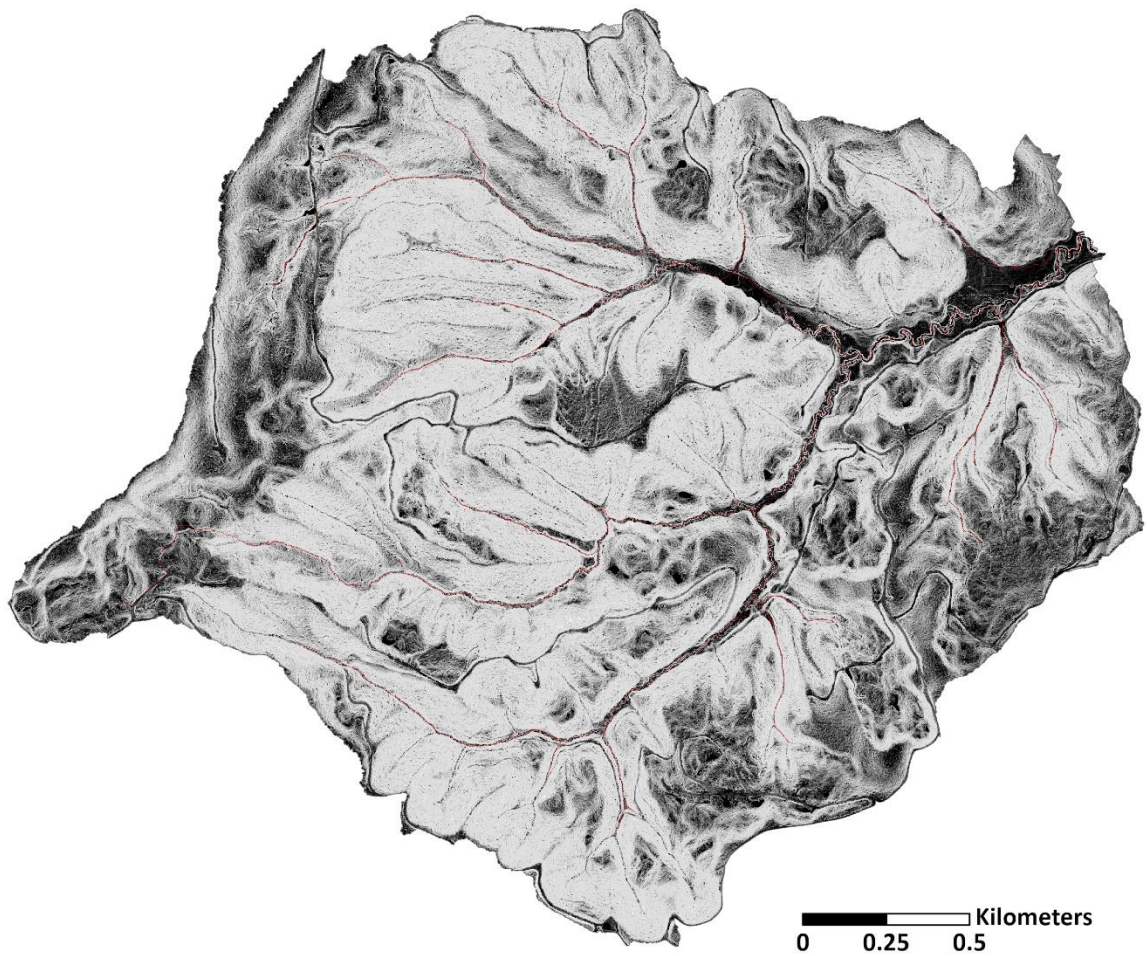
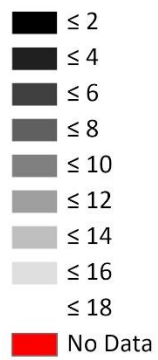


**Figure C29.** S factor with the MDS method for Site C at 1 m.

MDS (5 m)

Value

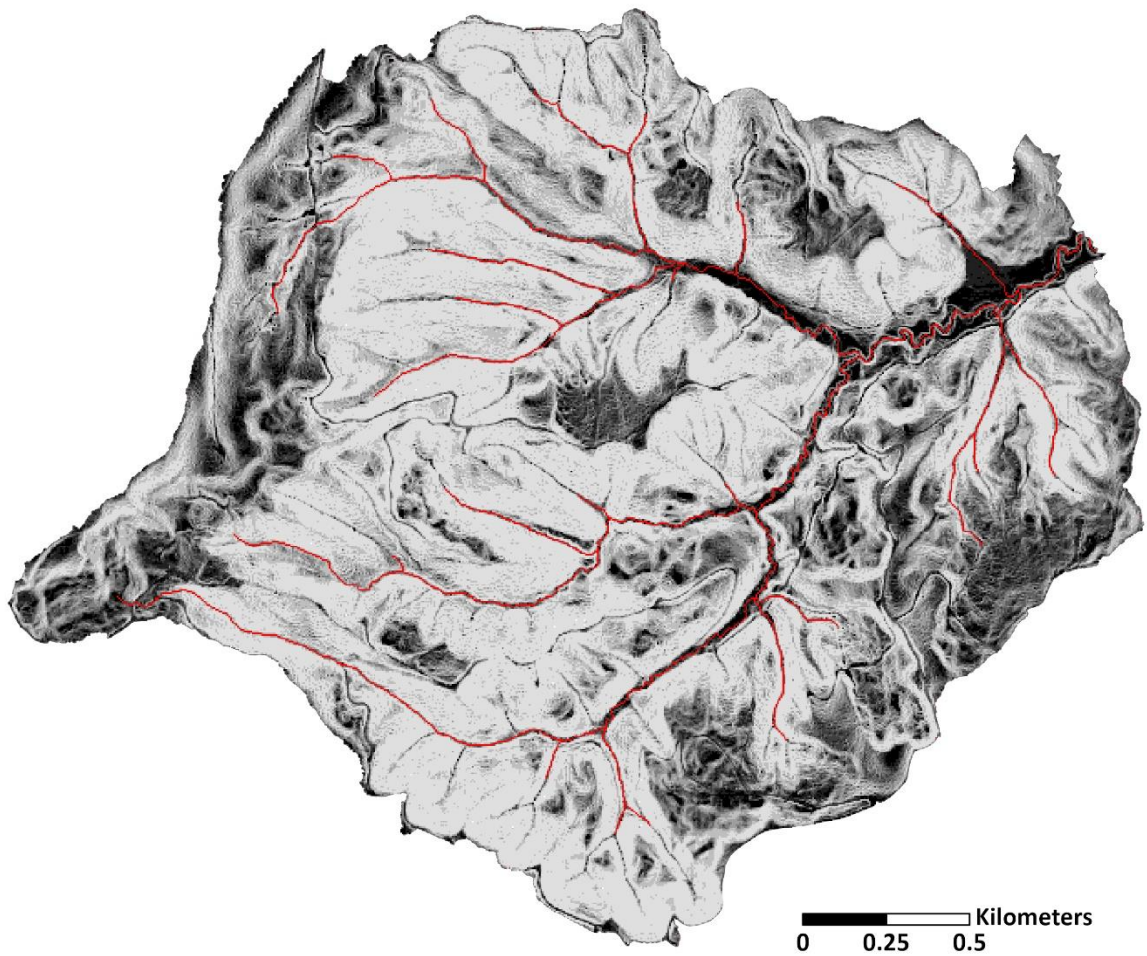
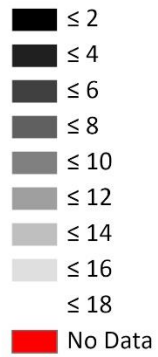


**Figure C30.** S factor with the MDS method for Site C at 5 m.

MDS (10 m)

Value

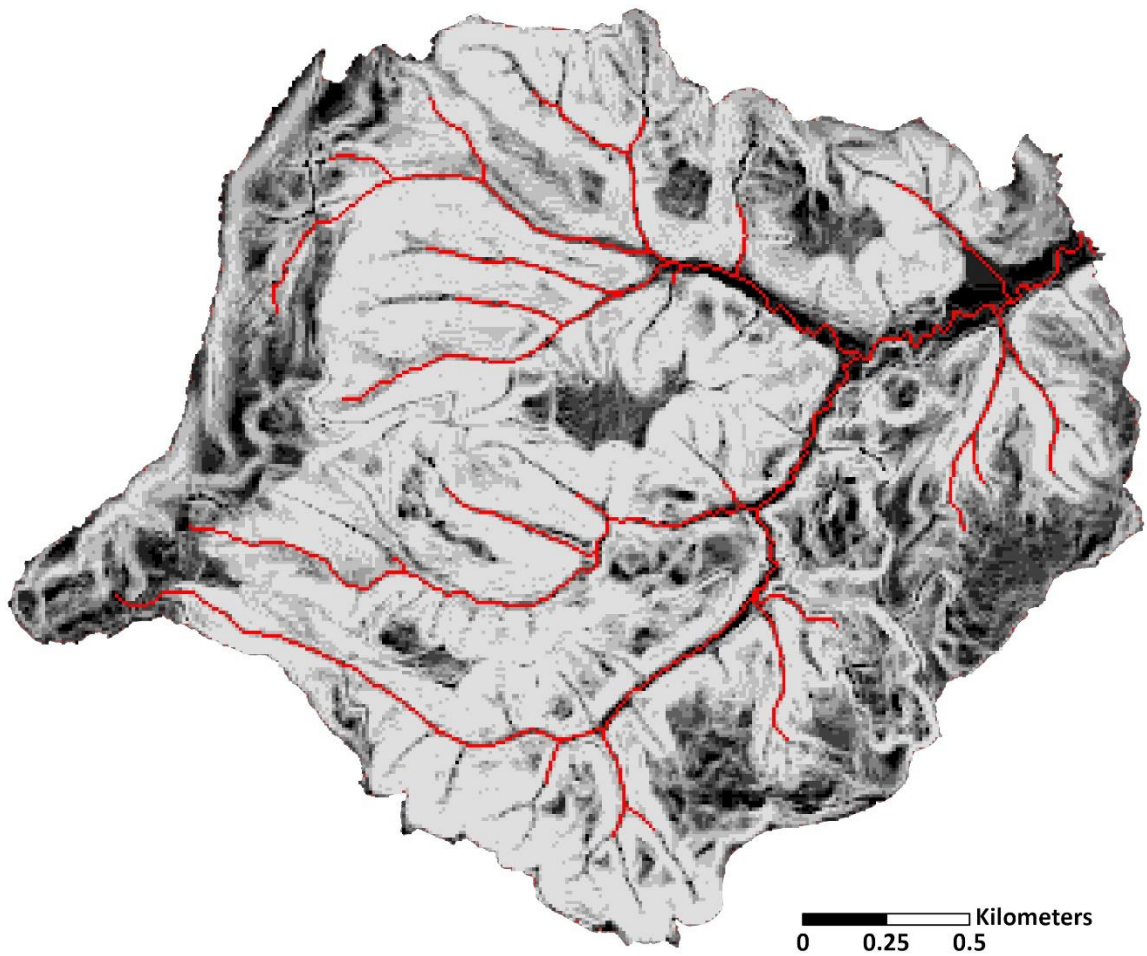
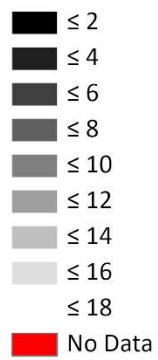


**Figure C31.** S factor with the MDS method for Site C at 10 m.

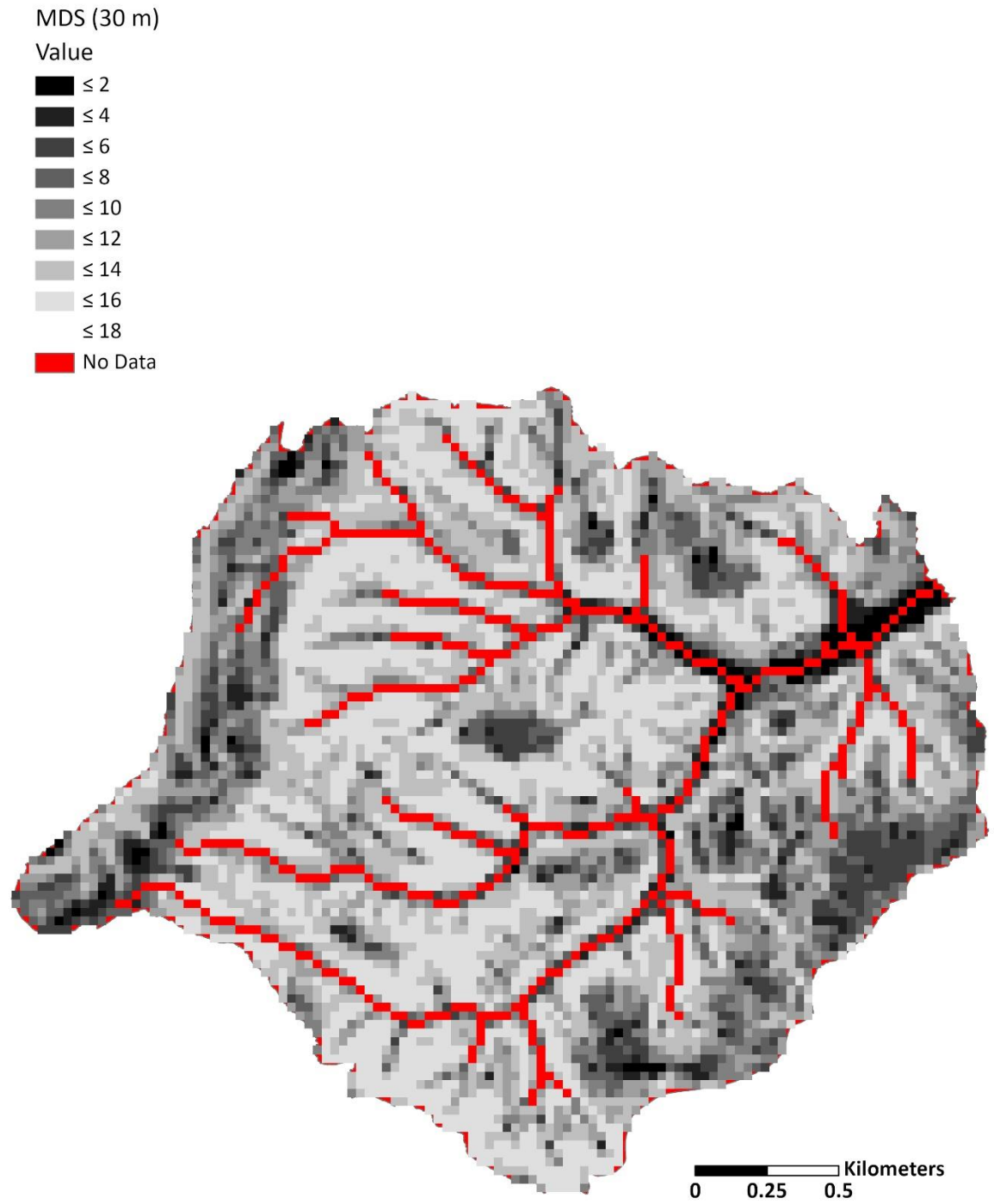


**Figure C32.** S factor with the MDS method for Site C at 30 m.

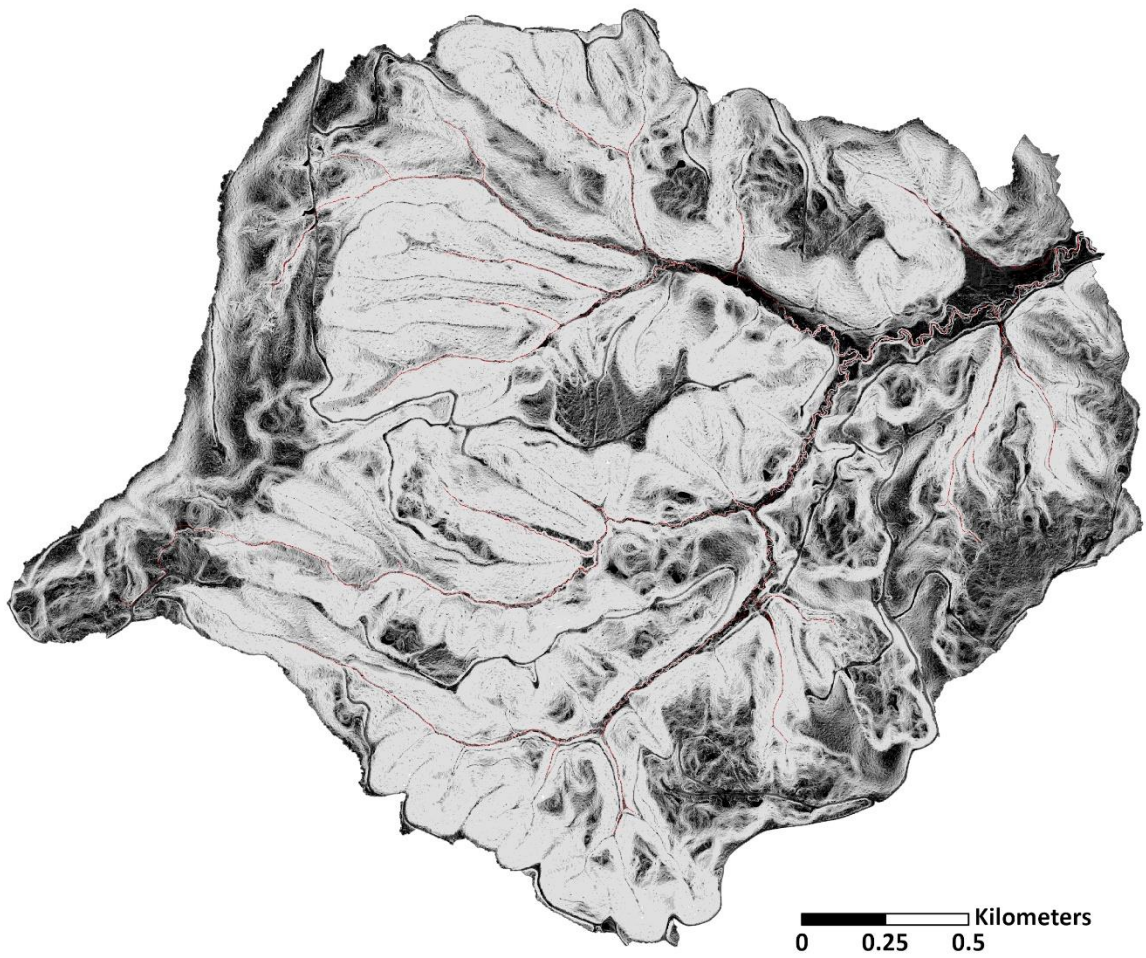
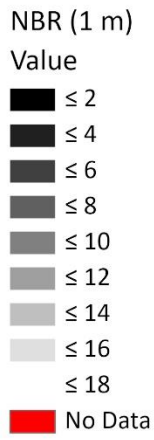


**Figure C33.** S factor with the NBR method for Site C at 1 m.

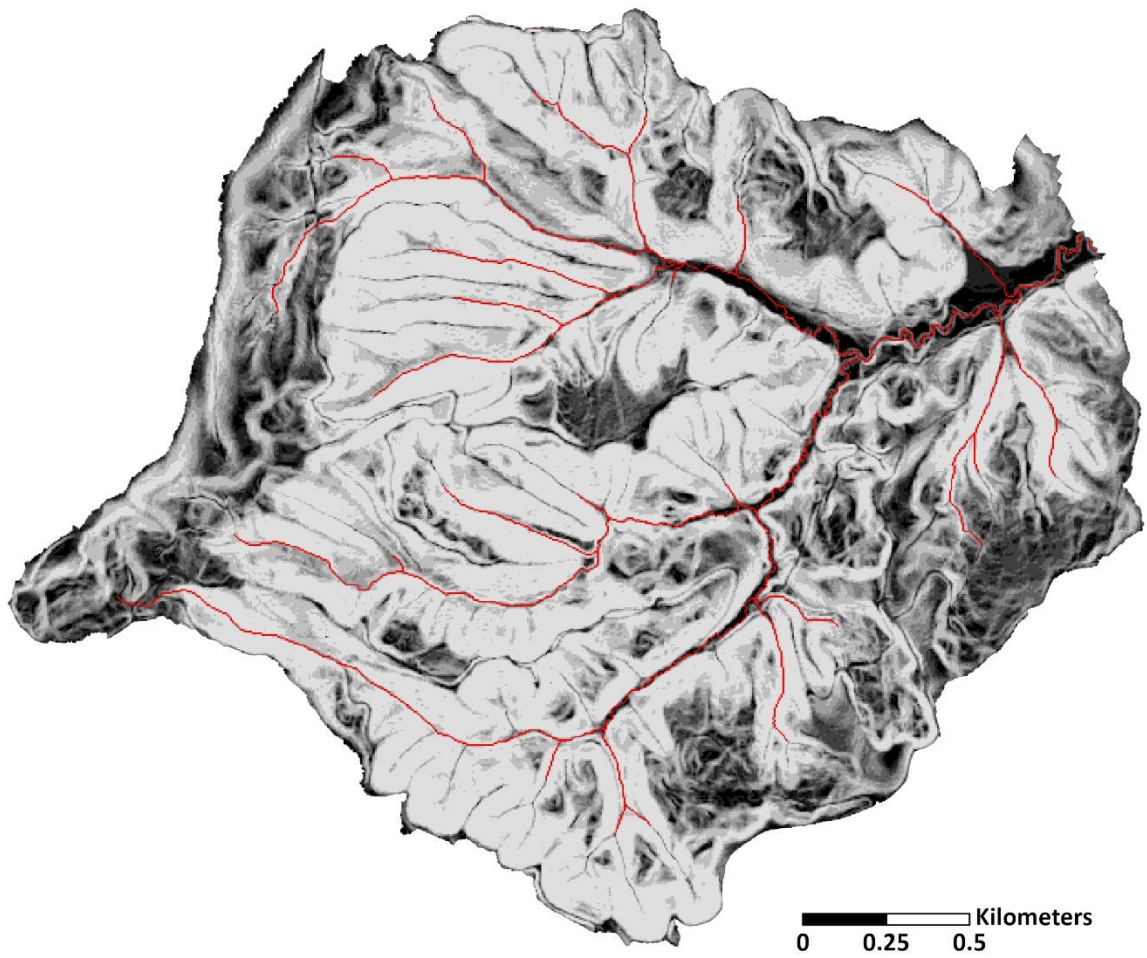
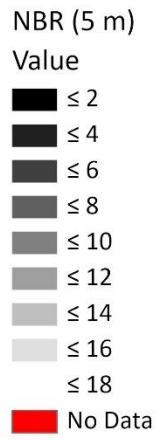


**Figure C34.** S factor with the NBR method for Site C at 5 m.

NBR (10 m)

Value

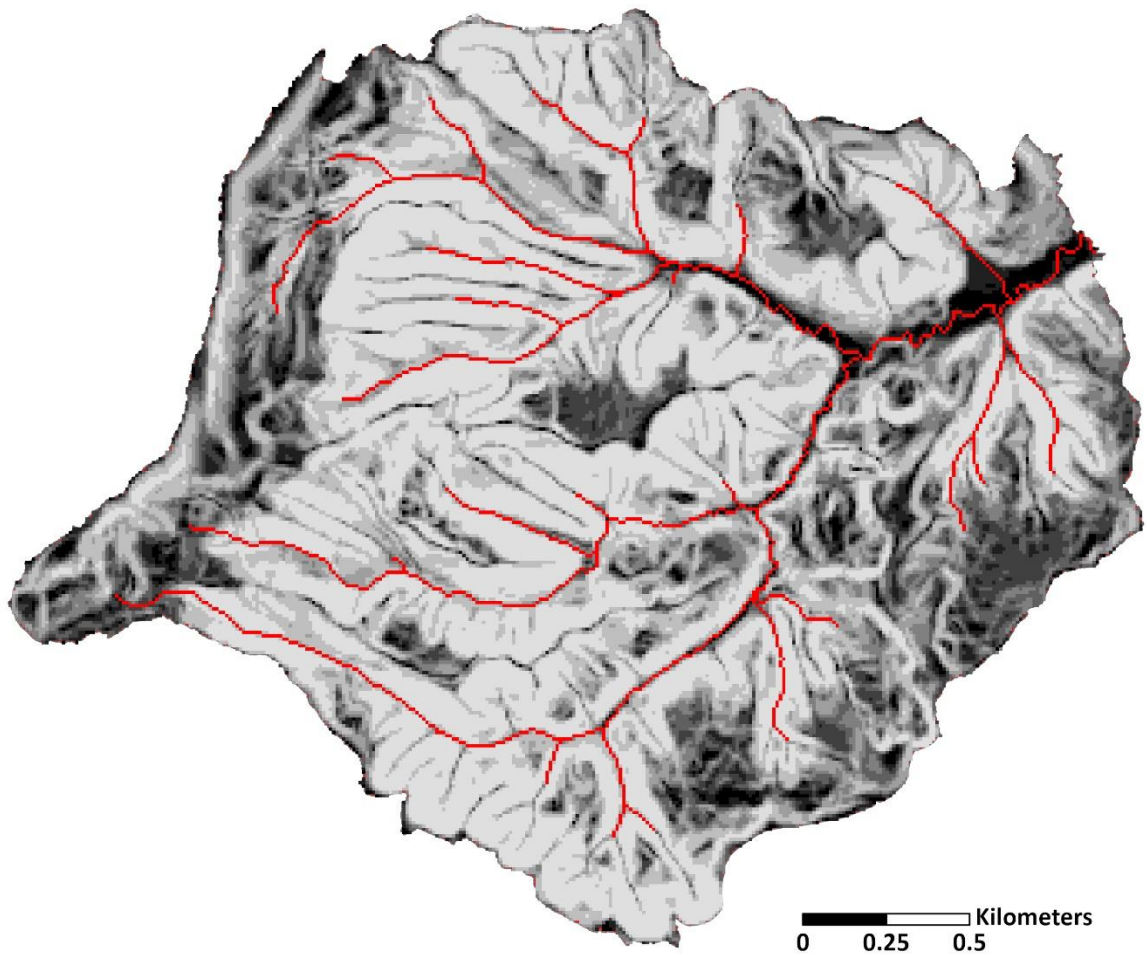
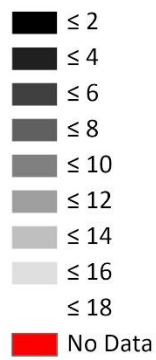


**Figure C35.** S factor with the NBR method for Site C at 10 m.

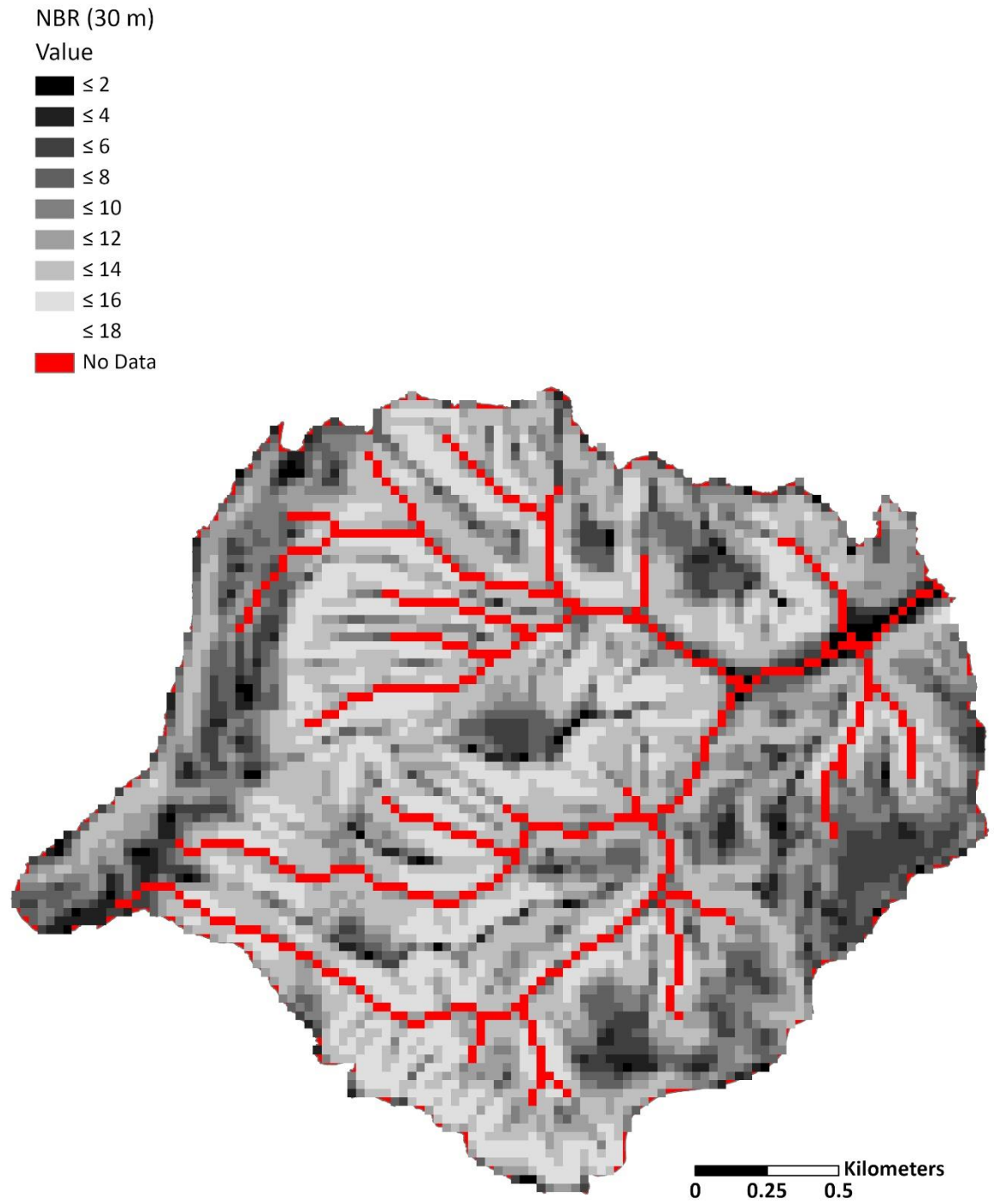


**Figure C36.** S factor with the NBR method for Site C at 30 m.

Difference  
NBR and MDS (1 m)

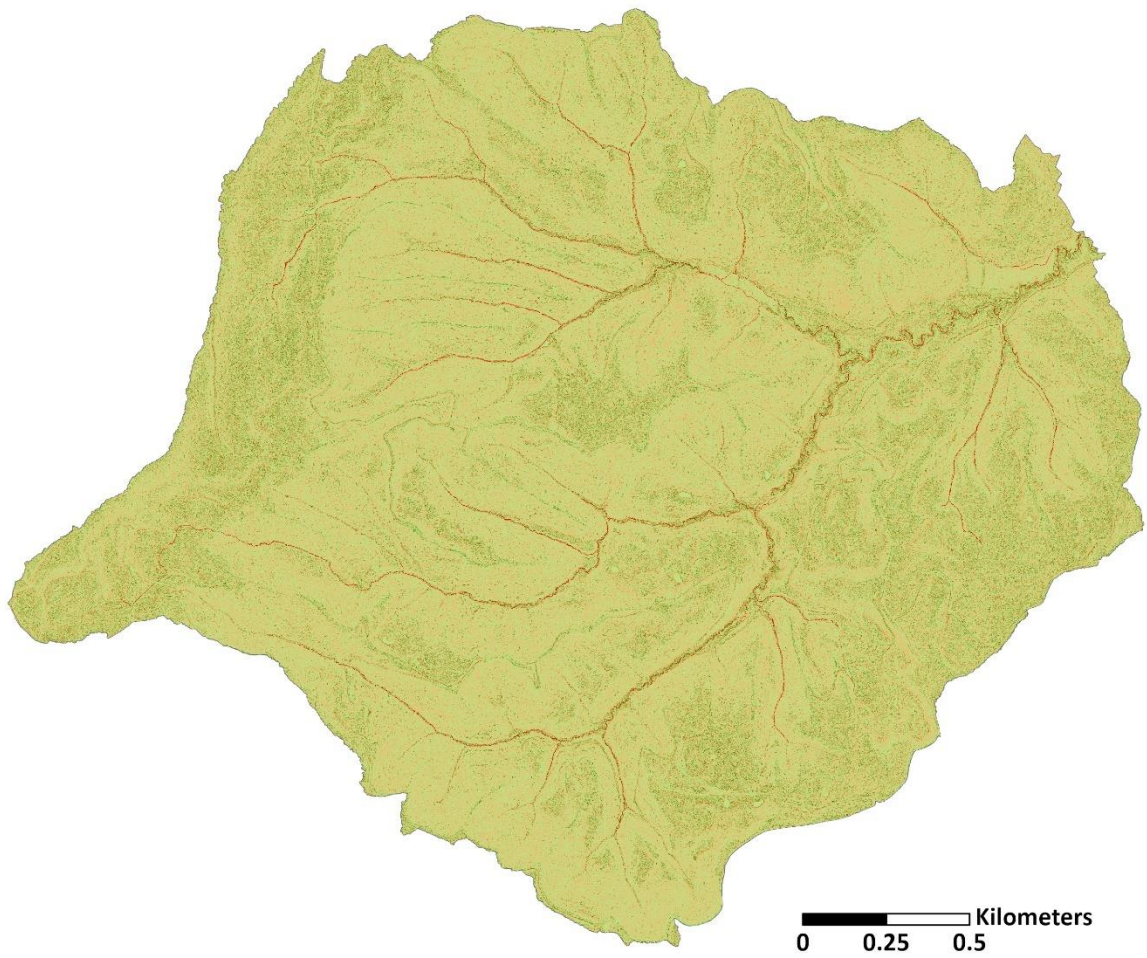
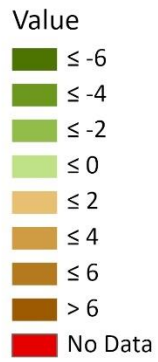


**Figure C37.** Site C difference raster (1 m) for the S Factor of the MDS method subtracted from the NBR method.

Difference  
NBR and MDS (5 m)

Value

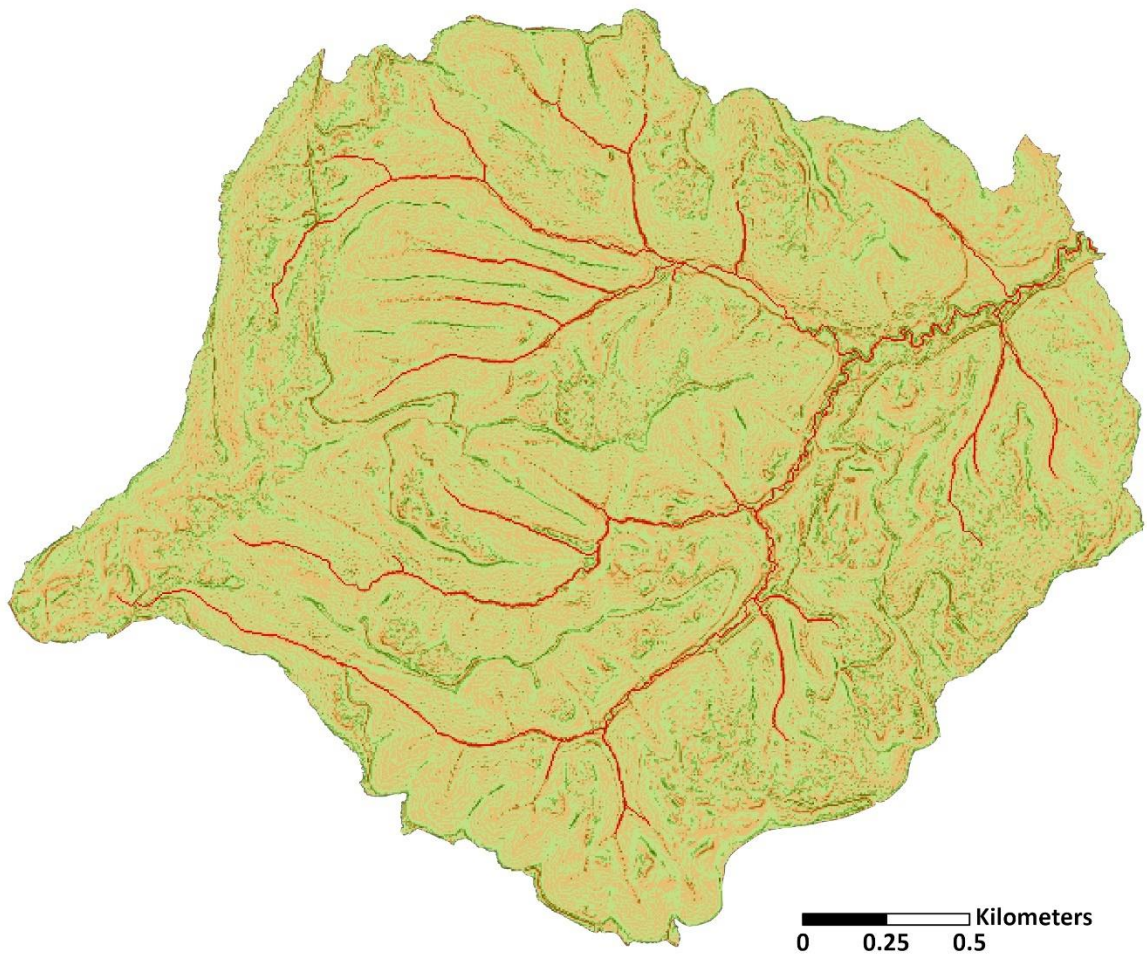
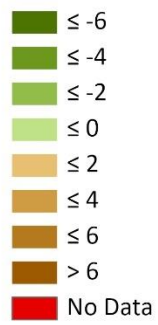


**Figure C38.** Site C difference raster (5 m) for the S Factor of the MDS method subtracted from the NBR method.

Difference  
NBR and MDS (10 m)

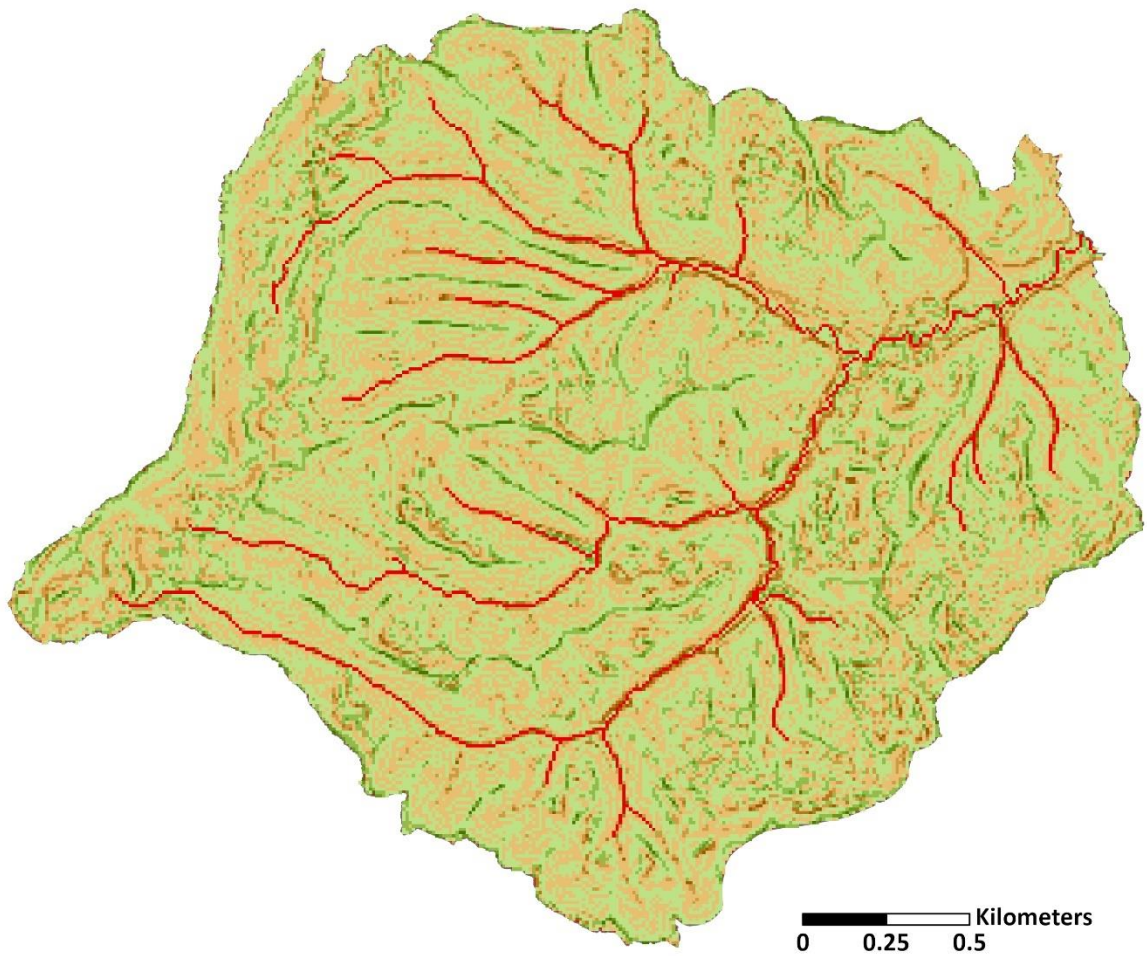
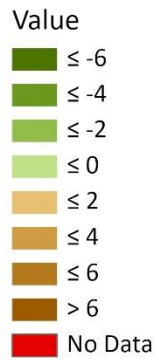


**Figure C39.** Site C difference raster (10 m) for the S Factor of the MDS method subtracted from the NBR method.

Difference  
NBR and MDS (30 m)

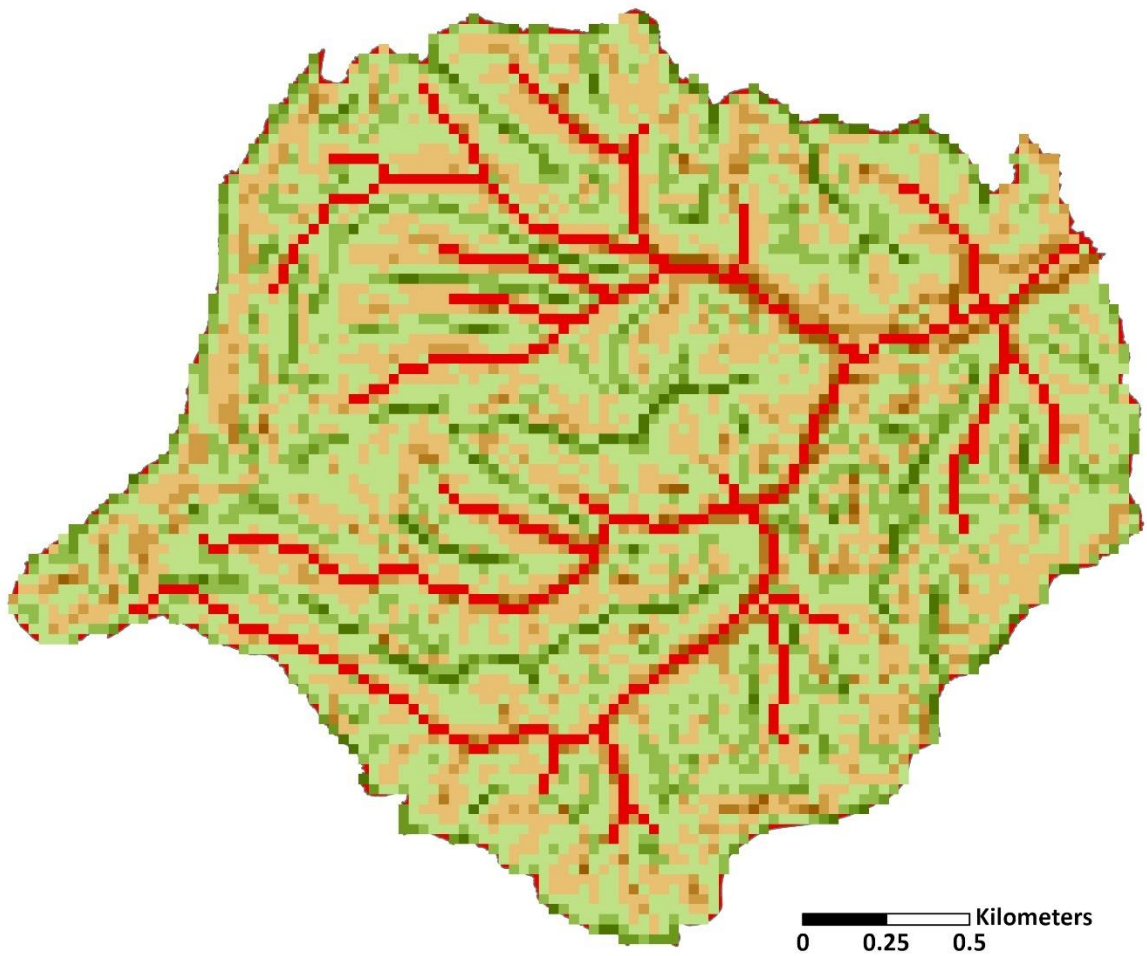
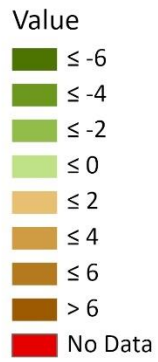


**Figure C40.** Site C difference raster (30 m) for the S Factor of the MDS method subtracted from the NBR method.

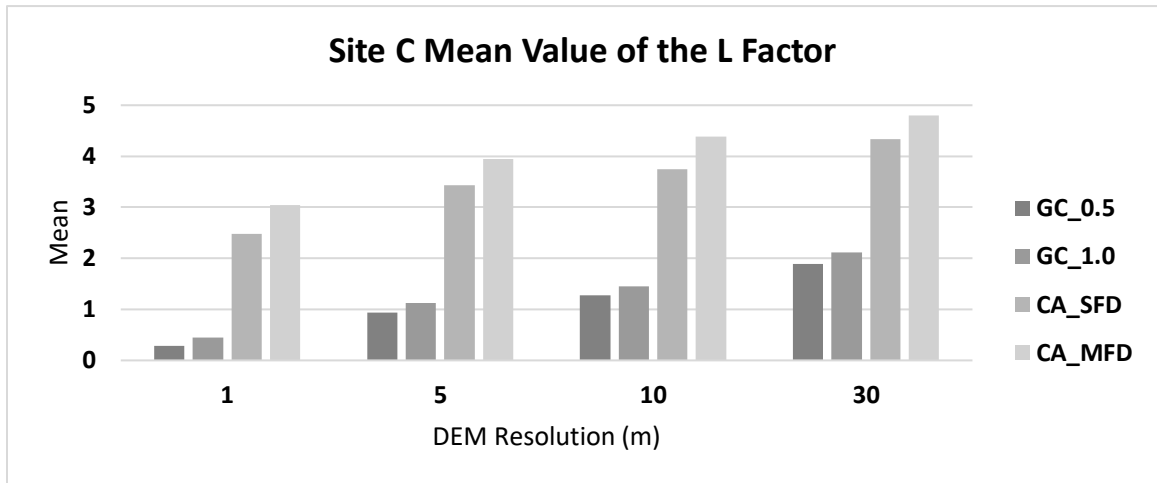


**Figure C41.** Mean value of L factor for Site C where GC\_0.5 is the GC method with slope cutoff set to 0.5, GC\_1.0 is the GC method without slope cutoff, CA\_SFD is the CA method using a SFD algorithm, and CA\_MFD is the CA method using a MFD algorithm.

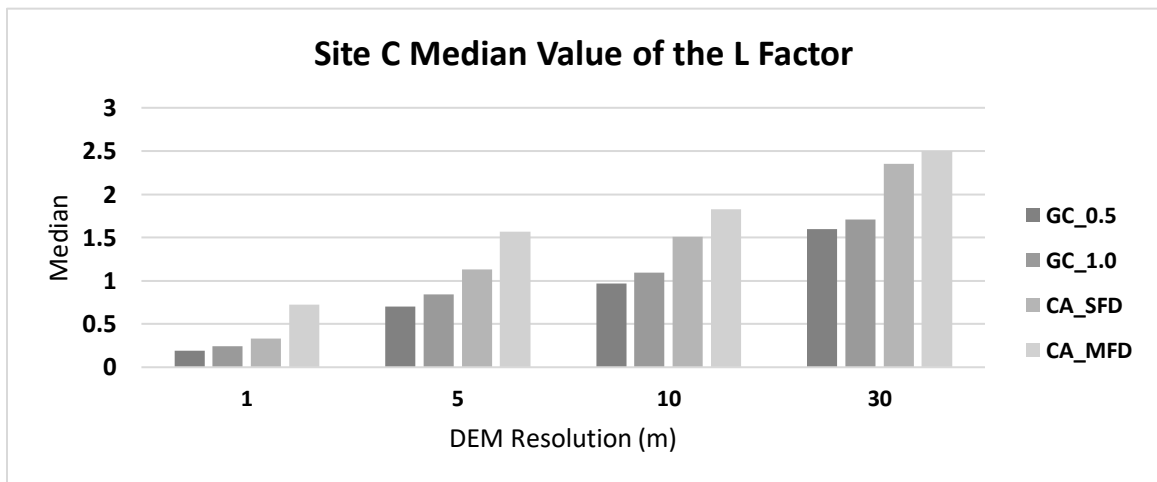


**Figure C42.** Median value of L factor for Site C where GC\_0.5 is the GC method with slope cutoff set to 0.5, GC\_1.0 is the GC method without slope cutoff, CA\_SFD is the CA method using a SFD algorithm, and CA\_MFD is the CA method using a MFD algorithm.

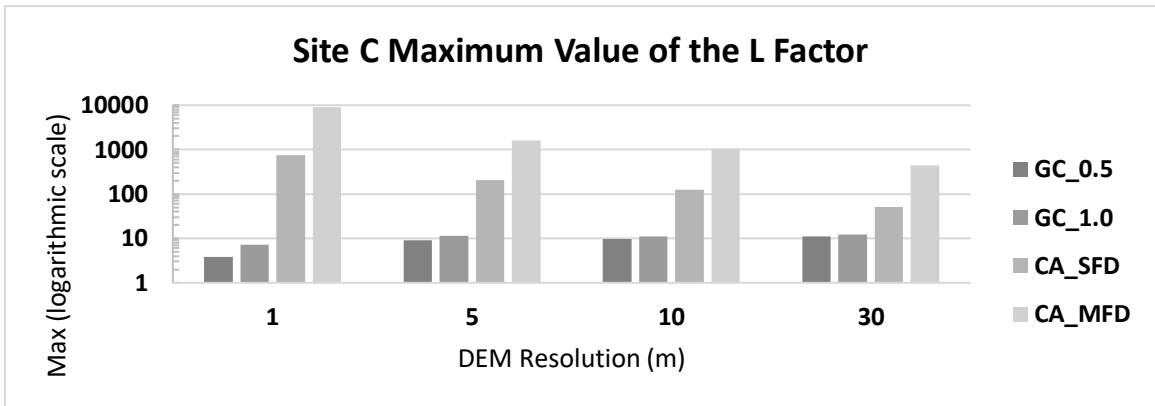


**Figure C43.** Maximum value of L factor for Site C where GC\_0.5 is the GC method with slope cutoff set to 0.5, GC\_1.0 is the GC method without slope cutoff, CA\_SFD is the CA method using a SFD algorithm, and CA\_MFD is the CA method using a MFD algorithm.

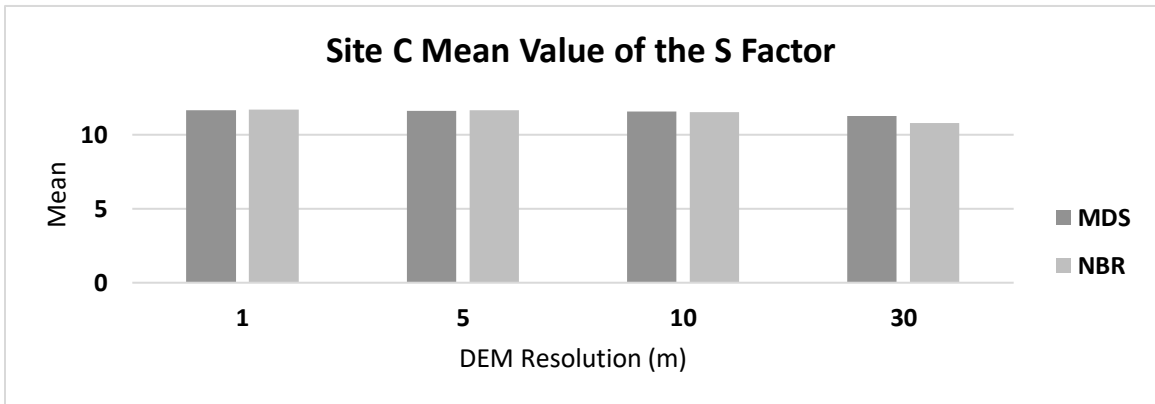


**Figure C44.** Mean value of S factor for Site C.

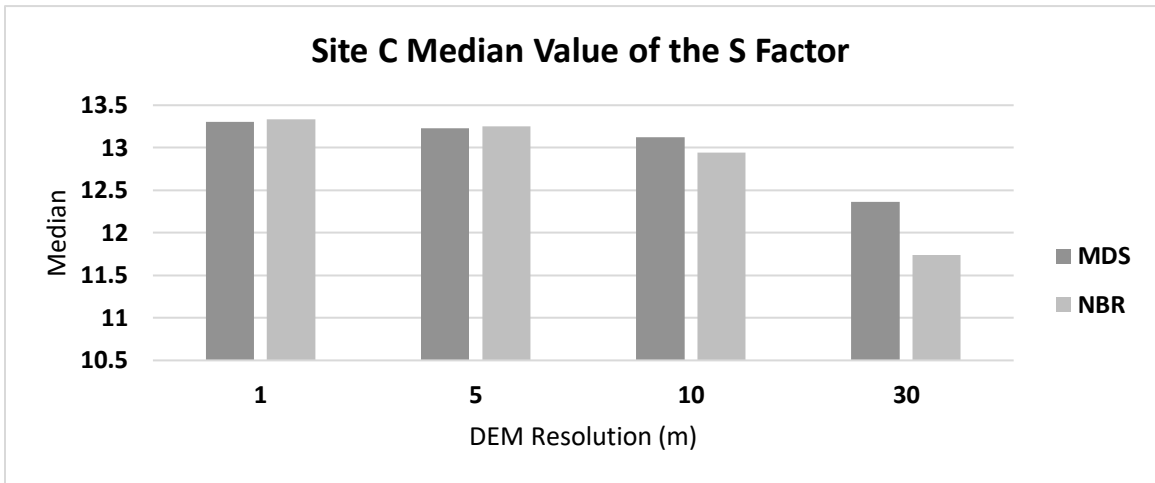


**Figure C45.** Median value of S factor for Site C.

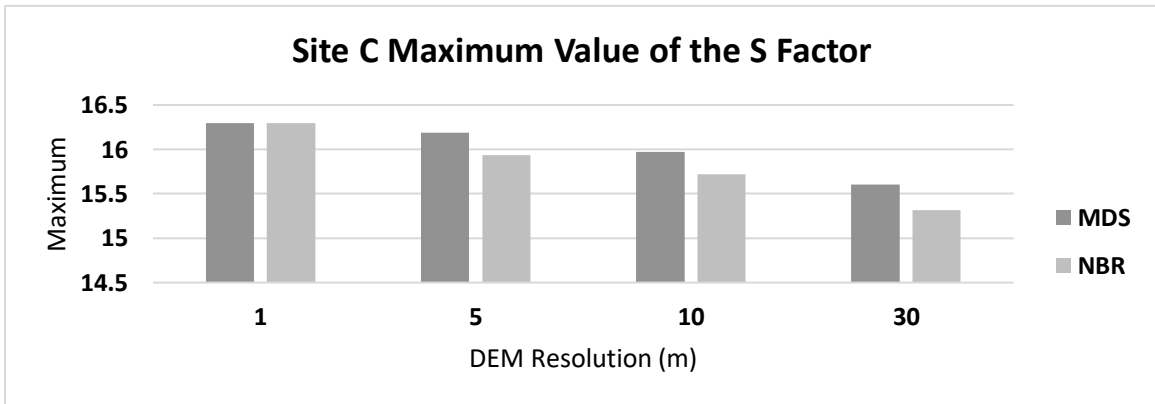


**Figure C46.** Maximum value of S factor for Site C.

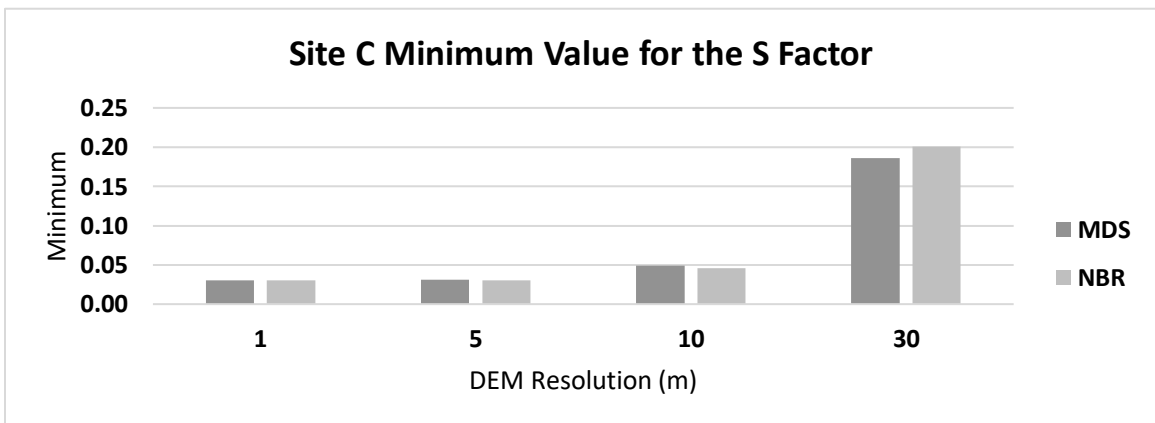


**Figure C47.** Minimum value of S factor for Site C.